Maria João Ribeiro
Cardoso

Regulação da biogénese e proliferação dos peroxissomas: caracterização de Pex16p e Pex11pβ

Regulation of peroxisome biogenesis and proliferation: characterization of Pex16p and Pex11pβ

Maria João Ribeiro
Cardoso

Regulação da biogénese e proliferação dos peroxissomas: caracterização de Pex16p e Pex11pβ

Regulation of peroxisome biogenesis and proliferation: characterization of Pex16p and Pex11pβ

Tese apresentada à Universidade de Aveiro para cumprimento dos requisitos necessários à obtenção do grau de Doutor em Bioquímica, realizada sob a orientação científica do Doutor Michael Schrader, Professor Associado do Departamento de Biociências da Universidade de Exeter e co-orientação científica da Doutora Margarida Sâncio da Cruz Fardilha, Professora Auxiliar Convidada da Secção Autónoma das Ciências da Saúde da Universidade de Aveiro

Ao Tiago, o meu menino, o maior e mais importante projeto da minha vida e para o qual as provas são diárias e eternas.

o júri

presidente

Doutor António Manuel Melo de Sousa Pereira
Professor Catedrático, Departamento de Eletrónica, Telecomunicações e Informática, Universidade de Aveiro

Doutor Carlos Jorge Alves Miranda Bandeira Duarte
Professor Associado com Agregação, Departamento de Ciências da Vida, Faculdade de Ciências e Tecnologia da Universidade de Coimbra

Doutor Vítor Manuel Vieira da Costa
Professor Associado, Instituto de Ciências Biomédicas Abel Salazar, Universidade do Porto

Doutora Margarida Sâncio da Cruz Fardilha
Professora Auxiliar Convidada, Universidade de Aveiro

Doutora Cláudia Patrícia Oliveira Grou
Investigadora em pós-doutoramento, Instituto de Biologia Celular e Molecular, Universidade do Porto

Doutora Daniela Maria Oliveira Gandra Ribeiro
Investigadora em pós-doutoramento, Instituto de Biomedicina, Universidade de Aveiro

palavras-chave

Célula, peroxissoma, biogénese e proliferação, regulação, fosforilação, PP1, Pex16p, Pex11pβ

resumo

Os peroxissomas são organelos multifuncionais e estão envolvidos em diversos processos metabólicos. As várias doenças graves provocadas por mau funcionamento dos peroxissomas e as crescentes evidências do seu envolvimento em várias patologias, desde a neurodegeneração, ao cancro e infeção viral, confere a este organelo um papel fundamental na saúde e desenvolvimento humanos. Os peroxissomas são extremamente dinâmicos, ajustando o seu número, morfologia e conteúdo proteico em resposta às necessidades da célula. A dinâmica peroxissomal, associada à sua devida regulação, está intimamente relacionada com a função deste organelo e, consequentemente, ao bem-estar humano. Assim sendo, o estudo dos mecanismos que regulam a biogénese e a proliferação dos peroxissomas é de extrema importância. Sendo a fosforilação reversível um dos principais mecanismos de controlo intracelular em eucariontes, tendo a PP1 um papel proeminente em eventos desfosforilativos, é altamente provável que seja um mecanismo importante na regulação também dos peroxissomas. De facto, têm surgido algumas evidências nesse sentido, embora sejam ainda muito escassas e não em células humanas. Interessantemente, um estudo em peroxissomas de rato revelou a presença de várias cinases e fosfatases, entre elas a PP1. O principal objetivo desta tese foi estudar o papel da fosforilação reversível nos peroxissomas humanos, através de um provável regulador da PP1, a Pex16p, e uma proteína potencialmente fosforilada, a Pex11pβ. Estas peroxinas são peças fundamentais na biogénese, crescimento e divisão dos peroxissomas. Os nossos estudos não confirmaram a interação putativa PP1-Pex16p e os resíduos S11 e S38 da Pex11pβ também não se revelaram envolvidos na sua regulação através de eventual fosforilação. Também investigámos uma possível regulação da Pex11pβ através de cisteínas-chave, sendo que C18, C25 e C85 não estão, aparentemente, envolvidas. Uma possível função para a intrigante zona rica em glicinas localizada na região intraperoxissomal também foi estuda, traduzindo resultados inconclusivos, sendo que esta parece ser dispensável ao crescimento e divisão dos peroxissomas induzidos por Pex11pβ. Também nos debruçámos sobre as hélices anfipáticas localizadas no N-terminal da Pex11pβ e verificámos que a hélice 2 é essencial para o alongamento da membrana peroxisomal, com provável envolvimento no processo de dimerização. Apesar de vários resultados serem negativos, o nosso estudo abriu alguns caminhos em direção a uma melhor compreensão dos mecanismos que regulam a biogénese e proliferação dos peroxissomas. Novos métodos de deteção de interações proteína-proteína desenvolvidos recentemente poderão ser úteis para verificar a interação PP1-Pex16p que, provavelmente será transiente. Além disso, constatámos que existem outras peroxinas com motivos de ligação à PP1, representando assim possíveis novos elos entre mecanismos de transdução de sinais intracelulares e peroxissomas. Também propomos a existência de outros domínios na Pex11pβ envolvidos na função de alongamento, uma vez que a região N-terminal, por si só, não é suficiente para promover o alongamento da membrana do peroxissoma. Também propomos que a zona inter-domínios transmembranares da Pex11pβ está, pelo menos parcialmente, embebida na bi-camada lipídica, desafiando a topologia pré-concebida. Mecanismos de regulação da Pex11pβ dirigidos por cisteínas e fosforilação continuam também a ser hipóteses em aberto, pois outros resíduos podem tomar parte nesses processos. O nosso trabalho trouxe dados importantes para o estudo dos enigmáticos mecanismos de regulação dos peroxissomas, organelos essenciais à função celular, com sérias consequências na saúde humana.

keywords

Cell, peroxisome, biogenesis and proliferation, regulation, phosphorylation, PP1, Pex16p, Pex11pβ

abstract

Peroxisomes are multifunctional organelles involved in various metabolic processes. The numerous severe disorders lead by peroxisomal malfunction in addition to the increasing evidences of the involvement of peroxisomes in several pathologies, from neurodegeneration to cancer and viral infection, renders this organelle an essential role for human health and development. Furthermore, peroxisomes are highly dynamic, adjusting their protein content, morphology and number in response to cellular needs. Peroxisome dynamics and their proper regulation are closely linked to organelle function and thus, human well-being. So that the study of the mechanisms that regulate peroxisomal biogenesis and proliferation is primordial. Being reversible phosphorylation a major intracellular control mechanism in eukaryotes with PP1 as the prominent player in dephosphorylation events, it is very likely that it represents an important regulation mechanism also in peroxisomes. As a matter of fact, some evidences in that direction have emerged, although they are still very scarce and mostly not for human cells. Interestingly, a large-scale blot screen on rat peroxisomes revealed the presence of several kinases and phosphatases, being PP1 one of them. The main goal of this thesis was to study the role of reversible phosphorylation in human peroxisomes through a very likely PP1 regulator, Pex16p, and a putative phosphorylated protein, Pex11pβ. Pex16p and Pex11pβ are essential players in the peroxisome biogenesis, elongation and division. Our studies were not able to verify a putative interaction between PP1 and Pex16p. S11 and S38 residues of Pex11pβ have also been demonstrated to not be involved in its regulation by putative phosphorylation. The regulation by key cysteines in Pex11pβ was also investigated, revealing that C18, C25 and C85 are apparently not involved in such mechanism. A possible role for an intriguing glycine-rich stretch in the intraperoxisomal region of Pex11pβ was also studied, with inconclusive results, being that it appears to be dispensable for Pex11pβ-driven peroxisomal growth and division. Our study also focused on the Pex11pβ N-terminally located amphipathic helices, reveling Helix 2 as essential for peroxisomal membrane elongation, with a probable involvement in the Pex11pβ dimerization process. Although with several negative results, our study opened some doors towards a better understanding of the mechanisms that regulate peroxisome biogenesis and proliferation. New protein-protein interaction methods which developed meanwhile may be useful to verify the likely transient PP1-Pex16p interaction. Moreover, we verified that other peroxins have putative PP1-binding motifs, representing possible further interconnectors between intracellular signal transduction and peroxisomes. Concerning Pex11pβ mechanisms of action and regulation, our study raised the hypothesis that other domains are involved in the elongation function since we demonstrated that N-terminal region in not sufficient to promote peroxisomal membrane elongation. We also propose that the inter-transmembrane domains area may be at least partially embedded within the lipid bilayer, defying the preconceived topology of this region of Pex11pβ. We further propose that other phosphorylation- and key cysteines-driven Pex11pβ regulation is still an open field since that other residues present as potentially active in such processes. Our study brought valuable insights in the mysterious regulation mechanisms of peroxisomes, essential organelles for cellular function, with serious consequences for human health.

TABLE OF CONTENTS

List of figures

List of tables

Abbreviations

3-AT	3-amino-1,2,4-triazole
α	alpha
aa	amino acid(s)
AAA	ATPases associated with diverse cellular activities
ABC	ATP-binding cassette
ABCD1	ATP-binding cassette sub-family D member 1
ACBD5	acyl-CoA-binding domain-containing protein 5
AD	DNA-activation domain
Ade	adenine
ADHAP	alkyl-dihydroxyacetone phosphate
ADHAPAT	acyl-CoA-dihydroxyacetone phosphate acyltransferase
ADHAPS	alkyl-dihydroxyacetone phosphate synthase
AGT	alanine:glyoxylate aminotransferase
ALDP	adrenoleukodystrophy protein
AMACR	2-methylacyl-CoA racemase
AMP	adenosine monophosphate
AOx/ACOX	acyl-CoA oxidase
approx.	approximately
APS	ammonium persulphate
ARD	adult Refsum disease
β	beta
bp	base pair(s)
BCA	bicinchoninic acid
BD	DNA-binding domain
BSA	bovine serum albumin
cAMP	cyclic AMP
CBC	Centre for Cell Biology
CPK1	calcium-dependent protein kinase 1
DAB	3, 3'-diaminobenzidine
DEPC	diethylpyrocarbonate
DBP	D-bifunctional protein
DHA	docosahexaenoic acid
DHAP	dihydroxyacetone phosphate
DHAPAT	dihydroxyacetone phosphate acyltransferase
DHCA	dihydroxycholestanoic acid
DLP1	dynamin-like protein 1
DMEM	Dulbecco's modified Eagle medium
DMSO	dimethyl sulphoxide

DNA	deoxyribonucleic acid
dNTPs	deoxynucleotide triphosphates
DSP	dithiobis[succinimidylpropionate]
DTT	dithiothreitol
ECL	enhanced chemiluminescence
EDTA	ethylenediaminetetraacetic acid
ER	endoplasmic reticulum
FBS	fetal bovine serum
fs	frameshift
γ	gamma
g	gram
GAP	GTPase-activating protein
GDAP1	ganglioside-induced differentiation-associated protein 1
GFP	green fluorescent protein
GSK3	glycogen synthase kinase-3
GST	glutathione S-transferase
HBS	HEPES buffered saline
HEPES	4-(2-Hydroxyethyl)piperazine-1-ethanesulfonic acid
His	histidine
HRP	horseradish peroxidase
IBMC	Institute for Molecular and Cell Biology
IF	immunofluorescence
IgG	immunoglobulin G
IP	immunoprecipitation
IPTG	isopropylthio-β-galactoside
IRD	infantile Refsum disease
IVT	*in vitro* translation
Kan	kanamycin
kb	kilo base pairs
kDa	kilo Dalton
KO	knockout
l	litre
Leu	leucine
LB	Luria Broth
LiAc	lithium acetate
LT-AG	large T antigen
μ	micro (10^{-6})
m	metre
m (prefix)	milli (10^{-3})

M	molar
MaMTH	mammalian-membrane two-hybrid
MAP	mitogen-activated protein
MAPK	mitogen-activated protein kinase
mc	monoclonal
Mff	mitochondrial fission factor
min	minutes
MKK6	dual specificity mitogen-activated protein kinase kinase 6
MKT1	MAP kinase phosphatase 1
MOPS	3-(N-Morpholino)propanesulfonic acid
mPTS	peroxisomal targeting signal of PMPs
MYTH	membrane-based yeast two-hybrid
n (prefix)	nano (10^{-9})
NALD	neonatal adrenoleukodystrophy
NOHLA	N^{ω}-hydroxy-L-arginine
Ω	ohm
OD	optical density
p (prefix)	pico (10^{-12})
PAGE	polyacrylamide gel electrophoresis
PAS	protein A-coupled sepharose
PBS	phosphate buffered saline
PBD	peroxisome biogenesis disorder
pc	polyclonal
PCR	polymerase chain reaction
PFD	peroxisome function disorder
PEG	polyethylene glycol
PEI	polyethylenimine
PEX	peroxin
PH	Pleckstrin homology
PH-1	primary hyperoxaluria type-1
PIP	PP1 interacting protein
PKA	cAMP-dependent kinase
PMP	peroxisomal membrane protein
PMP70	70 kDa peroxisomal membrane protein
PMSF	phenylmethylsulphonyl fluoride
PO	peroxisome
PP	peroxisome proliferator
PP1	protein phosphatase 1
PP1BM	PP1-binding motif

PP1c	PP1 catalytic subunit
PP2A	protein phosphatase 2A
PPAR	peroxisome proliferator-activated receptor
PPRE	PPAR response element
PSK	protein Ser/Thr-kinase
PSP	protein Ser/Thr-phosphatase
PTS	peroxisomal targeting signal
RCDP	rhizomelic chondrodysplasia punctata
RE	restriction endonuclease
Ref	reference
RNase	ribonuclease
RNS	reactive nitrogen species
ROS	reactive oxygen species
rpm	revolutions per minute
RXR	retinoid X receptor
s	seconds
SDS	sodium dodecyl sulphate
SEM	standard error of the mean
Ser	serine
T (suffix)	Tween 20
TAE	tris-Acetate-EDTA
TBS	Tris buffered saline
TE	Tris-EDTA
TEMED	tetramethylethylenediamine
THCA	trihydroxycholestanoic acid
Thr	threonine
T_m	melting temperature
Tris	tris(hydroxymethyl)aminomethane
TRITC	tetramethylrhodamine isothiocyanate
Trp	tryptophan
TRP	tetratricopeptide repeat
Tyr	tyrosine
U	units
UV	ultraviolet
V	volt
VLCFA	very long-chain fatty acids
v/v	volume per volume
w/v	weight per volume
WB	western blot

WD	tryptophan-aspartic acid
WT	wild-type
X-α-Gal	5-bromo-4-chloro-3-indolyl-α-D-galactopyranoside
X-ALD	X-linked adrenoleukodrystrophy
XOx	xanthine oxidase
YFP	yellow fluorescent protein
YPD	yeast extract peptone dextrose
YTH	yeast two-hybrid
ZS	Zellweger syndrome

1 Introduction

1.1 Peroxisomes – an overview

1.1.1 General features of the organelle

Peroxisomes are single-membrane subcellular compartments that are found in virtually all eukaryotic organisms (Figure 1). Despite their importance for human life and health, they were discovered only in the middle of the 20th century, and were initially termed microbodies (1). Later on, the discovery that the peroxisomal matrix contains a large number of hydrogen peroxide (H_2O_2)-producing oxidases as well as catalase, a H_2O_2-degrading enzyme finally coined the name "peroxisome" (2).
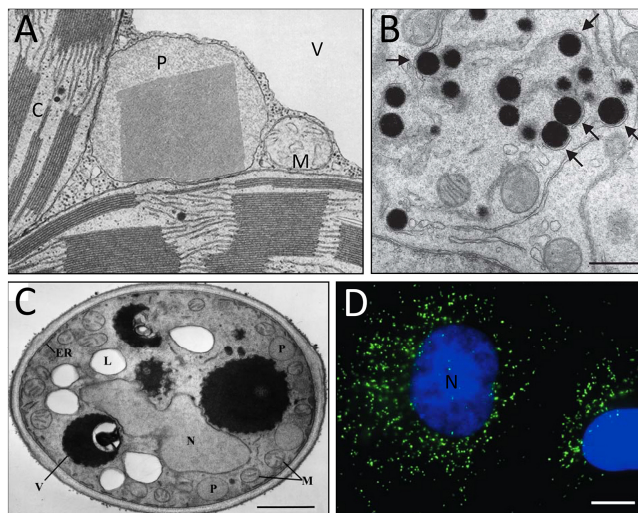
Figure 1: Peroxisomes
(**A**) Peroxisomes with crystalline inclusions in tobacco leaf cells. Adapted from (3). (**B**) Peroxisomes stained by DAB (black) in rat hepatoma cells. Note the close association with the smooth ER (arrows). Adapted from (4). (**C**) *Saccharomyces cerevisiae* cell. Adapted from (5). (**D**) Peroxisomes in mouse fibroblasts, peroxisomes stained in green. Adapted from (4). ER, endoplasmic reticulum; L, lipid droplet; M, mitochondrion; N, nucleus; P, peroxisome; V, vacuole. Bars, 500 nm (B), 1 µm (C) and 10 µm (D).

The investigation of peroxisomes was considerably facilitated by the development of experimental methods for inducing their proliferation (6) and to detect their enzymatic activity, e.g. alkaline 3, 3'-diaminobenzidine (DAB) staining, which explores catalase activity and allowed the specific staining of peroxisomes for electron and light microscopy in different tissues and organisms (7). Later, their important role in lipid metabolism and the existence of a peroxisomal β-oxidation pathway were discovered (8). Presently, it is known that peroxisomes, which together with glyoxysomes, glycosomes and Woronin bodies, constitute the organelle family of "microbodies", whose members are all evolutionarily related (9). Peroxisomes fulfil a wide range of metabolic functions (10)

which, along with their protein composition and morphological appearance, vary among different species, cell types and developmental stages (11). Peroxisomes are mainly found as spherical or rod-like forms (0,3 to 0,5 µm in diameter), but peroxisomes can also appear as tubular structures with up to 5 µm of length or even as interconnecting compartments forming tubular networks (5). Since peroxisomes are devoid of DNA all peroxisomal proteins are encoded by the nuclear genome. About 61 yeast and 85 human genes encoding peroxisomal proteins have been identified so far. Many of them are enzymes with metabolic functions, while the others, the so-called peroxins, are required for the biogenesis and maintenance of functional peroxisomes (12).

1.1.2   Metabolic functions

Peroxisomes show a broad functional diversity, justifying its designation as "multipurpose organelles" (13) (see Figure 2 and Table 1 for an overview). Peroxisome-specific metabolic functions vary depending upon organism and cell type, as well as developmental and environmental conditions (reviewed in (14) and (10)). Despite their enormous plasticity and dynamic behavior, peroxisomes do not exist as isolated entities, but are intimately linked to other organelles such as lipid droplets, the endoplasmic reticulum (ER) and mitochondria (15, 16).
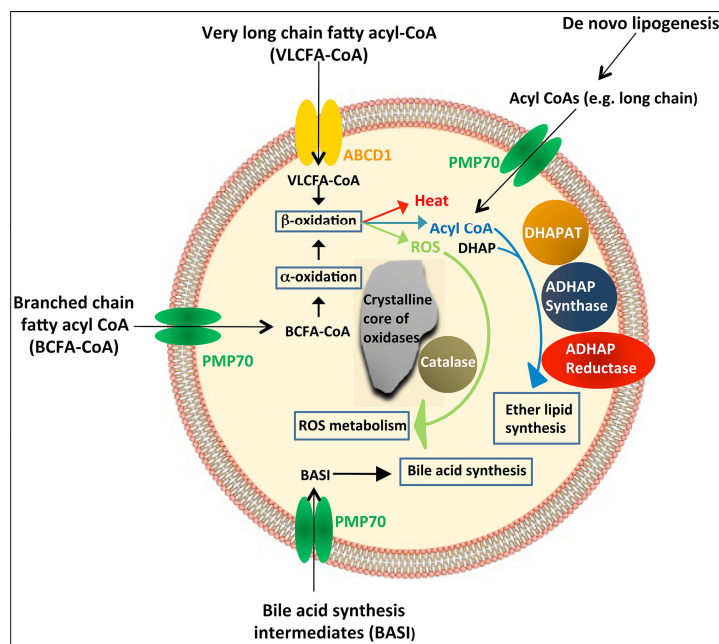
Figure 2: Overview of the major peroxisomal metabolic pathways
The main metabolic functions of peroxisomes in mammalian cells include β-oxidation of very long chain fatty acids, α-oxidation of branched chain fatty acids, synthesis of bile acids and ether-linked phospholipids, and removal of reactive oxygen species. Peroxisomes in many, but not all, cell types contain a dense crystalline core of oxidative enzymes. Adapted from (17). ABCD1, ATP-binding cassette sub-family D member 1; ADHAP, alkyl-dihydroxyacetone phosphate; DHAPAT, dihydroxyacetone phosphate acyltransferase; PMP70, 70 kDa peroxisomal membrane protein; ROS, reactive oxtgen species.

Table 1: Metabolic functions of mammalian peroxisomes

Function	Enzymes, substrates or products
Peroxide metabolism, ROS/RNS metabolism*	Catalase and H_2O_2-generating oxidases
Lipid biosynthesis	Ether phospholipids/plasmalogens, bile acids, fatty acid elongation (cholesterol and dolichol)
Fatty acid β-oxidation*	Very long-chain fatty acids, dicarboxylic acids, branched-chain fatty acids, unsaturated fatty acids, arachidonic acid metabolism
Fatty acid α-oxidation	Phytanic acid
Long/very long-chain fatty acid activation	
Regulation of acyl-CoA/CoA ratio	
Glycerol biosynthesis	
Protein/amino acid metabolism*	Biosynthesis of cysteine and sulphur assimilation, D-amino acid degradation, L-lysine metabolism, degradation of polyamines, proteases, transaminases
Catabolism of purines	
Glyoxylate and dicarboxylate metabolism	
Hexose monophosphate pathway	
Nicotinate and nicotinamide metabolism	
Retinoid metabolism	

*Functional cooperation of peroxisomes with mitochondria. Adapted from (12).

1.1.2.1 Lipid metabolism

In contrast to most other functions of peroxisomes (see Table 1), which may vary between different species and within specific cell types in a single organism (10), fatty acid β-oxidation is a universal property of peroxisomes in most, if not all, organisms. In yeast and plants, peroxisomes are the sole site of fatty acid β-oxidation, whereas in higher eukaryotes it may occur in both mitochondria and peroxisomes (14, 18, 19). In mammalian cells very long-chain fatty acids (VLCFA, ≥C_{24}) can only be degraded by peroxisomes and not by mitochondria (20). VLCFA are probably imported into peroxisomes as acyl-CoA esters by ABC transporters (e.g. ABCD1 = adrenoleukodystrophy protein, ALDP). After chain shortening by peroxisomal β-oxidation, the resulting (medium-chain) acyl-CoA esters can be transferred to mitochondria for full oxidation to CO_2 and H_2O – one example of the close metabolic cooperation between mitochondria and peroxisomes (15, 16). The final degradation of fatty acids in mitochondria supplies the cell with ATP, as the peroxisomal β-oxidation is not coupled to an electron transfer chain. Instead, electrons are transferred to oxygen via $FADH_2$, generating hydrogen peroxide

(H$_2$O$_2$, Figure 2). Therefore, the obtained energy is not used to power ATP synthesis, but is instead released as heat, contributing to thermogenesis (21). Besides VLCFA, other substrates such as prostaglandins and leukotrienes, bile acid intermediates, pristanic acid, certain polyunsaturated fatty acids, and the vitamins E and K are degraded by peroxisomal β-oxidation (14, 22). Trans-unsaturated fatty acids, i.e. those containing a methyl group at the C-3 position such as phytanic acid and xenobiotic compounds, cannot undergo β-oxidation directly and are thus first decarboxylated in peroxisomes by fatty acid α-oxidation (14, 23, 24).

Additionally, anabolic processes also take place in peroxisomes. The synthesis of etherphospholipids such as plasmalogens is a cooperative process between peroxisomes and the endoplasmic reticulum (25). Plasmalogens are essential components of myelin, thus they account for around 80% of the white matter of the brain (26), and represent around 18% of the total phospholipid mass in human body (27). The formation of the characteristic ether linkage is catalyzed by the peroxisomal enzyme alkyl-DHAP synthase while further biosynthesis is conducted in the smooth ER (14). Moreover, bile acid and glycerol biosynthesis are also performed by peroxisomal enzymes. The synthesis of cholesterol and dolichol in peroxisomes is debated (14, 28, 29).

1.1.2.2   ROS metabolism and other functions

Peroxisomes contain a number of O$_2$-consuming oxidases that produce H$_2$O$_2$ by oxidizing a large collection of substrates. H$_2$O$_2$ is ascribed to "reactive oxygen species" (ROS), as it can easily be converted into more aggressive radical species. Although ROS have been shown to have physiological functions (e.g. signaling), increased oxidative stress can provoke serious cell damage (30). Therefore a tight regulation of ROS is required. In addition to the enzymes involved in fatty acid α- and β-oxidation, oxidases metabolizing other substrates such as lactate, glycolate, other α-hydroxy acids, D-amino acids, oxalate, and urate (not in primates) produce H$_2$O$_2$. Xanthine oxidase (XOx), an enzyme involved in the catabolism of purines, even produces superoxide radicals (O$_2^{\bullet-}$) (31).

On the other hand, antioxidant enzymes located in peroxisomes counteract the production of H_2O_2 and $O_2^{\bullet-}$, with catalase being the most prominent one (reviewed in Bonekamp et al., 2009 (30)) . While catalase and other enzymes (see Table 2) decompose H_2O_2, superoxide anions and hydroxyl radicals ($^{\bullet}OH$, generated from hydrogen peroxide via Fenton-catalyzed reduction) are scavenged by manganese and copper-zinc superoxide dismutases (MnSOD, CuZnSOD) (32-35). Furthermore, the toxic metabolite glyoxylate is converted into glycine by alanine:glyoxylate aminotransferase (AGT), which localizes exclusively to peroxisomes in humans (36), and enzymes of the hexose monophosphate pathway are found in peroxisomes as well (37). More specialized functions are for instance fulfilled in the glyoxysomes of the parasite *Trypanosoma*, which contain enzymes of the glyoxylate cycle for the production of lipid-derived compounds required for gluconeogenesis (38), or in Woronin bodies, which seal septal pores in the hyphae of filamentous fungi (39). Additionally, peroxisomes are involved in several quite diverse processes such as penicillin biosynthesis (40), photorespiration in plants (41), or luciferase-based glowing of a firefly (42).

Table 2: Overview of ROS/RNS generated in mammalian peroxisomes

Type of ROS/RNS produced	Generating reaction	Produced in PO by	Scavenged in PO by
Hydrogen peroxide (H_2O_2)	$O_2^{\bullet-} + H^+ \rightarrow HO2^{\bullet-}$, $2HO2^{\bullet-} \rightarrow H_2O_2 + O_2$	Acyl-CoA oxidase (several types), Urate oxidase, Xanthine oxidase, D-amino acid oxidase, D-aspartame oxidase, Pipecolic acid oxidase, Sarcosine oxidase, L-α-hydroxy acid oxidase, Polyamine oxydase	Catalase, Glutathione peroxidase, Peroxiredoxin I, PMP20
Superoxide anion ($O2^{\bullet-}$)	$O_2 + e^- \rightarrow O2^{\bullet-}$	Xanthine oxidase	MnSOD, CuZnSOD
Nitric oxide ($^{\bullet}NO$)	L-Arg + NADPH + H^+ + O_2 $\rightarrow$ NOHLA + $NADP^+$ + H_2O, NOHLA + ½ NADPH + ½ H^+ + O_2 $\rightarrow$ L-citrulline + ½ $NADP^+$ + $^{\bullet}NO$ + H_2O	Nitric oxide synthase	

ROS, reactive oxygen species; RNS, reactive nitrogen species; PO, peroxisomes; NOHLA, N^{ω}-hydroxy-L-arginine. Adapted from (30).

1.1.3 Peroxisomal disorders

A pivotal role of peroxisomes in human health and development is indicated by the existence of several devastating genetic disorders caused by impaired peroxisomal activity or lack of peroxisomes due to defective peroxisomal biogenesis (Table 3) (43). Peroxisomal disorders are clinically heterogeneous. However, they are consistently associated with impaired peroxisomal lipid metabolism, resulting in the accumulation of VLCFAs and phytanic acid, and defective synthesis of ether lipids and bile acids (17). The most recent proposed classification divides the peroxisomal disorders into two groups: peroxisome biogenesis disorders (PBDs) and peroxisome function disorders (PFDs) (44).

Table 3: The peroxisomal disorders

	Abbreviation	MIM number	Defective protein	Mutant gene	Locus
Peroxisome biogenesis disorders	PBD				
PBD-group A (Zellweger spectrum disorders):					
			PEX1	*PEX1*	7q21.2
			PEX2	*PEX2*	8q21.1
			PEX3	*PEX3*	6q24.2
			PEX5	*PEX5*	12p13.3
			PEX6	*PEX6*	6p21.1
Zellweger syndrome	ZS	214100	PEX10	*PEX10*	1p36.32
Neonatal adrenoleukodystrophy	NALD	214110	PEX12	*PEX12*	17q12
Infantile Refsum disease	IRD	202370	PEX13	*PEX13*	2p14-p16
			PEX14	*PEX14*	1p36.22
			PEX16	*PEX16*	11p11.2
			PEX19	*PEX19*	1q22
			PEX26	*PEX26*	22q11.21
PBD-group B:					
Rhizomelic chondrodysplasia punctata type 1	RCDP-1	215100	PEX7	*PEX7*	6q21-q22.2
Peroxisome function disorders	PFD				
Fatty acid beta-oxidation					
X-linked adrenoleukodystrophy	X-ALD	300100	ALDP	*ABCD1*	Xq28
Acyl-CoA oxidase deficiency	ACOX-deficiency	264470	ACOX1	*ACOX1*	17q25.1
D-Bifunctional proteins deficiency	DBP-deficiency	261515	DBP/MFP2/MFEII	*HSD17B4*	5q2
Sterol-carrier-protein X deficiency	SCPx-deficiency	–	SCPx	*SCP2*	1p32
2-Methylacryl-CoA reacemase deficiency	AMACR-deficiency	604489	AMACR	*AMACR*	5p13.2-q11.1
Etherphospholipid biosynthesis					
Rhizomelic chondrodysplasia punctata type 2	RCDP-2	222765	ADHAPAT	*GNPAT*	1q42.1-42.3
Rhizomelic chondrodysplasia punctata type 3	RCDP-3	600121	ADHAPS	*AGPS*	2q33
Fatty acid alpha-oxidation					
Refsum disease	ARD/CRD	266500	PHYH/PAHX	*PHYH/PAHX*	10p15-p14
Glyoxylate metabolism					
Hyperoxaluria Type 1	PH-1	259900	AGT	*AGTX*	2q37.3
Bile acid synthesis (conjugation)					
Bile acid Co-A:amino acid N-acyltransferase deficiency	BAAT-deficiency	602938	BAAT	*BAAT*	
H₂O₂-metabolism					
Acatalasemia		115500	Catalase	*CAT*	11p13

From (44).

PBDs fall into four main phenotypic classes. Three of them, Zellweger syndrome (ZS), neonatal adrenoleukodystrophy (NALD), and infantile Refsum disease (IRD) have multiple

complementation groups and form a spectrum (Zellweger spectrum) of overlapping features. The fourth group, rhizomelic chondrodysplasia punctata type 1 (RCDP-1), is a distinct PBD phenotype (45, 46). Zellweger spectrum diseases result from mutations in one of the *PEX* genes involved in peroxisome biogenesis. Mutations in *PEX3*, *PEX16* and *PEX19*, which result in the complete absence of peroxisomes, cause the most severe phenotypes. Mutations in other *PEX* genes result in ghost peroxisomes, i.e. void of any matrix content. Features of ZS, which is the most severe end of the clinical spectrum, include craniofacial dysmorphism, hepatomegaly, and neurological abnormalities such as disruption of normal development, hypotonia, seizures, glaucoma, retinal degeneration, and deafness. Most Zellweger infants do not survive past one year of age due to respiratory compromise, gastrointestinal bleeding, and liver failure. The features of NALD and IRD are similar to those of Zellweger syndrome, but these disorders progress more slowly. Children with NALD usually die between the age of two and three years. Patients with IRD can live into early adulthood. RCDP-1 is clinically and genetically distinct from Zellweger syndrome spectrum disorders. It is characterized by distinctive facial features, including prominent forehead, hypertelorism (widely set eyes), and up-turned nose. These patients also suffer from growth failure, developmental delay, seizures, and congenital cataracts. Most die in early childhood. RCDP-1 is caused by mutations in Pex7, a chaperone for the three PTS2-containing peroxisomal matrix proteins (17, 43, 47).

The *PEX11B* patients known so far presented import-competent peroxisomes, although enlarged and undivided. His clinical symptoms are atypical for PBDs, with normal biochemical parameters (48, 49). This case, together with the newborn lethal case of a patient with a mutation in the *DLP1* gene which caused a defect in fission of both mitochondria and peroxisomes (50), raised the awareness for the importance of peroxisome (and mitochondria) morphology in health and disease (51).

The group of peroxisome function disorders (PFDs) involves the single peroxisomal enzyme deficiencies and the single peroxisomal substrate transport deficiencies (43). PFDs can be subclassified according to which peroxisomal function/biochemical pathway is lost or affected, namely (a) fatty acid β-oxidation, (b) etherphospholipid biosynthesis,

(c) fatty acid α-oxidation, (d) glyoxylate metabolism, (e) bile acid synthesis and (f) H_2O_2 – metabolism (Table 3, (44)).

The disorders of peroxisomal β-oxidation are the most abundant among PFDs, being X-linked adrenoleukodrystrophy (X-ALD) the most common peroxisomal disorder. X-ALD is the only single peroxisome substrate transport deficiency known so far and it is caused by mutations in the *ABCD1* gene, which encodes adrenoleukodystrophy protein (ALDP). This protein is a half-ABC transporter and mediates the ATP-driven transport of the CoA-esters of VLCFAs resulting in an accumulation of these molecules (52). The main symptoms of X-ALD are a progressive demyelination/neurodegeneration as well as adrenal insufficiency (53, 54).

Apart from the inherited peroxisomal disorders, peroxisomes have been linked to other pathological conditions, including Alzheimer's disease, diabetes and cancer. Santos and colleagues (55) demonstrated a direct link between the peroxisomal proliferation and neuroprotection against Aβ-driven degenerative alterations. Actually, peroxisomes seem to represent one of the first defense lines against oxidative stress induced by Aβ (56). The role of docosahexaenoic acid (DHA) in brain degeneration protection and the significant lower levels of plasmalogens in patients with severe dementia constitute other examples of the importance of peroxisomes for brain health (reviewed in (57)). Peroxisomes may also play noteworthy roles in type 2 diabetes by the involvement of peroxisome-generated H_2O_2 in fatty acid-induced toxicity in insulin-producing pancreatic β-cells (58, 59). Ether lipid levels are for a long time now known to be elevated in tumors (60-63) and recent work demonstrated that ADHAPS, a critical peroxisomal enzyme for ether lipid synthesis, is upregulated in several cancer cells and primary tumors. Moreover, its ablation impaired tumor pathogenicity; on the other hand, its overexpression elevated cancer cell motility, survival and tumor growth. Therefore, peroxisomes have a remarkable role in the generation of oncogenic signaling lipids (64). Furthermore, MCT2, a monocarboxylate transporter, was very recently demonstrated to be upregulated and localized mainly to peroxisomes in prostate cancer cells (65). Peroxisomes have also been liked to ageing (66-68) and antiviral response (reviewed in (69)).

1.2 Peroxisome biogenesis

The study of yeast mutants with defects in biogenesis of peroxisomes led to the identification of a set of peroxisomal proteins, collectively referred to as peroxins or PEX proteins, which are required for peroxisome biogenesis (70). The peroxins can be divided into three groups according to their role in peroxisome biogenesis: (a) peroxins involved in the import of peroxisomal matrix proteins, (b) peroxins required for peroxisomal membrane assembly/import of peroxisomal membrane proteins (PMPs) and (c) peroxins regulating peroxisomal proliferation (Table 4). At present, 31 different proteins/genes have been discovered in lower eukaryotes, 14 in mammals and 15 in plants (without counting isoforms). Most of the additional peroxins present in lower eukaryotes appear to be specific for one species and/or functionally redundant (71).

Table 4: Peroxisomal biogenesis proteins (Peroxins) in mammals, plants, filamentous fungi and yeast species

Peroxin	PEX1	PEX2	PEX3	PEX4	PEX5	PEX6	PEX7	PEX8	PEX10	PEX11	PEX12	PEX13	PEX14	PEX15	PEX16	PEX17	PEX18	PEX19	PEX20	PEX21	PEX22	PEX23	PEX24	PEX25	PEX26	PEX27	PEX28	PEX29	PEX30	PEX31	PEX32
Mammals	✓	✓	✓		✓	✓	✓		✓	✓	✓	✓	✓		✓			✓							✓						
Plants	✓	✓	✓	✓	✓	✓	✓		✓	✓	✓	✓	✓		✓			✓			✓										
F. fungi	✓	✓	✓	✓	✓	✓	✓	✓	✓	✓	✓	✓	✓		✓				✓	✓		✓	✓	✓							
Yeasts	✓	✓	✓	✓	✓	✓	✓	✓	✓	✓	✓	✓	✓	✓	✓[1]	✓	✓	✓	✓	✓	✓	✓	✓	✓	✓[2]	✓	✓	✓	✓	✓	✓

Peroxin function is indicated by color: blue – matrix protein import; red – membrane assembly; green – proliferation and division. PEX9 (absent), ORF misidentified, i.e. antisense sequence of PEX26. F, filamentous. [1]Only found in *Yarrowia lipolytica*. [2]PEX26 is absent in *Saccharomyces cerevisiae* and related yeast species. From (10).

1.2.1 Import of matrix proteins

All peroxisomal matrix proteins are synthesized on free polyribosomes in the cytosol and imported post-translationally (72). Unlike the translocation of unfolded polypeptides across the membranes of the ER, mitochondria, and chloroplasts (73), peroxisomes can transport cargoes in a folded, cofactor-bound, and/or oligomeric state (74). The specific import of peroxisomal matrix proteins is mediated by targeting signals which are recognized by cytosolic receptors. According to the model of the cycling receptor (Figure 3), the peroxisomal matrix protein import can be conceptually divided into six steps: I) cargo recognition in the cytosol and (II) docking of the receptor-cargo complexes to the

peroxisomal membrane; (III) formation of a transient pore; (IV) cargo-translocation into the peroxisomal matrix; (V) ubiquitination of the receptor and (VI) deubiquitination and export of the receptor back to the cytosol (75).

The sorting of proteins to peroxisomes depends on signal sequences, so called peroxisomal targeting signal (PTS) type 1 and type 2. PTS1, present in the majority of peroxisomal matrix proteins, is located at the extreme C-terminus and consists of three amino acids, serine-lysine-leucine (SKL), or variants of the motif fitting the consensus [SAC]-[KRH]-[LM] (76). Nowadays, PTS1 has been redefined as dodecamer, as additional amino acids might be crucial of receptor-cargo interaction (77, 78). PTS2 is N-terminally localized and comprised by the degenerated nonapeptide R-[LVIQ]-X-X-[LVIH]-[LSGA]-X-[HQ]-[LA] (79). In the cytosol, the PTS1 is recognized by receptor Pex5p (Figure 3, I), which contains a tetratricopeptide repeat (TPR) domain for PTS1-binding (80). PTS2-harbouring proteins are recognized by the soluble receptor protein Pex7p, which consists of six tryptophan-aspartic acid (WD) repeats, preceded by a distinct N-terminal region (81). Unlike Pex5p, the Pex7p-mediated import pathway requires species-specific auxiliary proteins known as co-receptors: a longer splice variant of the PTS1-receptor Pex5p (Pex5pL) fulfills this function in plants (82) and mammals (83, 84). Some peroxisomal proteins, such as *Yarrowia lipolytica* acyl-CoA oxidase (85), castor bean isocitrate lyase (86) or mammalian Cu/Zn superoxide dismutase (87), neither contain PTS1 nor PTS2. These so-called non-PTS proteins can be imported into peroxisomes by binding to a different region of Pex5p (88) or by "piggyback" complex formation with PTS-containing proteins (89). A new chapter of peroxisomal targeting signals has recently been opened by the finding that glycolytic enzymes of the analyzed fungi and mammalian species containing cryptic PTS. With few exceptions, these enzymes were thought to be strictly cytosolic in all species. However, they contain a cryptic peroxisomal targeting signal, which can be generated or eliminated in a species-specific manner by ribosomal read-through or alternative splicing (90).
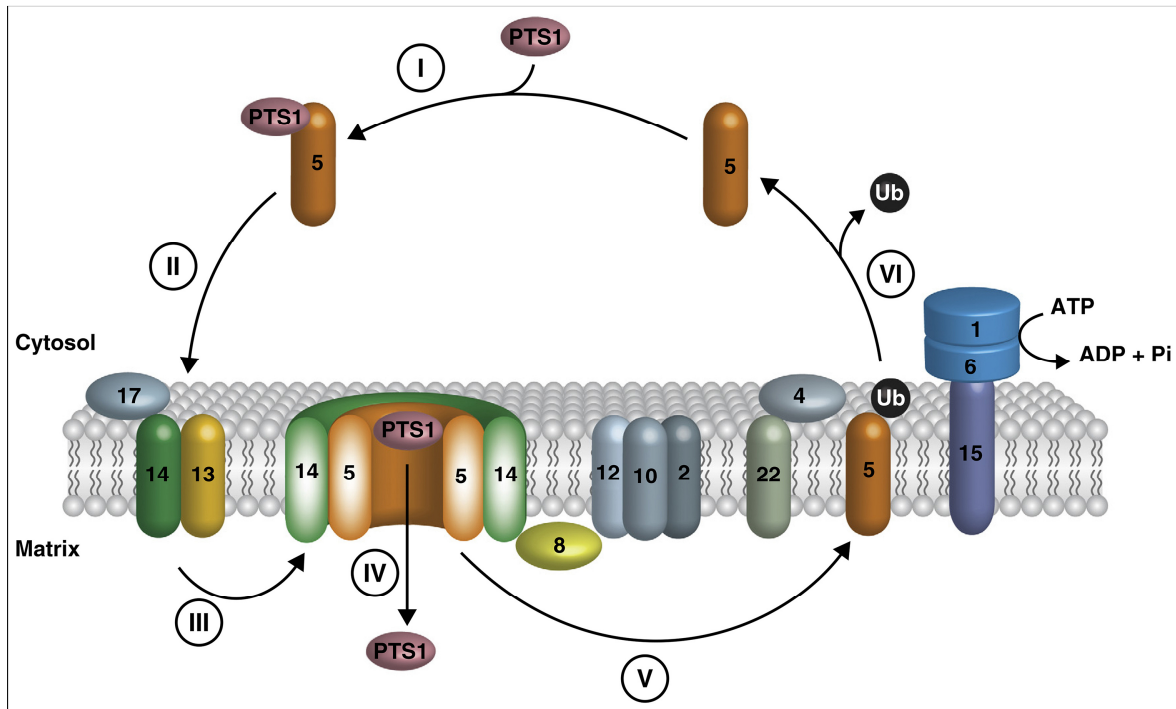
Figure 3: Peroxisomal matrix protein import
Model of peroxisomal matrix protein import in yeast. (**I**) Proteins harboring a peroxisomal targeting signal of type 1 (PTS1) are recognized by the import receptor Pex5 in the cytosol, (**II**) The cargo-loaded receptor is directed to the peroxisomal membrane and binds to the docking complex (Pex13p/Pex14p/Pex17p). (**III**) The import receptor assembles with Pex14p to form a transient pore and (**IV**) cargo proteins are transported into the peroxisomal matrix in an unknown manner. Cargo release might involve the function of Pex8p or Pex14p. (**V**) The import receptor is monoubiquitinated at a conserved cysteine by the E2-enzyme complex Pex22p/Pex4p in tandem with E3-ligases if the RING-complex (Pex2p, Pex10p, Pex12p). (**VI**) The ubiquitinated receptor is released from the peroxisomal membrane in an ATP-dependent manner by the AAA-peroxins Pex1p and Pex6p, which are anchored to the peroxisomal membrane *via* Pex15p. As the last step of the cycle, the ubiquitin moiety is removed and the receptor enters a new round of import. The designation is based on the yeast nomenclature, so note that Pex17p and Pex8p do not exist in mammals; moreover, the function of Pex22p/Pex4p is fulfilled by UbcH5a/b/c; and, in mammals, Pex26p anchors Pex6p at the membrane instead of Pex15p. From (75).

After cargo binding (Figure 3, I), the cargo-receptor complex docks at the peroxisomal membrane upon interaction with the resident docking complex, composed of the proteins Pex13p, Pex14p and additionally Pex17p in yeast (Figure 3, II) (91-94). In general, Pex14p is considered to be the initial binding partner for the cargo-bound PTS1-receptor. However, their exact roles are still matter of discussion (95). The current opinion for the mechanism on how cargo proteins enter the peroxisome is based in the concept of a transient pore that assembles at the peroxisomal membrane (Figure 3, III) and is disassembled after import, with its components being recycled for further rounds of protein import (96). Although the exact composition of this dynamic pore as well as the

driving force for cargo translocation (Figure 3, IV) remain elusive, it has been suggested that its major constituents are Pex14p and the PTS1-receptor Pex5p (96). Whether PTS1 and PTS2 proteins are imported via common or distinct pores in still a major question, as well as if the cargo-loaded receptor remains associated with the pore (shuttle hypothesis) or if it is released as a soluble receptor-cargo complex into the peroxisomal matrix (extended shuttle hypothesis) (75). The mechanism of how the cargo is released from the receptors isn't fully understood, but peroxins Pex14p (97) and Pex8p (98, 99) have been connected to this process. The signal sequence of a subset of the imported proteins is proteolytically removed after the import in peroxisomes of mammals and plants (100-102).

During or after dissociation of the cargo-receptor complex, the PTS1 receptor is mono-ubiquitinated at a conserved cysteine (Figure 3, V), which serves as a signal for ATP-dependent dislocation of the receptor from the membrane to the cytosol (103, 104). E2 ubiquitin-conjugating enzyme is required for this modification which, in mammals, is assisted by UbcH5a/b/c (105). Proper mono-ubiquitination of Pex5p also depends on the RING-finger proteins Pex2p, Pex10p and Pex12p which are protein-ubiquitin ligases (E3) (106, 107). Afterwards, extraction of ubiquitinated Pex5p (Figure 3, VI) is catalyzed by Pex1p and Pex6p, two members of the AAA-protein family (108, 109), which in mammals are anchored to the peroxisomal membrane by the tail anchored protein Pex26p (110, 111). Although the exact molecular mechanism for the exportation of ubiquitinated Pex5p to the cytosol is still unclear (112), the binding and hydrolysis of ATP by Pex1p and Pex6p is supposed to induce conformational changes that generate the force to pull the receptor out of the membrane (113, 114). Subsequent removal of the ubiquitin moiety (Figure 3, VI) is catalyzed by the ubiquitin hydrolase USP9X in mammals (115). Finally, Pex5p is once again available for promoting further cycles of protein transportation (Figure 3, VI).

1.2.2   Import of membrane proteins

The import of peroxisomal membrane proteins (PMPs) occurs independently of matrix import *via* a different set of import factors. The mechanistic details are not completely clarified so far, but three proteins, so-called early peroxins, were identified to be required for peroxisomal membrane assembly in several species, including humans: Pex3p, Pex16p and Pex19p (116-125). The loss of any of these proteins/genes leads to complete loss of peroxisomes, while defects in matrix protein import result in the formation of empty peroxisomal "ghosts" (118, 126, 127).

The model that better describes the peroxisomal biogenesis has been a subject for intense discussions as studies with conflicting results have been released (128). In 1985, Lazarow and Fujiki (72) suggested that peroxisomal matrix and membrane proteins were directly imported into peroxisomes from the cytosol, which led to the classical view that peroxisomes were autonomous organelles and the proposal of a "growth and division" model for peroxisome biogenesis. Accordingly, peroxisomes grow by import of newly synthesized proteins and are subsequently divided into daughter organelles (129). However, in 1960s, the ER was proposed to be the source of phospholipids for the peroxisomal membrane (130). Moreover, cell lines missing Pex3p, Pex16p and Pex19p that lack any detectable peroxisomal remnants are still able to restore *de novo* peroxisome formation upon reintroduction of the missing gene, involving ER. Therefore, an ER-dependent "*de novo* synthesis" model for peroxisomal biogenesis was suggested (119, 120, 131, 132). These two models were, for some time, apparently irreconcilable and both were questioned in terms of physiological importance under normal conditions as well as their applicability to evolutionary distant organisms, such as fungi, plants and mammals. Nevertheless, both models agreed that the Pex3p/Pex16p/Pex19p trio is fundamental to PMP import to peroxisomes and, consequently, peroxisome biogenesis (Figure 4, lower panel). Pex19p serves in all peroxisome-containing species as a soluble receptor for nascent PMPs by binding and targeting them to the peroxisomal membrane (128, 133). In the yeast *Saccharomyces cerevisiae*, Pex19p functions also in peroxisome inheritance (134). Pex3p is a conserved membrane-bound docking receptor for incoming complexes of Pex19p and its PMP cargo (135, 136). Pex3p serves also in the peroxisome

inheritance and degradation (137-139). Pex16p is an integral membrane-bound PMP receptor at the ER and peroxisomes (140-144) and is absent in all yeasts except *Yarrowia lipolytica* (Table 4). In that species Pex16p is a matrix-localized peripheral protein and seems to be involved in peroxisomal fission (145, 146).
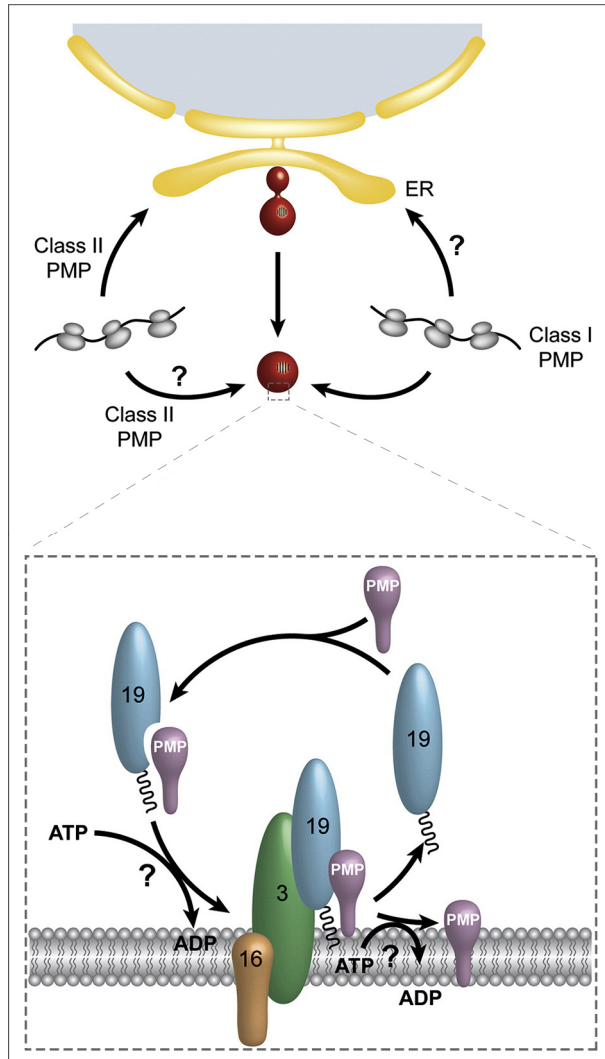
Figure 4: Peroxisomal membrane protein insertion

(upper panel) Topogenesis of peroxisomal membrane proteins. Two routes are proposed for the targeting of PMPs. Class I proteins are directly imported into existing peroxisomes. Class II proteins are first targeted to the ER, where they concentrate in pre-peroxisomal vesicles which then are targeted to existing peroxisomes or function as an origin for the *de novo* formation of peroxisomes.

(lower panel) Pex19p-dependent import of PMPs. Class I PMPs harbor a mPTS, which is recognized in the cytosol by the import receptor and/or PMP-specific chaperone Pex19p. Cargo-loaded Pex19p docks to the peroxisomal membrane via association with its docking factor Pex3p. Then the PMP is inserted into the membrane in an unknown manner but presumably with assistance of Pex19p, Pex3p and, in some organisms, Pex16p. Adapted from (147).

In latest years, several studies have been suggesting that (at least) some PMPs pass through the ER before being transported/routed to peroxisomes. Thus, until recently, two classes of PMPs[1] were distinguished based on their Pex19p dependence for targeting to peroxisomes (75, 128). Class I PMPs require Pex19p for post-translational transport, while class II PMPs are Pex19p-independent and traffic to peroxisomes via the ER (148, 149)

---

[1] Confusingly, class I and class II PMPs are also known as Group II and Group I PMPs, respectively.

(Figure 4, upper panel). Newly translated class I PMPs bind Pex19p, which has been shown to bind to a range of PMPs (150-153). Pex19p is a predominantly cytosolic protein thought to serve as a PMP chaperone, preventing aggregation and degradation of newly synthesized proteins (123, 149, 154, 155). A portion of Pex19p is also found in the peroxisome, which led to the notion that it acts as a shuttling receptor (123, 149, 151, 156), delivering PMPs to Pex3p which acts as a docking factor in the peroxisomal membrane (148). Although there is no easily recognizable consensus sequence that constitutes a targeting signal for PMPs (termed mPTS), several studies highlight the importance of a cluster of basic residues predicted to form an α-helix, adjacent to one or more transmembrane segments (157) and algorithms have been developed for the prediction of the mPTS (151, 158). Pex19p has also been characterized as both an insertion factor and assembly/disassembly factor at the peroxisomal membrane (152, 154, 159). The PMPs are inserted into the peroxisomal membrane by an unknown mechanism and Pex19p is recycled back to the cytosol (156).

Pex3p is the best-studied example of class II PMPs. Since its initial designation as a class II PMP and studies demonstrating its origin in the ER (140, 143, 149, 160-162), several peroxins, such as Pex2p, Pex10p, Pex11p, Pex13p, Pex15p, Pex16p, Pex26, Pex30p, Pex31p, Pex34p and Pex36p have been reported to traffic to peroxisomes via the ER in fungi, mammals and plants (133, 140-143, 163-166). However, discrepant data from the several studies may reflect differences in PMP biogenesis in different cell types and perhaps also differences in metabolic status and rates of PMP turnover (128). Pex3p in *Saccharomyces cerevisiae* has been shown to localize first in the ER and then in a subdomain of the ER before moving to peroxisomes. Pex19p is required for this process, justifying the absence of peroxisomes in *pex3* and *pex19* mutants. Noteworthy, this happens both in yeast lacking peroxisomes and in the wild-type yeast (160, 162). In a similar way, experiments with mammalian Pex16p demonstrated that this protein also traffics to peroxisomes in mammals via ER (140-143, 166) as is also required for *de novo* peroxisome synthesis (143), although a direct import route for Pex3p from the cytosol into the mammalian peroxisomes mediated by Pex19p and Pex16p has also been described (144, 167).

Recently, the segregation of PMPs in two classes has been challenged by the possibility of existence of a third class of PMPs, represented so far by Pex13p and Pex14, which sort to peroxisomes independently of Pex3p and Pex19p (75, 159, 167-169).

It is now generally accepted that peroxisomes can form from the ER, however, questions remain about the extent and timing of this process and its role within the lifecycle of a peroxisome (128). In 2007, Motley and Hettema (170) provided important evidences that the *de novo* pathway largely operates under conditions where cells have lost their peroxisomes and, under normal conditions, division predominates. However, a conflicting view is that most (if not all) PMPs are delivered first to the ER (171), but there are reports that components required for secretory vesicle formation aren't required for trafficking of PMPs (124, 172). The ability of so-called "pre-peroxisomal vesicles" to fuse in a Pex1p- and Pex6p-dependent manner has also been documented (173, 174) and provides a mechanism by which peroxisomes can be (re)formed. Actually, van der Zand et al. (174) demonstrated that the docking and the RING finger components of the translocon are kept physically separate until a late stage in biogenesis.

To sum up, at the present time, two models for peroxisome biogenesis and PMP trafficking are under debate. In their extreme forms, they appear mutually exclusive: either (i) most, if not all, PMPs enter the ER first (171), or (ii) only very specific so-called class II PMPs enter the ER and form ER-derived vesicles that bring lipids and a very limited complement of proteins to pre-existing peroxisomes which can then divide (Figure 4) (175). Consensually, Pex19p is important in both scenarios, but its role has been ascribed differently. In the latest years, new data over this issue has been produced and the view of *de novo* formation from the ER and division as segregated and independent mechanisms for peroxisome biogenesis has become out of date. Although many questions remain to be answered, more integrated and cooperative models have been proposed (75, 128, 167).

1.3   Peroxisome proliferation – growth and division

Regardless whether PMPs insert peroxisomes directly from cytosol or indirectly from the ER, peroxisomes are recognized to proliferate under a "growth and division" manner, in which spherical organelles form tubular structures that acquire a "beads-on-a-string"-like morphology prior to their fragmentation into smaller organelles (176-179). This sequence of events occurs in a multi-step fashion by the action of a set of evolutionarily conserved proteins throughout yeast, mammalian and plant systems (129). Initial elongation of the peroxisomal membrane is mediated by Pex11 proteins, and after subsequent constriction by a yet unidentified mechanism, final fission is carried out by dynamin-like GTPases (such as mammalian DLP1), mechano-enzymes that are recruited to the peroxisomal membrane by distinct adaptors (Fis1, Mff) (explored on section 1.3.2). Notably, these key components are shared with mitochondria (16).

In addition, peroxisomes may also interconnect to form tubulo-reticular networks and a variety of morphologically distinct types of peroxisomes has been observed in different organs of mammalian organisms and cell lines (176, 180-187). Besides growth and division, more complex structures such as elongated tubules or a peroxisomal reticulum may be related to other peroxisomal processes (e.g. in metabolism, membrane signaling or stress protection), but information on the exact correlation between peroxisome dynamics/morphology and function is still scarce.

1.3.1   The Pex11 family of proteins

The peroxin 11 (Pex11) family is comprised of conserved membrane proteins in fungi, plants and mammals that control peroxisome proliferation and regulate peroxisome morphology, size and number (188-195). However, not all Pex11 isoforms in a given species promote peroxisome proliferation or even membrane elongation pointing to distinct functions in peroxisome biogenesis. Accordingly, membrane association and topology may vary across organisms, ranging from a peripheral association in *Saccharomyces cerevisiae* to multi-membrane spanning proteins in plants and mammals (for detailed overview, see (129)). Furthermore, and besides their partial redundancy, not

all Pex11 proteins can complement each other (192). *Sc*Pex11p was the first protein discovered being involved in proliferation or division (188, 196). Meanwhile, a large number of Pex11 proteins, or proteins affecting peroxisome number, have been identified (Pex11-type peroxisome proliferators, reviewed in (197)). Every organism studied so far contain several Pex11 orthologues. The three mammalian Pex11 proteins are encoded by different genes and termed Pex11pα, Pex11pβ and Pex11pγ. Plants (*Arabidopsis thaliana*) possess five different Pex11 isoforms, *At*Pex11a to *At*Pex11e, while yeast (*Saccharomyces cerevisiae*), filamentous fungi (*Aspergillus nidulans*) and trypanosomes contain three Pex11 family proteins (Pex11p, Pex25p and Pex27p, or *Tb*Pex11, GIM5A and GIM5B, respectively) (overview in (129)). Besides some exceptions (e.g. *Sc*Pex25p and *Sc*Pex27p), Pex11 proteins have a molecular weight of 27-32 kDa and a length of roughly 230 to 260 amino acids. Different functions have been attributed to Pex11 proteins, such as playing a role in β-oxidation in *Saccharomyces cerevisiae* (198), organelle inheritance (199), membrane structure determination (200), or direct regulation of peroxisome size and number. Overexpression of Pex11p in *Penicillium chrysogenum* increases penicillin production (201). A common observation among all Pex11 proteins is that the modulation of its levels affects the number of peroxisomes (177, 188, 190, 196, 202). Generally, an increase of Pex11 levels induces peroxisome proliferation, while inhibition of its function reduces the peroxisome number or impairs peroxisome proliferation.

In mammals, the three Pex11p isoforms control peroxisome proliferation under both basal and induced conditions. However, different expression patterns were observed for all isoforms: while Pex11pβ is constitutively expressed in all tissues, both Pex11pα and Pex11pγ show tissue-specific expression, but are most prominent in the liver (15, 189, 203-208). Among the three isoforms, only Pex11pα is induced by peroxisome proliferators activating the nuclear transcription factor PPARα (207). Nonetheless, Pex11pα is dispensable for PPARα-mediated peroxisome proliferation in Pex11pα knockout (KO) mice suggesting functional redundancies (208). Although the Pex11pα KO mouse is viable, it shows reduced abundance of functional peroxisomes and aggravated renal interstitial lesions (209). Pex11pβ KO, however, causes neonatal lethality and defects similar to the Zellweger syndrome phenotype in mouse models (205), confirming

its role as the central regulator of peroxisome proliferation in mammals. As expected, peroxisome abundance in Pex11pβ KO mice is reduced, but peroxisomal protein import and metabolism are only slightly affected. A comparative analysis of primary neuronal cultures and brain samples from wild-type mice, Pex11pβ homozygous and heterozygous knockouts indicated a higher degree of cell death in heterozygous than in wild-type mice. Moreover, heterozygotes also showed delayed neuronal differentiation, indicating that deletion of a single allele of *PEX11B* already causes neuronal defects in mice (210). Curiously, the first *PEX11B* patient described has different phenotype, far less serious and life threatening, despite carrying a homozygous non-sense mutation, producing a truncated peptide with only 22 amino acids. With 26 years of age, the patient presented clinical symptoms atypical for peroxisome biogenesis disorders, like mild intellectual disability, migraine-like episodes, gastrointestinal problems and skin abnormalities. Patient's fibroblasts presented peroxisomes, enlarged and undivided though. Notwithstanding the abnormal peroxisome morphology, his biochemical parameters were within the normal range (48, 51). Very recently, seven additional patients have been identified with null mutation in the *PEX11B* gene (49). All patients presented with congenial cataracts and the older ones had mild intellectual disability, ataxia and sensorineural deafness. In addition, most of them presented with short stature and convultions. Biochemical parameters plasma and fibroblasts did not show clear peroxisomal abnormalities. However, analysis of patient skin fibroblasts often revealed enlarged and elongated peroxisomes indicative of a defect in peroxisome division and proliferation. This heterogeneity among mammal species indicates that functions of Pex11 proteins may vary considerably among evolutionarily close species and extrapolations concerning this issue must be made with extra precautions.

All mammalian Pex11 isoforms are tightly associated with the peroxisomal membrane and possess two predicted membrane spanning helices with both C- and N-termini protruding into the cytosol (177, 189, 203, 211). They are also capable of forming homo-dimers (193, 212, 213). Heterodimers were also observed, however, no interaction of Pex11pα and Pex11pβ was detected (193). Furthermore, it has been also demonstrated that Pex11pβ interacts with Fis1 (193, 213) and Mff (214, 215), tail anchor proteins

involved in the recruitment of DLP1 (section 1.3.2). Interestingly, besides Pex11pβ's capacity to promote peroxisome elongation upon expression, it was also observed to concentrate at constriction sites, indicating a non-uniform distribution of the protein at the peroxisomal membrane (177) (Figure 5). Pex11pβ initially localizes to spherical, pre-existing organelles where it initiates the formation of a nose-like protrusion at one side of the peroxisome (216). The protrusion extends to form a membrane tubule that acquires a specific set of PMPs, segments and becomes import-competent for peroxisomal matrix proteins prior to its final fission by the action of Fis1, Mff and DLP1 (Figure 5). Importantly, predominantly newly-synthesized matrix proteins are imported into the newly formed peroxisomes, pointing to an inherent mechanism of peroxisomal quality control linked to growth and division (216). Transient expression of various Pex11 family members of different origins led to the formation of similar membrane protrusions in mammalian cells which developed into large stacks of peroxisomal membranes (193). This pattern of Pex11p-dependent formation of specific membrane subdomains and its role in the induction of a differential distribution of PMPs was also detected in the yeast *Hansenula polymorpha* (217).

The membrane deforming capacities of the various Pex11 proteins were linked to the presence of several N-terminal motifs within Pex11p that are conserved in yeast, fungi and human proteins and display amphipathic properties (191). Negatively charged liposomes, resembling the phospholipid composition of peroxisomes, were shown to hyper-tubulate upon the addition of a Pex11 peptide containing the most conspicuous amphipathic helix of *Penicillium chrysogenum*. The conservation of the amphipathic properties and its helical structure is essential to mediate tubulation, an intrinsic property apparently conserved throughout species (191, 215). Thus, Pex11p-induced membrane remodeling is induced by the insertion of an amphipathic helix into one leaflet of the lipid bilayer which causes membrane asymmetry and bending (218) (Figure 5).

In regard to the regulation of Pex11p itself by post-translational modifications and/or other mechanisms, monomeric *Sc*Pex11p was suggested to be inactivated by homo-dimerization, hence dimerization was proposed to regulate membrane remodeling in a

redox-sensitive fashion (219). Furthermore, phosphorylation of *Sc*Pex11p at the S165/167 residue was shown to be required for Pex11p action (220).
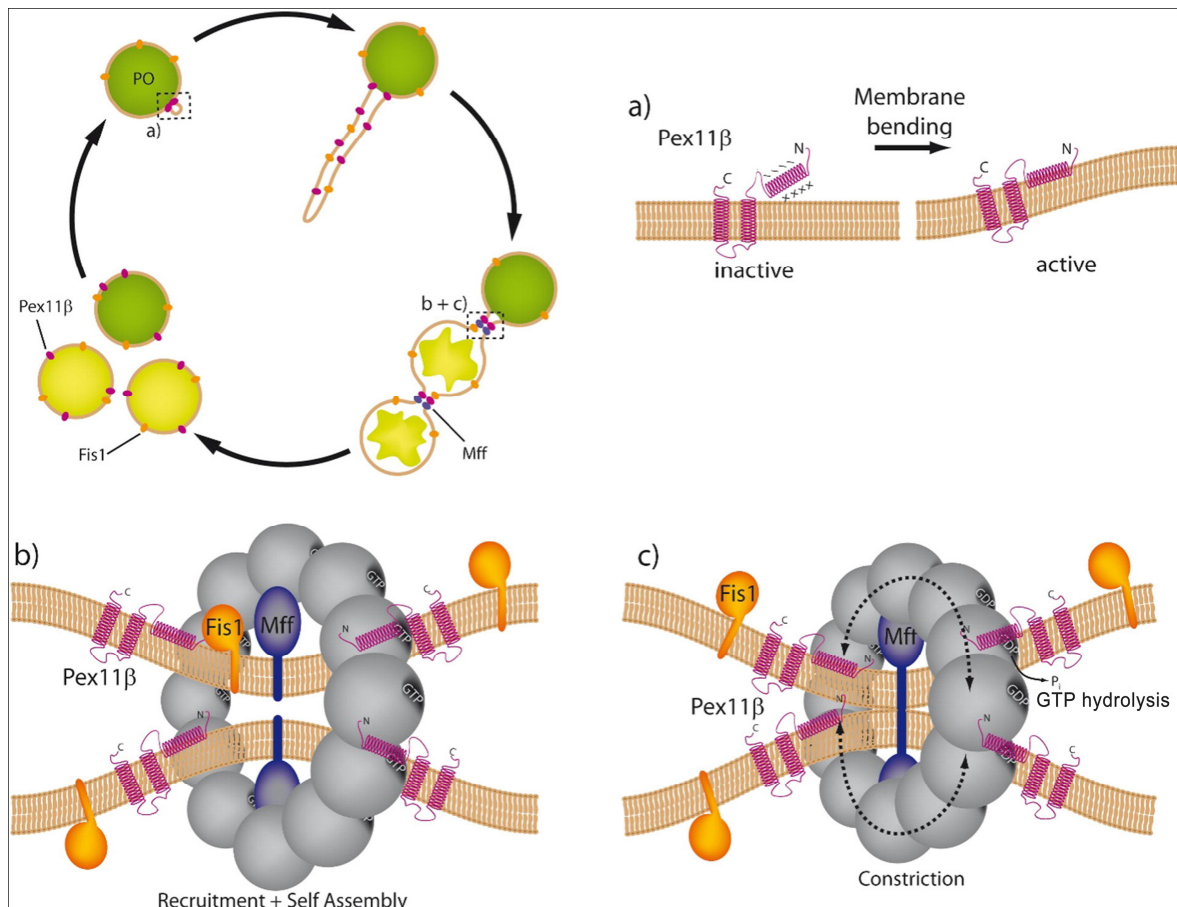
Figure 5: Model of peroxisomal growth and division in mammalian cells
Peroxisome proliferation in mammalian cells involves a well-defined sequence of morphological changes, including membrane elongation (growth), constriction, and final membrane scission. Pex11pβ initiates membrane remodeling and the formation of a tubular membrane extention at pre-existing peroxisomes. (a) Peroxisomal membrane remodeling *via* Pex11p in induced by the insertion of amphipathic, N-terminal helices into one leaflet of the lipid bilayer causing membrane asymmetry and bending (191, 221). Oligomerization is required for Pex11pβ function in membrane elongation and may as well stabilize membrane tubules. The growing membrane extention acquires a specific set of peroxisomal membrane proteins (e.g. Pex11pβ, Fis1), before it constricts and import of predominantly newly synthesized matrix proteins is initiated (216). Pex11pβ and the Mff-DLP1 complex concentrate at the sites of constriction, possibly driven by alterations in membrane curvature. The role of Fis1 is currently unclear. (b) Cytosolic DLP1 is recruited by the membrane receptor Mff. After targeting, DLP1 self-assembles into large ring-like structures. (c) Pex11pβ acts as a GTPase activating protein on DLP1 (222). GTP hydrolysis by DLP1 leads to constriction of the DLP1 ring and results in final membrane scission. From (223).

1.3.2 The fission machinery

Dynamin-like proteins (DLP or Drp, dynamin-related proteins) were the first components to be identified as key players in peroxisome fission (178, 212). Moreover, DLP1 was the

first indicated shared component of both peroxisome and mitochondrial fission (224, 225). DLPs belong to the dynamin family of large GTPases known to function in tubulation and fission events of cellular membranes. These cytosolic proteins are recruited to organelle membranes and assemble, probably as rings or spirals, in multimeric complexes around constricted parts of the organelle, where they induce GTP-dependent final membrane scission (178, 226, 227). Thus, dynamin proteins are supposed to act as pinchase-like mechano-enzymes. Classical dynamins have a size of approximately 100 kDa and possess five domains: GTPase domain, middle domain, Pleckstrin homology (PH) domain, GTPase effector domain, and proline-rich domain (PRD) (228-232). DLPs lack the SH3-binding PRD domain and the PH domain required for membrane association. The middle domain functions in the higher-order assembly, which is required for the formation of functional multimeric spirals (233, 234). Therefore, mutations in the DLP1 middle domain result in abnormal elongation of peroxisomes and hypertubulation of mitochondria (50, 235). These elongated peroxisomes still have a constricted morphology, indicating that DLP1 is required for final scission, but not for organelle constriction (179). Similar morphologies were observed in fibroblasts from a patient, leading to discovery of a new lethal disorder based on a mutation in *DLP1* (50). In mammals, overexpression of DLP1 does not induce organelle fragmentation, demonstrating that the division is regulated by other factors. Dynamin-like mechano-enzymes are also required for peroxisome fission in other species, such as Dnm1 (and Vps1) in yeast (170, 236, 237) and DRP3A, DRP3B and DRP5B in plants (192, 238, 239).

DLP1 action is extensively regulated by protein phosphorylation, sumoylation, ubiquitination and S-nitrosylation (240). Notably, starvation-induced phosphorylation of DLP1 by Protein Kinase A was demonstrated to decrease its recruitment to mitochondria thus resulting in the formation of elongated mitochondrial networks that resist autophagic degradation (241). Very recently, a study demonstrated that both yeast and mammalian DLP1 (Dnm1 and Drp1, respectively) need Pex11p/Pex11pβ for final peroxisome scission. Pex11p/Pex11pβ physically interacts with Dnm1/Drp1 and acts as GTPase-activating protein (GAP), identifying a previously unknown requirement of a GAP in DLP1 function (222) (Figure 6).
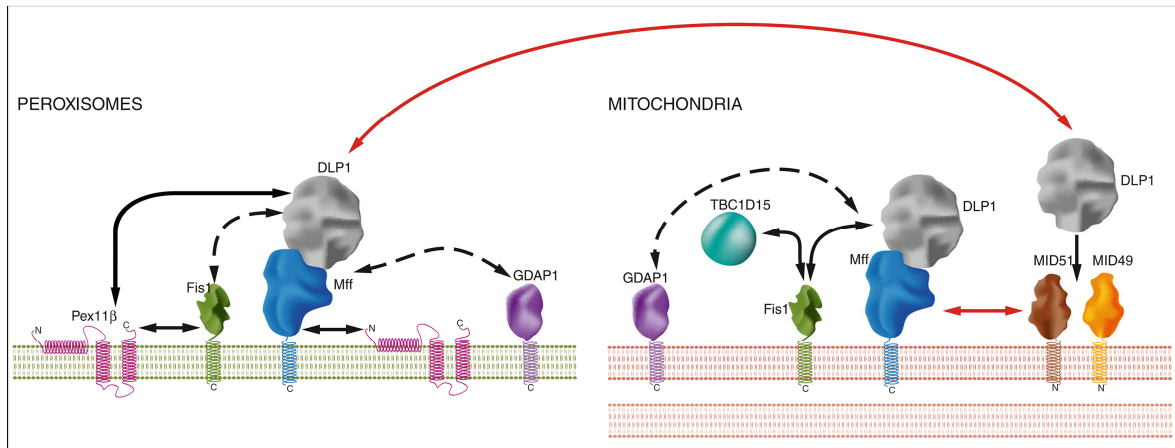
Figure 6: Key fission proteins on peroxisomes and mitochondria in mammals
Shared key components of the mitochondrial and peroxisomal fission machineries include DLP1, a large dynamin-like GTPase involved in final membrane scission of constricted membranes, and the DLP1-membrane adaptors Mff and Fis1. Mff is supposed to be the major DLP1 receptor for organelle fission. GDAP1 can regulate both mitochondrial and peroxisomal morphology and division in an Mff- and DLP1-dependent manner. The peroxin Pex11pβ is an exclusively peroxisomal membrane protein involved in the regulation of peroxisome abundance and in membrane deformation/elongation prior to fission. Pex11pβ can oligomerize and interacts with both Fis1 and Mff, which can homodimerize as well. Pex11pβ also interacts with DLP1 and acts as GTPase-activating protein. MiD51 and MiD49 are mitochondrial membrane adaptors which can sequester DLP1 and inhibit its function. This process may be regulated by mitochondrial Fis1, which interacts with TBC1D15, a Rab GTPase activating protein. Upregulation of MiD49 on mitochondria can deplete DLP1 from peroxisomes resulting in peroxisome elongation due to reduced division (red arrow). Adapted from (242).

The mechanistic basis of peroxisomal membrane constriction prior to fission remains to be elucidated. In *Yarrowia lipolytica*, intra-peroxisomal lipid remodeling, and thus membrane constriction, was linked to the AOX-dependent modulation of *Yl*Pex16p activity (146). In mammalian cells, the concerted action of non-muscle myosin A, Rho kinase II and the actin cytoskeleton was suggested to mediate membrane constriction (243).

As DLP1 lacks a PH domain for direct lipid binding, it is recruited to mitochondrial and peroxisomal membranes by membrane adaptor proteins. Initially, the tail-anchored protein Fission 1 (Fis1) was proposed to recruit DLP1 to mitochondria and peroxisomes, and thus mediate organelle division (213, 244, 245). The majority of Fis1 faces the cytosol (246) and TPR repeats in its N-terminus were suggested to facilitate protein-protein interactions (247, 248). Fis1 is targeted to peroxisomes in a Pex19p-dependent manner where it acts in complex with Pex11pβ (213, 215, 249) (Figure 6).

Another tail-anchored protein, the mitochondrial fission factor (Mff), was suggested to regulate fission of mitochondria and peroxisomes (250). Detailed analyses of Mff have revealed that it represents the major membrane receptor for DLP1, challenging the aforementioned role of Fis1 (214, 251) (Figure 6). Itoyama and colleagues (214) observed that overexpression of *MFF* increases the interaction between DLP1 and Pex11pβ, while knockdown of *MFF*, but not Fis1, abolishes that interaction. Thus, the function of Fis1 at mitochondria and peroxisomes has to be reconsidered. Interestingly, Mff was only identified in metazoans (250), thus the recruitment of the yeast DLP1 homologue Dnm1 to mitochondria and peroxisomes is still supposed to depend on the action of yeast Fis1. However, yeast Fis1 requires the additional action of the soluble molecular linkers Caf4 and Mdv1 (170, 252), two WD40 proteins that bind to yeast Dnm1 and well as Fis1. Additional factors involved in the recruitment and regulation of DLP1 action continue to emerge: MiD49 and MiD51, two novel N-terminally anchored mitochondrial membrane proteins, have been found to recruit DLP1, at least to mitochondria (253, 254) (Figure 6). Similarly to Mff, they are not found in yeast.

Recently, ganglioside-induced differentiation-associated protein 1 (GDAP1), a glutathione S-transferase, was found to localize to both peroxisomes and mitochondria and to influence their dynamics and division (255) (Figure 6). Mutations in GDAP1 have been associated with Charcot-Marie-Tooth disease, the most common inherited neuropathy (256, 257). Loss of GDAP1 function results in peroxisomal (and mitochondrial) elongation, which with respect to peroxisomes is less prominent than that observed after loss of DLP1 or Mff. On the other hand, overexpression of GDAP1 induces peroxisomal (and mitochondrial) division in an Mff- and DLP1-dependent manner. Whereas alterations in a hydrophobic domain of GDAP1 or at the C-terminal tail affect both peroxisomal and mitochondrial fission, N-terminal autosomal recessively inherited disease mutants are still able to promote peroxisome but not mitochondrial fission (255, 258).

Whereas key division components are shared by peroxisomes and mitochondria, the key proteins for mitochondrial fusion (e.g. the dynamin-related GTPases Mfn1, Mfn2 or OPA1) are not present on peroxisomes. In contrast to mitochondria, mature peroxisomes

have not been observed to fuse (259, 260). However, Bonekamp and colleagues (259) demonstrated that transient and long-term peroxisome-peroxisome contacts occur, although without exchange of matrix or membrane markers. These interactions may contribute to the equilibration of the peroxisomal compartment in mammalian cells (242).

1.4   Regulation of peroxisomal abundance

The capacity of peroxisomes to adapt their morphology and number upon exposure to external stimuli has been known for a long time already (261). Peroxisome response to peroxisome proliferators (PPs) and regenerating rat liver after partial hepatectomy are classical models of peroxisome proliferation in mammals (182, 262). Other peroxisome proliferation-inducing factors in mammals include high-fat diet (263), cold exposure (264) and hypolipidemic drugs as well as industrial compounds and environmental pollutants such as phthalates and plasticizers (265). The PP-induced peroxisome proliferation is commonly accompanied by an increase in both amount and activity of fatty-acid β-oxidation enzymes (8). However, it is important to note that different species respond with different intensities to PPs, e.g. a massive peroxisome proliferation upon treatment is observed in rodents, but not in humans. Similarly, prolonged PP exposure gives rise to hepatocellular tumors in rodents, but not in humans (129).

1.4.1   PPARs and expression of peroxisomal genes

Peroxisome proliferation in mammals is regulated by the activation of the peroxisome proliferator-activated receptor (PPAR)α *via* changing the expression of peroxisomal genes (266). Long-chain fatty acids are ligands for PPARα and thus transmit signals for the requirement of enhanced lipid catabolism (267). The other two PPAR subtypes, β/δ and γ, have partially overlapping substrate specificity but don't transmit the signals of classical PPs (268, 269). Notably, constitutive expression of peroxisomal genes is not dependent on PPARα (270). Along with fatty-acid β-oxidation enzymes, expression of genes involved in peroxisome proliferation, e.g. Pex11pα, is also enhanced by the activation of PPARα

(129). However, a potential functional compensation by the other Pex11 isoforms or by other, so far, unknown factors, is denounced by the *PEX11A* knockout mouse model which is capable to induce peroxisome proliferation upon treatment with PPARα-dependent PPs (208). Ligand binding induces conformational changes in PPARα that allows it to form heterodimers with retinoid X receptor (RXR)α, which are capable of recognizing PPARα-responsive elements (PPREs) (Figure 7). PPERs not only regulate all peroxisomal lipid β-oxidation enzymes, but also other proteins (271). PPARα is moderately expressed in human, but highly in rodents (272), in which PPARα-mediated peroxisome proliferation was linked to carcinogenesis in liver, pancreas and testis (273), which was linked to increased ROS damage (274). In addition, both primate PPERs and the corresponding DNA-binding domain of PPARα exhibit significant sequence differences, possibly leading to differential activation of PPAR-controlled genes. Thus, differences in the regulation of peroxisome proliferation appear to have developed through a species-specific co-evolution of PPARα and the respective DNA-binding site elements. Perhaps this allowed the adaptation to different physiological needs (129). Other pathways for peroxisome proliferation involving PPARγ and β/δ, and even in PPAR-independent way, have been found and shown to have relevant roles as well (129).
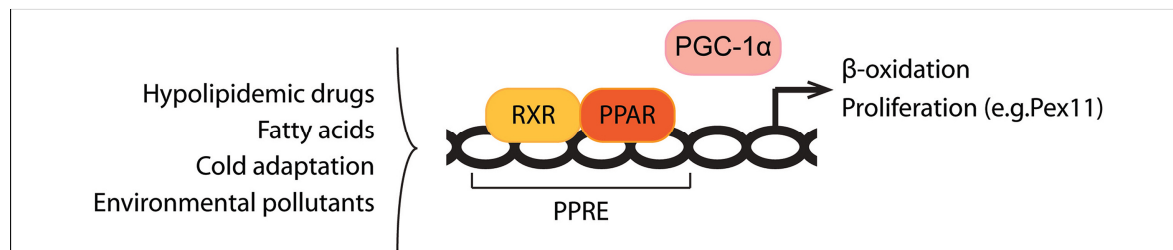
Figure 7: Activation of peroxisome proliferation in mammals
In most organisms, peroxisome proliferation is preceded by the induction of genes associated with fatty acid β-oxidation and membrane elongation (e.g. Pex11). Activation of these pathways depends on several environmental and developmental conditions. In mammals, PPARα and RXR coordinately bind to PPRE to upregulate gene expression. Other mechanisms independent of PPARα have also been described (e.g. PGC1α-dependent) (275). Adapted from (276).

1.4.2 Protein phosphorylation in peroxisomes

Beyond the regulation of the expression of peroxisomal genes, peroxisome proliferation and/or activity may be regulated by mechanisms of signal transduction, by which

information is spread out through the cell. Much of the molecules that transmit the information are molecular switches, i.e. proteins that switch from an inactive to an active state and vice-versa in response to signals. The largest class of molecular switches that occur in cells consists of proteins that are activated or inactivated by phosphorylation (277). In those cases, the switch is turned into one direction by a protein kinase, which covalently adds one or more phosphate groups to specific amino acids and into the other direction by a protein phosphatase, which removes the phosphate groups (Figure 8). The human genome encodes about 520 protein kinases and about 150 protein phosphatases. Each protein kinase is responsible for phosphorylating a protein or a set of proteins. On the other hand, some protein phosphatases are specific for only one or a few proteins, whereas others act on a broad range of proteins and are targeted to specific substrates by regulatory subunits (278). The activity of any protein regulated by phosphorylation depends on the balance between the activities of the kinases and phosphatases that phosphorylate and dephosphorylate it, respectively. There are two main types of protein kinases and phosphatases, distinguished by the specific target amino acids: serine/threonine (Ser/Thr) and tyrosine (Tyr) (279).
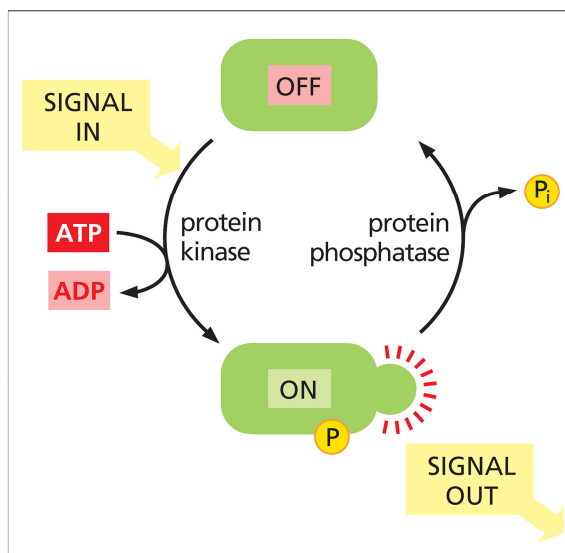
Figure 8: Phosphoproteins that act as molecular switches
A protein kinase covalently adds a phosphate from ATP to the signaling protein, and a protein phosphatase removes the phosphate. Although not shown, many signaling proteins are activated by dephosphorylation rather than by phosphorylation. Adapted from (279).

A recent meta-analysis on *Arabidopsis thaliana*'s phospho-proteome driven by van Wijk and colleagues (280), revealed that only 1% of the cell's phosphorylated proteins are localized to peroxisomes, with an enrichment in tyrosine-phosphorylated proteins, when

compared to other subcellular localizations. Despite this, and although the scarce data concerning localization of protein kinases or phosphatases to peroxisomes, phosphorylation seems to be an important mechanism for the regulation of peroxisome metabolism and biogenesis. Concerning metabolism, fatty-acid transport to peroxisomes was found to be regulated by phosphorylation in tyrosine residues of PMP70 and ALDP (281). Tanaka and colleagues (282) recently found that ScHrr25, a multifunctional serine/threonine kinase, phosphorylates Atg36, which recognizes superfluous peroxisomes and initiates pexophagy. Phosphorylation is also a regulation mechanism for Pex14p (283) and Pex15p (284), peroxisomal membrane proteins involved in matrix protein import (section 1.2.1). Peroxisome fission may also be regulated by phosphorylation: DLP1, a shared component of the mitochondrial and peroxisomal fission machinery (section 1.3.2), is phosphorylated by several kinases with consequences on mitochondrial morphology (285, 286) and implications on health (287-289). Moreover, Pex11 family proteins have been shown to be phosphorylated in *Saccharomyces cerevisiae* (220) and in *Pichia pastoris* (290), influencing peroxisome morphology and abundance. Thus, the study of the effect of phosphorylation in human Pex11p reveals to be crucial to understand its mechanism of action and consequent regulation of peroxisome biogenesis.

1.4.2.1 *Protein kinases and phosphatases in peroxisomes*

As previously mentioned, there aren't many studies localizing protein kinases or phosphatases to peroxisomes and most of them are predictions based on bioinformatics and/or mass spectrometry data (291-293). However, some proteins known to interact with kinases and phosphatases where reported to localize to peroxisomes. Akap11 (A-kinase anchor protein 11) of *Rattus norvegicus*, which possesses a PTS1 signal, was localized in testicular peroxisomes (294) and it is known to bind to the type II regulatory subunits of cAMP-dependent protein kinase (PKA), to glycogen synthase kinase-3 (GSK3) β, as well as to protein phosphatase 1 (PP1) catalytic subunit (295, 296). Human Limkain-B1, a protein involved in the female meiosis and predicted to bind RNA (297), was found

to localize in a subset of peroxisomes (298) and a fragment of it was demonstrated to interact with PP1α (299). Although unpublished, Limkain-B1 was originally annotated as Lim-kinase 2 interactor (accession number AB012134). Matre and colleagues (300) have shown that, in *Arabidopsis thaliana*, the regulatory subunit B'θ of protein phosphatase 2A (PP2A), a Ser/Thr-specific phosphatase, is targeted to peroxisomes via a PTS1 signal. Indeed, *At*PP2A targeting to peroxisomes was very recently confirmed by the same research group (301). Catalytic and scaffolding subunits of *At*PP2A appear to be imported into peroxisomes by piggyback transport dependent on B'θ regulatory subunit. The presence of a full *At*PP2A complex positively affects β-oxidation of fatty acids (301). In a subsequent report, Kataya and colleagues (302) identified another phosphatase that is targeted to peroxisomes in *Arabidopsis thaliana*. In this case, they found that MAP kinase phosphatase 1 (MKP1), a regulator for mitogen-activated protein kinases (MAPKs), possesses a non-canonical PTS1, which leads MKP1 to peroxisomes under stressful conditions. Interestingly, MAPK signaling is involved in the upregulation of catalase transcription and activity in salt-stressed *Arabidopsis thaliana* (303). Calcium-dependent protein kinase 1 (CPK1) was also found to localize in peroxisomes (304, 305). As in the previous cases, these studies on CPK1 were conducted in *Arabidopsis thaliana* as well.

Aside Akap11 (294) and Limkain-b1 (298), there are no other evidences for the presence of protein kinases/phosphatases or its regulators at mammalian peroxisomes. However, the importance of studying protein phosphorylation events in the regulation of peroxisome abundance became evident with the study of Saleem and colleagues (306) on the phosphoproteome of *Saccharomyces cerevisiae*. In this study, phosphorylated forms of several signaling proteins involved in fatty acid-induced peroxisome proliferation where identified to increase in oleic acid-treated cells, as well as in glucose-treated (peroxisome proliferation-repressing) cells. The amount of the phosphorylated forms of some signaling molecules involved in peroxisome morphology also varied between treatments. Thus, protein phosphorylation seems to be a relevant mechanism of signal transduction on the regulation of peroxisome abundance/proliferation.

Another evidence of a possible role of protein kinases/phosphatases in peroxisomes was the discovery of the early peroxin Pex16p in a human PP1 interactome study realized by Esteves and colleagues (307), at the time members of the Signal Transduction Laboratory of the Centre for Cell Biology, University of Aveiro. This finding defines Pex16p as a putative PP1-interacting protein, making this possible interaction of crucial importance for the regulation of peroxisome biogenesis, since as Pex16p is an "early peroxin" which is pointed to act as a PMP receptor during the early stages of the *de novo* peroxisome formation at the ER, as well as in mature peroxisomes (140, 141, 143, 144).

1.4.2.1.1 PP1 and PP1-binding motifs

As mentioned before (section 1.4.2), there are more than 500 putative protein kinases in the human genome, being the great majority of these Ser/Thr-kinases (278, 308, 309). On the other hand, the number of putative protein phosphatases is much less, with a twist on the target amino acids: the majority of protein phosphatases dephosphorylate tyrosine residues. Serine and threonine residues are dephosphorylated by only about 40 protein phosphatases (310-312). Whereas the numbers of protein Tyr-kinases and Tyr-phosphatases are well balanced, intriguingly, the number of protein Ser/Thr-kinases (PSKs) is about ten times higher than Ser/Thr-phosphatases (PSPs). The mechanism on how these few PSPs manage to reverse the actions of that large number of PSKs in a specific and regulated manner bases on the ability of PSPs to form stable protein-protein complexes. This property results in the accumulation of an abundant number of phosphatase holoenzymes, each with its own substrate and mode of regulation (313). This concept has been well illustrated for protein phosphatases -1 (PP1) and -2A (PP2A), which belong to the phosphoprotein phosphatase (PPP) superfamily of PSPs, and together account for more than 90% of the protein phosphatase activity in eukaryotes (278). PP1 is one of the most conserved eukaryotic proteins, being over 70% similar with early-branching eukaryotes. Its function is highly conserved as well (312). Janssens and colleague's (314) data suggest that mammals may contain as many as 650 distinct PP1 complexes and approximately 70 PP2A holoenzymes, indicating that PP1 catalyzes the

majority of protein dephosphorylation events in eukaryotic cells (278). CBC's Signal Transduction Laboratory has published several interactome studies of PP1 in human brain and testis which may significantly increase the number of confirmed PP1 complexes (307, 315, 316).

Unlike many protein kinases, PP1 does not recognize a consensus sequence surrounding the phosphorylated residue. Instead, efficient substrate binding depends on docking motifs for PP1 surface grooves that are remote from the active site. Under controlled buffer conditions, the free PP1 catalytic subunit has exceptionally broad substrate specificity (278). However, each functional PP1 complex is thought to have a stringent substrate specificity, each triggering a specific cellular pathway response (310, 312, 317, 318). The PP1 holoenzyme consists of a catalytic subunit (PP1c) and regulatory subunits (PP1 interacting proteins – PIPs). Mammalian genomes contain three PP1 encoding genes that together encode four distinct catalytic subunits: PP1α (gene *PPP1CA*), PP1β/δ (gene *PPP1CB*) and the *PPP1CC* gene splice variants PP1γ1 and PP1γ2, which differ mainly in their extremities (312, 319, 320). The approximately 90% amino acid sequence similarity between all forms of PP1c denotes a remarkable degree of evolutionary conservation, which is related to their essential role in the regulation of fundamental cellular processes (317, 319, 321). With the exception of the testis-enriched PP1γ2, all three mammalian isoforms are ubiquitously expressed (312, 322).

PIPs can function as modulators of PP1 activity, determining targets and substrate specificity, as well as subcellular localization of the holoenzyme or may even serve as substrate themselves (319). PP1 has diverse effects on substrate PIPs, activating or deactivating them by dephosphorylation, and some of these function as PP1 activity regulators themselves (278). Most PIPs contain a primary PP1-docking motif, commonly referred to as the RVxF motif, that binds, with high affinity, to hydrophobic amino acids on the surface of PP1, typically remote from the catalytic site (323, 324). Several studies permitted further characterization of the consensus sequence, and the RVxF motif was redefined. Other PP1-binding motifs (PP1BMs) have been described, and these strengthen the interaction of the PIPs with PP1, e.g. SILK motif (see Table 5).

Table 5: PP1-binding motifs

Motif		Consensus sequence	Reference(s)
RVxF motifs		[RK]-X(0,1)-[VI]-{P}-[FW]	(325)
		[HKR]-[ACHKMNQRSTV]-V-[CHKNQRST]-[FW]	(326)
		[KRL]-[KRSTAMVHNQ]-[VI]-{FIMYDP}-[FW]	(299)
RVxF-supporting motifs	SILK	[GS]-I-L-[RK]	(299, 325, 327-329)
	MyPhoNE	F-X-X-[RK]-X-[RK]	(299, 330)
	Apoptotic signature	R-X-X-Q-[VIL]-[KR]-X-[YW]	(331, 332)
	RARA	R-A-R-A	(333)
Other degenerated motifs		R-[KR]-X-H-Y	(329, 334, 335)
		K-S-Q-K-W	(329)
		R-N-Y-F	(336)

"X" is any amino acid; "X(0,1)" is any amino acid, present or absent; "[]" is one of those amino acids; "{}" is any amino acid except those.

Pex16p was detected in a yeast two-hybrid (YTH) study of PP1γ using a human brain cDNA library and two RVxF motifs were found on its sequence (307). Despite being also present in the brain (322, 337), the PP1γ2 isoform is particularly enriched in the testis and sperm (315). Interestingly, Akap11 was found in testicular peroxisomes of *Rattus norvegicus* which, as mentioned before, is a binding partner for PKA and PP1 (294, 295). Within testis, peroxisomes are present in Leydig, Sertoli and germ cells and residual bodies (338-342). Although the exact physiological role of peroxisomes in testis is still enigmatic, their metabolic pathways have to be of vital importance for normal spermiogenesis since adult X-ALD patients show impaired spermiogenesis and infertility (343).

2   Objectives

Peroxisomes are ubiquitous organelles that catalyze numerous metabolic processes. The crucial role of peroxisomes for human health is exemplified by the severe phenotype of peroxisomal disorders. Some are known to derive from mutations of peroxins, genes involved in the dynamic processes of peroxisome biogenesis and proliferation. Nonetheless, these mechanisms are far from being fully understood. A multitude of external stimuli was identified to induce peroxisome proliferation; however, there is only limited knowledge on their intracellular signal transduction at the peroxisomal level. Being protein phosphorylation/dephosphorylation a major intracellular signal transduction mechanism, with PP1 as the protagonist on the majority of dephosphorylation events in eukaryotic cells, our study focused on the putative role of PP1 and phosphorylation post-translational modifications in the regulation of peroxisomal biogenesis and proliferation.

The very first aim of this study was to find potential PP1-binding partners in peroxisomes by a screening for PP1-binding motifs among peroxins. Pex16p revealed to have several putative PP1-binding motifs and it was identified in a yeast two-hybrid screen on PP1. In addition, Pex16p is an early peroxin which function in peroxisome biogenesis is still not fully clear. So that Pex16p was selected to proceed our studies on the potencial role for PP1 in peroxisomes. On the other hand, Pex11 proteins, fundamental for peroxisome elongation and fission, had previously been suggested to be regulated by phosphorylation events in fungal cells. Being so, we selected also Pex11pβ to study the effect of phosphorylation in peroxisome proliferation. The specific aims of our study were the following:

I.   PP1-binding motifs search in human peroxins and other players in matrix protein import and fission machineries

    a.   Study of the role of PP1 on peroxisome biogenesis *via* the putative interaction with Pex16p

        i.   Verification of the putative PP1-Pex16p interaction

        ii.   Manipulation of the putative PP1-Pex16p interaction

II.   Study the mechanisms of action and regulation of Pex11pβ

a) Study the function of two potentially phosphorylated residues

b) Determination of Pex11pβ topology

c) Investigation of putative functional domains/residues

    i. Glycine-rich region

    ii. Amphipathic helices

    iii. Key cysteines

3   Material and methods

3.1   Chemicals and reagents

3.1.1   Chemicals

Chemicals (analytical or molecular biology grade) and cell culture reagents were obtained from commercial suppliers (Amersham Biosciences, Bayer, Bio-Rad, Bioron, Clontech, Fisher, Formedium, GE Healthcare, Merck, Polysciences, Roth, Sanol-Schwarz and Sigma). Low fat powder milk, from Nestlé, was obtained in the supermarket.

3.1.2   Loading dyes and markers

Table 6: Commercial loading dyes and markers

Product	Company
6x Orange Loading Dye	Fermentas
O'Gene Ruler DNA Ladder Mix	Fermentas
Precision Plus Protein Standards	BioRad

3.1.3   Kits

Table 7: Kits

Product	Company
Illustra Plasmid Prep Mini Spin Kit	GE Healthcare
NucleoSpin Plasmid	Macherey-Nagel
NucleoBond Xtra Midi	Macherey-Nagel
NucleoSpin Gel and PCR Clean-up	Macherey-Nagel
Quant-iT dsDNA BR Assay Kit	Invitrogen/Molecular Probes
TNT T7 Quick Coupled Transcription/Translation System	Promega

3.2 Immunological reagents

Table 8: Primary antibodies

Antigen	Technique	Dilution	Dilution buffer	Raised in	Source
ACOX	IF	1:200	PBS	Rabbit (pc)	A. Völkl, University of Heidelberg, Germany
GFP (tag)	IF WB	1:200 1:2000	PBS, PBS	Rabbit (pc)	Invitrogen
GST (tag)	WB	1:1000	3% milk in TBS-T	Goat (pc)	Amersham Pharmacia Biotech
Myc 9E10 (tag)	IF WB IP	1:200 1:2000 1:200	PBS, PBS	Mouse (mc)	Santa Cruz
Pex11pβ	IF	1:200	PBS	Rabbit (pc)	Abcam
Pex14p	IF	1:1400	PBS	Rabbit (pc)	D. Crane, Griffith University, Brisbane, Australia
PMP70	IF	1:100	PBS	Rabbit (pc)	A. Völkl, University of Heidelberg, Germany
His (tag)	WB	1:1000	3% milk in PBS	Mouse (mc)	E. da Cruz e Silva, CBC, Aveiro, Portugal
PP1γ	IF WB	1:1000 1:5000	PBS, 3% milk in PBS (or TBS-T)	Rabbit (pc)	E. da Cruz e Silva, CBC, Aveiro, Portugal
PP1α	IF	1:500	PBS	Rabbit (pc)	E. da Cruz e Silva, CBC, Aveiro, Portugal

ACOX, Acyl-CoA oxidase 1; GFP, green fluorescent protein; IF, immunofluorescence; IP, immunoprecipitation; mc, monoclonal; pc, polyclonal; WB: Western blot.

Table 9: Secondary antibodies

Antigen	Technique	Dilution	Dilution buffer	Raised in	Source
Alexa-488 conjugated Mouse IgG	IF	1:400	PBS	Donkey	Invitrogen
Alexa-488 conjugated Rabbit IgG	IF	1:500	PBS	Donkey	Molecular Probes
HRP conjugated Mouse IgG	WB	1:5000	PBS	Goat	BioRad
HRP conjugated Rabbit IgG	WB	1:5000	PBS	Goat	BioRad
HRP conjugated Rabbit IgG	WB	1:5000	PBS	Donkey	GE Healthcare
TRITC conjugated Mouse IgG	IF	1:100	PBS	Donkey	Jackson ImmunoResearch
TRITC conjugated Rabbit IgG	IF	1:200	PBS	Donkey	Jackson ImmunoResearch

HRP, horseradish peroxidase; IgG, immunoglobulin G; TRITC, tetramethylrhodamine isothiocyanate.

3.3 Molecular biology reagents

3.3.1 Plasmids

Table 10: Commercial vectors and plasmids received as a gift

Plasmid	Expressed protein	Source/Company
pACT2	GAL4AD	Clontech
pAS2-1	GAL4BD	Clontech
pAS2-1-Clone 18	GAL4BD-Pex16p (not full length), retrieved from and YTH screen	E. da Cruz e Silva, CBC, Aveiro, Portugal
pAS2-1-PP1γ1	GAL4BD-PP1γ1	E. da Cruz e Silva, CBC, Aveiro, Portugal
pcDNA3	(empty vector)	Invitrogen
pcDNA3.1-Myc-Pex16	Myc-Pex16p	G. Dodt, University of Tübingen, Germany
pcDNA3.1-PP1γ1	PP1γ1	M. Fardilha, CBC, Aveiro
pCMV-tag3A-ACBD5.2	Myc-ACBD5.2	M. Islinger, University of Heidelberg, Germany
pCMV-tag5A	(Myc tag adding empty vector)	Stratagene
pET28b	(His and T7 tags adding empty vector)	Novagen
pGEX-5X-1-Pex16	GST-Pex16p	J. Azevedo, IBMC, Porto, Portugal
pTD1-1	GAL4AD-SV40 large T antigen (aa87-708)	Clontech
pVA3-1	GAL4BD-p53 (aa72-390, murine)	Clontech

GAL4AD, GAL4 activation domain; GAL4BD, GAL4 DNA binding domain.

Table 11: List of plasmid constructs already present in the laboratory

Plasmid (vector+insert)	Expressed protein	Reference
pcDNA3-Pex11β-Myc	Pex11pβ-Myc	Schrader et al, 1998
pCMV-tag3A-Pex11β	Myc-Pex11pβ	Delille et al, 2010
pmEYFP-C1-Pex11β	YFP-Pex11pβ	Delille et al, 2010
pmEYFP-N1-Pex11β	Pex11pβ-EYFP	Delille et al, 2010

Table 12: List of plasmids constructed for this study

Plasmid (vector-insert)	Expressed protein	Construction		
		Template	Primers	Enzymes
pACT2-Pex16 C-ter	GAL4AD-Pex16p aa244-336	pcDNA3.1-Myc-Pex16	P16-244-249X Pex16-X-RV	XmaI XhoI
pACT2-Pex16 WT	GAL4AD-Pex16p	pcDNA3.1-Myc-Pex16	Pex16-XmaI-FW Pex16-X-RV	XmaI XhoI
pACT2-Pex16-PP1BM1	GAL4AD-Pex16p^{PP1BM1} (R298A_F301A)	pcDNA3.1-Myc-Pex16	Pex16PP1BM1FW Pex16PP1BM1RV Pex16-XmaI-FW Pex16-X-RV	XmaI XhoI
pACT2-Pex16-PP1BM1&2	GAL4AD-Pex16p$^{PP1BM1\&2}$ (R298A_F301A_K329A _F332A)	pcDNA3.1-Myc-Pex16	Pex16PP1BM1FW Pex16PP1BM1RV Pex16PP1BM2FW Pex16PP1BM2RV Pex16-XmaI-FW Pex16-X-RV	XmaI XhoI
pACT2-Pex16-PP1BM2	GAL4AD-Pex16p^{PP1BM2} (K329A_F332A)	pcDNA3.1-Myc-Pex16	Pex16PP1BM2FW Pex16PP1BM2RV Pex16-XmaI-FW Pex16-X-RV	XmaI XhoI
pcDNA3-Pex11b-C18S-C25S-C85S-Myc	Pex11pβ$^{C18S\_C25S\_C85S}$-Myc	pcDNA3-Pex11b-C18S-C25S-Myc	Pex11C85Sfw Pex11C85Srv	KpnI XbaI
pcDNA3-Pex11b-C18S-C25S-Myc	Pex11pβ$^{C18S\_C25S}$-Myc	pcDNA3-Pex11b-C18S-Myc	Pex11C25Sfw Pex11C25Srv	KpnI XbaI
pcDNA3-Pex11b-C18S-Myc	Pex11pβ^{C18S}-Myc	pcDNA3-Pex11β-Myc	Pex11C18Sfw Pex11C18Srv	KpnI XbaI
pcDNA3-Pex11b-C25S-Myc	Pex11pβ^{C25S}-Myc	pcDNA3-Pex11β-Myc	Pex11C25Sfw Pex11C25Srv	KpnI XbaI
pcDNA3-Pex11b-C85S-Myc	Pex11pβ^{C85S}-Myc	pcDNA3-Pex11β-Myc	Pex11C85Sfw Pex11C85Srv	KpnI XbaI
pcDNA3-Pex11β-S11A-Myc	Pex11pβ^{S11A}-Myc	YFP-Pex11β	Pex11bS11Afw Pex11bS11Arv Pex11bKpnI-F Px11bnoStopDown	KpnI BamHI
pcDNA3-Pex11β-S11D-Myc	Pex11pβ^{S11D}-Myc	YFP-Pex11β	Pex11bS11Dfw Pex11bS11Drv Pex11bKpnI-F Px11bnoStopDown	KpnI BamHI
pcDNA3-Pex11β-S38A-Myc	Pex11pβ^{S38A}-Myc	YFP-Pex11β	Pex11bS38Afw Pex11bS38Arv Pex11bKpnI-F Px11bnoStopDown	KpnI BamHI
pcDNA3-Pex11β-S38D-Myc	Pex11pβ^{S38D}-Myc	YFP-Pex11β	Pex11bS38Dfw Pex11bS38Drv Pex11bKpnI-F Px11bnoStopDown	KpnI BamHI
pcDNA3-Pex11βΔN40-Myc	Pex11pβΔN40-Myc	pcDNA3-Pex11β-Myc	Px11b-dN40-Up MycStopXbaI-Down	KpnI XbaI
pcDNA3-Pex11βΔN60-Myc	Pex11pβΔN60-Myc	pcDNA3-Pex11β-Myc	Px11b-dN60-Up MycStopXbaI-Down	KpnI XbaI
pcDNA3-Pex11βΔN70-	Pex11pβΔN70-Myc	pcDNA3-Pex11β-Myc	Px11b-dN70-Up	KpnI

Plasmid (vector-insert)	Expressed protein	Construction		
		Template	Primers	Enzymes
Myc			MycStopXbaI-Down	XbaI
pCMV-tag3A-Pex11β-ACBD5	Myc-Pex11pβ-ACBD5	pcDNA3-Pex11β-Myc and pCMV-tag3A-ACBD5.2	Pex11βup P11b_ACBD5rv P11b_ACBD5fw ACBD5_Eco_rv	BamHI EcoRI
pCMV-tag3A-Pex11βΔGly	Myc-Pex11pβΔGly	pcDNA3-Pex11β-Myc	Pex11βup Px11b-dGly-Left Px11b-dGly-Right Pex11β-wt-down	BamHI EcoRI
pCMV-tag3A-Pex16 WT	Myc-Pex16p	pcDNA3.1-Myc-Pex16	Pex16-H2-FW Pex16-X-RV	HindIII XhoI
pCMV-tag3A-Pex16-PP1BM1	Myc-Pex16p^{PP1BM1} (R298A_F301A)	pcDNA3.1-Myc-Pex16	Pex16PP1BM1FW Pex16PP1BM1RV Pex16-H2-FW Pex16-X-RV	HindIII XhoI
pCMV-tag3A-Pex16-PP1BM1&2	Myc-Pex16p$^{PP1BM1\&2}$ (R298A_F301A_K329A_F332A)	pcDNA3.1-Myc-Pex16	Pex16PP1BM1FW Pex16PP1BM1RV Pex16PP1BM2FW Pex16PP1BM2RV Pex16-H2-FW Pex16-X-RV	HindIII XhoI
pCMV-tag3A-Pex16-PP1BM2	Myc-Pex16p^{PP1BM2} (K329A_F332A)	pcDNA3.1-Myc-Pex16	Pex16PP1BM2FW Pex16PP1BM2RV Pex16-H2-FW Pex16-X-RV	HindIII XhoI
pEGFP-C1-Pex16	GFP-Pex16p	pcDNA3.1-Myc-Pex16	Pex16-X-Fw Pex16-E-Rv	XhoI EcoRI
pET28b-Pex16	His-Pex16p*	pcDNA3.1-Myc-Pex16	Pex16-H-FW Pex16-X-RV	HindIII XhoI
pET28b-Pex16 C-ter	His-Pex16p^{CT}* (aa244-336)	Cut from pGEX-4T-3-Pex16 aa244-336	-	EcoRI XhoI
pEYFP-C1-Pex11β Myc(mid)	YFP-Pex11pβ-Myc(mid)	pcDNA3-Pex11β-Myc	Pex11beta C up Px11b1-8mycR Px11b2-10mycF Pex11beta C down	EcoRI BamHI
pGEX-4T-3-Pex16 C-ter	GST-Pex16p^{CT} (aa244-336)	pcDNA3.1-Myc-Pex16	P16-244-249E Pex16-X-RV	EcoRI XhoI

*pET28 vectors also add a T7 tag between His tag and the subcloned protein. All restriction endonucleases were from New England Biolabs. In frame insertion and mutations of all constructs were verified by sequencing (Eurofins MWG Operon). DNA sequences were analysed using the software FinchTV (Geospiza Inc.).

3.3.2   Primers

Table 13: Synthetic oligonucleotides used in this study

Name	Nucleotide sequence (5' → 3')
ACBD5_Eco_rv	CCC<u>GAATTCC</u>T**TCA**ATTTAGTTTTCTTCTCCTTCTTTG
MycStopXbaI-Down	CC<u>TCTAGA</u>**CTA**CAGGTCCTCCTCG
P11b_ACBD5fw	cacctcaatcgaTGGTGGCCCTTTGAGATGTCC
P11b_ACBD5rv	caaagggccaccaTCGATTGAGGTGACTAACAGTG
P11b1-8mycR	ctcctcggagatcagcttctgctcTGGGACTCCTCCTCCAGAACC
P11b2-10mycF	aagctgatctccgaggaggacctgCCAGGGACTCCAGGAGGAGGT
P16-244-249E	GC<u>GAATTC</u>CAAACCCTGGCTCTTGG
P16-244-249X	GT<u>CCCGGG</u>TAAACCCTGGCTCTTGG
Pex11beta C down	TT<u>GGATCC</u>**TCA**GGGCTTGAGTCGTAGCCAGGG
Pex11beta C up	TT<u>GAATTC</u>*ATG*GACGCCTGGGTCCGCTTC
Pex11bKpnI-F	CA<u>GGTACC</u>*ATG*GACGCCTGGGTCCGC
Pex11bS11Afw	CGCTTCAGTGCTCAGgccCAAGCCCGGGAGCGG
Pex11bS11Arv	CCGCTCCCGGGCTTGggcCTGAGCACTGAAGCG
Pex11bS11Dfw	CGCTTCAGTGCTCAGgacCAAGCCCGGGAGCGG
Pex11bS11Drv	CCGCTCCCGGGCTTGgtcCTGAGCACTGAAGCG
Pex11bS38Afw	CTGCAGAGGCATGGAGCCgctCCTGAGTTACAGAAACAG
Pex11bS38Arv	CTGTTTCTGTAACTCAGGagcGGCTCCATGCCTCTGCAG
Pex11bS38Dfw	CTGCAGAGGCATGGAGCCgatCCTGAGTTACAGAAACAG
Pex11bS38Drv	CTGTTTCTGTAACTCAGGatcGGCTCCATGCCTCTGCAG
Pex11C18Sfw	GGGAGCGGCTGtctAGGGCCGCCCAGTATG
Pex11C18Srv	CATACTGGGCGGCCCTagaCAGCCGCTCCC
Pex11C25Sfw	GCCGCCCAGTATGCTtccTCTCTTCTTGGCC
Pex11C25Srv	GGCCAAGAAGAGAggaAGCATACTGGGCGGC
Pex11C85Sfw	GATGTTGTCCTGAGATTCtccATCACTGTTAGTCACCTC
Pex11C85Srv	GAGGTGACTAACAGTGATggaGAATCTCAGGACAACATC
Pex11βup	TT<u>GGATCC</u>*ATG*GACGCCTGGGTCCGCTTC
Pex11β-wt-down	T<u>GAATTC</u>**TCA**GGGCTTGAGTCGTAGCCAGGG
Pex16-E-Rv	GCG<u>GAATTC</u>**TCA**GCCCCACATGTAGAAG
Pex16-H2-FW	GCG<u>AAGCTT</u>*ATG*GAGAAGCTGCGG
Pex16-H-FW	CAT<u>AAGCTT</u>*ATG*GAGAAGCTGCGGC
Pex16-H-FW2	CAT<u>AAGCTT</u>GCC*ATG*GAGAAGCTGC
Pex16NOSTOP-X	GAT<u>CTCGAG</u>GCCCCAACTGTAGAAG
Pex16PP1BM1FW	CGCTTCTCCGAGGCCgcgATCCTCgccCTGCTCCAGTTGCTG
Pex16PP1BM1RV	CAGCAACTGGAGCAGggcGAGGATcgcGGCCTCGGAGAAGCG
Pex16PP1BM2FW	GCCCACCTGGCAGgcaATCTACgccTACAGTTGGGGCTG
Pex16PP1BM2RV	CAGCCCCAACTGTAggcGTAGATtgcCTGCCAGGTGGGC
Pex16-X-Fw	GAT<u>CTCGAG</u>CT*ATG*GAGAAGCTGCGGC
Pex16-XmaI-FW	GT<u>CCCGGG</u>T*ATG*GAGAAGCTGCGG
Pex16-X-RV	GAT<u>CTCGAG</u>**TCA**GCCCCAACTGTAG
Px11b-dGlyLeft	cagttggggcagTTTCAGTCGCCGGCTACAAGC
Px11b-dGlyRight	gcgactgaaaCTGCCCCAACTGGCTCTGAAAC
Px11b-dN40-Up	TT<u>GGTACC</u>ATGTTACAGAAACAGATTCGACAACTGG
Px11b-dN60-Up	TT<u>GGTACC</u>ATGCTGGGTAACTCAGCAGATGCC
Px11b-dN70-Up	TT<u>GGTACC</u>ATGGCCAAAAGAGCTGTTC
Px11bnoStopDown	TT<u>GGATCC</u>GGGCTTGAGTCGTAGCCAGGG

Restriction sites are underlined, start codons are printed italic, stop codons are printed bold and mutagenesis codons are printed lowercase. All primers used in this study were synthesized by Eurofins

MWG Operon and reconstituted in DEPC-treated water (Roth) to a stock concentration of 100 pmol/µl. Working primer solution is diluted 1:10 (10 pmol/µl) in DEPC-treated water.

3.4 Frequently used buffers and solutions

All solutions were prepared with distilled water (RO-Pure infinity reverse osmosis water system) if not indicated otherwise.

3-AT, for SD media

- 1 M 3-AT, filter sterilize

Amino acids dropout stock (10x), for SD media, autoclave

- 200 mg/l L-Adenine hemisulfate salt
- 200 mg/l L-Arginine HCl
- 200 mg/l L-Histidine HCl monohydrate
- 300 mg/l L-Isoleucine
- 1000 mg/l L-Leucine
- 300 mg/l L-Lysine HCl
- 200 mg/l L-Methionine
- 500 mg/l L-Phenylalanine
- 2000 mg/l L-Threonine
- 200 mg/l L-Tryptophan
- 300 mg/l L-Tyrosine
- 200 mg/l L-Uracil
- 1500 mg/l L-Valine

Selective SD/dropout media lack specific amino acids (e.g. SD/-Leu have all amino acids except L-Leucine)

Ampicillin stock

- 100 mg/ml Ampicillin, filter sterilize

Blocking solution for immunofluorescence

- 1% (w/v) BSA in PBS

Stock: 2%

Blocking solution for western blots

- 5% (w/v) milk powder (low fat) in PBS (or TBS-T)

BSA stock, for protein concentration measurement

- 1 µg/µl BSA

Cell culture medium for COS-7

- DMEM, high glucose (4,5 g/l) with L-glutamine
- 10% (w/v) FBS
- 100 U/ml Penicillin
- 100 µg/ml Streptomycin

Dilution/wash buffer for GFP-Trap®_M

- 10 mM Tris-HCl, pH 7,5
- 150 mM NaCl
- 0,5 mM EDTA

Glucose stock (20x), for SD media

- 40% (w/v) Glucose, filter sterilize

HBS – HEPES buffered saline, pH 7,15, for electroporation, filter sterilize

- 5 g/l HEPES
- 8 g/l Sodium chloride
- 0,37 g/l Potassium chloride
- 0,1 g/l Sodium phosphate dibasic
- 1,08 g/l D(+)Glucose

Homogenization buffer, pH 7,5 (for bacterial cells), autoclave if needs to be stored

- 50 mM Tris-HCl
- 15% Glycerol

Fixative for immunofluorescence

- 4% (w/v) paraformaldehyde in PBS, pH 7,4

IPTG stock, for protein expression in bacteria

- 100 mM IPTG

Kanamycin stock

- 30 mg/ml Kanamycin, filter sterilize

LB agar medium/plates, autoclave

- 2,5% (w/v) LB-Broth Miller
- 1% (w/v) Agar, for plates
- 30 mg/l Kanamycin or 100 mg/l Ampicillin, if needed, added after autoclave

LiAc, stock 10x, autoclave

- 1 M Lithium acetate

pH 7,5, adjusted with 1:5 diluted acetic acid

Lysis buffer, pH 8.0

- 25 mM Tris
- 50 mM Sodium chloride
- 0,5% (w/w) Sodium deoxycholate
- 0,5% (w/v) Triton X-100

Lysis buffer stock (10x) for GFP-Trap®_M (RIPA)

- 10 mM Tris-HCl, pH 7,5
- 150 mM Sodium chloride
- 5 mM EDTA
- 0,1% SDS
- 1% Triton X-100
- 1% Deoxycholate

Mini DNA preparation solution I, pH 8, autoclaved

- 50 mM Glucose
- 25 mM Tris-HCl
- 10 mM EDTA

Optional: 100 µg/ml RNase (alternative: water supplemented with 20 µg/ml RNase to resuspend the pellet)

Mini DNA preparation solution II

- 0,2 M Sodium hydroxide
- 1% SDS

Mini DNA preparation solution III

- 3 M Potassium acetate
- pH 4,8 with glacial acetic acid (approx. 11,5% v/v)

Mounting medium for immunofluorescence

- 3 volumes Mowiol stock
- 1 volume Propylgalate stock

Mowiol stock

- 12 g Mowiol 4-88
- 40 ml PBS
- 20 ml Glycerol, stir overnight
  Centrifuge 1 hour, 15000 rpm, 4 °C

  Sodium azide added to the supernatant

PBS – phosphate buffered saline, pH 7,35

- 140 mM Sodium chloride
- 2,5 mM Potassium chloride
- 6,5 mM Sodium phosphate dibasic
- 1,5 mM Potassium phosphate dibasic
  Stock: 10x concentrated (pH re-adjustment is needed after dilution)

PEG 4000 stock, autoclave

- 50% (v/v) PEG 4000

PEG/LiAc

- 40% (v/v) PEG 4000
- 1x TE
- 1x LiAc

Permeabilization for immunofluorescence

- 0,2% (v/v) Triton X-100 in PBS

Permeabilization for immunofluorescence

- 1 mg/ml Digitonin stock
- 1:400 diluted in PBS

Peroxisome homogenization buffer, pH 7,4

- 5 mM MOPS
- 250 mM Sucrose
- 1 mM EDTA

(0,1% (v/v) Ethanol – for catalase activity measurement)

Propylgalate stock

- PBS
- 2,5% (w/v) Propylgalate
- 50% (v/v) Glycerol

Protease inhibitors mix (final concentrations)

- 0,1 mM PMSF (or 1 mM PMSF, for GFP-Trap®_M buffers)
- 0,01 mM FOY 305
- 0,25% (v/v) Trasylol

PMSF stock

- 0,1 M PMSF in methanol

SD/dropout medium/plates, autoclave

- 0,69% (w/v) Yeast nitrogen base
- 1,5% (w/v) Agar, for plates
- 10% (v/v) Amino acids dropout 10x, added after autoclave

- 2% (w/v) Glucose, added after autoclave
- 15 mg/l Kanamycin, added after autoclave (facultative)

60 mM 3-AT if needed, added after autoclave

SDS-PAGE loading buffer

- 60 mM Tris, pH 6,8
- 2% (w/v) SDS
- 10% (v/v) Glycerol
- 0,005% (w/v) Bromophenol blue
- 20 mM DTT
- 5% (v/v) β-Mercaptoethanol

Stock: 1x, 3x or 5x concentrated (DTT and β-Mercaptoethanol added freshly)

SDS running buffer

- 25 mM Tris
- 190 mM Glycine
- 0,1% (w/v) SDS

Stock: 10x concentrated

SDS solution, for cell lysis

- 1% (w/v) SDS

Semidry blotting buffer

- 48 mM Tris
- 39 mM Glycine
- 0,4% (w/v) SDS
- 20% (v/v) Methanol

Stripping buffer

- 2% (w/v) SDS
- 62,5 mM Tris-HCl, pH 6,7
- 100 mM β-Mercaptoethanol (added prior to use)

TAE, pH 8.0

- 40 mM Tris
- 20 mM Acetic acid
- 1 mM EDTA

Stock: 50x concentrated

TE buffer, stock 10x, pH7,5, autoclave

- 0,1 M Tris-HCl
- 10 mM EDTA

TE/LiAc

- 1x TE
- 1x LiAc

Tris buffer for separation gel, pH 8,8

- 2 M Tris

Tris buffer for stacking gel, pH 6,8

- 1 M Tris

TBS-T – Tris buffered saline buffer, pH 8

- 10 mM Tris
- 150 mM Sodium chloride
- 1 mM EDTA
- 0,005% (v/v) Tween 20

Stock: 10x concentrated

Wash buffer I for immunoprecipitation

- PBS, pH 7,35
- 0,5% (w/v) Trinton X-100
- 0,05% (w/v) Sodium deoxycholate

Wash buffer II for immunoprecipitation

- 500 mM Sodium chloride
- 125 mM Tris-HCl, pH 8

- 10 mM EDTA
- 0,5% (w/v) Triton X-100

YPD medium/plates

- 5% (w/v) YPD (supplemented with glucose)
- 1,5% (w/v) Agar, for plates
- 15 mg/l Kanamycin, added after autoclave (facultative)

3.5 Cells

Table 14: Cells used in this study

Species	Strain/Line	Source	Purpose
Cercopithecus aethiops (African green monkey), kidney	COS-7	ATCC, CRL-1651	Overexpression of recombinant proteins, localization and interaction studies
Cercopithecus aethiops (African green monkey), kidney	COS-GFP-SKL	G. Lüers, University of Marburg, Germany (Koch et al, 2004)	COS-7 cells stably transfected with GFP-SKL – overexpression of recombinant proteins, localization and interaction studies, especially on peroxisomes
Homo sapiens	Pex16p-deficient	ATCC, GM06231	Complemention studies
Escherichia coli	DH5α	Invitrogen	DNA manipulations
Escherichia coli	XL1-Blue	E. da Cruz e Silva, CBC, Aveiro, Portugal (Stratagene)	DNA manipulations, recombinant protein expression
Escherichia coli	Rosetta (DE3)	E. da Cruz e Silva, CBC, Aveiro, Portugal (Novagen)	Recombinant protein expression
Escherichia coli	C41 (DE3)	Lucigen	Recombinant protein expression
Saccharomyces cerevisiae (Yeast)	AH109	E. da Cruz e Silva, CBC, Aveiro, Portugal (Clontech)	Protein-protein interaction studies

ATCC, American Type Culture Collection, Rockville, MD, USA

3.5.1 Mammalian cells

3.5.1.1 *Mammalian cell culture*

COS-7 cells were cultured in Dulbecco's modified Eagle medium (DMEM), high glucose (4,5 g/l) supplemented with 10% FBS, 100 U/ml Penicillin and 100 µg/ml Streptomycin.

Cells were cultured at 37 °C, 5% CO_2 aeration and 95% humidity. Cell culture work was performed in a sterile laminar flow safety cabinet and all materials and solutions were sterilized by filtration, autoclaving or heat sterilization. Routinely, cells were grown in 100 mm dishes and seeded on 18 mm Ø glass coverslips in 60 mm dishes for immunofluorescence experiments.

3.5.1.1.1 Cell passage

Routinely, passaging or splitting of cell was performed twice per week, after the cells reached confluence. Cell were washed with PBS and incubated with 2 ml trypsin EDTA solution (0,5 mg/ml trypsin and 0,22 mg/ml EDTA) for 3-5 minutes at 37 °C. Cells were resuspended in 10 ml medium and pelleted by centrifugation for 3 minutes at 200x g. The pellet was resuspended in medium and a fraction of this single cell suspension was seeded again.

3.5.1.1.2 Cell freezing

For long term storage, cells were frozen and stored in the vapour phase of liquid nitrogen. Cell pellets prepared as described above were resuspended in freezing medium containing 20% FBS and 10% DMSO. Cell suspension aliquots of 1 ml were filled into cryovials, slowly frozen overnight at -80 °C and subsequently transferred into the liquid nitrogen storage tank. For unfreezing, cells were thawed quickly by mixing with pre-warmed culture medium, and the cells were seeded with pre-warmed medium in a regular dish. After adhesion of the cells to the bottom of the dish, the medium was changed to remove DMSO and debris.

3.5.1.2 *Transfection of mammalian cells*

3.5.1.2.1 PEI transfection

24 hours before transfection cells were seeded on coverslips in 60 mm dishes. 10 µg of DNA were diluted in 750 µl of 150 mM sodium chloride, and 100 µl of 1 mg/µl PEI were diluted in 650 µl of 150 mM sodium chloride. After 15 minutes of incubation at room temperature, the PEI solution was added drop-wise to the DNA solution and the mixture was incubated for additional 15 minutes. 500 µl of the mixture were added drop-wise to 2,5 ml medium into the cell dish and the cells were incubated for 3-6 hours at 37 °C. Afterwards cells were washed with PBS and incubated for 24-48 hours in fresh medium before fixation.

3.5.1.2.2 Electroporation

A confluent dish of cells was trypsinized as described in section 3.5.1.1.1. The cell pellet was washed by resuspension in 5 ml HBS buffer and re-centrifugation. The cell pellet was resuspended in 1 ml HBS buffer and 0,5 ml of this cells suspension were mixed with 10 µg DNA in a 4 mm gap electroporation cuvette. Electroporation was performed at 230 V, 1500 µF and 125 Ω. Subsequently, the cells were quickly mixed with 1 ml of complete medium and seeded.

3.6 Microscopy techniques

3.6.1 Immunofluorescence

Cells grown on coverslips were washed twice with PBS and fixed with 4% paraformaldehyde for 20 minutes at room temperature. The cells were washed three times with PBS (washing was performed in between all further incubation steps). Cellular membranes were permeabilized using 0,2% Triton X-100 for 10 minutes. Afterwards unspecific binding sites were blocked by incubation with 1% BSA for 10 minutes. Incubation with the primary antibodies was performed for 1 hour in a humid and dark environment to avoid drying of the cells, followed by incubation with the secondary

antibodies in the same way. If more than one protein is meant to be observed, the antibodies were incubated simultaneously. Antibodies were diluted in PBS (see Table 8 and Table 9). For visualization of the cell nuclei the DNA was stained by incubation of the cells with Hoechst 33258 dye solution for 2-3 minutes. The coverslips were washed with distilled water, mounted using Mowiol and dried overnight before microscopic examination. Alternative permeabilization methods were also used: incubation with methanol for 5 minutes at -20 °C or with digitonin solution for 5 minutes at room temperature.

3.6.2   Fluorescence microscopy

For the observation of the immunofluorescent preparations Olympus IX81 microscope was used at a magnification of 1000x. Digital images were taken with the CCD Camera F-View II and selected and optimized for contrast and brightness using Olympus Software Imaging Viewer and Adobe Photoshop.

3.6.3   Microscope quantitative examination

For quantification of the peroxisomal morphology, 100 cells per coverslip were characterized, two coverslips per experiment were analysed and each experiment was performed at least three times. Data analysis and preparation of diagrams were done using Microsoft Excel software. Data are presented as means ± standard error of the mean (SEM). An unpaired t-test was used to determine statistical differences between experimental groups. P values <0,05 are considered as significant (**) and P values <0,001 are considered as highly significant (***).

3.7 Biochemical techniques

3.7.1 Preparation of post-nuclear supernatants and peroxisome-enriched fractions

Confluent 100 mm dishes of COS-7 cells were rinsed with PBS and the cells were harvested in a total volume of 5 ml PBS. The cells were pelleted by centrifugation (3 minutes, 200x g), resuspended in 1 ml peroxisome homogenization buffer containing protease inhibitors (3.4) and transferred to a microcentrifuge tube on ice. The cells were homogenized by passing fifteen times through a 26 G 1/2 needle. Remaining intact cells were pelleted by centrifugation (5 minutes, 500x g, 4 °C), the supernatant was collected and the cell pellet was re-homogenized in 500 µl peroxisome homogenization buffer as described. This procedure was performed twice, and the nuclei were removed from the collected supernatant by centrifugation at 500x g for 5 minutes at 4 °C. The resultant supernatant is designated as "post-nuclear supernatant". The mitochondria-enriched fraction was prepared by centrifugation at 2000x g for 10 minutes at 4 °C. The supernatant was centrifuged for 25 minutes at 25000x g at 4 °C to generate a peroxisome-enriched fraction. The pellet was shortly dried and resuspended in 100 µl of lysis buffer containing protease inhibitors.

3.7.2 Protein precipitation

Proteins were precipitated to concentrate samples and this was performed using chloroform and methanol (344). One volume of protein-containing sample (100 µl, filled up with water to perform the volume) was mixed with four volumes of methanol (400 µl), followed by mixing with one volume of chloroform (100 µl) and three volumes of water (300 µl). Centrifugation for 3 minutes at 16000x g separated the solution in two phases divided by a white interphase containing the proteins. The top aqueous phase was removed and discarded, and three volumes of methanol (300 µl) were added. After another centrifugation step (3 minutes, 16000x g) the precipitated proteins were found in the bottom pellet and the supernatant was discarded. The pellet was air-dried and dissolved, e.g. in SDS loading buffer.

3.7.3 Measurement of protein concentration

3.7.3.1 Bradford method

Measurement of protein quantification, e.g. for equal gel loading, was performed using the Bradford assay. Standards containing 1 to 20 µg BSA, blank and samples (1 to 10 µl) were filled up to 100 µl with 0,1 M NaOH . Protein assay solution (Bradford, from BioRad) was diluted 1:5 with distilled water and 1 ml of the solution was added to each sample. All standards and samples were prepared as duplicates. After 15 minutes of incubation at room temperature the absorption at 595 nm compared to the blank was measured. Using the standard curve prepared from the mean values, the protein concentration of the samples was calculated.

3.7.3.2 BCA method

This method was used with 1% SDS-diluted protein samples. To standards containing 2 to 40 µg BSA and blank were added 5 µl of 10% SDS and filled with up to 50 µl with water. 1-2 µl of 1% SDS-diluted samples were filled up to 50 µl with water. 50 ml of BCA reagent A were mixed with 1 ml of BCA reagent B and 1 ml of the solution was added to each sample. All standards and samples were prepared as duplicates. After 30 minutes of incubation at 37 °C the absorption at 562 nm compared to the blank was measured. Using the standard curve from the mean values, the protein concentration of the samples was calculated. The BCA reagents were from Pierce.

3.7.4 SDS-PAGE

Standard SDS-PAGE was performed with 10% or 12,5% separating and 5% stacking gels. To exclude oxygen, which inhibits polymerization process, the separating gel solution was covered with a layer of isopropanol. Gel recipes are presented in Table 15. Before loading of the proteins on the gel, they were denatured at 95 °C for 5 minutes in SDS-containing loading buffer. Gel electrophoresis in mini slap gel chambers was conducted for approximately 30 minutes at 80 V until the proteins entered the separation gel and

continued at 130 V for approximately 90 minutes or until proteins reached the desired separation. The gel chambers were filled with SDS running buffer. To mark protein size, a pre-stained molecular weight marker was used and the sample running front was visualized by bromophenol blue added to the loading buffer.

Table 15: Gel solutions of SDS-PAGE

Component	Stacking gel	Separating gel	
	5%	10%	12,5%
30% Polyacrylamide	1,66 ml	5,33 ml	6,67 ml
2 M Tris pH 8,8 (360 mM)	-	2,98 ml	2,98 ml
1 M Tris pH 6,8 (125 mM)	1,25 ml	-	-
20% SDS (0,1%)	50 µl	80 µl	80 µl
dH$_2$O	6,85 ml	7,55 ml	6,21 ml
TEMED (0,1% / 0,05%)	10 µl	8 µl	8 µl
10% APS (0,8% / 0,3%)	80 µl	48 µl	48 µl
Total volume	**10 ml**	**16 ml**	**16 ml**

Final concentrations are in brackets.

3.7.5 Immunoblotting

After separation by SDS-PAGE (section 3.7.4), proteins were transferred to a nitrocellulose membrane by semi-dry Western blotting (345). The membrane and two Whatman papers (3 mm) were soaked with semidry blotting bufferand a stack of Whatman paper, membrane, gel, and Whatman paper was formed. Air bubbles in between the layers were removed to guarantee complete transfer. The stack was put into a semidry transfer chamber and the proteins were blotted for 45 minutes at 12 V.

After the transfer unspecific binding sites on the membrane were blocked by incubation with 5% low fat powdered milk in PBS for 1 hour, shacking. For incubation with the primary antibody the membrane was sealed in a plastic bag with the respective antibody dilution (Table 8). The incubation times and temperatures ranged from 1 hour to overnight and from 4 °C to room temperature, always with shaking. Afterwards the membrane was washed with PBS three times for 10 minutes to remove unbound antibody. The incubation with the secondary antibody was performed for 1 hour at room temperature. For the ECL reaction, ECL1 (containing luminol) and ECL2 (phenol-containing enhancer) solutions were mixed at a 1:1 ratio and the membrane was incubated for

approximately two minutes. Film exposition, development and fixation were performed in a light protected room. The exposition time varied from 2 to 45 minutes, depending on the antibody and protein amount. Films were afterwards scanned with Bio-Rad GS-710 or Bio-Rad GS-800 Calibrated Imaging Densitometer.

3.7.6 Protein membrane overlay

The proteins of interest were expressed in C41 DE3 *E. coli* strain. The lysates were boiled at 95 °C for 15 minutes with appropriate amount of 3x SDS loading gel. The samples were subsequently separated by SDS-PAGE (section 3.7.4) and transferred to a nitrocellulose membrane (section 3.7.5). The membrane was blocked with blocking solution (5% milk in TBS-T) for 1 hour at room temperature. The membrane was overlaid with 25 pmol/µl purified PP1γ1 protein (346), diluted in 3% low fat milk/TBS-T, for 1 hour at room temperature. After washing with TBS-T three times for 10 minutes, the bound PP1γ1 was detected by incubating the membrane with anti-PP1γ antibody (Table 8) for 1 hour at room temperature. Immunoreactive bands were revealed by incubating with horseradish peroxidase-conjugated secondary antibody (1:2000 in 3% low fat milk in TBS-T) for 1 hour at room temperature, and developed by ECL.

3.7.7 Membrane stripping

Membrane striping method was used to remove antibodies from blotted membranes. The membrane was submerged in striping buffer and incubated at 50 °C for 30 minutes, with agitation. The membrane was then washed twice, at room temperature, with a large volume of TBS-T, for 10 minutes with shacking. The membrane was re-blocked by incubation with blocking solution (5% milk in TBS-T) for 1 hour at room temperature.

3.7.8 Protein pull down

3.7.8.1 Immunoprecipitation

Protein A-coupled sepharose (PAS) beads were incubated twice overnight in PBS (5 ml PAS in 50 ml PBS) at 4 °C and for storage 0,1% sodium azide was added. For co-immunoprecipitation two confluent 100 mm dishes of COS-7 cells transfected by electroporation (section 3.5.1.2.2) with A) 10 μg pcDNA3.1-PP1γ1 and 10 μg empty pcDNA3 vector; B) 10 μg pcDNA3.1-Myc-Pex16 and C) 10 μg pcDNA3.1-PP1γ1 and 10 μg pcDNA3.1-Myc-Pex16. After 24 hours the cells were washed with PBS and carefully harvested in a total volume of 5 ml PBS by scraping. All further steps were performed on ice. A cell pellet was prepared by centrifugation (200x g, 3 minutes) and resuspended in 1 ml lysis buffer containing protease inhibitors. The cells were lysed by three ten seconds sonication steps (30 seconds of total time). The lysate was cleared by centrifugation at 10000x g for 5 minutes, at 4 °C, and the pellet was discarded. Two 25 μl samples were collected and stored. A pre-clearing step was performed to avoid unspecific binding to PAS: the cell lysate was incubated with 50 μl PAS and rotated for 4 hours at 4 °C; the lysate was then centrifuged to pellet the beads at 2400x g for 5 minutes at 4 °C; the supernatant was transferred into a new tube and a 25 μl sample was collected and stored; the beads were washed twice with wash buffer I and wash buffer II and stored; a 100 μl sample of the supernatant of the first wash was collected into a new tube. The rest of the pre-cleared lysate supernatant was divided into two new tubes with equal volumes (for immunoprecipitation and negative control, without antibody). Anti-Myc antibody was added to a final concentration of 1:200 into one of the pre-cleared supernatant tubes (no antibody was added to the other tube – negative control). Both tubes were incubated for 1 h at 4 °C with over-head rotation. Afterwards, 50 μl of PAS were added to each tube and incubated overnight at 4 °C with over-head rotation. The tubes were then centrifuged at 2400x g for 5 minutes at 4 °C and a 25 μl supernatant sample was collected from each tube and stored. The beads were washed twice with wash buffer I and wash buffer II and stored. A 50 μl sample of the supernatant of the first wash was collected into new tubes and stored. For the separation by SDS-PAGE (section 3.7.4), 40 μl of 3x Lämmli buffer were added to each sample of beads and boiled for 5 minutes at 95 °C. The other samples

were precipitated by chloroform-methanol method (section 3.7.2) and the pellets were resuspended in 25 µl 3x Lämmli buffer (3.4) and boiled for 5 minutes at 95 °C.

3.7.8.2   GFP-Trap®_M

GFP-Trap®_M (from Chromotek) contains a small GFP-binding protein covalently coupled to the surface of magnetic beads, enabling the purification of a protein of interest fused to GFP or GFP variants. COS-7 cells were transfected by electroporation (section 3.5.1.2.2) with GFP vector which induces the expression of a GFP-fused protein, and incubated at 37 °C for 16-24 hours. Cells transfected by electroporation with an empty GFP-expression vector were used as negative control. The cells were rinsed twice with PBS and harvested by scraping with a rubber policeman in 2 ml of PBS per dish. The cells were pelleted by centrifugation (200x g for 3 minutes) and resuspended in 100-200 µl of lysis buffer. The tubes were placed on ice for 30 minutes and extensively pipetted every 10 minutes. The cell lysates were spun at 17000x g for 15 minutes at 4 °C. The supernatant was transferred to a pre-cooled tube and the volume adjusted to 500-1000 µl with dilution/wash buffer. The protein concentration on the lysates was measured by Bradford method (section 3.7.3.1) and 75 µg of each sample were collected for western blot analysis (input fraction). For equilibration, the magnetic beads were resuspended by vortexing and 25 µl of bead slurry were transferred into 500 µl of dilution/wash buffer. The beads were magnetically separated until the supernatant was clear. The supernatant was discarded and the beads were washed two times more with 500 µl ice cold dilution/wash buffer. 1500 µg of lysate were added to equilibrated GFP-Trap®_M beads and incubated at 4 °C for two hours under constant mixing by rotation. Both lysis and dilution/wash buffers were supplied with protease inhibitors. Afterwards, the beads were magnetically separated until the supernatant was clear. For western blot analysis, 75 µl of the supernatant were collected (non-bound fraction), and the remaining supernatant was discarded. The beads were then washed two times with 500 µl of dilution/wash buffer. The beads were resuspended in 60 µl of 3x SDS loading buffer (3.4) and boiled at 95 °C for 10 minutes (bound fraction). The beads were magnetically separated and discarded. The

input and non-bound fractions were denatured by mixing with the necessary volume of 3x SDS loading buffer and boiled at 95 °C for 5-10 minutes. Input, bound and non-bound fractions of GFP-fused protein and GFP alone control were separated by SDS-PAGE (section 3.7.4) and analysed by western blot with the appropriated antibodies (section 3.7.5).

For protein pull down using a cross-linker, DSP was used. Prior to cell harvesting, each 10 cm dish was incubated with 4 mg of DSP, dissolved in 40 µl DMSO + 10 ml PBS solution, for 45 minutes, at room temperature. The dishes were then rinsed three times with PBS and the cells were harvested. The following procedures were performed as described above.

3.8 Molecular biology techniques

3.8.1 DNA subcloning

The DNA subclonings performed for this study were made as follows: the cDNA (or a portion of it) to be subcloned was used as template for a PCR (section 3.8.3) in which restriction endonuclease (RE) recognition sites and/or mutations were inserted. The PCR product was separated and the expected band purified in agarose gels (sections 3.8.4 and 3.8.5). The purified PCR product and the selected vector were then digested with the insertion enzymes (section 3.8.6) and purified in agarose gel (sections 3.8.4 and 3.8.5). The vector and insert fragments were ligated (section 3.8.7) and ligation product inserted in *E. coli* (section 3.8.8) for amplification (section 3.8.9) and selection of positive clones (sections 3.8.11 and 3.8.13). The selected positive clone was re-cultured (section 3.8.9) and isolated by kit mini preparation (section 3.8.11 and Table 7) in order to obtain a high quality DNA for sequencing (section 3.8.14). After confirmation of insert's frame and presence/absence of mutations, a high quality kit midi (Table 7) preparation was performed to conduct the subsequent assays.

3.8.2   Primer design

In general, the plasmids constructed for this study, were created by cDNA amplification by PCR (section 3.8.3) using a pair of forward and reverse primers which contained recognition sites for restriction endonucleases. The primers annealed to the cDNA on the beginning and the end of the area to be amplified by 15 to 20 nucleotides. Some nucleotides were added upstream and downstream the RE recognition sites to improve cutting efficiency and maintain the frame, respectively. The primer pairs were designed to have melting temperatures as close as possible.

For site-directed mutagenesis (section 3.8.3.1), in which one to three bases were mutated in order to change an amino acid, (e.g. Pex11pβ-S11A-Myc), both forward and reverse primers contain the desired mutation and anneal to the same sequence on opposite strands of the plasmid. The primers were designed to have 30-45 bases and a melting temperature (T_m) of ≥78 °C. The desired mutation was in the middle of the primer with 10-15 bases of correct sequence on both sides. The following formula was used to calculate T_m of mutational primers (N = primer length in bases; *%GC*, i.e. percentage of guanines and cytosines, and %mismatch are whole numbers):

$$Tm = 81,5 + 0,41(\%GC) - 675/N - \%mismatch$$

3.8.3   PCR

The PCRs performed for cloning in this study are listed with template, primer pair, restriction endonucleases cutting sites and target vector in Table 12. For standard PCR conditions see Table 16 and Table 17. For site-directed mutagenesis PCR condition see Table 18 and Table 19. The DNA polymerase, the $MgSO_4$ 25 mM and the dNTPs were from Novagen. The PCR components were mixed in DEPC-treated water (ROTH).

Table 16: Standard PCR assembly

Component	Amount
Template	100 ng
Primer forward (10 pmol/µl)	1 µl
Primer reverse (10 pmol/µl)	1 µl
dNTPs mix (2 mM each)	5 µl
$MgSO_4$ (25 mM)	3 µl
10x Buffer	5 µl
KOD Hot Start DNA polymerase (1 U/µl) (Novagen)	1 µl
H_2O	x µl
Final volume	**50 µl**

Table 17: Standard PCR protocol

Step		Temperature	Time	Cycles
Denaturation and activation		95 °C	2 min	1 cycle
First amplification[3]	Denaturation	95 °C	30 s	5 – 7 cycles
	Annealing[1]	43 °C – 62 °C	20 s	
	Elongation[2] (1 min/kb)	70 °C	20 s – 1 min 30 s	
Second amplification[3]	Denaturation[1]	95 °C	30 s	25 – 30 cycles
	Annealing[2]	62 °C – 70 °C	20 s	
	Elongation (1 min/kb)	70 °C	20 s – 1 min 30 s	
Final elongation		70 °C	10 min	1 cycle
Cooling		4 °C	∞	

[1] Annealing temperature was adjusted to the respective primer pair. [2] Elongation time was adjusted to template length. [3] The PCR reaction is divided in two parts because in the first cycles the whole primer doesn't anneal to the template due to the extensions to add RE recognition sites or other sequences (i.e. mutagenesis PCRs).

3.8.3.1 Site-directed mutagenesis

Some cDNAs were mutated for this study using the site-directed mutagenesis technique, following the general guidelines of the instruction manual of the QuikChange® Site-Directed Mutagenesis Kit, from Stratagene. The mutations were inserted by PCR (section 3.8.3), using mutational primers (section 3.8.2) to amplify the whole plasmid. Afterwards, 1 µl of DpnI (New England Biolabs) was added to the PCR product and incubated at 37 °C for approximately 3 hours. DpnI is a restriction enzyme that cleaves exclusively methylated DNA. Therefore only template DNA, which was amplified from a *dam+ E. coli* strain (XL1-Blue or DH5α), was digested. Afterwards, 1 µl to 4 µl of the digested PCR product were used to transform bacteria (section 3.8.8) to get single-cell colonies. Three

isolated colonies were then selected and cultured (section 3.8.9) to amplify and isolate the plasmid (section 3.8.11) for sequencing (section 3.8.14) and selection of the clone with the desired mutation. The mutated cDNA was subsequently re-cloned into a fresh vector. If the vector to be inserted in was the same, no PCR amplification was used, the insert was separated from the backbone vector by digestion (sections 3.8.6 and 3.8.5) and ligated (section 3.8.7) with fresh digested vector. Selection of positive clones was done as described in section 3.8.13.

Table 18: Site-directed mutagenesis PCR assembly

Component	Amount
Template	50 ng
Primer forward (10 pmol/µl)	125 ng
Primer reverse (10 pmol/µl)	125 ng
dNTPs mix (2 mM each)	5 µl
$MgSO_4$ (25 mM)	3 µl
10x Buffer	5 µl
KOD Hot Start DNA polymerase (1 U/µl) (Novagen)	1 µl
H_2O	x µl
Final volume	**50 µl**

Table 19: Site-directed mutagenesis PCR protocol

Step		Temperature	Time	Cycles
Denaturation and activation		95 °C	30 s	1 cycle
Amplification	Denaturation	95 °C	30 s	16 cycles
	Annealing	55 °C	1 min	
	Elongation[1] (1 min/kb)	70 °C	5 min 45 s – 7 min	
Final elongation		70 °C	15 min	1 cycle
Cooling		4 °C	∞	

[1] Elongation time was adjusted to template length.

3.8.4   Agarose gel electrophoresis

Agarose was dissolved in TAE buffer by boiling in a microwave. The solution was cooled down until being hand-hot, ethidium bromide was added (0,5 µg/ml) and the gel was poured into a horizontal gel chamber containing a comb to form loading wells. Routinely, 0,8-1% (w/v) agarose gels were used. DNA samples were mixed with 6x loading buffer and a DNA ladder was used to mark DNA sizes (Table 6). Separation was performed at 60-130

V and for 30-60 minutes. Digital images were taken using Alpha Innotech AlphaImager HP device and quantifications were made with the provided software.

3.8.5   DNA gel extraction

PCR products and other DNA samples were isolated from agarose gels (section 3.8.5) using a gel extraction kit (Macherey-Nagel, Table 7). The DNA bands visible with UV light in the agarose gel were sliced with a scalpel and transferred to a reaction tube. Agarose was melted at 50 °C and the DNA was extracted with spin columns (Table 7). Elution was performed using 30-50 µl of distilled water.

3.8.6   Digestion with restriction enzymes for DNA subcloning

PCR products extracted from the agarose gel (total volume) and the target vector (2 µg – 5 µg) were digested with the same two enzymes. Routinely, restrictive digestions for DNA subcloning were performed according to Table 20, at 37 °C, for approximately 24 h, separately, inactivating the first restriction enzyme (65 °C, 20 min) in between. Afterwards, successful digestion was checked on an agarose gel, the DNA was isolated and used for ligation. All the enzymes were from New England Biolabs.

Table 20: Standard RE reaction for DNA subcloning

Component	Amount
DNA (PCR product or vector)	x µl
Restriction endonuclease I	1,0 µl
Restriction endonuclease II (added after some hours)	1,0 µl
100x BSA (100 ng/µl; optional, depending on the enzymes)	0,5 µl
10x Buffer[1]	5,0 µl
H$_2$O	x µl
Final volume	**50 µl**

[1] The buffer used was the one recommended by New England Biolabs for double digestion with the selected enzymes.

3.8.7 DNA Ligation

To combine vector and insert DNAs both were enzymatically ligated using the T4 DNA ligase (from New England Biolabs). The digested vector and insert molecules were mixed by a ratio of 1:3. In some cases, depending on the sizes of both vector and insert, the ratios of 1:6 or 1:9 were also used. The reaction was assembled according to Table 21 and incubated at 16 °C overnight. Two negative controls were performed: vector without ligase and vector with ligase. 5 µl of the ligation products were transformed and amplified in *E. coli* (sections 3.8.8 and 3.8.9) and screened for correct ligations by RE digestion (section 3.8.13).

Table 21: Standard ligation reaction

Components	Negative controls		Ligation
	Vector without ligase	Vector with ligase	
Vector	25 ng	25 ng	25 ng
Insert	-	-	x ng*
T4 Ligase (400 U/µl)	-	1 µl	1 µl
10x Ligation buffer	2 µl	2 µl	2 µl
H$_2$O	x µl	x µl	x µl
Total volume	20 µl	20 µl	20 µl

*The amount of insert depends on its size and on the ratio vector:insert used

3.8.8 Bacterial transformation

50 µl of competent *E. coli* were mixed with the DNA (e.g. from a ligation reaction) and incubated on ice for 20 minutes. After a 90 seconds heat shock at 42 °C, the bacteria were chilled on ice (2 minutes, approximately) and 900 µl LB medium without antibiotics was added, followed by 30 min – 1 h shacking incubation at 37 °C. The cells were then centrifuged (1 minute at 12000x g) and the pellet resuspended in 50 µl – 100 µl of leftover supernatant LB medium. The suspension was spread on a LB agar plate containing a selective antibiotic using glass beads and grown overnight at 37 °C.

3.8.9 Bacterial culture

For cloning and amplification of DNA plasmids of *Escherichia coli* (XL-1 blue, DH5α or C41 strains) cultures were used. The bacteria were cultured in LB medium containing a

selective antibiotic (100 μg/ml ampicillin or 30 μg/ml kanamycin) at 37 °C and 200 rpm in a shaking incubator. Long-time storage of *E. coli* cultures was performed as 25% glycerol mixtures at -80 °C. For single-cell colonies bacteria were spread on LB agar plates (with selective antibiotic) and incubated overnight in a 37 °C incubator. Plates were short-term stored at 4 °C and the bacterial colonies were used for inoculation of liquid cultures (2 ml – 5 ml).

3.8.10 Protein expression in bacteria

E. coli strain C41 was transformed (section 3.8.8) with bacterial expression vectors containing the cDNAs of interest. One single colony was inoculated in 5 ml LB-containing selective antibiotic and incubated at 37 °C, overnight, with shaking. As control, one single colony of non-transformed bacteria was inoculated as well. Afterwards, 150 μl of these pre-cultures were inoculated in 20 ml of LB with antibiotic and incubated at 37 °C until OD_{600} reached 0,5-0,6. Each culture was divided in two batches: two test tubes were filled with 5 ml of this culture and 20 μl of 100 mM IPTG (final concentration of 0,4 mM) were added to one of the batches of each culture (induced batch). All tubes (induced and non-induced) were then incubated at 18 °C, overnight, with shaking. Two 1,5 ml aliquots of each batch of each culture were harvested by centrifugation at 12000x g for 1 minute and the supernatants discarded. The dried pellets were frozen at -20 °C until further analysis.

One aliquot of each induced cell pellet was used to separate the proteins in soluble and insoluble fractions. To do this, the pellets were resuspended in 300 μl of homogenization buffer and sonicated in 5 seconds cycles until light was able to pass through the sample. The sonication was performed on ice. The cell lysates were centrifuged at 4000 xg, 4 °C for 10 minutes. The supernatants (soluble fractions) were transferred into new tubes. The pellets (insoluble fractions) were resuspended in 100 μl of homogenization buffer (section 3.4). The pellets don't solubilize but can be resuspended).

To obtain total protein extracts, the other aliquot of each culture pellet was resuspended in 100 μl of SDS 1% and sonicated as previously described. The protein concentrations were measured by the BCA method (section 3.7.3.2).

3.8.11 Plasmid isolation

Plasmid DNA was isolated from *E. coli* cultures in two different amounts; as small scale (mini) preparation from 3 ml to 5 ml cultures or as large scale (midi) preparation from 200 ml cultures. Large scale preparations were performed using midi kit (Macherey-Nagel, Table 7). Mini preparations for sequencing or DNA testing purposes were performed using a mini kit (GE Healthecare or Macherey-Nagel, Table 7) and the plasmid DNA eluted in 50 µl of water. Mini preparations for colony screening after cloning were done according to the following protocol: 1,5 ml – 3 ml *E. coli* cultures inoculated from single colonies were grown overnight and sedimented by centrifugation at 12000x g for 2 minutes. The supernatant was carefully removed and the pellet was completely resuspended in 100 µl cold solution I. 200 µl of room temperature solution II were added and mixed by inverting the tube five times. 150 µl of cold solution III were added, the tube carefully inverted for mixing, and incubated on ice for 3 to 5 minutes. The precipitate formed was removed by centrifugation at 17000 – 20000x g, 4 °C for 10 minutes and the supernatant was transferred to a new tube. The DNA was precipitated by addition of 1 ml (approximately 2 volumes) 100% ethanol, incubation at room temperature for 2 minutes and centrifugation at 17000 – 20000x g, 4 °C for 5 minutes. The supernatant was removed and 1 ml 70% ethanol was added, the tube was vortexed and centrifuged at 17000 – 20000x g, 4 °C for 5 minutes. After supernatant removal and air-drying, the pellet was resuspended in 50 µl of water supplemented with 20 µg/ml RNase. Alternatively, RNase can be added to solution I at 100 µg/ml. DNA concentrations of midi and column mini preparations were measured as described in section 3.8.12.

3.8.12 Measurement of DNA concentrations

DNA concentration of column midi and mini preparations were measured in two different ways, either using the Qubit fluorometer and the respective fluorometric assay (Table 7) or by measuring the optical density at wavelengths of 260 nm and 280 nm. The DNA preparations were diluted in water in order to achieve $OD_{260/280}$ between 0,1 and 1. An OD_{260} of 1 corresponds to approximately 50 µg/µl of double stranded DNA. The ratio

OD_{260}:OD_{280}, which provides an estimate of the purity of the nucleic acid, was between 1,8 and 2,0. Water was used as blank.

3.8.13 Screening of positive DNA clones by restriction analysis

To find positive clones 5 to 15 isolated bacterial colonies transformed with the ligation product were selected and its plasmid DNA extracted. This DNA was analysed by digestion with one or two restriction enzymes which cut in specific sites (see Table 22), giving an expected and distinguishable band pattern after separation by agarose gel electrophoresis (section 3.8.4). Typically, the selected enzyme cut the vector and the insert. The insertion enzymes were used in some cases. Empty vector (negative control) was also digested in parallel.

Table 22: Standard RE reaction for screening of clones

Component	Amount
DNA	1 µl – 3 µl
Restriction endonuclease I	0,1 µl – 0,2 µl
Restriction endonuclease II (if needed)	0,1 µl – 0,2 µl
100x BSA (100 ng/µl; optional, depending on the enzymes)	0,1 µl
10x Buffer[1]	1 µl
H_2O	x µl
Final volume	**10 µl**

A master mix without the DNA was prepared, divided, and the DNA added in the end to each aliquot. The tubes were incubated at 37 °C for 2 h – 5 h.

3.8.14 DNA sequencing

The sequencing of all the constructs made for this study was conducted by Eurofins MWG Operon following their instructions. The sequencing primers were also provided by them.

3.8.15 Yeast co-transformation for protein-protein interaction assays

The yeast co-transformation assay was used to test protein-protein interactions and was performed following the guidelines of the small-scale LiAc yeast transformation procedure from Clontech's Yeast Protocols Handbook (PT3024-1). The vectors and

plasmids for positive controls are described in the Clontech's MATCHMAKER Gal4 Two-Hybrid Vectors Handbook (PT3062-1). Competent cells were prepared by inoculating one colony of *Saccharomyces cerevisiae* strain AH109, in 1 ml of YPD and vigorously vortexed to disperse cell clumps. The suspension was transferred into a flask containing 50 ml of YPD and incubated at 30 °C for 16 h – 18 h with shacking at 250 rpm until it reached the stationary phase ($OD_{600} > 1$). 20 ml to 40 ml of this overnight culture was transferred to a flask containing 300 ml of YPD in order to get a cell suspension with an OD_{600} of 0,2 – 0,3. This culture was incubated for 3 hours, at 30 °C, with shacking at 230 rpm. At this point, the culture's OD_{600} was between 0,4 and 0,6. The cells were then placed in 50 ml tubes and centrifuged at 1000x g for 5 minutes, at room temperature. The supernatants were discarded and the cells pellets were thoroughly resuspended in sterile distilled water. The cells were pooled into one tube (final volume of 25 ml – 50 ml) and centrifuged again at 1000x g for 5 minutes, at room temperature. The supernatant was discarded and the cell pellet resuspended in 1,5 ml freshly prepared sterile 1x TE/1x LiAc.

The plasmid DNAs to be inserted in the cells were prepared by mixing 0,1 µg of plasmid DNA (for simultaneous co-transformations, using two different plasmids, 0,1 µg of each plasmid were used) with 0,1 mg of herring testes DNA (previously boiled) in a 1,5 ml tube. Then, 100 µl of fresh yeast competent cells were added to each tube and well mixed by vortexing. 600 µl of PEG/LiAc solution were added to each tube and vortexed at high speed for 10 seconds. After incubation at 30 °C for 30 minutes with shacking at 200 rpm, 70 µl of DMSO were added to each tube and gently mixed by inversion. The cells were then heat shocked for 15 minutes at 42 °C, in a water bath, and chilled on ice for 1 to 2 minutes. Afterwards, the cells were centrifuged for 5 seconds at 17000x g at room temperature, the supernatants discarded and the cells resuspended in 200 µl – 500 µl of 1x TE buffer.

The selection of the desired transformants was made by plating 100 µl of each transformed cells tube on SD agar plates with the respective amino acid(s) dropout. Cells transformed with pAS2-1 and pACT2 backbone vectors are able to grow in dropout

medium without tryptophan and leucine amino acids (SD/-T-L), respectively. The plates were incubated up-side-down at 30 °C for 2 to 4 days, until colonies appeared.

To verify protein-protein interactions double transfected cell colonies and controls were re-picked into SD/dropout agar plates without histidine and/or adenine and with X-α-Gal (from BD Biosciences). 3-AT was added to some plates (to a final concentration of 60 mM) to suppress leaky *HIS3* expression. Kanamycin antibiotic was added to YPD and plates to a final concentration of 15 mg/l in order to reduce the growth of some contaminants.

3.9   *In silico* analysis

For *in silico* analyses of DNA and protein several online and offline programs were used as well as databases (see Table 23). References for the programs can be found in the respective websites.

Table 23: Databases and online and offline programs used for the *in silico* analyses

Purpose	Program/database	URL
Protein information search	UniProtKB	www.uniprot.org
	NCBI Protein Database	www.ncbi.nlm.nih.gov/protein
Peroxisome protein information search	PeroxisomeDB 2.0	www.peroxisomedb.org/home.jsp
Protein motifs prediction	ELM	elm.eu.org
	MotifScan	myhits.isb-sib.ch/cgi-bin/motif_scan
	ScanSite3	scansite3.mit.edu
Protein motifs canonical sequences screen	ScanProsite	prosite.expasy.org/scanprosite
Protein molecular weight prediction	Compute pI/Mw	web.expasy.org/compute_pi
Human protein-protein interactions search	HIPPIE	cbdm.mdc-berlin.de/tools/hippie
Protein alignments	Clustal Omega	www.ebi.ac.uk/Tools/msa/clustalo
Protein and DNA blasts	BLAST	blast.ncbi.nlm.nih.gov/Blast.cgi
Gene information search	NCBI GenBank	www.ncbi.nlm.nih.gov/genbank
DNA sequencing files analysis	FinchTV (offline)	www.geospiza.com/Products/finchtv.shtml
Primer melting temperature calculation	OligoCalc	www.basic.northwestern.edu/biotools/oligocalc.html
Buffer determination for double DNA restrictions	NEB Double Digest Finder	www.neb.com/tools-and-resources/interactive-tools/double-digest-finder
Plasmid map design	Clone Manager (offline)	www.scied.com/pr_cmbas.htm

3.10 Figure preparation

All figures of the present work were prepared using the software Adobe Photoshop CS6. In microscopy figures, manipulations in brightness and contrast parameters were made by a mask layer clipped to all layers or groups of layers from the same experiment.

4 Results

4.1 PP1 as a potential regulator of peroxisome biogenesis *via* interaction with Pex16p

Phosphorylation/dephosphorylation is a well-known molecular switch mechanism used to tightly regulate the active/inactive state of proteins. Although with unclear role, phosphorylation have been already demonstrated to be a post-translation modification in two players of the peroxisomal matrix import machinery – Pex14p and Pex15p (283, 284). Other peroxisome biogenesis players were shown to be phosphorylated as well, such as DLP1 (285, 286) and Pex11 family proteins (220, 290). So far, only the protein phosphatases PP2A and MKP1 and the kinase CPK1 were localized to peroxisomes, in *Arabidopsis thaliana* (300-302, 304). The only direct link of protein kinases/phosphatases and mammallian peroxisomes discovered so far is Akap11 and Limkain-b1, both PP1 interactors (295, 296, 298, 299). Human Pex16p was also identified as a putative PP1-interacting protein (PIP) by another research group of CBC, University of Aveiro (307). PP1 belongs to the PPP superfamily of protein Ser/Thr-phosphatases which contributes with more than 90% of protein phosphatase activity in eukaryotes (313, 347).

In a collaborative approach of our group, Signal Transduction group from CBC and the company Kinexus Bioinformatic Corporation (www.kinexus.ca), a large-scale blot screen for kinases and phosphatases in highly purified peroxisomal fractions from rat liver was made, with very interesting results (unpublished data). The fractions were obtained from 8 weeks old rats either untreated (controls) or bezafibrate fed for either 3 or 10 days[2]. Bezafibrate is a peroxisome-proliferator agent often used to analyse selected aspects of peroxisome biogenesis or lipid metabolism (348). An astonishing number of kinases (31 out of 78 tested) and phosphatases (11 out of 28 tested) were detected in the fractions. Although in a less expressive amount than other phosphatases (e.g. PP2A) or kinases (e.g. MKK6), all three PP1 isoforms were detected, being PP1γ the most abundant one. A significant variation on PP1 amount between the control and the three days bezafibrate-

---

[2] The rats weighted approximately 250 g each and the treated rats were fed with 250 mg/kg of bezafibrate. The fractions were prepared by Markus Islinger in the University of Heidelberg, Germany.

treated fractions was also detected (41%, 27% and 36% decrease for PP1α, PP1β and PP1γ, respectively). This result suggests a possible role of PP1 in the down-regulation of peroxisome proliferation, i.e. the proteins involved in the proliferation may need to be phosphorylated to become active and vice-versa.

In a yeast two-hybrid (YTH) screen using PP1γ in a human brain cDNA library, Esteves and colleagues identified Pex16p as a putative PP1 binding protein (307). They tested full length PP1γ1, full length PP1γ2 and the specific C-terminal 39 amino acids of PP1γ2. One clone of Pex16p was detected in the full length PP1γ2 YTH. Pex16p has 3 PP1-binding motifs, two RVxF and one SILK, an RVxF-cooperating motif (see section 1.4.2.1.1). The presence of these motifs re-enforced the confidence on a putative interaction between PP1 and Pex16p, making Pex16p a potential PIP, bringing PP1 to the vicinity of potential Ser/Thr dephosphorylation targets in the peroxisomal membrane.

All *PEX16* patients described up today had mutations that somehow affected the C-terminus of the protein (118, 349-351) (see section 1.1.3). Intriguingly, none of the mutations directly affected any known functional motifs of Pex16p (120, 141, 152, 352). However, the RVxF motifs identified in human Pex16p localize in the very C-terminus, turning them into good candidates to be functional PP1-binding motifs with implications on Pex16p function and in health.

4.1.1   Several peroxins have putative PP1-binding motifs

To identify potential PIPs in peroxisomal membrane, we screened all known human peroxins for PP1-binding motifs. The sequences were retrieved from UniProtKB database, loaded on the ScanProsite server and screened for the PP1-binding motifs' consensus sequences listed on Table 5 (Figure 9, Supplementary Table 1). The peroxins that returned no hits for PP1-binding motifs were Pex5pL, Pex11pβ, Pex14p and Pex19p. Pex2p and Pex6p have only RVxF-cooperating motifs. The peroxins considered more likely to be true PIPs were Pex3p, Pex10p and Pex16p because they presented both RVxF and RVxF-cooperating motifs. Importantly, Pex1p, Pex5p, Pex7p, Pex10p, Pex13p and Pex26p isoform 1 were recognized by RVxF canonical sequences that are more specific, making

those peroxins also good candidates for PIPs. Interestingly, human UbcH5a/b/c, an ubiquitin-conjugating enzyme that ubiquitinates PTS1 receptor Pex5p during the receptor-recycling step of matrix protein import (105), also revealed to have two RVxF motifs (Supplementary Figure 1, Supplementary Table 2). Human Fis1, DLP1, Mff and GDAP1, players in the peroxisomal (and mitochondrial) fission were also screened for PP1-binding motifs and all off them returned no hits (Supplementary Table 3).
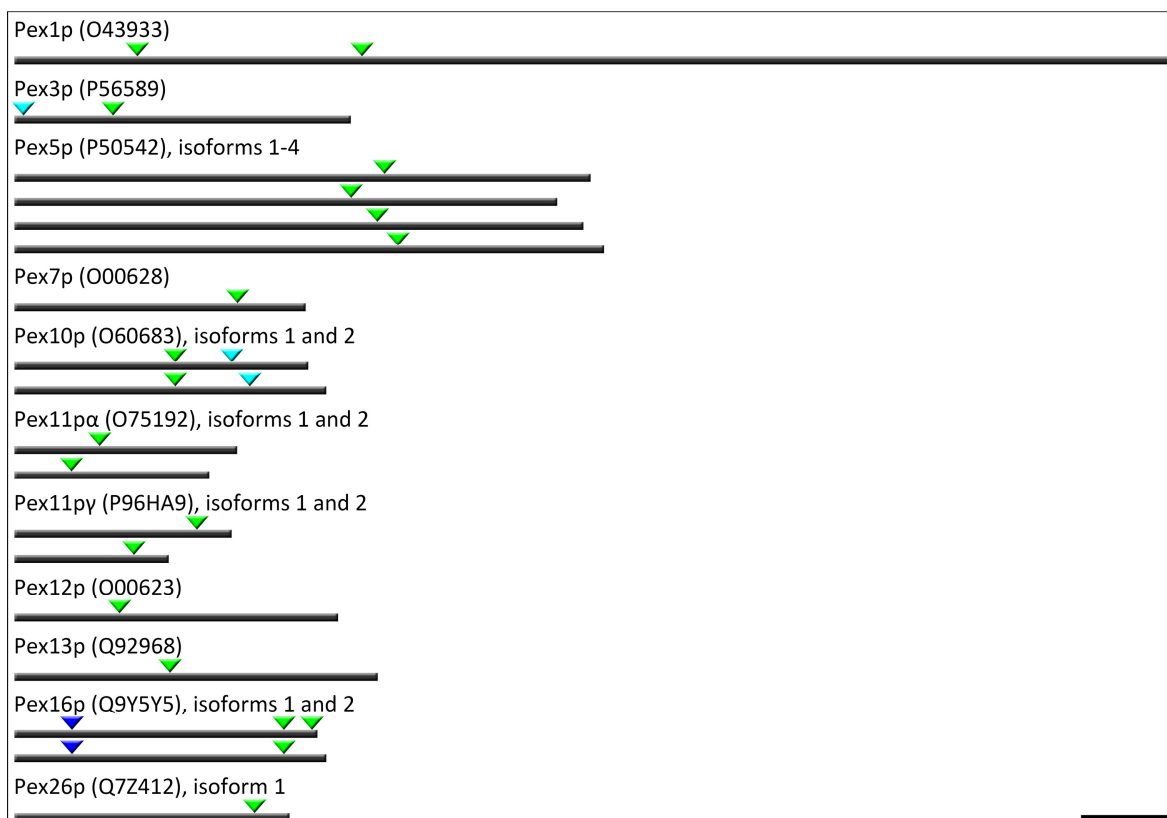
Figure 9: Several human peroxins possess PP1-binding motifs.
The sequences were collected from UniProtKB database and loaded in the ScanProsite program as well as the PP1-binding motifs canonical sequences listed on Table 5. Green triangles point matches with RVxF motifs. Dark blue triangles point matches with the SILK motif and light blue boxes point matches with other RVxF-cooperating motifs. Bar, 100 amino acids. For more detailed information, such as sequences and position of the matches within the proteins see Supplementary Table 1.

4.1.2 Pex16p as a potential PP1 interacting protein

Along with Pex3p and Pex19p, Pex16p is generally referred as an "early" peroxin because of its essential role in the initial steps of peroxisome biogenesis (353). However, the precise roles of these peroxins appear to vary considerably depending on the organism. For instance, besides the role on PMP reception of Pex19p (128, 133) and Pex3p (135,

136), they have been implicated in peroxisome inheritance in yeast (134, 137). Pex3p serves also in the degradation of yeast peroxisomes (138). Nonetheless, Pex16p seems to possess the most diverse set of functions, ranging from a matrix-localized, peripheral membrane protein involved in peroxisomal fission in the yeast *Yarrowia lipolytica* (145, 146), to an integral membrane-bound PMP receptor at the ER and peroxisomes in mammals (140, 143, 144) and plants (141, 142). Notably, Pex16p homologues are absent in some well characterized model organisms, including *Saccharomyces cerevisiae* (71) and *Caenorhabditis elegans* (354). The studies on Pex16p have helped to develop the current working models for peroxisome biogenesis, shedding significant light on the role that ER plays in this process in evolutionarily distant organisms (355). The species wherein this peroxin has been best studied are *Yarrowia lipolytica*, *Arabidopsis thaliana* and *Homo sapiens*. Pex16p was first identified in *Yarrowia lipolytica*, where it was found to be peripherally associated with the inner surface of the peroxisomal membrane and was referred to play a role in peroxisomal fission (145). *Yl*Pex16p was also one of the first PMPs experimentally shown to target indirectly to peroxisomes via the ER (356). In *Arabidopsis thaliana*, Pex16p is also among the class II PMPs that sort to peroxisomes via the ER and possesses two predicted transmembrane domains (142). *At*Pex16p has been pointed out to be a receptor for Pex3p and class I PMPs (142). Likewise, human Pex16p also has two transmembrane domains and a topological orientation whereby both N- and C-terminus face the cytosol (352). *Hs*Pex16p is also distinct from *Yl*Pex16p as it does not appear to be directly involved in regulating peroxisome division, but, instead, functions as a PMP receptor during the early stages of the *de novo* peroxisome formation at the ER, as well as in mature peroxisomes (143, 144). Consistent with this, the loss of *Hs*Pex16p, unlike *Yl*Pex16p, results in the complete absence of any peroxisomal structures (352). More recently, studies have demonstrated that *Hs*Pex16p is capable to recruit several PMPs, such as Pex3p, Pex34p, Pex26p, Pex10p, Pex11βp and Fis1 to the ER (140, 141). This property seems to be conserved at least between mammals and plants (141). Despite the similarities, Pex16p homologs from metazoans, yeast and plants are separated into distinct clades (Figure 10), indicating early diversification and perhaps functional specialization (355).
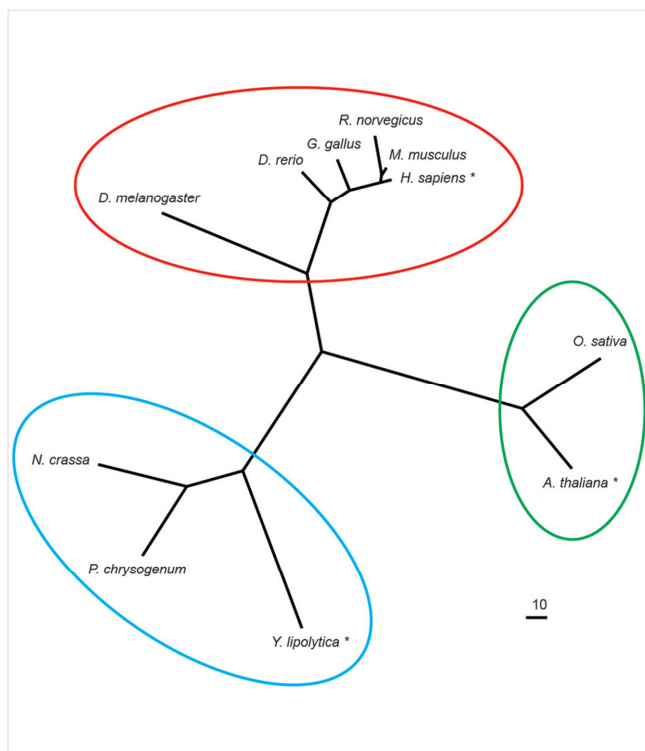
Figure 10: Phylogenetic analysis of Pex16p sequences from selected evolutionarily diverse species

Each protein is labeled based on its respective Genus and species, and circles represent Pex16p proteins of the metazoans (red), yeast (blue) and plants (green) that form distinct clades. Branch lengths of the tree are proportional to divergence with the "10" scale bar representing a 10% change. Sequence alignments were carried out using either CLUSTALW (357) and the phylogram was generated using the program TreeView (v1.6.6). Genbank® accession numbers are as follows: *Homo sapiens* (BAA88826.1), *Rattus norvegicus* (NP_001012088.1), *Mus musculus* (NP_660104.2), *Drosophila melanogaster* (NP_649252.1), *Neurospora crassa* (XP_963884.2), *Danio rerio* (NP_001020340.1), *Gallus gallus* (XP_421125.3), *Penicillium chrysogenum* (ABH11422.1), *Yarrowia lipolytica* (AAB41724.1), *Arabidopsis thaliana* (NP_566053.1), *Oryza sativa* (EEC72380.1). Adapted from (355).

4.1.2.1 Pex16p from other species also have PP1-binding motifs

Pex16p homologs were also screened for PP1-binding motifs (Figure 11, Supplementary Table 5). The species were selected based on organisms expressing Pex16p that are listed in Peroxisome DB 2.0 (www.peroxisomedb.org). The sequences were collected from UniProtKB database and screened for PP1-binding motifs using the ScanProsite server. The PP1-binding motifs' canonical sequences are listed in Table 5.
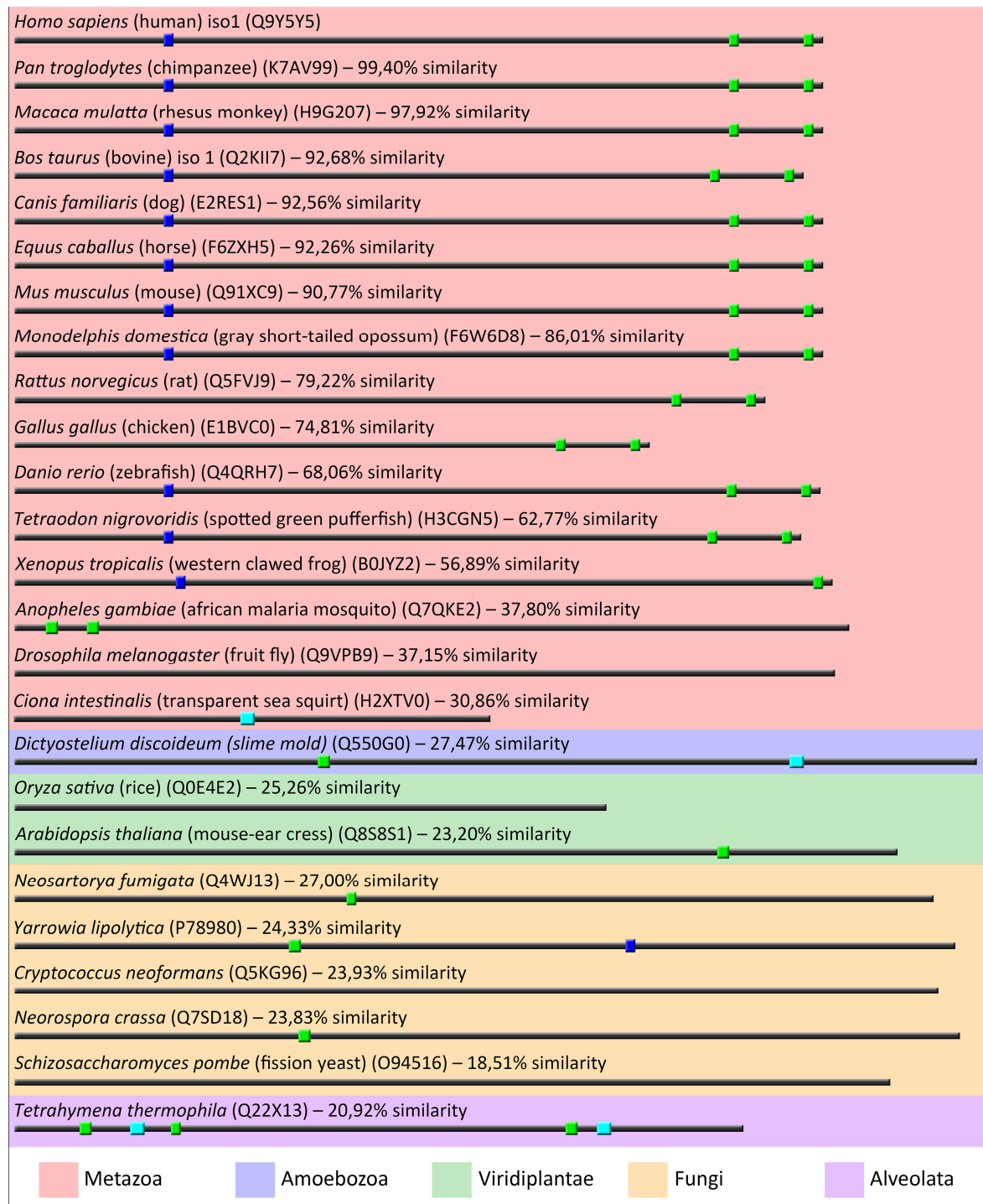
Figure 11: Homologs of Pex16p from different organisms also have predicted PP1-binding motifs
Sequences are ordered by percentage of similarity when compared with human Pex16p and by taxa. Similarity was calculated by alignment using the Clustal Omega program (Supplementary Table 4). The sequences were screened for PP1-binding motifs using the canonical sequences listed on Table 5. Green boxes represent matches with RVxF motifs. Dark blue boxes represent matches with the SILK motif and light blue boxes represent other RVxF-cooperating motifs. For more detailed information, such as sequences and position of the matches within the proteins see Supplementary Table 5.

PP1-binding motifs were found in almost all the screened sequences, even in evolutionarily distant species (Figure 11). *Anopheles gambiae* Pex16p has two RVxF motifs while *Drosophila melanogaster* Pex16p doesn't have any PP1-binding motif, but they share only 44,21% similarity (Supplementary Table 4), reflecting the extraordinary diversity among insects. Noteworthy, *Drosophila pex16* mutant, although reflecting broad symptoms of PBDs, it doesn't exhibit the infant death seen in Zellweger syndrome patients (358). *Ciona intestinalis* (tunicate) Pex16p does not possess a RVxF motif either; however, this is the most distant metazoan among the screened sequences. Within plants, only *Arabodipsis thaliana* Pex16p has an RVxF motif, nonetheless, it shares only 45,46% similarity with *Oryza sativa* Pex16p (Supplementary Table 4), which may indicate that Pex16p in these plant species has slightly different structure and/or function. Even with a similarity of only 56,89% *Xenopus tropicalis* Pex16p conserves one RVxF and SILK motifs. Curiously, most fungi also have RVxF motif, but it is positioned within the N-terminus. *Yarrowia lipolytica* Pex16p even has a SILK motif, although C-terminally localized. Noteworthy, *Yl*Pex16p is known to have a completely different topology from *Hs*Pex16p, without transmembrane domains and faced into the peroxisome lumen (145, 146).

The presence of PP1-binding motifs in most of *Hs*Pex16p homologs may indicate that a putative interaction with PP1 is of significant importance, implying that PP1 may have a role in peroxisome biogenesis through interaction with Pex16p.

4.1.2.2 PP1-binding motifs may be affected in PEX16 patients

4.1.2.2.1 RVxF motifs localize in the C-terminus

The two RVxF motifs of Pex16p localize at the residues 298-301 and 329-332 (Figure 12). Henceforward and for simplicity, first and second RVxF motifs are named PP1-binding motif 1 (PP1BM1) and PP1-binding motif 2 (PP1BM2). The RVxF-cooperating SILK motif localizes at the residues 63-66. SILK motif, with the consensus sequence [GS]-I-L-[RK], is present in several PP1 regulators and it usually occurs N-terminally to the RVxF motif. Furtermore, SILK motif docking site within PP1 differs from one of RVxF motif (β-sheets

12 and 13) (299). In Pex16p, the SILK motif is 231 and 262 amino acids apart from PP1BM1 and PP1BM2, respectively. Although very distant, Pex16p has two transmembrane domains (TMDs) and is supposed to expose both N- and C-termini to the cytosol (Figure 13) (120, 352). This topology might allow the SILK motif to become close enough to the PP1BMs to simultaneously interact with PP1.

```
MEKLRLLGLRYQEYVTRHPAATAQLETAVRGFSYLLAGRFADSHELSELVYSASNLLVLL 60
  SILK motif
NDGILRKELRKKLPVSLSQQKLLTWLSVLECVEVFMEMGAAKVWGEVGRWLVIALVQLAK 120

AVLRMLLLLWFKAGLQTSPPIVPLDRETQAQPPDGDHSPGNHEQSYVGKRSNRVVRTLQN 180

TPSLHSRHWGAPQQREGRQQQHHEELSATPTPLGLQETIAEFLYIARPLLHLLSLGLWGQ 240
                                                      PP1BM1
RSWKPWLLAGVVDVTSLSLLSDRKGLTRRERRELRRRTILLLYYLLRSPFYDRFSEARIL 300
                    PP1BM2
FLLQLLADHVPGVGLVTRPLMDYLPTWQKIYFYSWG 336
```

Figure 12: Human Pex16p and PP1-binding motifs
SILK motif (blue), PP1BMs (green), putative transmembrane domains (yellow). The underlined residues correspond to exon 11a, which in variant 2 are substituted by the residues TSQRAASPCLPARPHTQPWSPPAFLPGHP, reaching a total length of 346 amino acids.

The *PEX16* gene is localized at chromosome 11p12-p11.2 and consists of 11 exons. In humans, two different mRNA variants of PEX16 are produced as a result of alternative splicing, each with an alternative exon 11 (exon 11a and exon 11b). Pex16p variant 2, which harbours exon 11b, has a different C-terminus from residue 318, with a total length of 346 amino acids (Figure 12). Consequently, variant 2 possesses only PP1BM1. Both transcription variants are expressed in human fibroblasts, of which variant 1 containing exon 11a is the most abundant (350). The present work was focused on variant 1 which, in this document, is named solely Pex16p.

In addition to the transmembrane domains (120, 352), other domains have been identified (Figure 13). Residues 59-219 revealed to be necessary for the interaction with Pex19p (152). Moreover, residues 66-81 were demonstrated to be responsible for the targeting to peroxisomes and residues 83-103 for the PMP recruitment to the ER (141). Notably, all this domains localize in the N-terminus. Until now, no functional domains were identified within the cytosolic C-terminus.
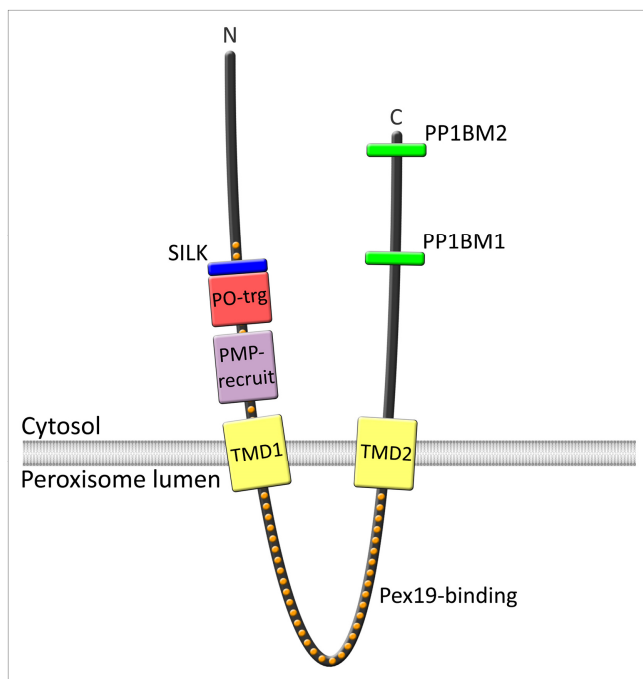
Figure 13: Pex16p predicted topology and functional domains
Boxes represent specific regions: SILK (aa 63-66), SILK domain; PO-trg (aa 66-81), peroxisome targeting domain; PMP-recruit (aa 83-103), PMP recruitment domain; TMD1 (aa 110-131), transmembrane domain 1; TMD2 (aa 222-243), transmembrane domain 2; PP1BM1 (aa 298-301), PP1-binding motif 1; PP1BM2 (aa 329-332), PP1-binding motif 2. Dashed area (aa 59-219) represents the necessary zone for interaction with Pex19p.

4.1.2.2.2   Mutations of *PEX16* patients affect the C-terminus

So far, ten patients with mutated *PEX16* gene have been reported (118, 349-351). Four of these patients belong to complementation group D, carrying the most severe form of Zellweger spectrum diseases, Zellweger syndrome (ZS). The first to be identified had a nonsense mutation, introducing a stop codon at position 176 (352) (Figure 14, a). Other two ZS patients, although unrelated, both carried a splice site mutation, which caused a frameshift at codon 298 introducing a stop codon at position 336 (349) (Figure 14, b). The latter ZS patient to be identified also carried a splice site mutation, which caused a frameshift at position 121 and an immediate stop at 122 (351) (Figure 14, c). Fibroblasts of all of the four patients presented the typical ZS cell phenotype caused by mutations of *PEX3*, *PEX16* and *PEX19*, characterized by the total absence of peroxisomes. Remarkably, the other six *PEX16* patients presented an unexpected mild variant of peroxisome biogenesis disorder. These patients developed progressive spastic paraparesis and ataxia in the preschool years (with a characteristic pattern of progressive leucodystrophy and brain atrophy); latter developed also cataracts and peripheral neuropathy. Plasma analysis revealed biochemical abnormalities suggesting a peroxisomal disorder. Surprisingly, their fibroblasts showed import-competent peroxisomes, which were

increased in size but reduced in number (350). From these six patients, five homozygotic mutations of *PEX16* were identified: patients 1 and 2, siblings, carried a single-nucleotide deletion in exon 11a, provoking a frameshift and introducing a stop codon at position 356 (Figure 14, e) (exon 11b is intact in both patients); patient 3 carried an in frame deletion of a valine at position 252 (Figure 14, f), affecting both variants; patient 4 carried a missense mutation leading to the substitution of a threonine for a proline at position 289 (Figure 14, g), affecting both variants; patient 5 carried a missense mutation leading to the substitution of a cysteine for a tyrosine at position 331 (Figure 14, h), affecting only variant 1; patient 6 carried a large intragenic deletion leading to the expression of three splice variants, causing frameshifts from positions 296 (with a stop at position 328) and 318 (with stop codons at positions 355 and 455) (Figure 14, i). Despite the differences in the mutations, these patients had similar fibroblasts, all with import-competent, reduced in number and enlarged peroxisomes.
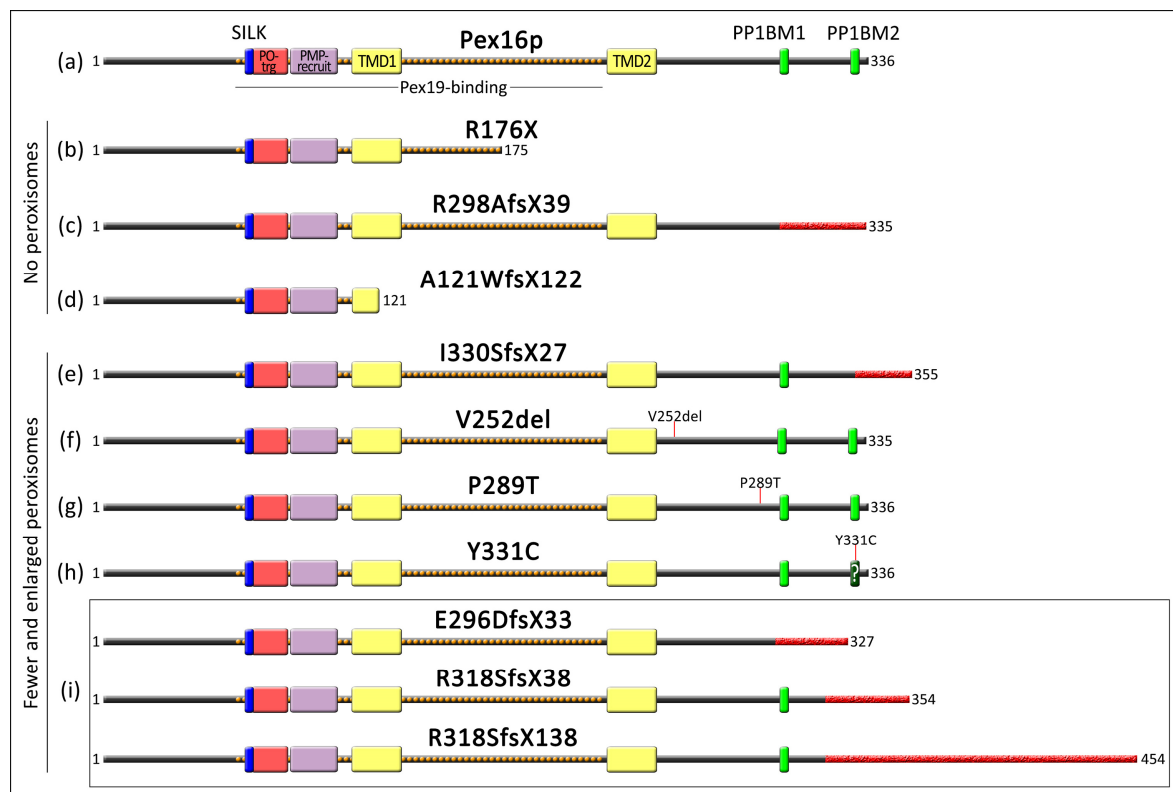
Figure 14: *PEX16* mutations identified in PBD patients
(a) Schematic representation of wild type Pex16p (variant 1) and (b-h) Pex16p mutations of reported patients. Known and putative domains are depicted: SILK (aa 63-66), SILK domain; PO-trg (aa 66-81), peroxisome targeting domain; PMP-recruit (aa 83-103), PMP recruitment domain; TMD1 (aa 110-131), transmembrane domain 1; TMD2 (aa 222-243), transmembrane domain 2; PP1BM1 (aa 298-301), PP1-

binding motif 1; PP1BM2 (aa 329-332), PP1-binding motif 2. Dashed area (aa 59-219) represents the necessary zone for interaction with Pex19p. Red areas indicate frameshifted parts of the proteins. Fibroblasts from patients carrying the mutations represented by (b), (c) and (d) were peroxisomes lacking (118, 349, 351); fibroblasts from patients carrying the mutations represented by (e) to (i) contained import-competent peroxisomes which were reduced in number and enlarged (350).

All the patients had mutations that affected solely the C-terminus, not involving any of the up to date known functional domains. The exceptions are the first and the last patients identified (Figure 14, b and d), which do not have the TMD2 or both TMDs (118, 351). However, the patients described by Shimozawa and colleagues (349) harbour both TMDs and approximately half of the cytosolic C-terminus (Figure 14, c) but Pex16p function is equally extensively affected. This can be due to the lack of the last 39 amino acids and/or the changed C-terminus may structurally affect its function. The intriguing cases reported by Ebberink and colleagues (350) suggest that Pex16p function in those patients is just mildly affected. These results indicate that, besides membrane assembly, Pex16p may be involved in morphology and division of peroxisomes.

So a question arises: which functional domains are localized in the C-terminus? Can PP1-binding motifs and a consequent interaction with PP1 be the answer? Curiously, in the case represented by letter e in Figure 14, the frameshift starts exactly in the PP1BM2. Also in the case represented by i in Figure 14, no PP1BM2 is present in any of the transcript variants. In the case where a tyrosine is substituted by a cysteine in position 331 (Figure 14, h), a single amino acid is changed in the RVxF motif. This change occurs in the most variable residue of the RVxF motif and a cysteine is accepted in this position by all published consensus sequences (Table 5). Actually, tyrosine is an excluded residue for this position in the more specific consensus sequences, but less sensitive though. Tyrosine is an aromatic amino acid and cysteine is not, but both are hydrophobic and uncharged. In any case, it is curious to notice that a single amino acid mutation can affect Pex16p's function as extensively as a frameshift from residue 298. These clinical cases lead us to conclude that some crucial domain(s) are localized in the more distal C-terminus of the protein. Also noteworthy are the other two cases, in which a single in frame deletion (Figure 14, f) and a single amino acid substitution (Figure 14, g) also affect Pex16p function, causing a similar phenotype. In the latter case, a proline in substituted by a

tyrosine. Proline is an amino acid with exceptionally rigid conformation, which influences protein secondary structure. This way, the substitution of proline by any other amino acid may considerably affect protein's structure and, possibly, its function. In the case of this patient (Figure 14, g), the proline-to-tyrosine substitution affects the distal C-terminus, another evidence that some functional domain in this area is being influenced. On the other hand, such structural changes in the protein may affect its stability and/or influence its degradation rate.

4.1.3   PP1-Pex16p binding studies do not prove the putative interaction

For this study, several PEX16 mutants were created (Figure 15) to serve as tools to clarify the putative PP1-Pex16p interaction and its role in peroxisome biogenesis. Being the first and fourth residues of the RVxF motif the most conserved ones (299), we considered that substituting these residues for alanines would be sufficient to interfere with the potential binding of Pex16p to PP1. These mutants were inserted in mammalian (pCMV-tag3A, pEGFP-C1), yeast (pACT2) and bacterial (pET28b, pGEX-4T-3) expression vectors. Cloning strategies are described in Material and methods, Table 12.
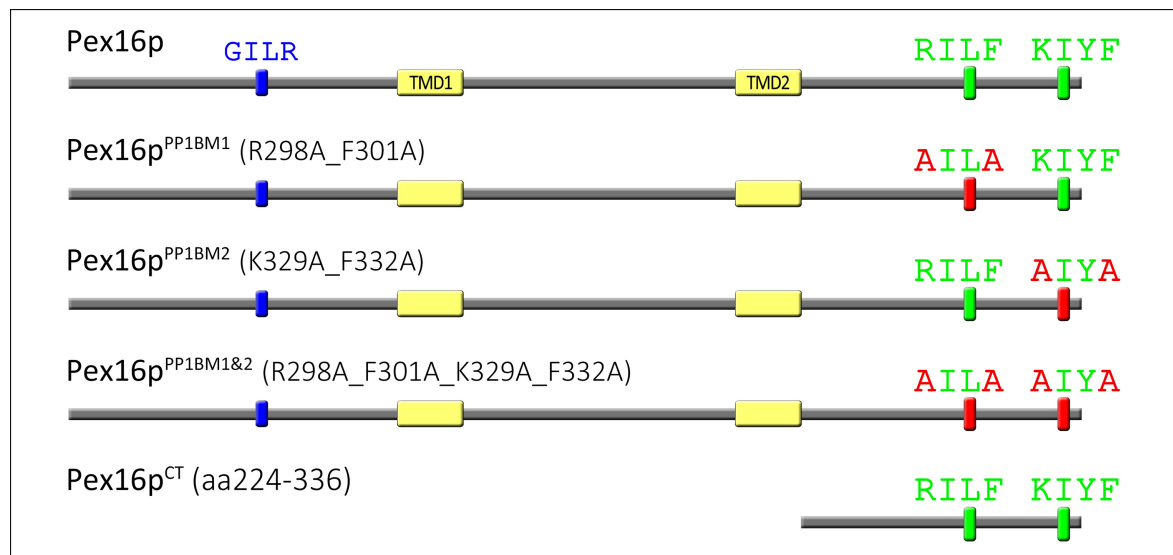
Figure 15: Pex16p mutants generated for this study
Residues depicted in red are the ones that were mutated. Yellow-shaded areas correspond to transmembrane domains (TMD).

To confirm a protein-protein interaction between Pex16p and PP1, different approaches were established and applied. As Pex16p was identified in a yeast two-hybrid screen with PP1γ2 (307), PP1γ isoform was the one elected to perform the studies on the putative Pex16p-PP1 interaction. In the cases in which the splice isoforms needed to be discriminated, e.g. experiments in which PP1γ overexpression is induced, PP1γ1 was the selected isoform because PP1γ1, contrary to PP1γ2, is ubiquitously expressed (312).

4.1.3.1 Two co-immunoprecipitation techniques give inconclusive results

One of the chosen protein-protein techniques to investigate the PP1-Pex16p interaction was pull-down by co-immunoprecipitation (co-IP). Two approaches were tested, both by Pex16p overexpression in COS-7 cells. In one of them were used antibody-coupled beads (section 4.1.3.1.1) and in the other one were used magnetic beads coupled to a GFP-binding peptide – GFP-Trap_M® system from Chromotek (section 4.1.3.1.2). This peptide is derived from the antigen-binding domain of alpaca-raised anti-GFP antibody. In co-immunoprecipitation assays, the results can be influenced by several parameters, such as buffers, temperature, antibodies, tags, expression levels, etc. For this study, several setup conditions were tried and the following two sections report the clearer results from the multiple co-immunoprecipitation experiments that were executed.

4.1.3.1.1 PP1γ1 co-immunoprecipitates with Myc-Pex16p

COS-7 cells were transfected with the respective plasmids encoding either A) PP1γ1, B) Myc-Pex16p or C) PP1γ1 and Myc-Pex16p (Figure 16, panel I). The overexpressed PP1γ1 was untagged. In previous experiments we observed that the transfection with pcDNA3.1-PP1γ1 alone promoted a very high level of PP1γ1 expression, provoking its aggregation and high cell morbidity, which didn't occur while co-transfected with pcDNA3.1-Myc-Pex16 (data not shown). Given that, cells from group A were co-transfected with both empty and PP1γ1-coding cDNA expression plasmids. The transfection was verified by immunofluorescence (Figure 16, panel I). The IP (Figure 16, panel II) was performed with anti-Myc antibody as described in section 3.7.8.1.
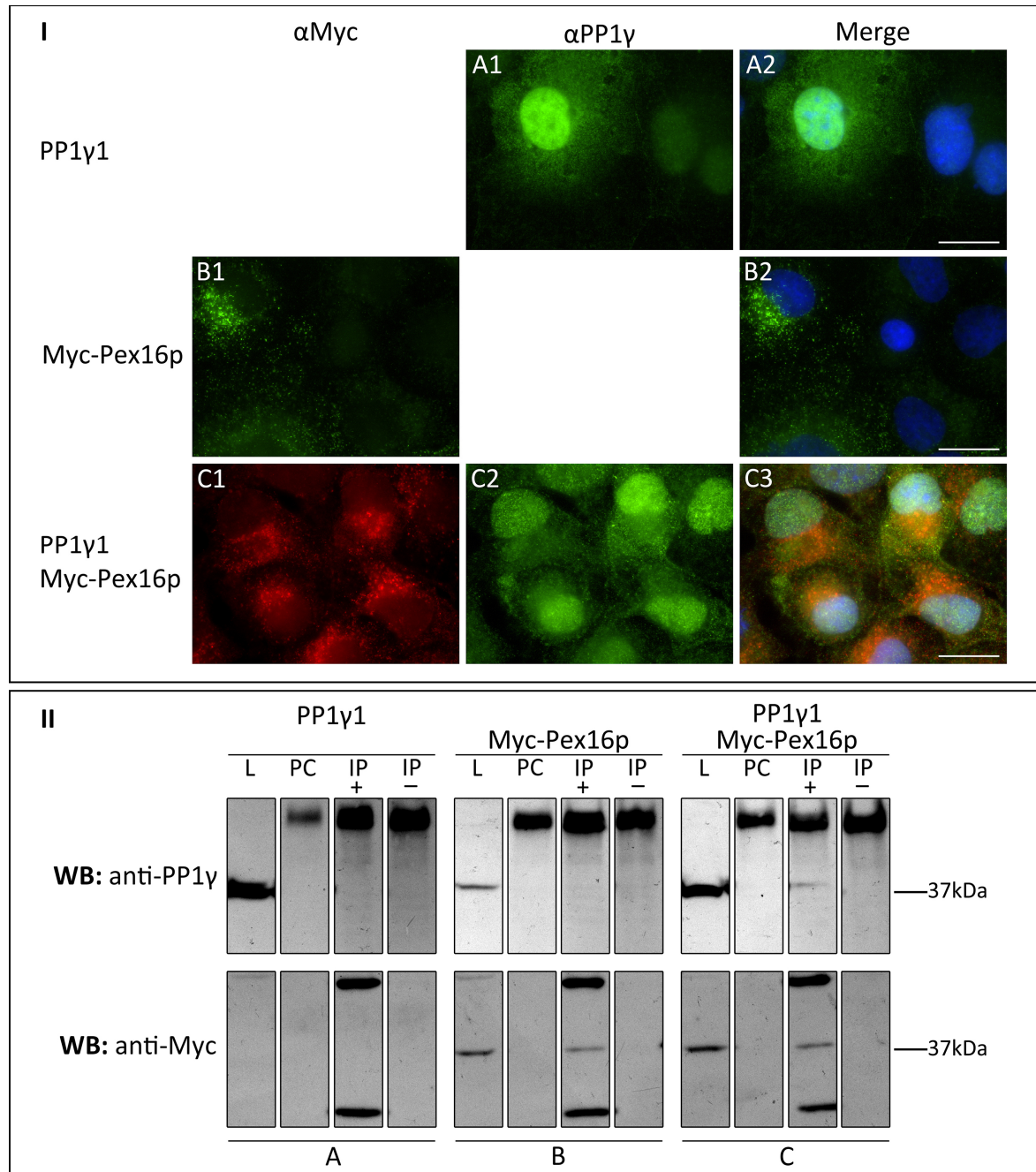
Figure 16: PP1γ1 co-immunoprecipitates with Myc-Pex16p
COS-7 cells were transfected with (A) PP1γ1, (B) Myc-Pex16p or (C) both. Panel I: immunofluorescence with anti-PP1γ (A1 and C2) and anti-Myc (B1 and C1) antibodies. Nuclei were labelled with Hoechst 33258. Bars, 20 μm. Panel II: Co-immunoprecipitation on cell lysates with anti-Myc antibody conjugated with protein-A-sepharose beads. The fractions were separated by 12,5% SDS-PAGE and blotted to a nitrocellulose membrane. Immunoblotting was performed with anti-PP1γ (top) and anti-Myc (bottom) antibodies. L, lysate; PC, pre-cleared beads; IP, immunoprecipitation beads with (+) and without (−) antibody.

To avoid unspecific binding to the beads, all lysates were subjected to a preclearance step by incubation of the lysates with beads without antibody (Figure 16, panel II, PC).

Afterwards, each precleared lysate was divided into two tubes and incubated with beads with and without anti-Myc antibody (Figure 16, panel II, IP+ and IP–, respectively). The latter was used as negative control to verify that PP1γ1 did not bind unspecifically to the beads. Group A was not expected to present any band on the IP lanes because the IP was made with anti-Myc antibody. Nonetheless, it was used as negative control to rule out any unspecific binding to the beads due to PP1γ1 overexpression (Figure 16, panel II, A). On group B, which cells overexpressed Myc-Pex16p alone, PP1γ is not detected in the IP with antibody (Figure 16, panel II, top, B, IP+). This means that endogenous PP1γ was not co-precipitated with Myc-Pex16p. However, PP1γ co-precipitated with Myc-Pex16p on group C, which cells overexpressed both PP1γ1 and Myc-Pex16p (Figure 16, panel II, top, C, IP+). Due to the fact that PP1γ1 and Myc-Pex16p have similar molecular weights, all samples were split in two and ran in separate gels to enable western blots with both anti-PP1γ (Figure 16, panel II, top) and anti-Myc antibodies (Figure 16, panel II, bottom). Anti-Myc labeling allowed verifying the expression of Myc-Pex16p and its specific binding to the beads.

4.1.3.1.2 PP1γ does not co-immunoprecipitate with GFP-Pex16p

Protein pull down using the GFP-Trap®_M method is very similar to immunoprecipitation with antibody-coupled beads; however, instead of an antibody, magnetic agarose beads are covalently coupled to a small GFP-binding protein. This technique is claimed to enable fast, reliable and one-step precipitations of a protein of interest fused to GFP or GFP variants. This system uses only the antigen-binding domain of alpaca-raised antibodies (359). This way, no heavy-chain bands appear in the gels and blots, possibly covering bands of interest. Another advantage of this system would be the use of GFP-tagged Pex16p, which significantly increases its molecular weight allowing using the whole fractions to detect Pex16p and PP1γ. Given this, we decided to use this approach to further verify the result from the conventional immunoprecipitation (previous section).
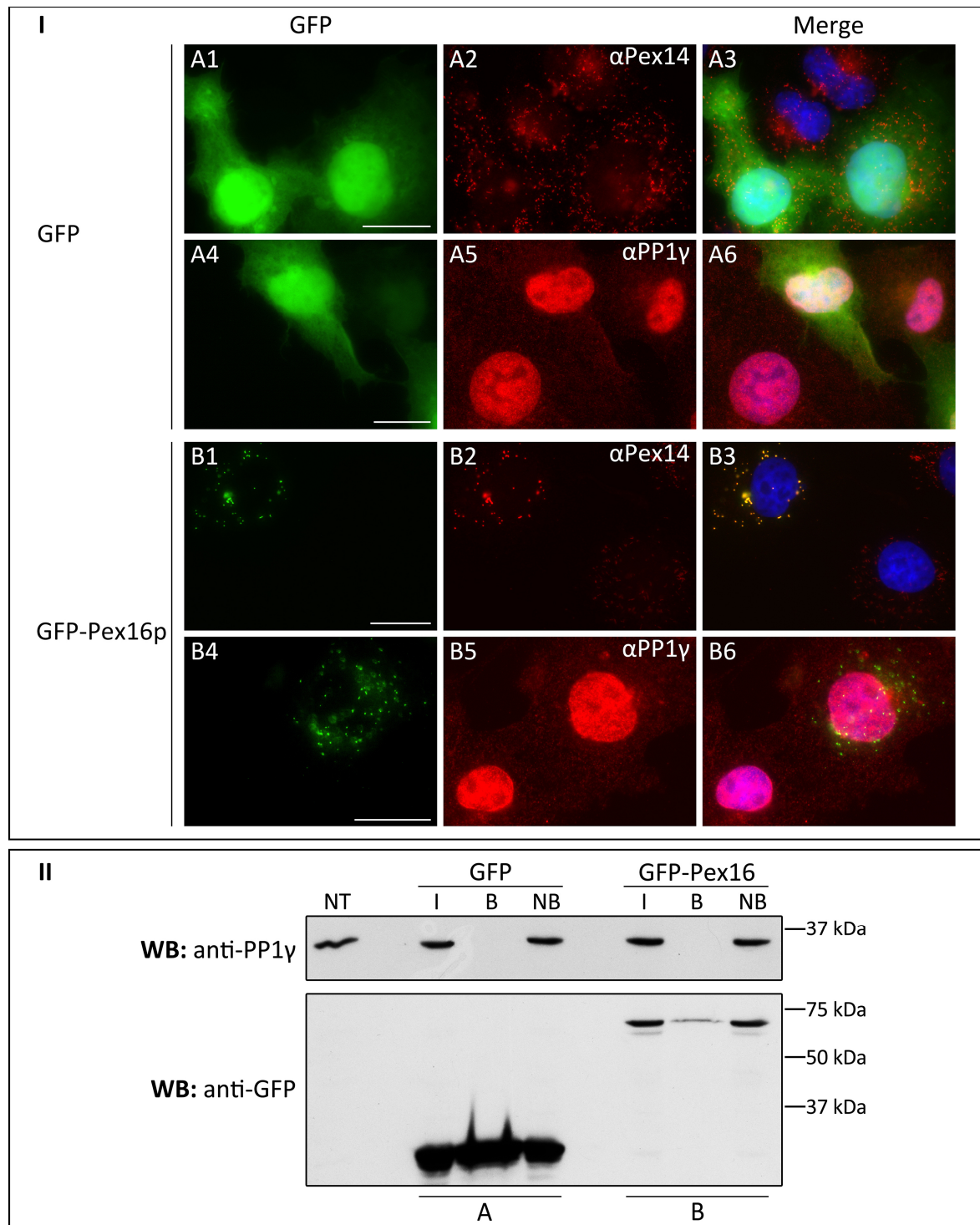
Figure 17: PP1γ does not co-immunoprecipitate with GFP-Pex16p

COS-7 cells were transfected with (A) GFP and (B) GFP-Pex16p. Panel I: immunofluorescence with anti-Pex14 (A1-A3, B1-B3) antibodies. Nuclei were labelled with Hoechst 33258. Bars, 20 μm. Panel II: co-immunoprecipitation on 1500 μg of cell lysates with GFP-binding protein-coupled magnetic beads. Non-transformed cells were harvested and lysed as well. 75 μg of protein of non-transformed (NT), input (I) and non-bound (NB), and the whole bound (B) fraction were separated by 12,5% SDS-PAGE and blotted to a nitrocellulose membrane. Immunobloting was performed with anti-PP1γ (top) and anti-GFP (bottom) antibodies.

For this approach, COS-7 cells were transfected by electroporation with either pEGFP-C1-Pex16 or empty pEGFP-C1 vector as negative control. The transfection was verified by immunofluorescence with anti-Pex14 and anti-PP1γ antibodies (Figure 17, panel I). GFP-Pex16p was targeted to peroxisomes (Figure 17, B1-B3), however, they are fewer and enlarged when compared to non-transfected cells or cells transfected with pEGFP-C1 empty vector, which can be due to GFP-induced clustering. In addition, being Pex16p an early peroxin involved in PMP import to peroxisomes, GFP-Pex16p overexpression could induce alterations on peroxisome morphology and number. Moreover, the cell mortality was very high.

The co-immunoprecipitation was performed as described in section 3.7.8.2. The lysates of the transfected cells (input fraction, Figure 17, panel II, I) were incubated with the magnetic beads, which were afterwards magnetically pelleted. The pellets constituted the bound fractions (Figure 17, panel II, B) and the supernatants the non-bound fractions (Figure 17, panel II, NB). The fractions were separated by SDS-PAGE and blotted to a nitrocellulose membrane. Immunoblotting was performed with anti-PP1γ antibody (Figure 17, panel II, top). PP1γ is present, as expected, on input and non-bound fractions at its predicted size, 37 kDa. PP1γ was not present in the bound fraction of the GFP control. However, PP1γ was not detected in the bound fraction of GFP-Pex16p as well. The membrane was even re-incubated with a more powerful ECL substrate (from BioRad) and exposed for a longer time, but PP1γ was still undetectable in the bound fractions. To confirm the presence of GFP and GFP-Pex16p in the bound fractions, the membrane was subsequently incubated with H_2O_2 for 30 minutes at 37 °C to erase the ECL signal and the membrane was re-blocked and incubated with anti-GFP antibody. As expected, GFP expressed at very high levels and was pulled down by the magnetic beads. GFP-Pex16p band was at the predicted size (66 kDa), but its expression level was considerably lower, and only a fraction of it bound to the beads.

The experiment was repeated either using a cross-linker or using a buffer with lower amount of detergents (10 mM Tris/Cl pH 7,5; 150 mM NaCl; 0,5 mM EDTA; 0,5% NP-40), but the results remained negative (not shown).

4.1.3.2 Pex16p does not interact with PP1γ1 in co-transformed yeast

The yeast co-transformation assay to probe protein-protein interactions uses the fact that most eukaryotic transcription activators have two functionally independent domains, the DNA-binding domain (BD), that recognizes a specific DNA sequence in the promoters of different genes, and activation domain (AD), which brings the transcriptional machinery to the promoter vicinity (360). Interaction of the BD fusion with the AD fusion positions the AD in the proximity of the reporter gene, thus activating its transcription (Figure 18). In the present work, AD (aa 768-881) and BD (aa 1-147) elements of GAL4, a yeast transcription factor involved in galactose metabolism, were fused with the two potentially interacting proteins, Pex16p and PP1γ1 respectively, and co-introduced into yeast cells that possess several reporter genes that were made to be transcriptionally dependent on activation through a binding site to the BD. Interacting proteins allow co-transfected yeast to grow in synthetic media lacking histidine and/or adenine by the activation of the reporter genes *HIS3* and *ADE2*, respectively. Interacting proteins also activate the reporter gene *MEL1*, which promotes the expression of α-galactosidase that is secreted to medium. X-α-Gal is a chromogenic substrate, which can be added to the medium and is hydrolysed by α-galactosidase causing yeast colonies to turn blue.
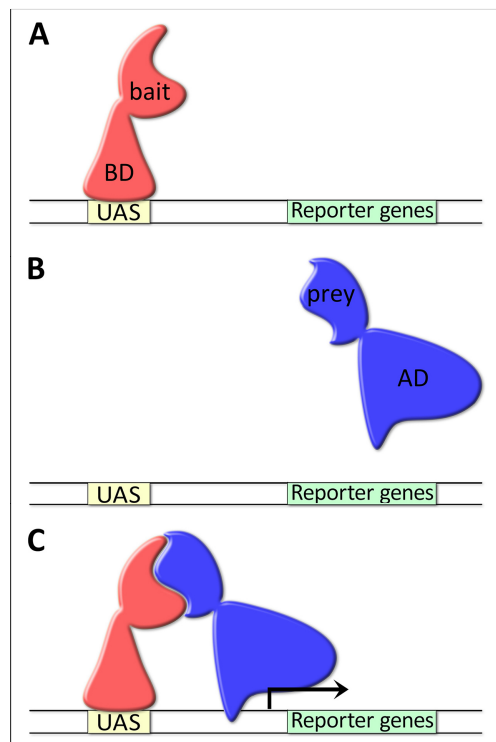
Figure 18: The yeast two-hybrid system
Two chimeric proteins are expressed in yeast: (A) GAL4 DNA-binding domain (BD) fused to a bait protein. The BD-bait hybrid protein can bind to upstream activation sites (UAS) but cannot activate transcription. (B) GAL4 activation domain (AD) fused to a prey protein. The AD-prey protein cannot recognize the UAS, thus, alone is not capable of initiating transcription. (C) When the bait and the prey interact, BD and AD are brought together and can activate reporter gene transcription.
pACT2 and pAS2-1 yeast expression vectors were used in this assay to generate GALAD- and GAL4BD-fused proteins, respectively. pACT2 contains *LEU2*, a nutritional gene that allows yeast auxothophs to grow on synthetic media lacking leucine amino acid. On the other hand, pAS2-1 contains *TRP1* gene that allows the growth in tryptophan-lacking media. pVA3-1 and pTD1-1 plasmids, encoding GAL4BD-p53 (aa72-390, murine) and GAL4AD-SV40 large T antigen (LT-AG, aa87-708) respectively, were used as positive control.

The previously generated pAS2-1-PP1γ1 construct (encoding GAL4BD-PP1γ1) that was used in the YTH screen of human brain cDNA library (307) was used in this study as bait as well. pACT2-Clone 18 (encoding GAL4AD-Clone 18), extracted from the YTH, was also used in order to reproduce the YTH results and test possible auto-activation of reporter genes. In addition to GAL4AD-fused wild-type Pex16p, other Pex16p versions were used: (a) with mutated PP1BMs and (b) cytosolic C-terminal tail (see Figure 15). The PP1BMs mutants were tested to verify if these domains were responsible for the putative PP1γ1-Pex16p interaction. On the other hand, despite pACT2 vector adding a nuclear targeting signal to the GAL4AD-fused proteins, the two transmembrane domains could arrest Pex16p to enter the nucleus and activate the transcription of the reporter genes. To overcome this possible setback, we also used a truncated Pex16p version containing solely the cytosolic C-terminal tail (aa244-336) (352), i.e. without the transmembrane domains but with the RVxF PP1-binding motifs. Table 24 summarizes the constructs that were used in this assay.

Table 24: List of constructs that were used in the protein-protein interaction assay by yeast co-transformation

	Plasmid name	Encoded recombinant protein
Baits	pAS2-1	GAL4AD
	pAS2-1-PP1γ1	GAL4AD-PP1γ1
	pVA3-1	GAL4AD-p53 (aa 72-390) (murine)
Preys	pACT2	GAL4BD
	pACT2-Clone 18	GAL4BD-Clone 18 (Pex16 YTH clone)
	pACT2-Pex16	GAL4BD-Pex16p
	pACT2-Pex16 PP1BM1	GAL4BD-Pex16p^{PP1BM1} (R298A_F301A)
	pACT2-Pex16 PP1BM2	GAL4BD-Pex16p^{PP1BM2} (K329A_F332A)
	pACT2-Pex16 PP1BM1&2	GAL4BD-Pex16p$^{PP1BM1\&2}$ (R298A_F301A_K329A_F332A)
	pACT2-Pex16 C-ter	GAL4BD-Pex16p^{CT} (aa244-336)
	pTD1-1	GAL4BD-SV40 LT-AG (aa 87-708)

The plasmids were inserted in the AH109 strain of *Saccharomyces cerevisiae* following the method described in section 3.8.15. To select transformed and co-transformed yeasts, cells were plated and incubated for 2-4 days at 30 °C in a synthetically defined medium supplemented with amino acids, excluding leucine (SD/-L), tryptophan (SD/-T) or both (SD/-T-L), according to the vectors that were inserted. Three single colonies transformed

with the desired plasmid(s) were then re-picked to the same SD/Dropout (SD/DO) which they have been collected from and incubated again for 2-3 days at 30 °C in order to get a higher and fresh amount of yeast to be re-picked later on into SD/DO interaction selective media. The SD/DOs that were used to select the yeasts with activated interaction reporter genes lacked histidine and/or adenine. 3-AT was used in some plates to supress leaky *HIS3* expression and to obtain a more accurate His⁻ phenotype. X-α-Gal was added to some plates as well. Yeasts were grown on interaction selective plates for 3-6 days at 30 °C.

In a first stage, the preys alone were inserted in yeast and grown in selective media and with X-α-Gal additive to test if they themselves were able to activate reporter genes. Empty pACT2 vector, encoding GAL4AD, was used as negative control; GAL4AD-p53 + GAL4BD-SV40 LT-AG was used as positive control (Figure 19, panel A). None of the yeasts transformed with the preys or bait alone were able to grow on interaction selective medium or to turn blue in the presence of X-α-Gal, meaning that they were unable to activate the reporter genes (Figure 19, panel A). This allowed us to use them further for the protein-protein interaction assay with PP1γ1 (Figure 19, panel B).

To perform the protein-protein interaction assay, baits and preys were co-inserted into the yeast. Several negative controls were used: GAL4BD + GAL4AD, GAL4BD-PP1γ1 + GAL4AD and GAL4BD + GAL4AD-Pex16p wild-type/mutants. GAL4BD-p53 + GAL4AD-SV40 LT-AG was used as positive control. GAL4BD-PP1γ1 + GAL4AD-Pex16p wild-type/mutants were used to verify PP1γ1-Pex16p putative interaction (Figure 19, panel B). As expected, the negative controls GAL4BD + GAL4AD and GAL4BD-PP1γ1 + GAL4AD did not grow in the interaction selective media. However, they presented some minor growth on SD/-T-L-H plates due to leaky *HIS3* expression, which is completely supressed by the addition of 3-AT.
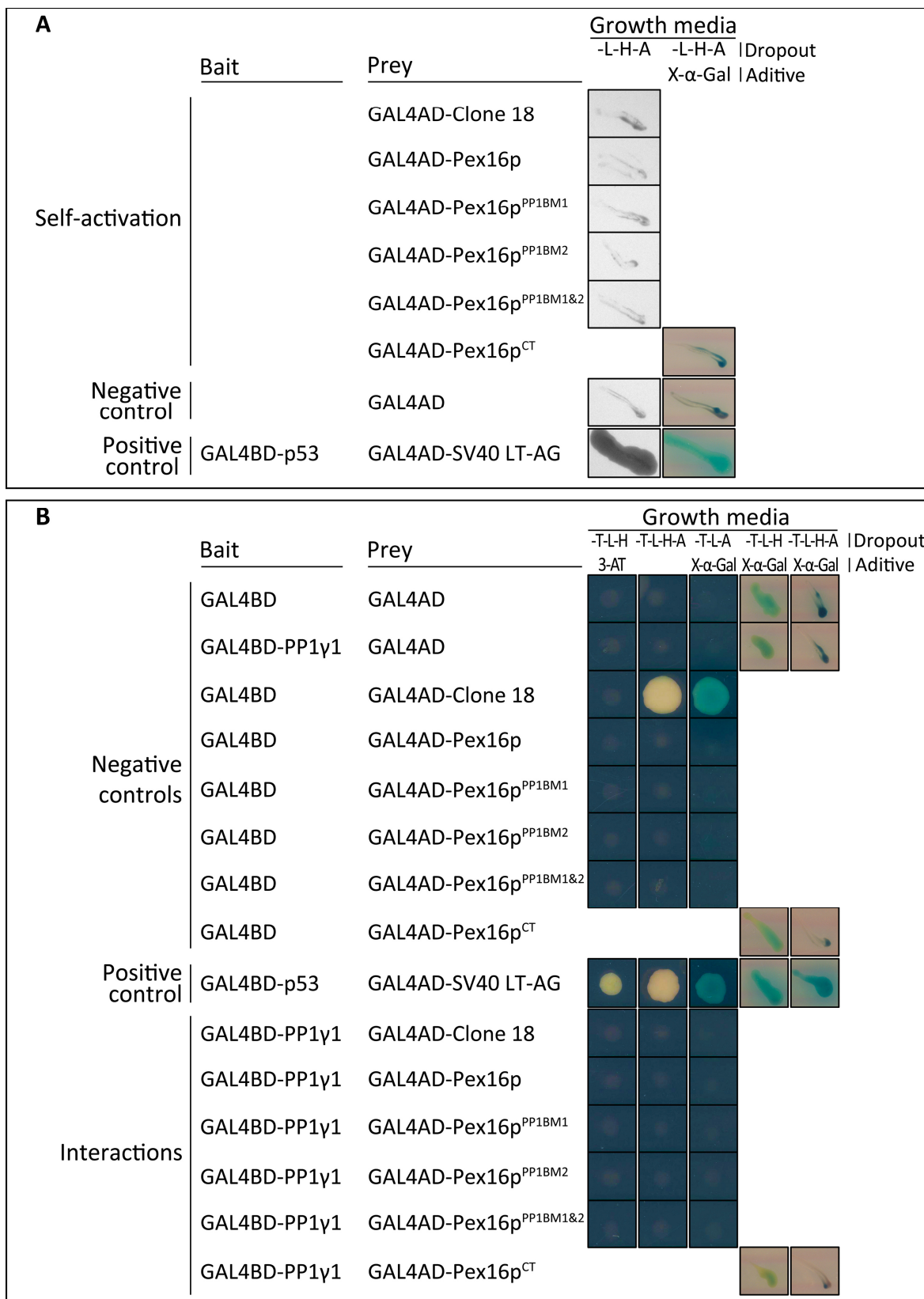
Figure 19: Protein-protein interaction assay by yeast co-transformation using strain AH109 reveals no interaction between PP1γ1 and Pex16p

The yeast growth media (agar plates) were composed by a synthetically defined medium supplemented with amino acids, excluding leucine (-L), tryptophan (-T), histidine (-H) and/or adenine (-A). 3-AT, added to

some plates, acts as leaky *HIS3* expression suppressor. X-α-Gal was added to some plates to test the activation of *MEL1* reporter gene. The pictures were taken after 2-6 days incubation at 30 °C. For this figure, one representative clone of each co-transformed yeast was selected. Panel A: self-activation control. Panel B: protein-protein interaction assay.

Yeasts co-transformed with GAL4AD-Clone 18 and GAL4BD were able to grow on SD/-T-L-H-A and SD/-T-L-A and to degrade X-α-Gal (Figure 19, panel B). The growth was inhibited on SD/-T-L-H by 3-AT. Although GAL4AD-Clone 18 alone was not able to self-activate the reporter genes (Figure 19, panel A), the presence of GAL4BD, although not recombined with another protein, allowed these yeasts to activate some of the reporter genes. The other negative controls, GAL4BD + GAL4AD-Pex16p wild-type/mutants did not activate any reporter gene (Figure 19, panel B).

When co-expressed with GAL4BD-PP1γ1, any of the GAL4AD-fused Pex16p versions were able to activate the reporter genes, even the truncated version. This means that none of the Pex16p versions interacted with PP1γ1 in our experimental set-up (Figure 19, panel B).

4.1.3.3   *PP1γ1 does not overlay in blot with Pex16p*

The protein blot overlay technique involves fractionating proteins on SDS-PAGE, blotting to a membrane, and the incubating with a probe of interest. Is this work, the probe used was purified PP1γ1, which was then visualized by antibody.

For this study, we examined several methods to express Pex16p. One of the methods used was the *in vitro* translation, using the kit TNT T7 Quick Coupled Transcription/Translation System from Promega. Two plasmids were used, pET28b-Pex16 and pET28b-Pex16 C-ter, (encoding His-Pex16p and His-Pex16p^{CT}). The expression was induced both in the presence and absence of recombinant Pex19p. In every case, there was no detectable expression (data not shown).

In vivo expression in mammalian cells was also approached. Two 10 cm confluent dishes of COS-7 cells were transfected by electroporation with pcDNA3.1-Myc-Pex16 plasmid,

encoding Myc-Pex16p. Non-transfected COS-7 cells were used as negative control. The cells were harvested and post-nuclear supernatants were prepared. The protein concentration of both samples was determined by the Bradford method and two 100 µg portions of each sample were precipitated by chloroform-methanol and separated by 12,5% SDS-PAGE. The gels were blotted onto nitrocellulose membranes. One of the membranes was used for immunoblotting with anti-Myc antibody to control for Myc-Pex16p expression (Figure 20, top).
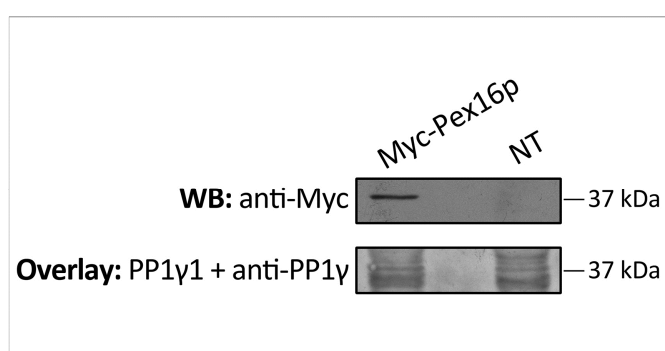
Figure 20: Protein blot overlay in mammalian cell lysates shows no interaction between PP1γ1 and Myc-Pex16p 100 µg of post nuclear supernatants of COS-7 cells transfected with Myc-Pex16p and non-transfected (NT) were separated by 12,5% SDS-PAGE and blotted to nitrocellulose membranes. WB: western blot using anti-Myc antibody. Overlay: protein blot overlay with purified PP1γ1 and detection with anti-PP1γ antibody.

As expected, the lane of the transfected cells (Figure 20, left) shows a protein band around 37 kDa, the predicted size for Myc-Pex16p. The other membrane was overlaid with purified PP1γ1 and labelled with anti-PP1γ antibody (Figure 20, bottom). Endogenous PP1γ, expressed in both transfected and non-transfected cells, should be labelled in the blot because anti-PP1γ antibody was used. However, this band would be indistinguishable from putative PP1γ1 overlaid on Myc-Pex16p because Myc-Pex16p and PP1γ have very similar expected molecular weight. Nonetheless, in case of positive interaction, the band intensity was expected to be significantly distinct due to the overexpression of Myc-Pex16p in transfected cells. However, both lanes displayed a similar band pattern, revealing no evident interaction between Myc-Pex16p and PP1γ1. Moreover, the overlay showed a significant amount of "unspecific" bands. This may be explained by the very high number of proteins that bind to PP1 (307). To try to circumvent this problem, the overlay was repeated, with peroxisome-enriched fractions using the same parameters. This was expected to significantly reduce "unspecific"

binding, but too many bands were still visible after immunoblotting and no differences between transfected and non-transfected cells were detected (data not shown). The problem concerning the similar molecular sizes of Pex16p and PP1γ1 could be overcome by the expression of Pex16p with a larger tag. By the time this assay was performed, a Pex16p-GFP construct was available but, as GFP was localized at the C-terminus, nearby the PP1BMs, it could potentially interfere with the PP1γ1-Pex16p interaction.

Pex16p was also expressed in bacteria. Several *E. coli* strains (XL-1 Blue, Rosetta DE3 and C41 DE3) were transformed with pET28b-Pex16 and tested under different conditions, such as temperature, incubation time and IPTG concentration (data not shown). His-Pex16p did not express under any of the tested conditions or strains. For this reason, pGEX family vectors were used. pGEX vectors add a glutathione S-transferase (GST) tag at the N-terminus of the protein as well as a protease cleaving site in between. These vectors are commonly used for protein purification. On the other hand, since GST composes a very large tag, it could reduce possible toxicity of the target protein. In fact, unlike His-Pex16p, it was possible to express GST-Pex16p, in Rosetta DE3 (vestigially) and C41 DE3. The C41 DE3 strain is used to generate membrane proteins that are difficult to express. Another approach to overcome this difficulty was to generate a construct without the transmembrane domains (Figure 15). This way, we generated the pGEX-4T-3-Pex16 C-ter, which encodes GST-Pex16^{CT}. The resulting fusion protein conserves the PP1BMs but lacks the transmembrane domains. Empty pGEX-4T-3 vector and non-transformed cells were used as negative controls. The determined optimal conditions for the expression were induction with 0,4 mM IPTG and overnight incubation at 18 °C.

In order to verify the molecular masses of the expressed proteins and to evaluate the expression levels in order to optimize the overlay experiment, one of the prepared aliquots were lysed, separated on 12,5% SDS-PAGE (equal protein amounts) and immunoblotted with anti-GST antibody (data not shown). The molecular masses were as expected. GST and GST-Pex16p^{CT} presented much higher expression levels than GST-Pex16p, indicating that a higher amount of the latter's lysate should be loaded for the subsequent protein blot overlay.

For the overlay (Figure 21) we used the stored aliquots of C41 DE3 induced to express GST, GST-Pex16p and GST-Pex16p^{CT}. As negative control, non-transformed cells were used. Total protein was obtained by resuspending and sonicating the pellets in 100 μl 1% SDS. As a well-known PIP, Nek2A (307) was used as positive control: 1% SDS lysate of Rosetta DE3 transformed with pET28c-Nek2A and induced to express the resulting recombinant His-Nek2A was used in this experiment (kindly provided by Luis Gregório, CBC, University of Aveiro). Protein concentration measurement of all samples was done by the BCA method. 1% SDS lysate of rat cortex was used as control for the anti-PP1γ antibody (kindly provided by Sara Esteves, CBC, University of Aveiro). In this sample, a 37 kDa band was expected, corresponding to the endogenous PP1γ in the rat cortex. The SDS-PAGE was loaded with different amounts of each sample, considering the expression levels of each recombinant protein observed previously (data not shown). After separation, the proteins were blotted to a nitrocellulose membrane and overlaid with 25 pmol/μl purified PP1γ1. Overlaid PP1γ1 was detected by subsequent incubation with anti-PP1γ antibody (Figure 21, panel A). The membrane was afterwards stripped and re-probed with anti-GST and anti-Myc antibodies (Figure 21, panel B).
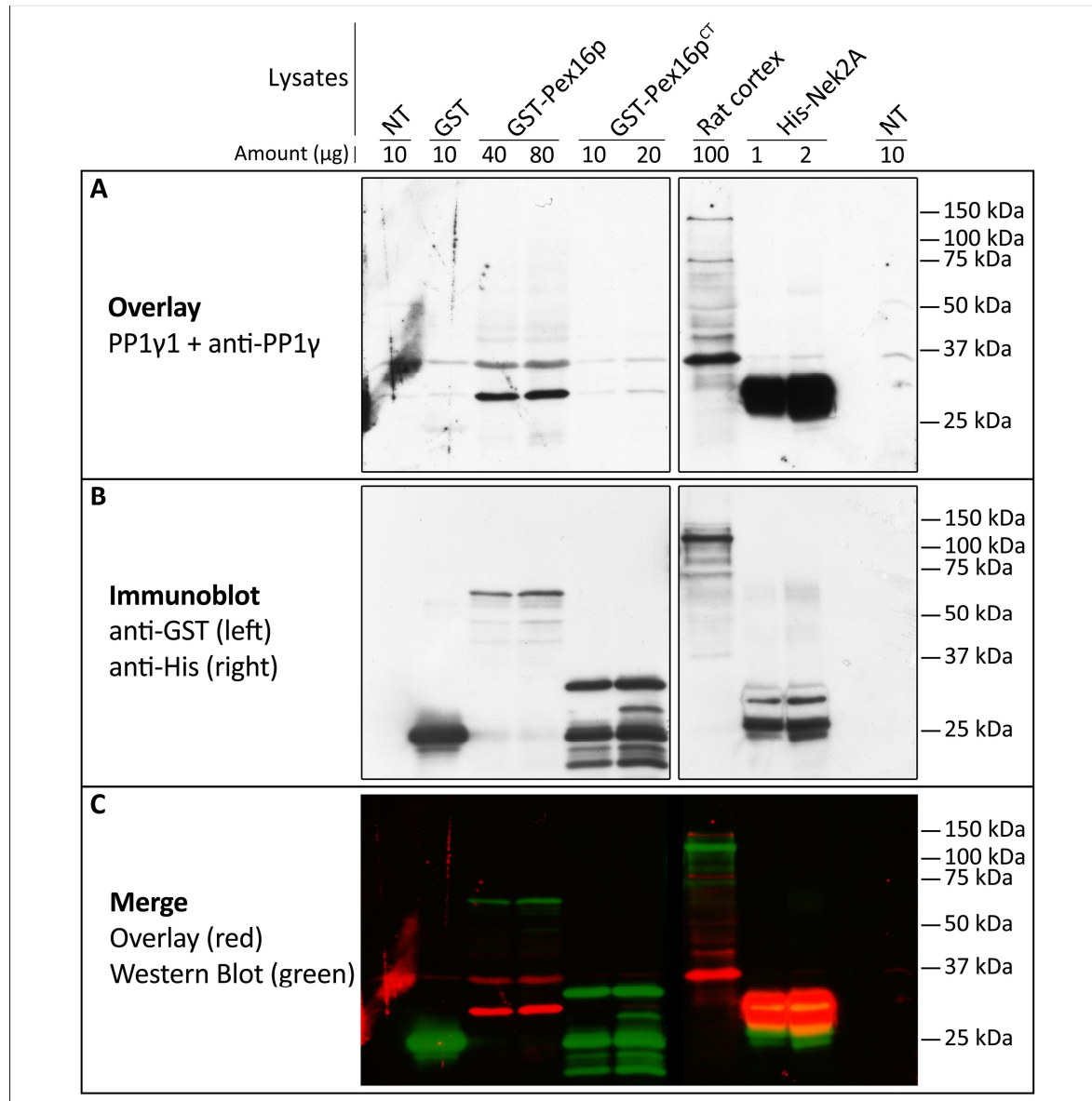
Figure 21: Protein blot overlay in bacterial lysates shows no interaction between PP1γ1 and GST-Pex16p or GST-Pex16^{CT}

C41 DE3 bacteria were transformed and induced to express GST, GST-Pex16p and GST-Pex16p^{CT}. 1% SDS buffer and sonication was used to lyse the cells and obtain total protein. Lysates of non-transformed (NT) and GST expressing bacteria were used as negative controls. Pre-prepared lysate of Rosetta DE3 transformed and induced to express His-Nek2A was used as positive control. Rat cortex lysate was used as control for anti-PP1γ antibody. The amount of protein (in µg) of each cell lysate loaded in the gel is indicated by the numbers on the top of each lane. The lysates were separated by 12,5 % SDS-PAGE and blotted to a nitrocellulose membrane. Panel A: the membrane was blocked and overlaid with 25 pmol/µl purified PP1γ1; the overlaid PP1γ1 was detected by subsequent incubation with anti-PP1γ antibody. Panel B: the membrane was stripped, cut and re-probed with anti-GST (left) and anti-His (right) antibodies. Panel C: merge image with the protein overlay (red) and the immunoblot (green). The signal of PP1γ1 overlay on His-Nek2A was so strong that the membrane stripping was not completely effective to remove it, which led to the emergence of a ghost band superimposed to His-Nek2A band.

On the overlay blot (Figure 21, panel A) two bands between 25 kDa and 37 kDa appear in all bacterial samples, including the non-transformed (NT) ones, indicating that they are unspecific. In the lane loaded with rat cortex lysate there is a band at the expectable size of 37 kDa, indicating that the anti-PP1γ antibody was functional (Figure 21, panel A). As expected, His-Nek2A gives a very strong overlay signal (Figure 21, panel A). This band overlaps with the His-Nek2A band on the immunoblot (Figure 21, panels B and C). GST-Pex16p and GST-Pex16p^{CT} samples do not present any band overlapping to the corresponding bands on the immunoblot, revealing no overlay with PP1γ1 (Figure 21, panel C).

Despite the samples were continuously handled on ice, there was some extent of protein degradation. Although no protease inhibitors were added to the lysis buffer, it was a denaturing buffer (1% SDS), making protein degradation by the action of proteases after cell lysis not expectable. It is likely that the observed protein degradation happens within the cells. As a matter of fact, pGEX vectors add a protease recognition site between the GST tag and the sub-cloned proteins.

4.1.4 Manipulation of the putative PP1-Pex16p interaction does not change peroxisome dynamics

4.1.4.1 *Pex16p overexpression in COS-7 cells does not change endogenous PP1α and PP1γ sub-cellular localization*

One of the first questions raised in this study was whether the overexpression of Pex16p in mammalian cells would influence the subcellular localization of PP1 which, during interfase, localizes in the cytoplasm and enriched in the nucleus (361). To test the overexpression and localization of Myc-Pex16p, COS-7 cells were transfected with pcDNA3.1-Myc-Pex16 by the PEI method and endogenous Pex14p was labelled as a marker for peroxisomes (Figure 22). Overexpressed Myc-Pex16p co-localizes with Pex14p, indicating that it is correctly targeted to the peroxisomal compartment.
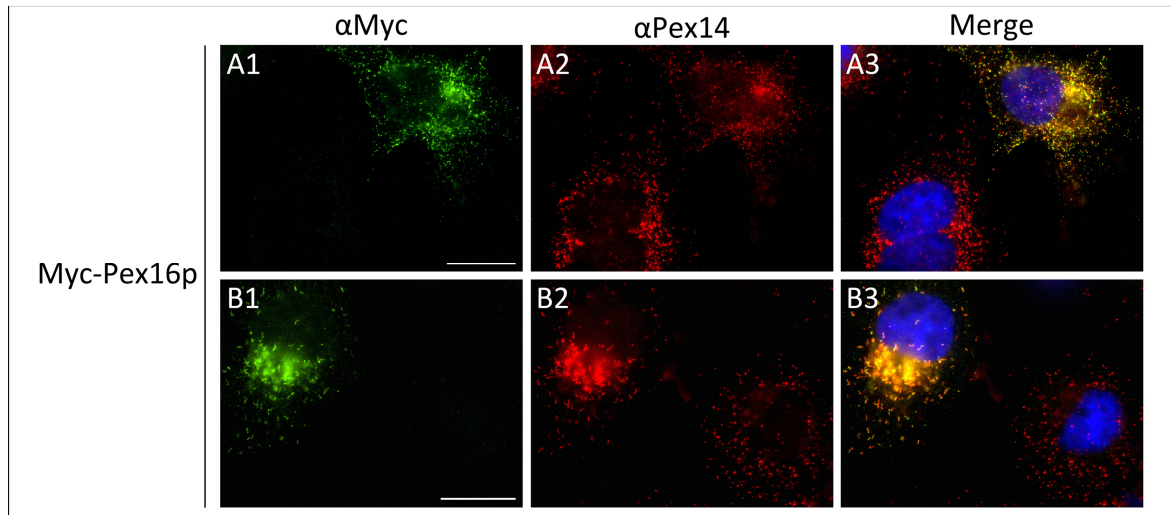
Figure 22: Overexpressed Myc-Pex16p localizes to peroxisomes
COS-7 cells were transfected with Myc-Pex16p and processed for immunofluorescence microscopy using anti-Myc (A1 and B1) and anti-Pex14 (A2 and B2) antibodies. Nuclei were labelled with Hoechst 33258. Bars, 20 μm.

Then, COS-7 cells were transfected with the same construct and endogenous PP1γ and PP1α proteins were labelled with the respective antibodies (Figure 23). Comparing transfected and non-transfected cells one cannot see any difference in the subcellular localization of both PP1α and PP1γ. Moreover, no co-localization is visible between Pex16p and PP1, which could mean that the amount of PP1 in peroxisomes is too low and/or the putative interaction has a transient nature, which could make it difficult to detect by fluorescence microscopy.
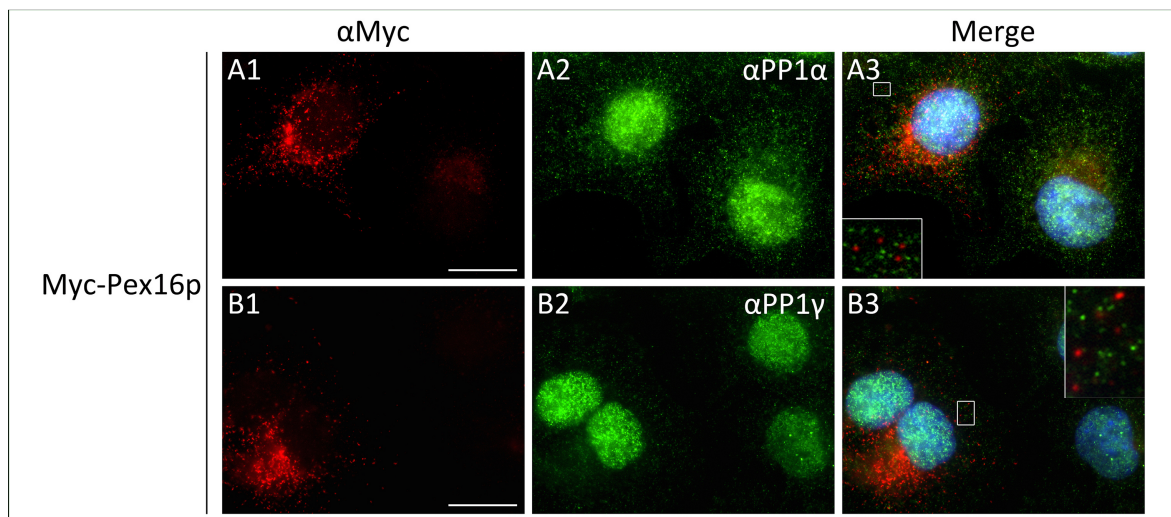
Figure 23: Overexpression of Myc-Pex16p does not change PP1 sub-cellular localization
COS-7 cells were transfected with Myc-Pex16p and processed for immunofluorescence with anti-Myc (A1 and B1) and anti-PP1α (A2) or anti-PP1γ (B2) antibodies. Nuclei were labelled with Hoechst 33258. Bars, 20 μm.

4.1.4.2 Overexpression of Pex16p PP1BMs mutants in COS-7 cells does not change peroxisomal morphology or number

In parallel to the interaction assays, experiments were performed in order to unravel the physiological role of a putative interaction between PP1γ1 and Pex16p. First, wild-type and PP1BMs mutants (see Figure 15) were cloned into the mammalian expression vector pCMV-tag3A, which adds a Myc tag N-terminally. COS-7 cells stably expressing GFP-SKL (COS-GFP-SKL), which display green fluorescent peroxisomes were transfected by PEI with the wild-type and the mutated versions of PEX16 (Figure 24). Observing the peroxisomes from transfected cells, there are not visible differences in peroxisome morphology, size or number between cells expressing with any of Myc-Pex16p PP1BMs mutants and Myc-Pex16p. However, GFP-SKL is a matrix protein, so an alteration of the membrane could not be visible in this approach.

Thus, COS-7 cells were transfected with Myc-Pex16p and Myc-Pex16p$^{PP1BM1\&2}$, which carry mutations in both RVxF motifs (see Figure 15). The cells were then labelled with anti-Pex14 and anti-ACOX antibodies to label membrane and matrix, respectively (Figure 25). Similarly to the experience with COS-GFP-SKL cell (Figure 24), no differences were visible concerning peroxisome morphology, size and/or number between cells expressing Myc-Pex16p and Myc-Pex16p$^{PP1BM1\&2}$. Nonetheless, a possible interaction between PP1 and Pex16p could not influence the peroxisomal number or morphology. Moreover, a difference could be only visible under specific conditions or stimuli. On the other hand, COS-7 cells endogenously express Pex16p, which could surpass the effect of the overexpression of a mutated Pex16p version.
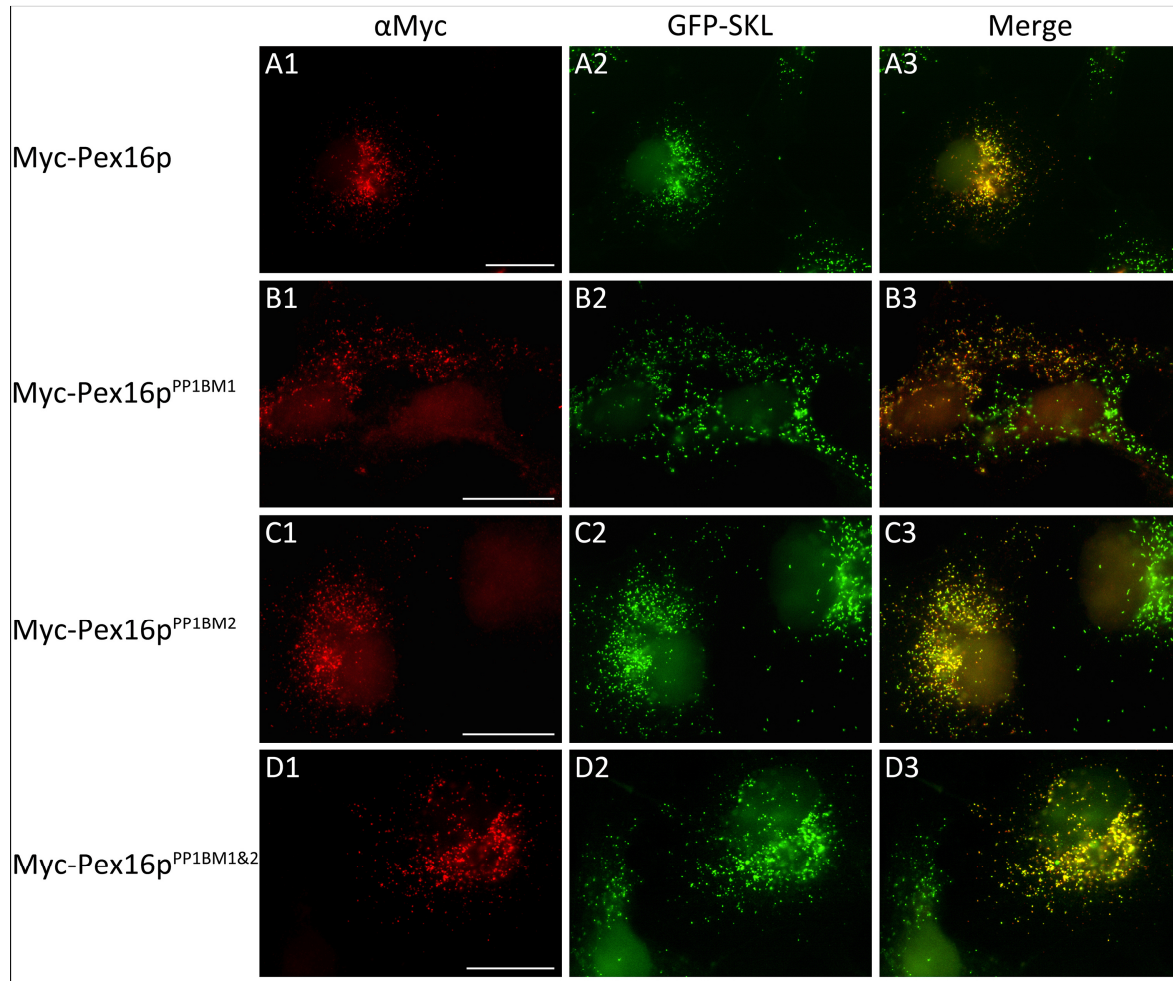
Figure 24: Overexpression of Myc-Pex16p with mutated PP1BMs does not change peroxisomal morphology or number

COS-GFP-SKL cells were transfected by PEI to express Myc-Pex16p, as well as Myc-Pex16p with mutations in the first RVxF motif (Myc-Pex16p^{PP1BM1}) or in the second (Myc-Pex16p^{PP1BM2}) or in both (Myc-Pex16p$^{PP1BM1\&2}$). The cells were labelled with anti-Myc antibody. Bars, 20 µm.
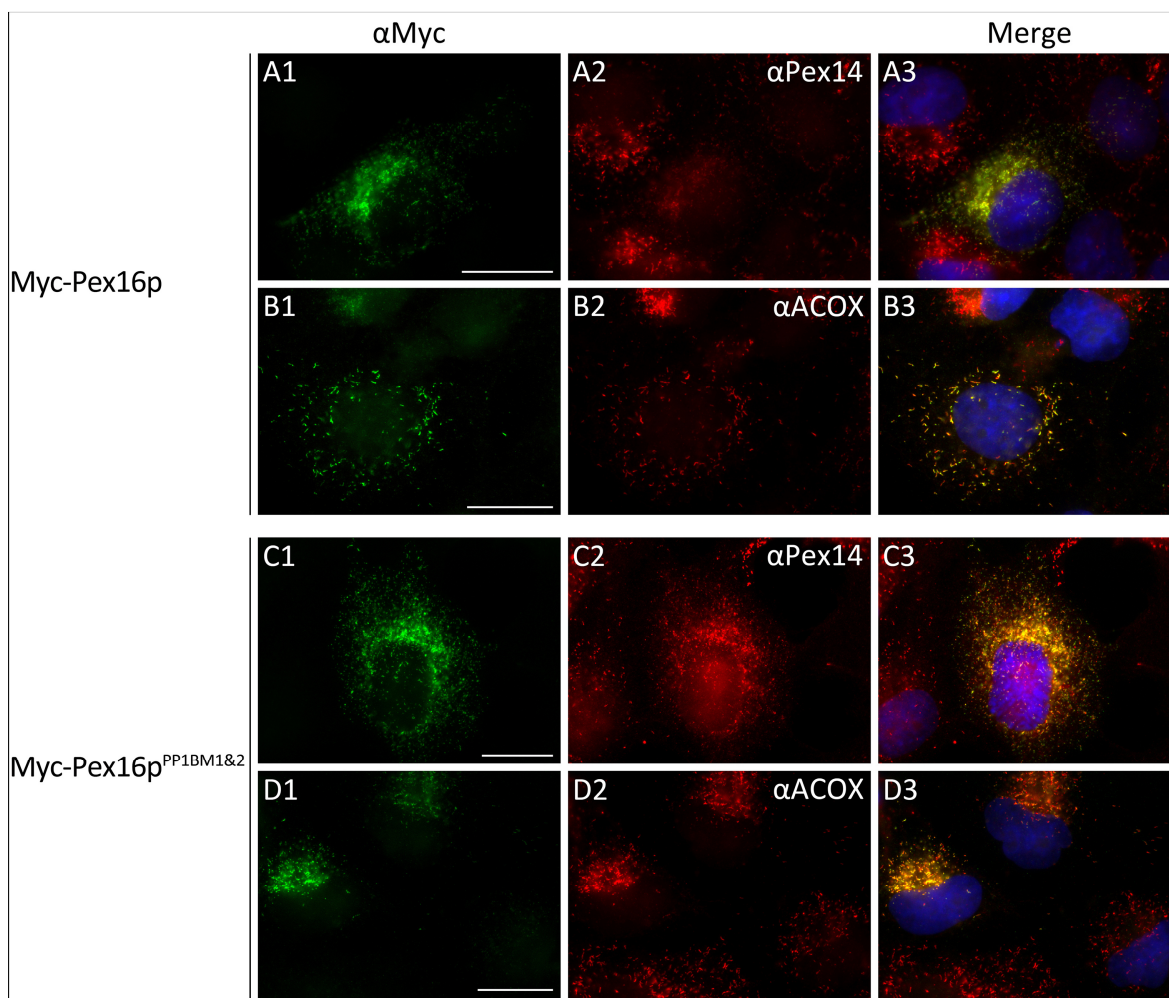
Figure 25: Overexpression of Myc-Pex16p with both PP1BMs mutated does not change peroxisomal morphology or number
COS-7 cells were transfected by PEI to express Myc-Pex16p, a well as with mutations on both RVxF motifs (Myc-Pex16p[PP1BM1&2]). The cells were labelled with anti-Myc and anti-Pex14 or anti-ACOX antibodies. Nuclei were labelled with Hoechst 33258. Bars, 20 µm.

4.1.4.3 Pex16p PP1BMs mutants are able to complement the peroxisomal phenotype in Pex16p-deficient cells

The re-introduction of Pex16p in Pex16p-deficient cells is known to complement its phenotype characterized by the total absence of peroxisomes (118, 120, 350). In order to test if Pex16p with mutated RVxF motifs was able to complement the phenotype and result in *de novo* synthesis of peroxisomes, Pex16p-deficient cells were transfected with Myc-Pex16p wild-type and with mutated PP1BMs. This work was made in collaboration with the group of M. Fransen in the University of Leuven, Belgium. The cells were transfected using the Neon® Transfection System and fixated four days after transfection.

The cells were labelled with anti-Pex14 (Figure 26) and anti-catalase (not shown) antibodies. Both wild-type and mutated versions were able to restore peroxisomes biogenesis. Co-localization of Pex14p and catalase (not shown) indicated that the newly-formed peroxisomes were also import-competent. In our study, despite the peroxisomes from the complemented cells do not appear absolutely normal, one cannot see differences between the wild-type and any of the mutated versions. This result clearly demonstrates that the putative PP1-binding sites within Pex16p are not essential for the *de novo* formation of peroxisomes.
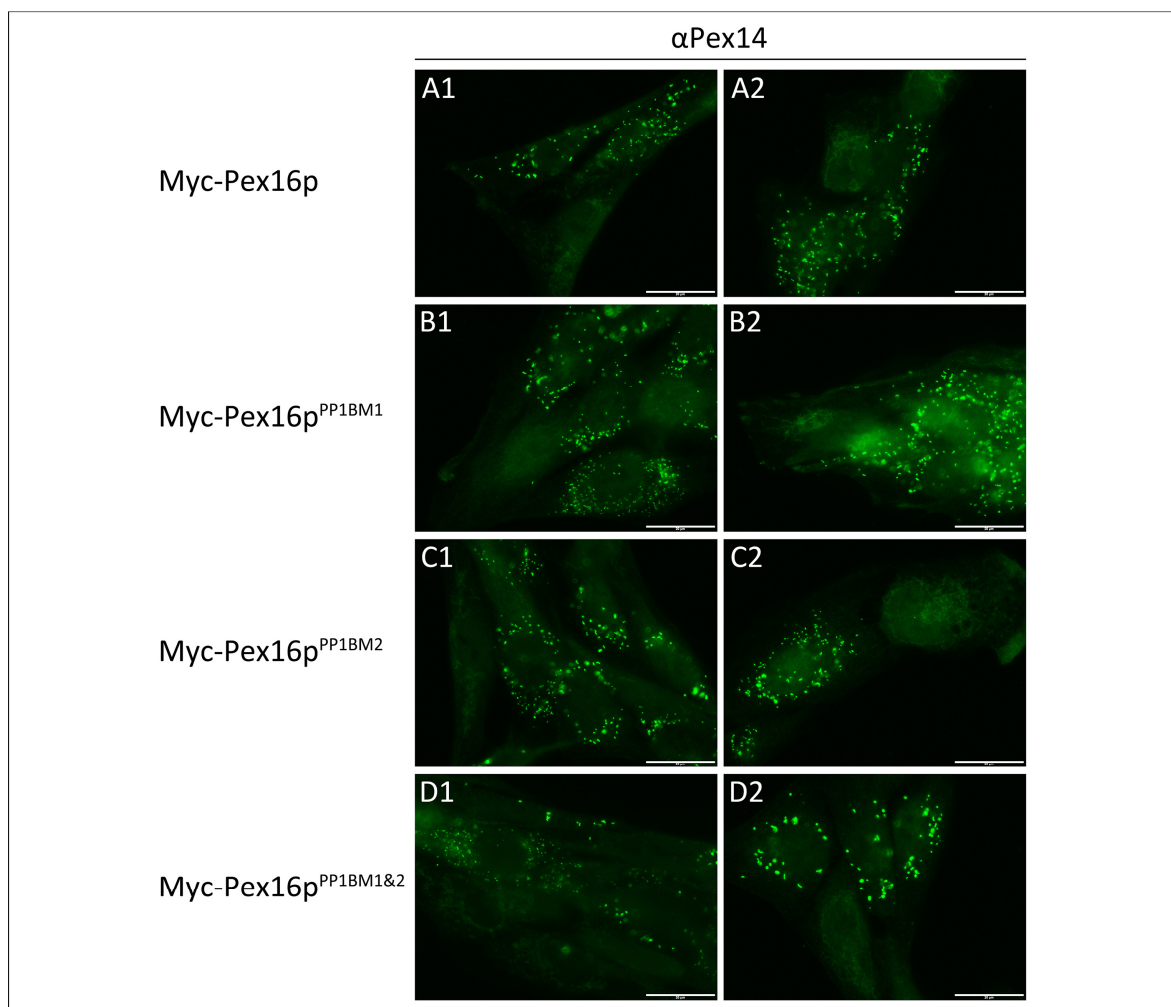
Figure 26: Pex16p PP1BMs mutants are able to complement the phenotype in Pex16p-deficient cells
Pex16p-deficient cells were transfected using the Neon® Transfection System to express Myc-Pex16p, as well as Myc-Pex16p with mutations in the first RVxF motif (Myc-Pex16p[PP1BM1]) or in the second (Myc-Pex16p[PP1BM2]) or in both (Myc-Pex16p[PP1BM1&2]). The cells were fixated four days after transfection and labelled with anti-Pex14 antibody. Bars, 20 µm. With kind support of M. Fransen, Univ. of Leuven, Belgium.

4.1.5 Discussion

Protein phosphorylation represents one of the most common post-translational modifications in eukaryotes. It affects 30-70% of all cellular proteins and some cellular processes are associated with thousands of phosphorylation events, the majority of which are highly dynamic owing to their ability to be rapidly reversed by protein phosphatases (278). The protein Ser/Thr phosphatase PP1 has been pointed to be the catalyzer for the majority of protein phosphorylation events in eukaryotic cells (278, 314). As PP1 does not recognize a consensus sequence surrounding thephosphorylated residue, efficient and specific substrate binding depends on regulatory subunits, so-called PP1-interacting proteins (PIPs) (319). Most PIPs contain a primary PP1-docking motif and some even possess interaction-strengthening motifs (see Table 5, section 1.4.2.1.1).

The signal transduction mechanisms that may regulate peroxisome biogenesis and proliferation are yet to be discovered. Being phosphorylation/dephosphorylation a major signal transduction mechanism and PP1 the major player, we investigated a possible role for PP1 in peroxisome biogenesis and proliferation by searching for possible PIPs among peroxins and other important players on the matrix import and fission machineries (section 4.1.1). We identified PP1-binding motifs in several peroxins (Figure 9) and considered Pex3p, Pex10p and Pex16p the most likely to be true PIPs since they harbor primary and strengthening PP1-docking motifs. In parallel, another evidence emerged pointing out to a putative interaction between PP1 and Pex16p: Pex16p was identified in a yeast two-hybrid screen for PP1γ2 interactors in human brain (307). Moreover, all three PP1 isoforms were identified in a large scale blot screen on highly purified rat liver peroxisome fractions. Altogether, we considered Pex16p as very likely to be a PP1-interacting protein, possibly regulating PP1's activity during peroxisome biogenesis.

One of the aims of this work was to verify the putative PP1-Pex16p interaction by binding studies. Several techniques were used; however, we could not confirm the interaction. We used two pull-down techniques, co-immunoprecipitation using anti-Myc antibody and GFP-binding peptide coupled to magnetic beads. In the first case, we used COS-7 cells overexpressing PP1γ1 and/or Myc-Pex16p. The fraction from double transfected cells

presented a positive result, pointing to a true interaction between PP1γ1 and Myc-Pex16p. However, no interaction between Myc-Pex16p and endogenous PP1γ was verified (Figure 16). On the second case, we used COS-7 cells overexpressing GFP-Pex16p in a GFP-Trap_M® system, with negative results (Figure 17). The same experiment using a cross-linker also turned negative (data not shown). In addition to the pull-down assays, other approaches were applied to unravel whether PP1 interacts with Pex16p. GST-tagged Pex16p expressed in bacteria was separated by SDS-PAGE, blotted to nitrocellulose membrane and was afterwards overlaid with purified PP1γ1. Both full length and cytosolic C-terminal tail versions of Pex16p gave a negative result (Figure 21). The interaction was also verified in yeast, mimicking the conditions of the YTH assay in which Pex16p was identified. Several Pex16p versions were used: full length, cytosolic C-terminal tail and with mutated PP1-binding motifs. In all cases, we did not verify an interaction (Figure 19). Moreover, we also used the clone collected from the YTH screen and verified that it was able to self-activate the reporter genes. This raises the possibility of Pex16p being a false-positive. PP1α and PP1γ cellular sub-localization in mammalian cells was also verified and no co-localization with peroxisomes was found, both in Pex16p-tranfected an untransfected cells (Figure 23).

Several aspects could have been improved in each approach individually. In the pull-down assays, a crosslinker could have been used in the co-IP with anti-Myc antibody in order to enhance the signal on co-transfected cells or pull-down endogenous PP1γ. Nonetheless, this was done in the GFP-Trap_M® assay with negative results. An inverse approach could have been tried, using PP1 as bait instead of Pex16p. However, this approach was rejected right at the beginning because of the multitude of PP1-binding proteins that exist in the cell, which could complicate the observation of a possible PP1-Pex16p interaction. In the GFP-Trap_M® assay, we verified that GFP-Pex16p had a considerably low binding rate to the beads. Increasing the amount of protein bound to the beads would raise the visibility of a possible interaction. However, raising even more the amount of total protein would be very difficult, since we verified that GFP-Pex16p-transfected cells had an extremely high level of death rate, obligating us to use a very high number of culture dishes. Actually, artefacts (such as peroxisome agglomeration) and miss-targeting of

overexpressed Pex16p were relatively common in Pex16p-overexpressing cells (data not shown) and an interaction between PP1 and Pex16p could possibly be hampered by this fact. Perhaps the use of expressing vectors with weaker promoters could overcome this issue. Both co-immunoprecipitation assays would benefit from the use of positive controls. Ideally, Pex16p-binding partners should have been used to verify the effectiveness of the pull-down. Anti-Pex3p and anti-Pex19p antibodies were being planned to be used for that purpose; however, temporal limitations precluded us to execute these controls on the co-IPs in time to be included in this dissertation. In general, all the experiments could have been further optimized in several parameters, such as buffers and incubation times or temperatures.

Regardless of the improvements that could have been done to each approach individually, completely different techniques were used, recurring to an whole panoply of tools: mammalian/yeast/bacterial cells; native/denaturing conditions; diverse detection techniques, such as immunoblot and activation of reporter genes. Taken together, we could affirm that the putative PP1-Pex16p interaction does not occur; however, we are able to identify reasons for the negative results in each protein-protein interaction detection method that was used. For example, the overlay method was executed under denaturing conditions, which may hamper the interaction. On the other hand, full length Pex16p expression in bacteria was extremely low, which could reduce a positive signal to undetectable levels. PP1γ1 also did not overlay with Pex16p^{CT} – however, this peptide lacks the SILK motif, which can be essential for the interaction. The same principle applies to the experiments in yeast: Pex16p^{CT} does not have the transmembrane domains, which may prevent the full length protein to enter the nucleus and activate the reporter genes and justify the negative result. Pex16p^{CT} is presumably soluble; nonetheless, the lack of the SILK motive could render the PP1-Pex16p complex not stable enough to activate the reporter genes. The overexpression of Pex16p in mammalian cells provoked, in many cases, the occurrence of artefacts, such as peroxisome agglomeration or miss-targeting to ER (data not shown). This could prevent the interaction either by altering the physiological conditions needed for it to occur or by sequestration of the overexpressed protein in inaccessible structures. In every case, a possible transient nature of the

putative PP1-Pex16p interaction may prevent its detection. In addition, one or more specific stimulus may be required for the interaction to occur, such as peroxisome proliferation-induction stimulus, e.g. ROS.

Nonetheless, other approaches could be attempted. Membrane-based yeast two-hybrid (MYTH) is a technique based on the split-ubiquitin protein complementation assay and detects protein interactions directly at the membrane, thereby allowing the use of full-length integral membrane proteins and membrane-associated proteins as baits to hunt for interaction partners (362). Very recently, a membrane-based two-hybrid system (MaMTH) was developed for mammalian cells (363). Similarly to MYTH, MaMTH allows the detection of protein-protein interactions of full-length integral membrane proteins based on the split-ubiquitin complementation assay. However, using mammalian cells, better *in vivo* mimicking conditions are achieved, as protein-protein interactions may be dependent on, for example, post-translational modifications to occur. Moreover, the system can be used to track the effect of certain stimuli or post-translational motifications, e.g. phosphorylation, on a given protein-protein interaction. Another approach could be the co-separation in a native gel. In this technique, *in vitro* translated proteins are incubated with the putative binding partners and separated in native gels. A shift in the protein molecular weight would indicate a positive interaction. In this technique radiolabeled proteins can be used, which detection is much more sensitive than immunoblot. For this work, *in vitro* translation of Pex16p was attempted, without success. However, this experiment needed further adjustments and/or other conditions, such as the presence of peroxisome-like membranes.

Besides the verification of PP1-Pex16p interaction, other experiments were done in parallel to manipulate the putative interaction and verify its effect in mammalian cells. To achieve that, Myc-Pex16p was overexpressed in COS-7 cells and the PP1 sub-cellular localization was verified and compared with non-transfected cells – no differences were found (Figure 23). Nonetheless, Myc-Pex16p constructs carrying mutations in the RVxF motifs were overexpressed as well. No differences were found between cells transfected with Myc-Pex16p and any of the PP1BMs mutants concerning peroxisome morphology or

number (Figure 24 and Figure 25). This does not necessarily mean that they do not interact. Influencing the putative interaction may not have an effect on these parameters. As mentioned before, one or more specific stimuli may be required in order for the interaction to occur and to provoke visible differences. As Pex16p function is still unclear, finding those stimuli may be a challenge. One of the few facts known about Pex16p is that its re-introduction in Pex16p-deficient cells complements the peroxisome-lacking phenotype (118, 120, 350). We verified that Myc-Pex16p with mutated RVxF motifs were able to complement Pex16p-deficient cells, suggesting that the putative PP1-binding sites within Pex16p are not essential for the *de novo* formation of peroxisomes (Figure 26). Actually, the re-introduction of mutant Pex16p from the *PEX16* patients with mild symptoms also complemented the phenotype in Pex16p-deficient cells, although the peroxisomes had altered morphology and number, like in patient fibroblasts (350). Recent advances on the study of Pex16p function (140, 141) opened new routes for future research on putative PP1-Pex16p interaction, guiding to possible conditions needed for the interaction to occur.

In summary, our results suggest that PP1 does not interact with Pex16p and the PP1-binding motifs seem to be irrelevant for Pex16p function, at least under the tested conditions. Nonetheless, two questions still need to be clarified: 1) which functions or motifs are being affected in *PEX16* patients and 2) what are the roles of kinases and phosphatases that have been shown or suggested to be targeted to peroxisomes? The answer to the first question is primordial to further understanding the molecular mechanism of Pex16p function – a mysterious yet fundamental peroxin. We analyzed the human Pex16p sequence (accession number Q9Y5Y5) via the ELM server to search for possible functional domains within the C-terminus and some interesting ones were identified. Two of them, localized within residues 313-323, are recognized by SH3 (Src Homology 3) domains. SH3 domains mediate protein-protein interactions and are involved in several and diverse biological processes, e.g. signal transduction and organelle assembly. This domain is abrogated in some patients, namely the ones with sequence frameshifts (Figure 14). ELM also found several putative phosphorylation sites by proline-directed kinases, e.g. MAPK, in the intraperoxisomal region of Pex16p. Curiously, MAPK

phosphatase 1 (MKP1) has been found to be targeted to peroxisome in plants (302). Another one of these sites is the residue S288 which is next to P289, mutated to threonine in one of the patients (Figure 14). On one hand, the mutation P289T may avoid S288 putative phosphorylation because the motif is no longer recognized by the proline-directed kinases. On the other hand, phosphorylated [ST]-P domains are recognized by Pin1, a peptidyl-prolyl *cis*/*trans* isomerase. This protein interconverts prolines between *cis* and *trans* conformations, provoking structural alterations and plays a role as post-phosphorylation control in regulating protein function. Intriguingly, ELM did not identify any domain involving valine in position 252, which is deleted in one of the patients (Figure 14). Resuming, the C-terminal tail of Pex16p seems to be an important object of study to understand Pex16p function which seems to have been neglected up today. Allying bioinformatics tools and directed mutagenesis, the Pex16p C-terminus could be extensively studied, which would certainly clarify Pex16p function and molecular mechanisms of action.

As protein phosphorylation/dephosphorylation reactions are an ancient and ubiquitous mechanism for signal transduction, peroxisomes are likely not an exception. This way, it is urgent to identify the protein kinases and phosphatases that act on peroxisomes as well as their binding partners and substrates. PP1, as the most conserved eukaryotic protein (312) and catalyzing the majority of protein dephosphorylation events in eukaryotic cells (278), is certainly an unneglectable phosphatase which role on peroxisomes needs to be extensively studied. Indeed, its presence on peroxisomes was suggested by the large-scale blot screen with highly purified peroxisome fractions from rat liver. Nevertheless, PP1 activity is regulated by binding partners that often target PP1 to certain locations within the cell, bringing it to the vicinity of its substrate(s). Previous data suggested that Pex16p could be a PP1 interacting protein, turning Pex16p into a possible player in peroxisomal signaling cascades. As Pex16p is an early peroxin, this putative interaction could have a primordial role in peroxisome biogenesis. Although this study was not able to confirm the interaction, this it not a closed chapter, as many experiments and approaches can still be done as discussed earlier. Nevertheless, we verified that other peroxins represent possible PP1 interacting proteins, as they also possess PP1-binding

motifs. This way, other proteins are also good options in the study of the possible role for PP1 in the regulation of peroxisome biogenesis and/or proliferation. Interestingly, PP2A and MKP1 were very recently identified to be targeted to peroxisomes in *Arabidopsis thaliana* (301, 302). Nonetheless, their targeting seems to be conditioned to certain stimuli. MKP1 is targeted to peroxisomes only under stressful conditions. Probably not a coincidence, MAPK signaling is involved in the upregulation of catalase transcription and activity and H_2O_2 production under oxidative stress conditions (302, 303). Along with CDK1 (304), PP2A (301) and MKP1 (302) are the only kinases/phosphatases identified to be targeted to peroxisomes. However, this was observed in *Arabidopsis thaliana* and has been associated to the regulation of peroxisomal metabolism. The protein kinases/phosphatases involved in the regulation of peroxisome biogenesis and proliferation in mammals are completely unknown. The possible connection of Pex16p and/or other peroxins with PP1 is then a very important line of study to better understand peroxisome function in mammalian cells.

4.2 Regulation of Pex11pβ during peroxisome proliferation

Protein of Pex11 family is known to control peroxisome proliferation and to regulate peroxisome morphology, size and number across fungi, plants and mammals (188-195). However, the mechanisms that regulate the function of Pex11 proteins during peroxisome proliferation are still obscure. It has been demonstrated in yeast, that *Saccharomyces cerevisiae Sc*Pex11p and *Pichia pastoris Pp*Pex11p are regulated by phosphorylation (220, 290). Phospho-mimicking "off" and "on" mutants either interfered with peroxisome division giving rise to enlarged and clustered peroxisomes (constitutively dephosphorylated), or resulted in hyperdivision (constitutively phosphorylated) of peroxisomes. Furthermore, the phosphorylation of S173 in *Pp*Pex11 also influences its interaction with Fis1 (290). This project aimed to contribute to an investigation on whether phosphorylation events contribute to the regulation of human Pex11pβ and consequently peroxisome proliferation, focusing on selected putative phosphorylation sites (Figure 27).

Figure 27: Human Pex11pβ protein sequence (accession number O96011)
Yellow and blue residues correspond to transmembrane domains and a glycine-rich region, respectively (211). H1, H2 and H3 – predicted amphipathic helices (191). S11 and S38 – potential conserved phosphorylation sites. C18, C25 and C85 – cysteine residues with a putative role in Pex11pβ conformation and/or dimerization. Light and dark green-shaded residues correspond to hydrophobic and very hydrophobic amino acids (364).

On the other hand, dimerization of Pex11 has also been identified in fungi as a mechanism to regulate its function. Marshall and colleagues (219) suggested that *Sc*Pex11 is inactivated by homodimerization. Moreover, one of *Sc*Pex11 cysteines was identified to be involved in the homodimer formation, suggesting that *Sc*Pex11 may regulate membrane remodeling in a redox-sensitive fashion. Human Pex11pβ has also been

shown to self-interact forming homodimers (193, 211-213), controlling its activity. Moreover, *Hs*Pex11pβ possesses cysteine residues (Figure 27) which present as possible players in the dimer formation, hence this project also aimed to investigate whether these residues interfer with Pex11pβ-driven peroxisome proliferation.

To further comprehend the mode of action and regulation of human Pex11pβ, its topology was also studied. As mentioned in the introduction of this dissertation (section 1.3.1), the topology of Pex11 proteins varies considerably across organisms (129). All mammalian isoforms, including *Hs*Pex11pβ, are tightly associated with the peroxisomal membrane and possess two predicted membrane spanning helices with both C- and N-termini protruding into the cytosol (177, 189, 203, 211) (Figure 28). Nonetheless, the intra-peroxisomal region between the two transmembrane domains facing to the peroxisomal matrix is still unclear, since we do not know if this region fully embeds within the peroxisomal matrix or if (at least parts of) it interacts with the matrix site of the peroxisomal membrane or even if it is buried within the membrane. Moreover, a glycine-rich region between the transmembrane domains of *Hs*Pex11pβ was identified (Figure 27) and it was targeted in our studies to clarify its role in peroxisome proliferation and to better understand the topology of Pex11pβ.
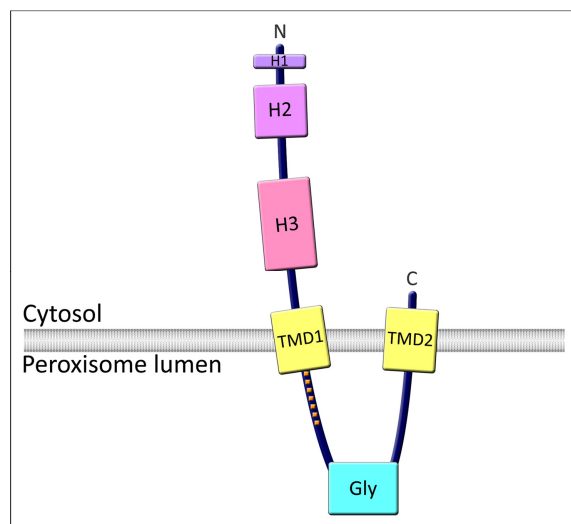
Figure 28: Pex11pβ predicted topology and functional domains
Boxes represent specific regions: H1 (aa 3-8), Helix 1; H2 (aa 14-31), Helix 2; H3 (aa 45-75), Helix 3; TMD1 (aa 90-110), transmembrane domain 1; TMD2 (aa 230-255), transmembrane domain 2; Gly, glycine-rich region (aa 159-182), dashed area corresponds to the epitope recognized by an anti-Pex11β antibody (aa 110-140) (see Table 8). Pex11pβ-induced peroxisomal membrane remodeling may be driven by the insertion of one or more amphipathic helices into one leaflet of the lipid bilayer.

Another important topology aspect of Pex11p is the presence of regions located within the N-terminus that display amphipathic properties (Figure 27 and Figure 28). *In vitro*

studies indicated that these amphipathic helices were shown to be essential to mediate membrane tubulation, a property apparently conserved throughout species (191, 215). Thus, membrane asymmetry and bending caused by the insertion of one or more amphipathic helices into one leaflet of the lipid bilayer (218) seems to be the mechanism of Pex11p-induced peroxisomal membrane remodeling. This work aimed to complement and verify these findings by mutational studies of the N-terminus of *Hs*Pex11pβ *in vivo*.
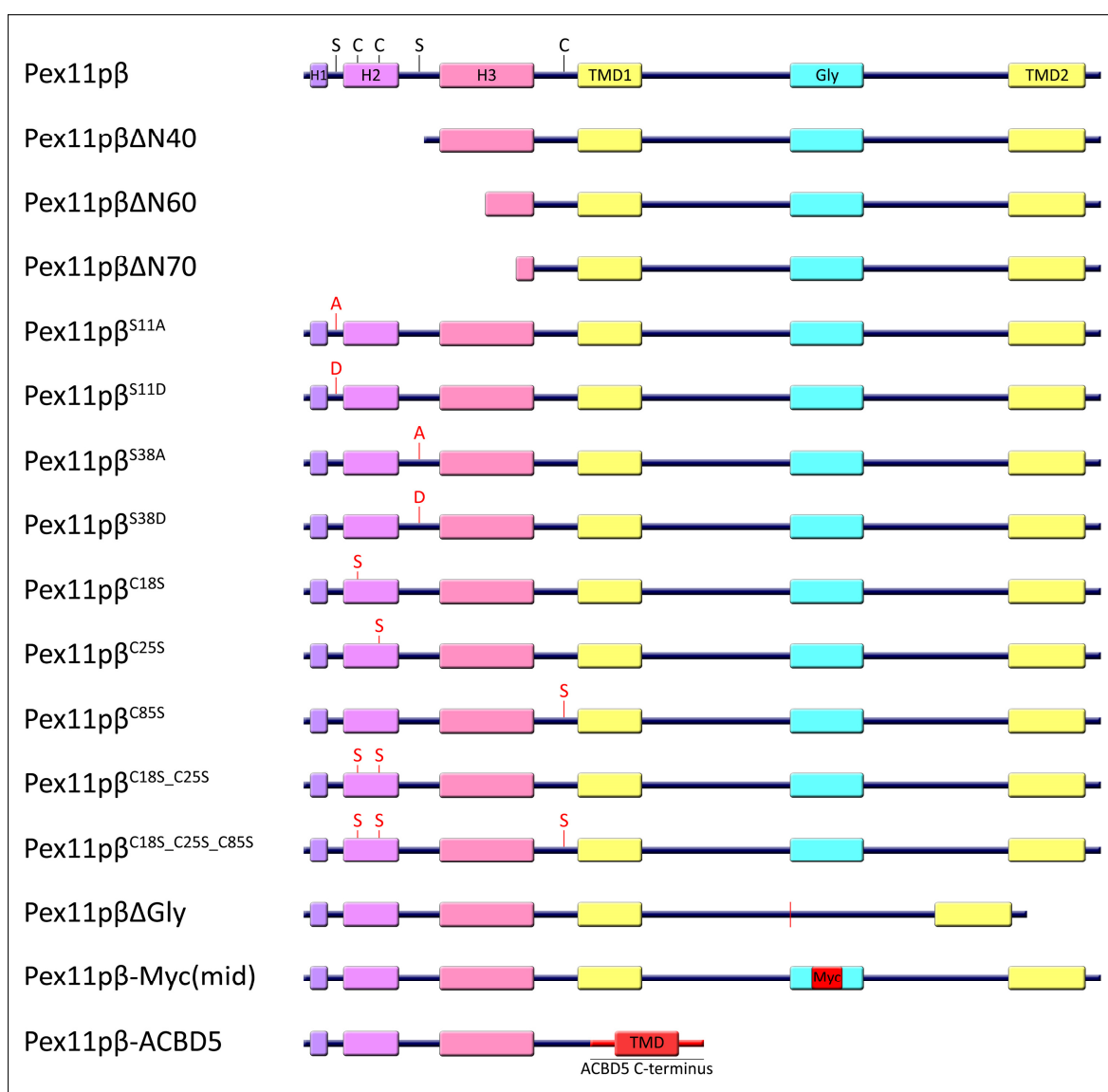
Figure 29: PEX11β mutants created for this study
Residues depicted in red are the ones that were mutated. Boxes represent specific regions: H1 (aa 3-8), Helix 1; H2 (aa 14-31), Helix 2; H3 (aa 45-75), Helix 3; TMD1 (aa 90-110), transmembrane domain 1; TMD2 (aa 230-255), transmembrane domain 2; Gly, glycine-rich region (aa 159-182).

To perform our studies towards a better understanding of Pex11pβ topology and regulation during peroxisome proliferation, we created several mutants. A schematic view of these mutants is depicted in Figure 29. To study the effect of those mutations on Pex11pβ function in promoting peroxisome elongation, we took advantage of the known effect of overexpression of wild type Pex11pβ in mammalians cells, which induces prominent elongation of peroxisomes, followed by division into spherical organelles over time (177, 179, 216).

4.2.1 A glycine-rich region within Pex11pβ is dispensable for peroxisomal growth and division

We observed that human Pex11pβ contains a glycine-rich region at aa positions 159-182 (Figure 27), between the transmembrane domains and, based on several topology studies including from our group (211), it is exposed to the peroxisomal matrix. Curiously, this glycine-rich stretch is absent in Pex11pα and Pex11pγ (Supplementary Figure 2). To examine if this region (which also contains proline residues) is required for Pex11pβ function, we deleted those 30 amino acids resulting in the construct Myc-Pex11pβΔGly (Figure 29) and compared the effect of its expression with the wild type version, Myc-Pex11pβ. Expression in COS-7 cells showed proper targeting to peroxisomes as revealed by immunofluorescence microscopy (Figure 30, D-F, J-L). However, deletion of the glycine-rich region had no effect on peroxisome elongation and subsequent division over time when compared to controls expressing wild type Myc-Pex11pβ (Figure 30, M). Our data demonstrate that the glycine-rich region within Pex11pβ is dispensable for the targeting to peroxisomes as well as membrane elongation and division.
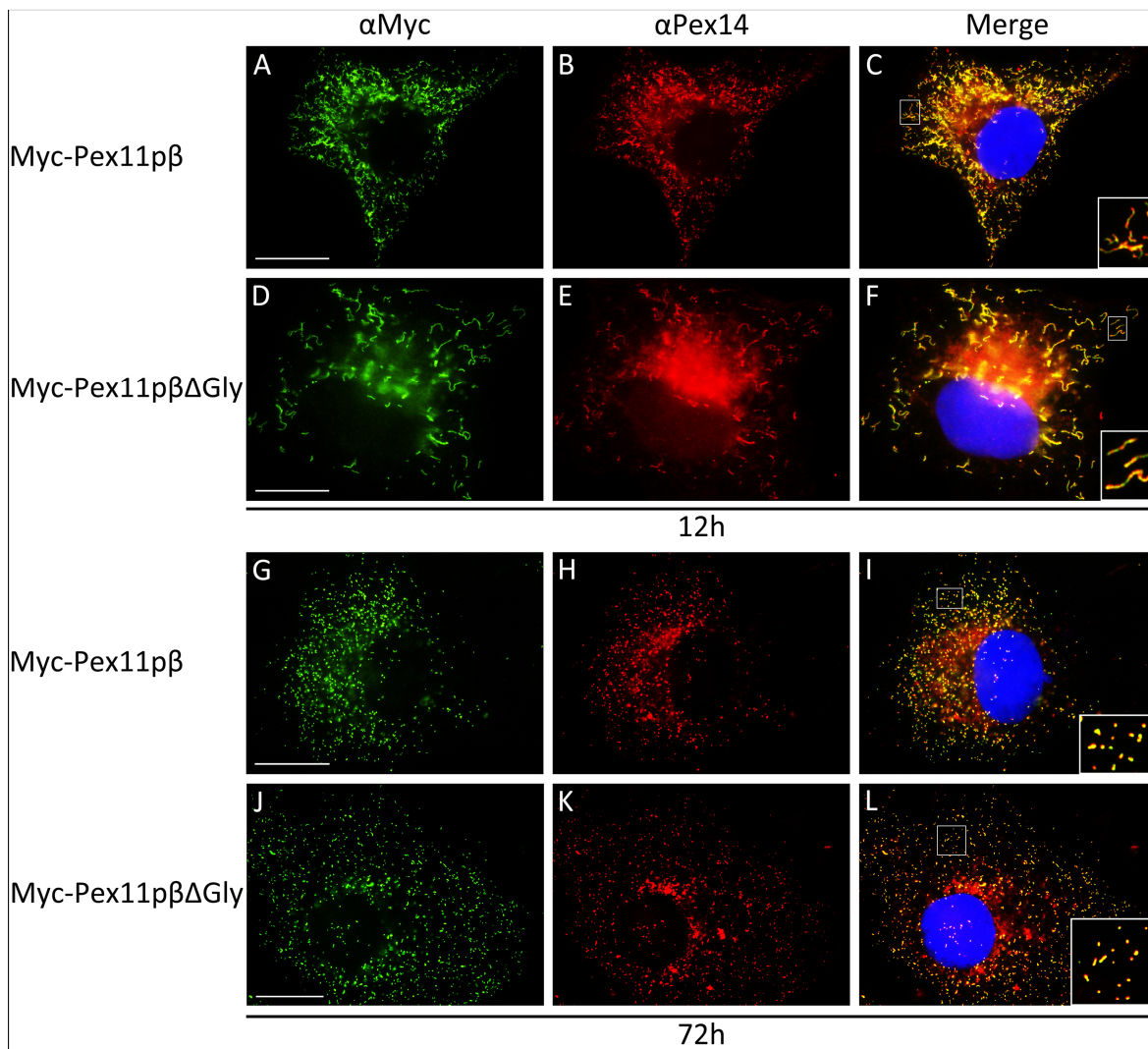
Figure 30: A glycine-rich internal region specific for human Pex11pβ is dispensable for peroxisome elongation and division

COS-7 cells were transfected by electroporation with Myc-Pex11pβ (A-C and G-I) and Myc-Pex11pβΔGly (D-F and J-L), and were processed for immunofluorescence microscopy 6h, 12h (A-F), 24h, 48h and 72h (G-L) after transfection using anti-Myc (A, D, G, J) and anti-Pex14 (B, E, H, K) antibodies. Nuclei were labelled with Hoechst 33258. The transfected cells were quantitatively evaluated for peroxisome morphology (M). Data are from five independent experiments and are presented as means ± SEM. No significant differences were found between the mutants and wild-type, for all time points. Bars, 20 μm.
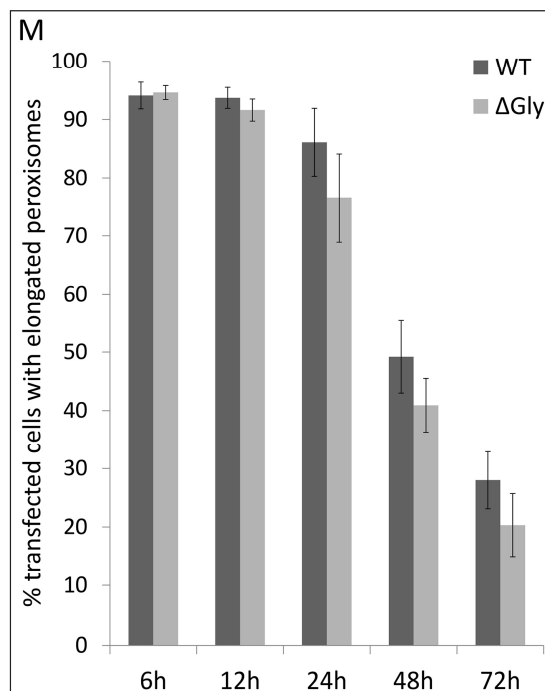
4.2.2 An inter transmembrane region of Pex11pβ may be buried within the peroxisomal membrane

Our research group has recently published a thorough analysis of the membrane topology of Pex11pβ at the peroxisomal membrane (211), which confirms that it possesses two transmembrane domains at amino acids 90-110 and 230-255. The data also demonstrated that Pex11pβ is an integral membrane protein with N- and C-termini directed towards the cytosol and the intra-peroxisomal region between the two transmembrane domains facing the peroxisomal matrix. However, one cannot rigorously exclude that parts of this region may interact with the matrix site of the peroxisomal membrane, or are partially buried within the membrane. Indeed, several N- and C-flanking amino acids of the glycine-rich region have hydrophobic properties (Figure 27).

In the present work we have demonstrated that a glycine-rich stretch within the intra-peroxisomal region is dispensable for the properties of Pex11pβ to promote membrane elongation and division of peroxisomes (section 4.2.1). Taking advantage of this fact, we generated a construct in which the central 10 amino acids of the glycine-rich stretch were substituted by the sequence EQKLISEEDL, which corresponds to a Myc tag (Figure 29). With this experiment, we intended to further clarify Pex11pβ topology. We transfected COS-7 cells with YFP-Pex11pβ-Myc(mid), which were processed for immunofluorescence microscopy using different permeabilization techniques and antibodies (Figure 31). To obtain complete and selective permeabilization of the peroxisomal membrane, methanol and digitonin were used, respectively. As peroxisomal markers, we used AOX, a matrix protein which is inaccessible to the antibody in digitonin-permeabilized cells; Pex14p and PMP70, membrane proteins which are accessible to the antibody in either permeabilization conditons. YFP-Pex11pβ-Myc(mid) co-localized with all the peroxisomal markers AOX (Figure 31, G-I), Pex14p (not shown) and PMP70 (not shown) in methanol-permeabilized cells, indicating that the fusion protein was correctly targeted to peroxisomes. Co-localization between YFP-Pex11pβ-Myc(mid) and anti-GFP antibody in both methanol- and digitonin-permeabilized cells was also observed (not shown), which confirms the expected topology with the Pex11pβ N-terminus facing towards the cytosol. As also observed in a previous study from a member of our research group, anti-Pex11β

antibody, directed against the internal site aa 110-140, was unable to label YFP-Pex11pβ-Myc(mid) in cells permeabilized with digitonin, confirming that this region resides in the intra-peroxisomal part of the fusion protein (211, 365). However, an intriguing observation was that the Myc epitope was accessible to the anti-Myc antibody in both full and selective permeabilization conditions (Figure 31, A-F). The lack of anti-AOX signal in digitonin-permeabilized cells confirmed that peroxisomal membrane was not permeabilized by this detergent (Figure 31, J-L).
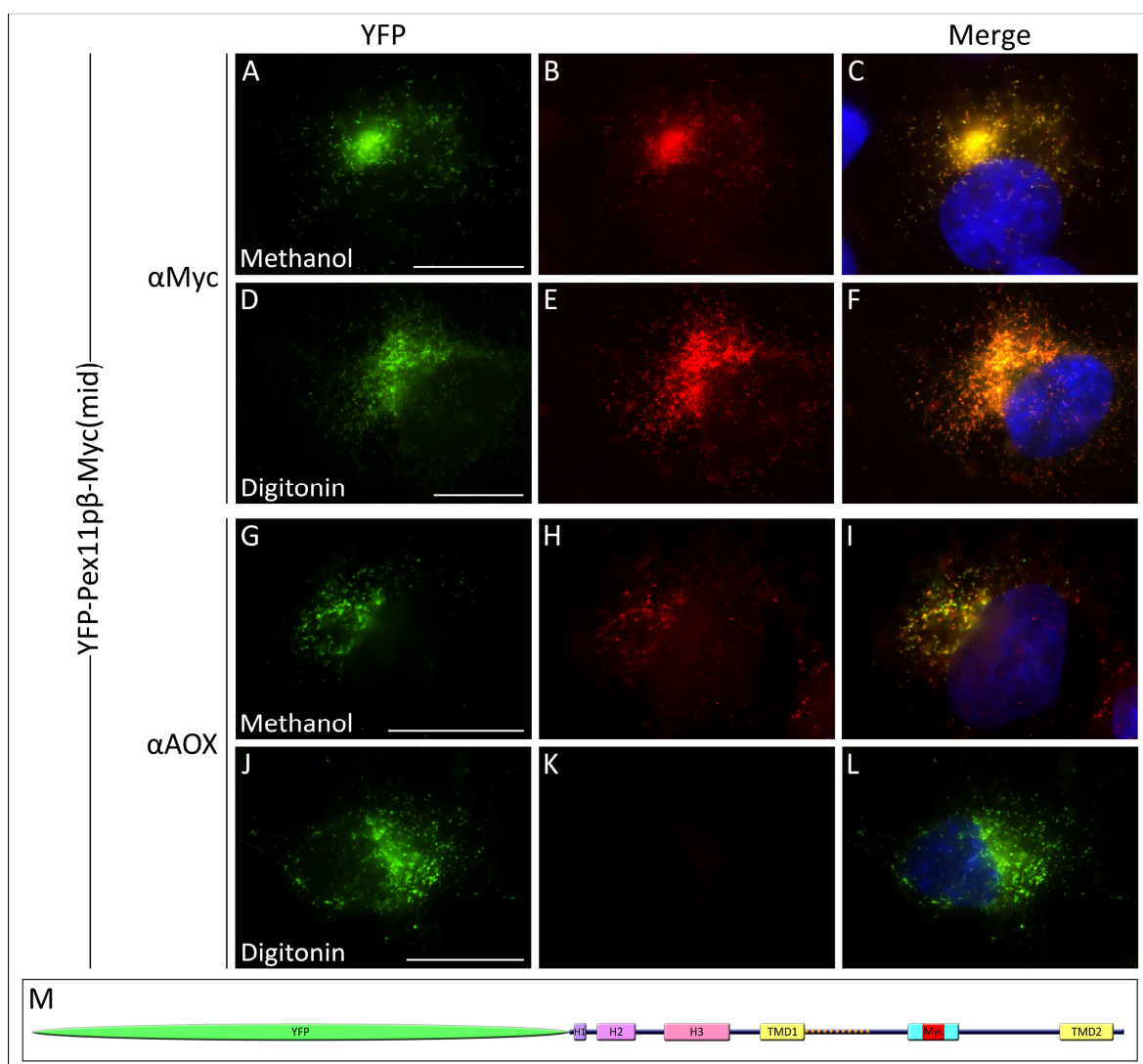
Figure 31: A Myc epitope inserted between the Pex11pβ transmembrane domains is accessible from the cytosol under selective permeabilization conditions
COS-7 cells were transfected by PEI with YFP-Pex11pβ-Myc(mid), permeabilized with either methanol (A-C, G-H) or digitonin (D-F, J-L) and labelled with anti-Myc (A-F) or anti-AOX (G-L) antibodies. Nuclei were labelled with Hoechst 33258. Bars, 20 µm. Panel M, schematic representation of the YFP fusion protein YFP-Pex11pβ-Myc(mid). YFP, yellow fluorescent protein; H1, helix 1; H2, helix 2; H3, helix 3; TMD1, transmembrane domain 1; Myc, Myc tag; TMD2, transmembrane domain 2; dashed area, anti-Pex11pβ epitope.

Although the Myc tag could influence the three-dimensional structure of Pex11pβ and impair a proper insertion into the membrane, this finding may suggest that a part or the entire internal region between the transmembrane domains is buried within the membrane bilayer (Figure 32). As a matter of fact, excluding the glycine-rich stretch, the inter-transmembrane domain region is as rich in hydrophobic residues as the transmembrane domains and the amphipathic helices (Figure 27), possibly allowing this region (or a portion of it) to bury within the lipid bilayer.
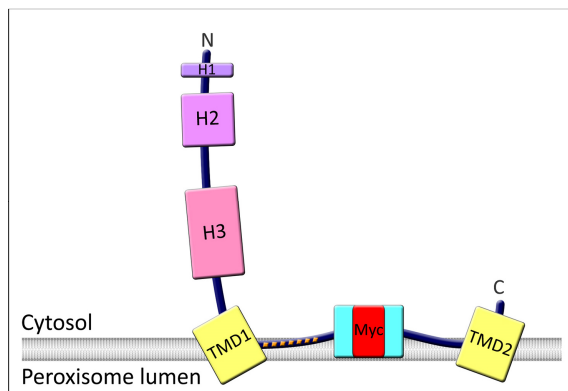
Figure 32: Predicted Pex11pβ topology based of the experiments with YFP-Pex11pβ-Myc(mid)
Boxes represent specific regions: H1 (aa 3-8), Helix 1; H2 (aa 14-31), Helix 2; H3 (aa 45-75), Helix 3; TMD1 (aa 90-110), transmembrane domain 1; TMD2 (aa 230-255), transmembrane domain 2; Myc, Myc tag added substituting the middle 10 amino acids from the glycine-rich region (aa 159-182, blue box), dashed area corresponds to the epitope recognized by an anti-Pex11β antibody (aa 110-140). Pex11pβ-induced peroxisomal membrane remodeling may be driven by the insertion of one or more amphipathic helices into one leaflet of the lipid bilayer.

4.2.3 Serine residues S11 and S38 are not involved in the regulation of Pex11pβ by putative phosphorylation

The information on the regulation mechanisms of Pex11 proteins is still very scarce. The emergence of evidences pointing to phosphorylation events as one of those mechanisms in yeast (220, 290) elevated the need to investigate this matter in human cells, as Pex11pβ has a crucial role in peroxisome proliferation, with impacts on health (48, 49, 51). To identify potential phosphorylation sites in human Pex11pβ, a member of our research group performed an *in silico* analysis using various prediction tools that either calculate putative phosphorylation sites within the protein or screen for potential kinase binding sites. The results were combined with a homology screen of various Pex11pβ protein sequences examined for conservation of putative phosphorylation sites. Several conserved sites were identified at positions S11, S38, S70, S154, S160, S168, and T178

within the human protein, which showed high probability for possible phosphorylation (Supplementary Figure 3) (211).

In this project, we focused our study on residues S11 and S38, which are present in the cytosolic portion and are thus potentially accessible to cytosolic kinases. Individual point mutations were generated by site-directed mutagenesis. We converted the respective serines to alanines to block putative phosphorylation, resulting in the constructs Pex11pβ^{S11A}-Myc and Pex11pβ^{S38A}-Myc (Figure 29). Furthermore, to generate phospho-mimicking (constitutively phosphorylated) versions we mutated the sequences encoding S11 or S38 to aspartate, resulting in the constructs Pex11pβ^{S11D}-Myc and Pex11pβ^{S38D}-Myc (Figure 29). The wild type and mutant Pex11pβ versions were overexpressed in COS-7 cells and alterations of peroxisome morphology were analyzed at different time points by immunofluorescence microscopy using anti-Myc and anti-Pex14 antibodies (Figure 33). As expected, wild type Pex11pβ-Myc induces a prominent elongation of peroxisomes which is followed by division into spherical organelles over time (Figure 33, A1-2). A similar pattern of morphological alterations was observed in all generated mutants. No enlarged or otherwise altered morphologies were detected and division proceeded normally over time for all mutants. Unlike the observations in fungi (220, 290), neither phospho-off mutants (S11A and S38A) promotes hypertubulation nor phospho-on mutants (S11D and S38D) promotes hyperdivision. These findings indicate that modifications of S11 and S38 have no impact on peroxisome elongation or division, but do not exclude that other putative phosphorylation sites within Pex11pβ may modulate its activity. Parallel work performed by another member of our research group indicated that, under the experimental conditions applied so far (e.g. by phospho-labelling), human Pex11pβ is presumably not phosphorylated (365).
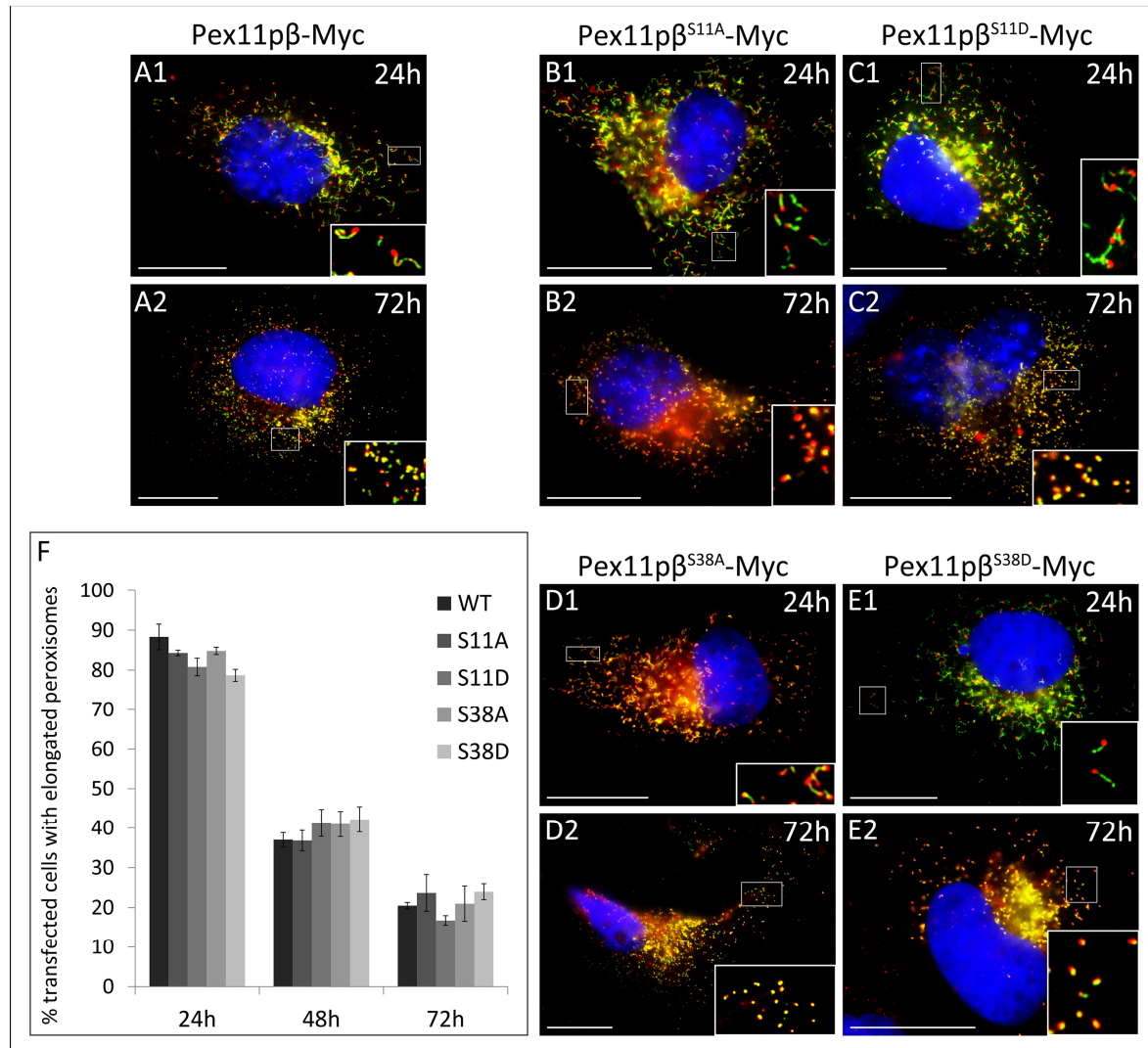
Figure 33: Phospho-mimicking mutants of Pex11pβ have no effect on peroxisome elongation and division
COS-7 cells were transfected by electroporation with Pex11pβ-Myc (A), Pex11pβ^{S11A}-Myc (B), Pex11pβ^{S11D}-Myc (C), Pex11pβ^{S38A}-Myc (D), Pex11pβ^{S38D}-Myc (E). Cells were fixed after 24h (A1-E1), 48h and 72h (A2-E2), processed for immunofluorescence and labelled with anti-Myc (green) and anti-Pex14 (red) antibodies. Nuclei were labelled with Hoechst 33258. The transfected cells were quantitatively evaluated for peroxisome morphology (F). Data are from three independent experiments and are presented as means ± SEM. No significant differences were found between the mutants and wild-type, for all time-points. Bars, 20 µm.

4.2.4 The predicted amphipathic helix 2 within the first 40 N-terminal amino acids of Pex11pβ is required to elongate the peroxisomal membrane

Pex11 proteins possess conserved amphipathic regions which are supposed to play important roles in membrane remodeling and peroxisome proliferation (191). Indeed, the

N-terminal 80 amino acids of Pex11pβ, containing three potential α-helices, have been shown to be indispensable for peroxisome proliferation activity (213). Helix 1 is only composed of 6 residues, whereas Helix 2 and Helix 3 display larger amphipathic stretches with Helix 3 being the largest one (Figure 27). Opalinski and colleagues (191) demonstrated that Helix 3 is able to tubulate membranes *in vitro* and this is conserved among species, as it was demonstrated for several fungal Pex11 proteins and for human Pex11pα. To study the potential role of the helices in the regulation of Pex11pβ *in vivo*, we generated N-terminally truncated versions (Pex11pβΔN40-Myc, Pex11pβΔN60-Myc, Pex11pβΔ70-Myc, Figure 29) and analyzed their effect on peroxisome morphology compared to the expression of Pex11pβ-Myc (Figure 34). Upon expression in COS-7 cells, all truncated fusion proteins localized to peroxisomes, as shown by co-localization with the peroxisomal marker PMP70. Interestingly, cells expressing the truncated versions did not exhibit a prominent elongation of peroxisomes (Figure 34, M). This is in contrast to the expression of full-length Pex11pβ-Myc, which typically induced a significant membrane elongation. Whereas the ΔN60 and ΔN70 truncations remove all helices, the ΔN40 truncation leaves Helix 3 intact (Figure 29). This indicates that although peptides matching Helix 3 are capable of elongating liposomal structures *in vitro*, also Helix 2 (and possibly region H1) is required for peroxisome elongation in living cells.
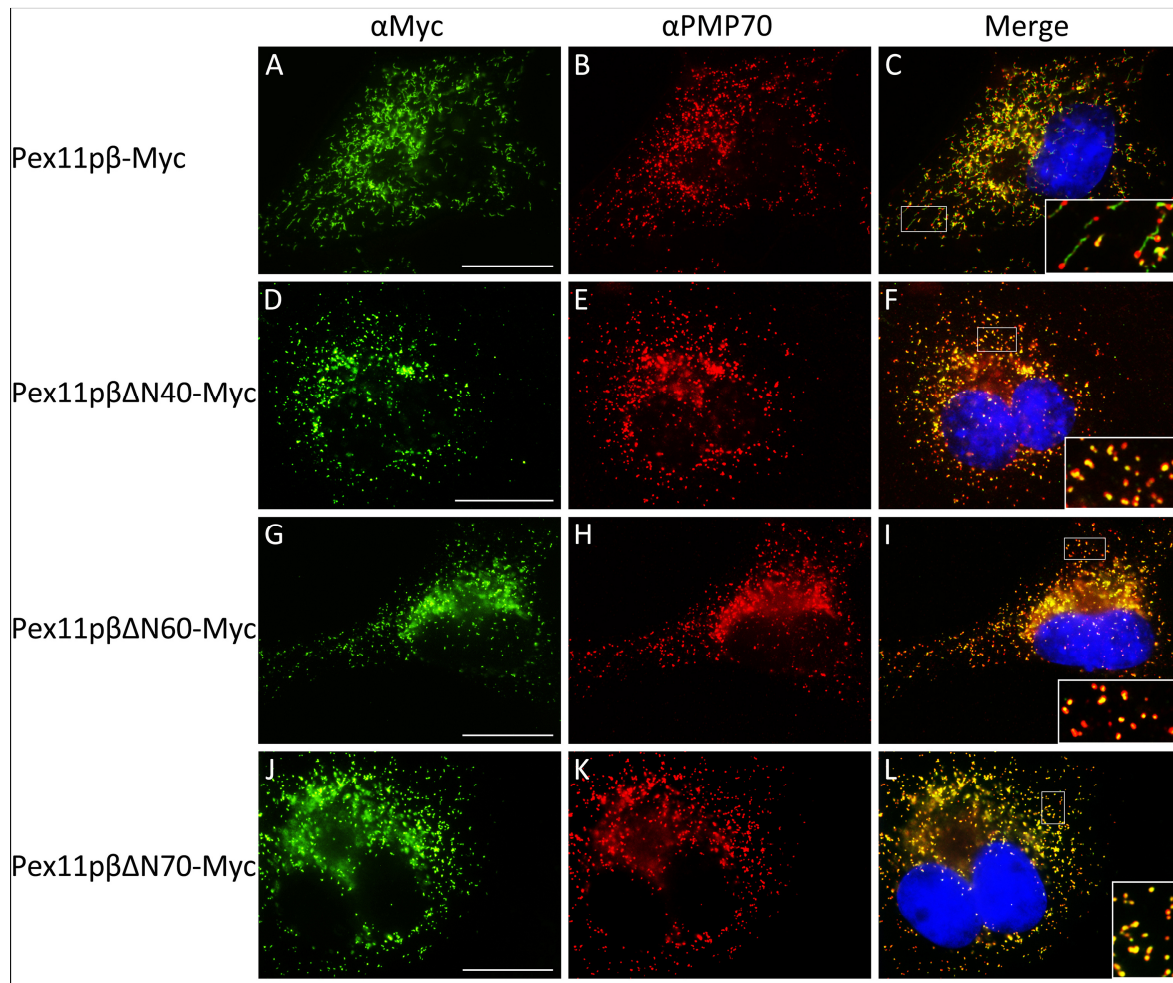
Figure 34: Intact first 40 N-terminal amino acids of Pex11pβ are required to elongate the peroxisomal membrane

COS-7 cells were transfected by PEI with Pex11pβ-Myc (A-C) and the N-terminal deletions Pex11pβΔN40-Myc (D-F), Pex11pβΔN60-Myc (G-I) and Pex11pβΔ70-Myc (J-L). Cells were processed for immunofluorescence microscopy after 24h using anti-Myc (A, D, G, J) and anti-PMP70 (B, E, H, K) antibodies. Nuclei were labelled with Hoechst 33258. The transfected cells were quantitatively evaluated for peroxisome morphology (M). Data are from three independent experiments and are presented as means ± SEM (** p<0,01, compared to wild-type). Bars, 20 μm.
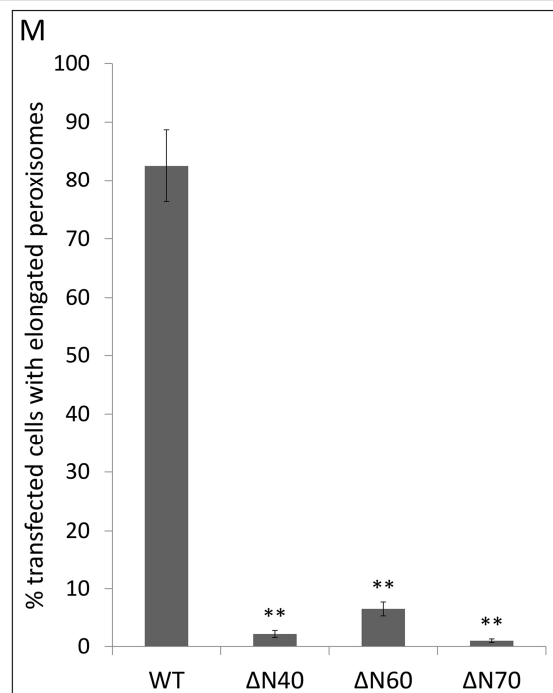
Interestingly, a parallel study from our research group confirmed the importance of Helix 2 by mutating the alanine at position 21 into a proline, which breaks the helical structure of region H2. Similarly to the N-terminally truncated versions, the expression of this mutant (Pex11pβ-Myc[A21P]) did not result in prominent peroxisome elongation (211). Our group also studied the effect of the truncation of the first 40 amino acids and the A21P mutation on the dimer formation capacity of Pex11pβ. Interestingly, while Pex11pβ-Myc was able to form dimers, Pex11pβΔN40-Myc and Pex11pβ-Myc[A21P] were unable to do so (211). These findings strongly support that the Helix 2 within the first 40 amino acids of Pex11pβ participates in homodimer formation.

4.2.5 Pex11pβ-mediated peroxisomal elongation do not rely solely on the N-terminal region

Unlike the studies performed *in vitro* (191), we have demonstrated that Helix 3 is not sufficient to induce prominent peroxisome elongation (section 4.2.4). However, Opalinski and colleagues (191) also reported that incubation of small unilamellar vesicles with bacterial lysates expressing the entire soluble N-terminal domain of *Pc*Pex11p also resulted in membrane tubulation. To verify if this *in vivo* and with human Pex11pβ, we generated a fusion protein containing the N-terminal domain of *Hs*Pex11pβ (aa 1-93) and the C-terminally located transmembrane domain of rat ACBD5 (aa 471-506) (Figure 29). ACBD5 (acyl-CoA-binding domain-containing protein 5) was chosen because it is a tail-anchored protein which is exclusively targeted to peroxisomes in mammalian cells and contains one transmembrane domain (348).

We verified that this chimeric protein (named Myc-Pex11pβ-ACBD5) was targeted to peroxisomes as confirmed by its co-localization with PMP70. However, unlike with Myc-Pex11pβ, cells transfected with Myc-Pex11pβ-ACBD5 were unable to elongate peroxisomes (Figure 35). We suggest that the predicted amphipathic helices alone, even within a peptide correctly targeted to peroxisomes, are not sufficient to elongate peroxisomes *in vivo*.

Figure 35: Pex11pβ-mediated peroxisomal elongation do no rely solely on the N-terminal region

COS-7 cells were transfected by PEI with Myc-Pex11pβ (A-C) or Myc-Pex11pβ-ACBD5 (D-F). Cells were processed for immunofluorescence microscopy after 24h using anti-Myc (A, D) and anti-PMP70 (B, E) antibodies. Nuclei were labelled with Hoechst 33258. The transfected cells were quantitatively evaluated for peroxisome morphology (G). Data are from three independent experiments and are presented as means ± SEM (*** p<0,001, compared to wild-type). Bars, 20 μm.

4.2.6 The N-terminal cysteines C18, C25 and C85 are not essential for membrane elongation

Phosphorylation/dephosphorylation is the most prominent post-translational modification used as regulation mechanism. Nonetheless, versatile redox modifications of key cysteine residues are stepping forward as a non-negligible distinct class of modifications which can often work in concert with other regulation mechanisms (366). Among the twenty common amino acids in proteins, cysteine is one of the two least

abundant yet the most conserved residue that is frequently present in functionally important sites (367). Cysteine residues serve numerous functions, such as protein activity regulation and structure determination. Regulatory cysteines modulate protein activity by changing their redox state, which may involve reversible intra- and intermolecular disulfide bonds. Structural cysteines participate in protein structure and folding through formation of stable disulfide bonds (367).

A redox-sensitive homodimerization of ScPex11p regulated by a key cysteine has been proposed by Marshall and colleagues (219) some time ago. Given that, we considered that a study on human Pex11pβ cysteines and their importance for Pex11pβ function could bring important clues towards understanding how Pex11pβ is regulated during peroxisome proliferation. Human Pex11pβ possesses eight cysteines, with C18, C25 and C85 localized in the cytosolic N-terminal region (Figure 27) and considered a priority for this study. To analyze whether those cytosolic cysteines contribute to Pex11pβ function of promoting peroxisome proliferation, we generated several mutants: single (Pex11pβ^{C18S}-Myc, Pex11pβ^{C25S}-Myc and Pex11pβ^{C85S}-Myc) was well as double (Pex11pβ$^{C18S\_C25S}$-Myc) and triple mutants (Pex11pβ$^{C18S\_C25S\_C85S}$-Myc). Upon expression in COS-7 cells, all versions were properly targeted to peroxisomes as demonstrated by immunofluorescence microscopy using anti-Myc and anti-Pex14 antibodies (single mutants not shown) (Figure 36, A-I). When compared to wild-type Pex11pβ-Myc, the triple and double mutations did not interfere with the property of Pex11pβ to elongate peroxisomal membranes as confirmed by statistical evaluation (Figure 36, J). Similar results were obtained with the single mutants (not shown). These findings indicate that the three cysteines within the N-terminus of Pex11pβ are not essential for membrane elongation, as they probably do not contribute to its structure by the formation of disulfide bonds.
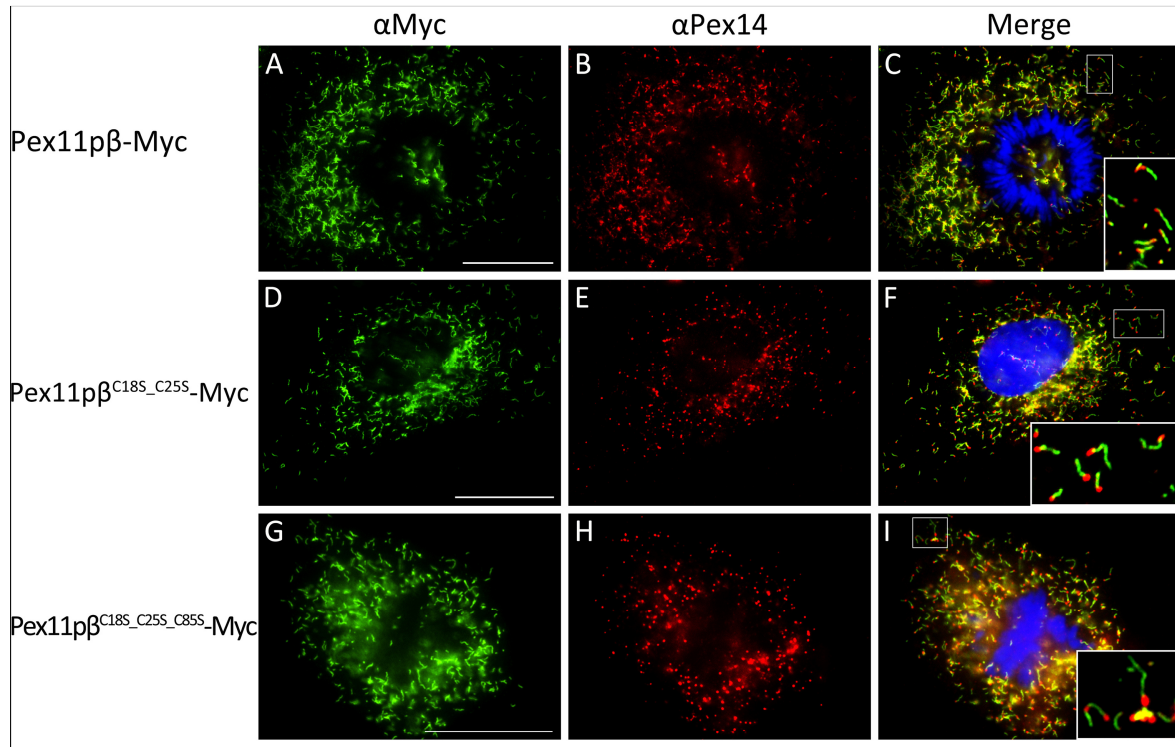
Figure 36: Mutations on N-terminal cysteines within Pex11pβ do not affect peroxisome membrane elongation

Fig x. Mutations on N-terminal cysteines within Pex11pβ do not affect peroxisome membrane elongation. COS-7 cells were transfected by PEI with Pex11pβ-Myc (A-C) Pex11pβ$^{C18S\_C25S}$-Myc (D-F) and Pex11pβ$^{C18S\_C25S\_C85S}$-Myc (G-I), and were processed for immunofluorescence microscopy proximately 30h after transfection using anti-Myc (A, D, G) and anti-Pex14 (B, E, H) antibodies. Nuclei were labelled with Hoechst 33258. The transfected cells were quantitatively evaluated for peroxisome morphology (J). Data are from three independent experiments and are presented as means ± SEM. No significant differences were found between the mutants and wild-type. Bars, 20 μm.
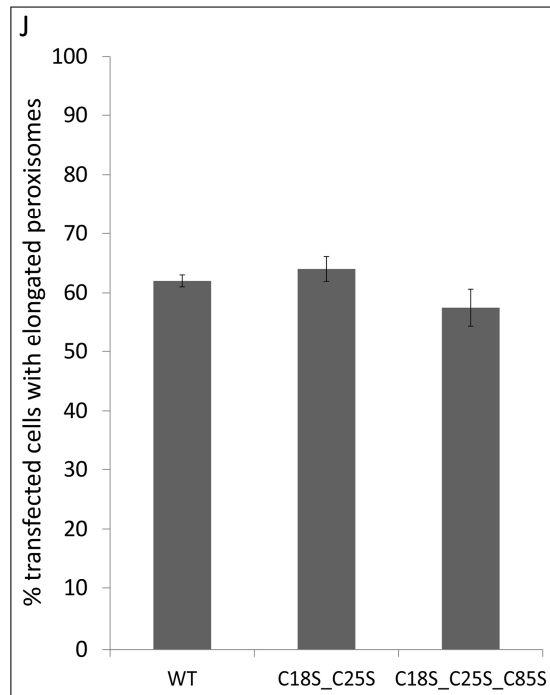
4.2.7 Discussion

Pex11 proteins in yeast, plant and animal cells contribute to the formation of peroxisomes and regulation of their abundance (129, 194, 197, 368). Mammalian Pex11pβ has been shown to elongate and proliferate peroxisomes in conjunction with the peroxisomal division machinery and has been proposed to possess membrane remodeling/deforming properties (191, 215). Its loss is embryonically lethal in knockout mice (205), but on the other hand, in humans, several patients with milder clinical phenotypes but several disabilities have been reported (49, 51, 350). Thus, there is currently great interest in the molecular and biochemical characterization of Pex11 proteins, their mode of action and regulation of peroxisome abundance.

Within this project, we carried out a series of experiments that complemented previous knowledge as well as work from other members of our research group towards a better understanding of the mechanisms involved in the regulation of Pex11pβ function as well as its mode of action. Regardless the diverse topologies proposed for Pex11 proteins in different organisms (190, 219), studies from our group clearly confirmed the previous evidences based on *in silico* analysis and differential permeabilization experiments that pointed to human Pex11pβ as being a transmembrane protein with two membrane spanning domains and with both N- and C-termini facing the cytosol (177, 189, 211). Nonetheless, it was unclear if the region between the transmembrane domains is embedded in or interacting with the peroxisomal membrane or, by the opposite, it fully stands out from the membrane and reaches into the peroxisomal matrix. Within this region, we observed a glycine-rich stretch of thirty amino acids (which also contains three proline residues) that is absent in Pex11pα and Pex11pγ. This unique feature led us to wonder if this particular region had a role in the function of Pex11pβ to promote membrane elongation and division of peroxisomes. However, deletion of the entire glycine-rich stretch revealed it to be dispensable for those functions of Pex11pβ (Figure 30). Using this information, we designed an experiment that could help us to clarify the topology of the intraperoxisomal region of Pex11pβ – we substituted the middle ten amino acids from the glycine-rich area by a Myc tag and performed a selective permeabilization study. That study revealed that the Myc tag is exposed to the cytosol

and not to the peroxisomal matrix (Figure 31). Based on this finding, we suggest that the area between the transmembrane domains may be at least partially buried into the lipid bilayer (Figure 32). The inter-transmembrane region flanking the Gly-rich stretch is very rich in hydrophobic residues (Figure 27), which could allow that region to interact to or even embed into the membrane. This can possibly help to explain why Pex11pβ is extracted from peroxisomal membrane by postfixation Triton X-100 treatment (211, 369), since Pex11pβ may not completely cross peroxisomal membrane.

The insertion of the Myc tag could significantly alter the structure of Pex11pβ, hampering a proper insertion in the membrane and, consequently, alter Pex11pβ function. Overexpression of YFP-Pex11pβ is known to promote peroxisome elongation and division (216). Analyzing the differentially permeabilized cells, one cannot conclude that YFP-Pex11pβ-Myc(mid) mutant had the same effect. However, to undoubtedly clarify that, a time-course experiment comparing with wild type YFP-Pex11pβ could be done.

This study also revealed that S11 and S38 are not involved in the regulation of Pex11pβ by putative phosphorylation. This is consistent with the fact that Pex11pβ has not been demonstrated to be phosphorylated so far. Although Pex11 proteins from fungi were shown to be phosphorylated (220, 290, 370), the phosphorylation sites are not conserved among organisms and, in *Hansenula polymorpha*, phosphorylation do not regulate Pex11p localization and function (370). It is possible that other mammalian Pex11 isoforms, i.e. Pex11pα and Pex11pγ) are phosphorylated and/or other diverse regulatory mechanisms have evolved. Nonetheless, the potential phosphorylation sites of human Pex11pβ have not been exhaustively studied. Indeed, we have chosen S11 and S38 residues because those localize in the cytosolic N-terminal part of Pex11pβ and because they localize in the first 40 amino acids that we had already observed to be essential for Pex11pβ function. Internally localized putative phosphorylated residues were not selected for this study due to the fact that no kinases or phosphatases have been localized in the matrix of mammalian peroxisomes so far. However, the topology studies with the internally tagged YFP-Pex11pβ-Myc(mid) raised the possibility that the glycine-rich are may be exposed to the cytosol instead of to the matrix. Actually, the potential

phosphorylation targets S160, S168 and T178 localize within the glycine-rich area, turning them into interesting targets for further studies on Pex11pβ putative phosphorylation. Interestingly, YFP-Pex11pβ-Myc(mid) protein does not possess the S168 residue and, as mentioned before, this protein seems to be unable to promote peroxisome proliferation (although more extensive studies are needed). A possible malfunction of this protein could be due to the absence of the possible phosphorylation target S168.

The amphipathic Helix 3 of Pex11 proteins from several fungal species and human (Pex11pα) was suggested to play the central role in membrane elongation as it was able to elongate small unilamellar vesicles *in vitro* (191). However, no evidences for that was obtained *in vivo* mammalian cells. Given that and to further characterize human Pex11pβ, we made N-terminally truncated versions that eliminated the first 40 (ΔN40), 60 (ΔN60) and 70 (ΔN70) amino acids. In all cases, the loss of those amino acids abolished membrane elongation of peroxisomes (Figure 34). Whereas the ΔN60 and ΔN70 truncations disrupt all helices, the ΔN40 truncation leaves Helix 3 intact (Figure 29). This means that Helix 2 within the first 40 amino acids is crucial for membrane elongation. This assumption was further supported by the work of other member of our team demonstrating that breaking the helical structure of Helix 2 by mutating alanine at position 21 into a proline (A21P) was sufficient to inhibit peroxisome elongation (211). Moreover, ΔN40 and A21P mutant versions of Pex11pβ were demonstrated to prevent homodimer formation which is presumed to be a prerequisite for membrane retention and elongation of the peroxisomal membrane (211, 213). Marshall and colleagues (219) suggest that, by the contrary, the active form of *Sc*Pex11p is the monomeric one. So, further studies are needed to undoubtedly verify which form is active in human Pex11pβ as dimerization/oligomerization seems to be an activity regulation mechanism for this peroxin.

Another important protein activity regulatory mechanism is the versatile modification of key cysteine residues. These residues may either contribute to protein structure by establishment of stable inter- and intramolecular disulfide bonds. On the other hand, reversible bonds may be established in response to redox state alterations as cysteine

residues possess a thiol group (366). In this study we demonstrated that the N-terminally located cysteines C18, C25 and C85 are not essential for peroxisome membrane elongation (Figure 36). Given that Pex11pβ self-interactions in co-immunoprecipitation studies are lost in the presence of Triton X-100 (212), it is unlikely that these residues contribute to dimer formation by covalent bonds, which is in line with our results on mutational studies on the aforementioned cysteine residues. Nonetheless, it is possible that transient, intra- or intermolecular disulfide bridges occur which may change or stabilize Pex11pβ structure or protein interactions later on during the division process. To clarify that, a time-course experiment with these mutants could be done. Importantly, being peroxisomes a shelter for numerous ROS producing/degrading metabolic reactions, a redox-sensitive proliferation control system would make much sense. Moreover, peroxisome division control has been suggested to be regulated by a signal from inside the peroxisome in *Yarrowia lipolytica*: Guo and colleagues (146, 371) proposed that, in mature peroxisomes, an AOx pool binds to Pex16p, cancelling its inhibitory effect on peroxisome division. Now, a proliferation-favorable redox-state within peroxisomes could be sensed by Pex11pβ *via* its internal cysteine residues, namely C153 and C216, which localize in the inter-transmembrane domains region (Figure 27). Redox-state sensing by these cysteines could provoke conformational alterations on Pex11pβ signaling for peroxisome proliferation. Thus, cysteines C153 and C216 may represent very interesting targets for future investigations on human Pex11pβ activity regulation.

Pex11p proteins were known to act in concert with the tail-anchored proteins Fis1 and Mff for the recruitment of DLP1 and promote final peroxisome scission after elongation and constriction (214). However, a very recent study revealed that both yeast and mammalian Pex11p/Pex11pβ interact directly with Dnm1/Drp1 (DLP1 yeast and mammalian homologs) (222). Moreover, Pex11p/Pex11pβ was shown to function as a GTPase-activating protein (GAP) for Dnm1/Drp1. GAPs have the capability to increase the hydrolysis rate of GTP into GDP. DLP1 forms oligomeric ring-like structures around constricted sites on organelle membranes and, as a large GTPase, its scission activity is powered by GTP hydrolysis (222). Given this, Pex11pβ assumes nowadays a new role in peroxisome proliferation: that of a direct player in membrane scission. This finding re-

enforces the need to deeply study the mechanisms of action and, very importantly, the mechanisms of regulation of Pex11pβ as it seems to be a crucial player in virtually the whole peroxisome proliferation process, from elongation to constriction and final scission.

The recent finding of seven more *PEX11B* patients (48, 49), which present atypical symptoms for a peroxisome biogenesis disorder, brought the urgency of a wider comprehension of this peroxin to the front. The peroxisomes from these patients are import-competent, although enlarged and undivided. In the case of the patient with a newborn lethal mutation in the *DLP1* gene, the fibroblasts presented elongated and constricted peroxisomes as well as hypertubulated mitochondria. These cases alert for the necessity to be aware of the importance of peroxisome (and mitochondria) morphology in health and disease, as peroxisomes have been demonstrated to be involved in several pathological conditions such as Alzheimer's disease (55), diabetes (58, 59) and cancer (64).

5   General discussion and future perspectives

Since the discovery of peroxisomes around 60 years ago (1) that evidences of their pivotal role in human health and development have increased, as several devastating disorders have been found to be caused by impaired peroxisomal activity or defective peroxisome biogenesis (43). Besides, peroxisomes have also been implicated in several non-inherited pathological conditions, such as Alzheimer's disease, diabetes, cancer and viral infection (reviewed in (276)). Peroxisomes are involved in numerous metabolic pathways, which implies a cooperation with several other subcellular compartments including mitochondria, ER, lipid droplets or lysosomes (242, 372, 373). They also constitute an important intracellular platform for redox-, lipid-, inflammatory- and antiviral signaling (69, 374, 375). Peroxisomes are also dynamic organelles, having the capacity to proliferate in response to environmental stimuli and being degraded to maintain default numbers when stimuli dissipate. This way, control of peroxisome number must be achieved by tight regulation of peroxisome biogenesis, proliferation and degradation (11, 72, 376). Being protein reversible phosphorylation a major signal transduction mechanism in eukaryotic cells (278), we focused our studies in the role of such events in peroxisome dynamics, focusing on two key peroxins, Pex16p and Pex11pβ.

Pex16p is known to be one of the three early peroxins, as its absence provokes the absolute inexistence of peroxisomal structures (118, 120). The exact function of Pex16p in human cells is still a matter of debate, but evidences have been pointing into a role in PMP reception during the early stages of the *de novo* peroxisome formation at the ER, as well as in mature peroxisomes (140, 141, 143, 144). This property appears to be conserved at least between mammals and plants (141). On the other hand, Pex11pβ belongs to a family of proteins known to control peroxisome proliferation and to regulate peroxisome morphology, size and number across fungi, plants and mammals (188, 190-195). Pex16p and Pex11pβ seem to operate in different stages of peroxisome dynamics but they have one thing in common: obscure regulation mechanisms.

Concerning Pex16p, our project followed the clues that pointed to Pex16p as a putative PP1-interacting protein (PIP): Pex16p harbours three putative PP1-binding motifs and it

was identified in a yeast two-hybrid screen with PP1. Until now, Akap11 (294) and Limkain-b1 (298) are the only evidences of protein kinases/phosphatases or its regulators at mammalian peroxisomes. Moreover, PP1 is one of the most abundant serine/threonine phosphatases which, together with PP2A, accounts for more than 90% of the protein phosphatase activity in eukaryotes (278) and it relies on complex formation with PIPs for substrate specificity and binding (313). As a putative PIP, Pex16p presented as a link between cell signaling cascades and peroxisome biogenesis as it could bring PP1 into the vicinity of dephosphorylation substrates on the peroxisome. Despite our efforts, we could not verify the interaction. Several technical barriers stickled our experiments, such as the transmembrane topology of Pex16p which, for example, may have hampered its expression in bacteria or the activation of reporter genes in the yeast two-hybrid assays. In addition, the results of *in vitro* assays, such as protein membrane overlay, could have been affected by denaturing conditions. Moreover, a possible transient nature of this putative interaction may have restrained its verification by some methods, like subcellular co-localization and co-immunoprecipitation. As previously discussed, several other approaches could be used to verify the putative PP1-Pex16p interaction. However, we highlight mammalian-membrane two-hybrid assay (MaMTH) as it presents as the best native conditions-mimicking for membrane protein-protein interactions (363). This technology was recently developed and it is a split ubiquitin-based method, similar to the one that already existed for yeast (362). Being a method that uses the activation of reporter genes instead of a direct detection of the protein-protein interaction, it is ideal for verification of transient interactions. Moreover, it doesn't depend on the direct binding of the protein-protein complex with the nuclear DNA to activate the reporter genes (as in the yeast two-hybrid system we used); instead, a membrane bait protein is tagged with the C-terminal half of ubiquitin and a chimeric transcription factor, and a cytosolic or membrane-bound prey is tagged with the N-terminal half of ubiquitin. Upon interaction of bait and prey, the split halves form pseudoubiquitin, which is recognized by cytosolic deubiquitination enzymes, resulting in the cleavage of the transcription factor and expression of a reporter gene (363). Finally, since the system works in mammalian cells, the proteins on study would be as close to the natural environment as possible. This

system even allows the tracking of the effect of post-translational modifications (e.g. phosphorylation) or stimuli (e.g. ROS) on the interaction (363). Given all this, we think that this could be a very interesting method to further verify and manipulate PP1-Pex16p putative interaction. Moreover, the method could also be an efficient, fast and cost effective method to search for PP1 interactors among other peroxins, primarily the ones that revealed to harbor PP1-binding motifs as well (e.g. Pex3p and Pex10p). A search for PP1-binding motifs in the proteins of the peroxisome fission machinery revealed that the ubiquitin-conjugating enzyme that ubiquitinates Pex5p during the receptor-recycling step of matrix protein import (UbcH5a/b/c) (105) also harbors two PP1-binding motifs. Pex14p and Pex15p, other members of the matrix import machinery, have been demonstrated to be phosphorylated, although the role of this post-translational modification in those peroxins is still unclear. Nonetheless, the possibility of UbcH5a/b/c to function as a regulator subunit of a PP1 holoenzyme in the vicinity of Pex14p and Pex15p is a very interesting matter to be further studied. On the other hand, some PIPs are PP1 substrates themselves and their controlled dephosphorylation serves a regulatory function (278), so that it would also be interesting to search for potential phosphorylated residues on Pex16p (and the other potential peroxisomal PIPs).

The few studies published so far demonstrating the presence of kinases or phosphatases in peroxisomes were carried out in *Arabidopsis thaliana* (PP2A, MKP1 and CPK1) (300-302, 304). Being phosphorylation a major regulation and signal transduction mechanism, it is urgent to intensify the studies on that matter also in mammalian peroxisomes. Indeed, PP1, as well as other kinases and phosphatases (e.g. MKK6 and PP2A) were identified in a large scale blot screen in highly purified rat peroxisome fractions. This result, not only supported a putative role for PP1 in peroxisomes as it opened new routes for further investigations on this field. As a matter of fact, the role of some of those kinases and phosphatases on mammalian peroxisomes is being currently investigated by other members of our research group.

Another issue that urges to be explored is whether functional domains are present in the C-terminus of Pex16p and what is their contribution to the function of this early peroxin.

All *PEX16* patients (some with Zellweger syndrome, others with milder phenotypes) described up today had mutations that somehow affected the C-terminus of the protein (118, 349-351). Nonetheless, none of the mutations directly affected any of the known Pex16p functional domains, such as the peroxisome targeting- and the PMP recruitment domains (120, 141, 152, 352), which localize in the cytosolic N-terminus. An *in silico* analysis of human Pex16p sequence revealed several putative functional domains, such as potentially phosphorylated residues. The clarification of these issues is of primordial importance for a full comprehension of Pex16p function and mechanisms of action and regulation, which would consequently enlighten us concerning peroxisome biogenesis process and regulation.

In addition to a putative phosphatase regulator (Pex16p), our study also addressed a potentially phosphorylated peroxin – Pex11pβ, which is involved in proliferation of peroxisomes by membrane remodeling (194) and as a GTPase-activating protein for DLP1 (222). Nonetheless, its regulation mechanisms remain unclear. While Pex11p proteins have been revealed to be regulated by phosphorylation in fungi (220, 290), that has not been verified in human Pex11pβ so far. Our studies revealed that serines S11 and S38 are not involved in the regulation of Pex11pβ by phosphorylation. However, more exhaustive studies are needed to be done, as other residues may have that function. Another aspect regarding regulation mechanisms that urges to be extensively analyzed is the capacity of Pex11pβ to form dimeric/oligomeric structures (211, 213). Studies from our research group suggest that homodimerization of Pex11pβ is a pre-requisite for peroxisomal membrane elongation and that amphipathic helix 2 is needed to the self-interaction (211). However, this subject is still open for discussion. Using the fact that monomeric and dimeric forms of Pex11pβ are extracted from post-fixated peroxisomal membranes by Triton X-100 detergent (211), a time-course experiment at, for instance, 24 h, 48 h, and 72 h after transfection could elucidate us about which form is predominant in each phase of peroxisome proliferation.

Another important regulation mechanism to be explored in Pex11pβ is possible modifications by key cysteines. Cysteines are recognized for having the capacity to

establish permanent and transient disulfide bridges that contribute to the protein structure and inter-molecular interactions. Moreover, transient conformational changes conducted by cysteine residues are often driven by redox-state alterations in protein's environment (366). Given that one of the multiple functions of peroxisomes is peroxide and ROS metabolism (12), together with the fact that oxidative stress has been shown to induce pronounced peroxisome elongation in a human cell line (377), exhaustive studies on the role of Pex11pβ cysteines is a must. Our results suggest that cysteines C18, C25 and C85, which are localized in the N-terminal region of human Pex11pβ, are not relevant for the Pex11pβ-induced peroxisome elongation. However, a time-course experiment would clarify if those residues have a role on later proliferation stages, such as constriction or fission. Moreover, other Pex11pβ cysteines may also be interesting to study, namely the ones that localize in the region between the transmembrane domains. In addition, a possible role of these cysteines could only be detectable under redox-state destabilizing conditions. So that we suggest that studies such as the ones conducted by Schrader and colleagues (377) are repeated using cells expressing cysteine-mutated Pex11pβ.

Several studies have addressed the cytosolic N-terminal region of Pex11 proteins (191, 211). However, the area in between the transmembrane domains is still a mystery. The apparently dispensable glycine-rich stretch localized in this region rises an important question: why does it occur in Pex11pβ isoform and not in Pex11pα or Pex11pγ? Does it traduce a particular role of Pex11pβ isoform? Is it evolutionarily relevant? An *in silico* analysis of Pex11p homologs in other species is needed to understand the meaning of the presence of such an exceptional amino acid stretch in human Pex11pβ. That way, new experiments could be designed to figure out the function of this domain. Furthermore, our studies have pointed to the necessity to put efforts on the definition of the topology of the inter-transmembrane domains area, given that it may not be fully embedded on peroxisomal matrix as assumed up to nowadays. The clarification of the exact topology of this area – matrix and/or membrane embedded – is very important because it influences the putative role of key amino acids (e.g. potentially phosphorylated residues and cysteines).

The understanding of the mechanisms that regulate peroxisome biogenesis and proliferation is extremely valuable to help to comprehend certain pathological processes and possibly contribute for better disease diagnostics and treatment. As an example, given that peroxisomes represent one of the first defense lines against Aβ(and other neurodegenerative conditions)-induced oxidative stress (56, 378, 379), manipulating peroxisome proliferation could eventually be a treatment approach in early-stage patients. Hence, the research of such regulation mechanisms is off extreme importance, since it is still an underexplored field and it has serious repercussions on human health and disease.

Bibliography

1. Rhodin J. Correlation of ultrastructural organization and function in normal experimentally changed convoluted tubule cells of the mouse kidney. Stockholm: Aktiebolaget Godvil; 1954.

2. De Duve C, Baudhuin P. Peroxisomes (microbodies and related particles). Physiological reviews. 1966;46(2):323-57. Epub 1966/04/01.

3. Frederick SE, Newcomb EH. Cytochemical localization of catalase in leaf microbodies (peroxisomes). J Cell Biol. 1969;43(2):343-53. Epub 1969/11/01.

4. Schrader M, Fahimi HD. Mammalian peroxisomes and reactive oxygen species. Histochem Cell Biol. 2004;122(4):383-93.

5. Purdue PE, Lazarow PB. Peroxisome biogenesis. Annual review of cell and developmental biology. 2001;17:701-52.

6. Reddy JK, Krishnakantha TP. Hepatic peroxisome proliferation: induction by two novel compounds structurally unrelated to clofibrate. Science. 1975;190(4216):787-9. Epub 1975/11/21.

7. Novikoff AB, Goldfischer S. Visualization of peroxisomes (microbodies) and mitochondria with diaminobenzidine. The journal of histochemistry and cytochemistry : official journal of the Histochemistry Society. 1969;17(10):675-80. Epub 1969/10/01.

8. Lazarow PB, De Duve C. A fatty acyl-CoA oxidizing system in rat liver peroxisomes; enhancement by clofibrate, a hypolipidemic drug. Proc Natl Acad Sci U S A. 1976;73(6):2043-6. Epub 1976/06/01.

9. Pieuchot L, Jedd G. Peroxisome assembly and functional diversity in eukaryotic microorganisms. Annual review of microbiology. 2012;66:237-63. Epub 2012/09/22.

10. Islinger M, Cardoso MJ, Schrader M. Be different--the diversity of peroxisomes in the animal kingdom. Biochim Biophys Acta. 2010;1803(8):881-97. Epub 2010/03/30.

11. Schrader M, Fahimi HD. Growth and division of peroxisomes. International review of cytology. 2006;255:237-90. Epub 2006/12/21.

12. Schrader M, Fahimi HD. The peroxisome: still a mysterious organelle. Histochem Cell Biol. 2008;129(4):421-40. Epub 2008/02/16.

13. Pfeifer S, Zimmer C. [Biotransformation and pharmacokinetics of beta-receptor blockaders]. Die Pharmazie. 1975;30(10):625-33. Epub 1975/10/01. Biotransformation und Pharmakokinetik von beta-Rezeptorenblockern.

14. Wanders RJ, Waterham HR. Biochemistry of mammalian peroxisomes revisited. Annu Rev Biochem. 2006;75:295-332. Epub 2006/06/08.

15. Schrader M, Yoon Y. Mitochondria and peroxisomes: are the 'big brother' and the 'little sister' closer than assumed? BioEssays : news and reviews in molecular, cellular and developmental biology. 2007;29(11):1105-14. Epub 2007/10/16.

16. Camoes F, Bonekamp NA, Delille HK, Schrader M. Organelle dynamics and dysfunction: A closer link between peroxisomes and mitochondria. J Inherit Metab Dis. 2009;32(2):163-80. Epub 2008/12/11.

17. Lodhi IJ, Semenkovich CF. Peroxisomes: a nexus for lipid metabolism and cellular signaling. Cell Metab. 2014;19(3):380-92. Epub 2014/02/11.

18. Poirier Y, Antonenkov VD, Glumoff T, Hiltunen JK. Peroxisomal beta-oxidation--a metabolic pathway with multiple functions. Biochim Biophys Acta. 2006;1763(12):1413-26. Epub 2006/10/10.

19. Shen YQ, Burger G. Plasticity of a key metabolic pathway in fungi. Functional & integrative genomics. 2009;9(2):145-51. Epub 2008/09/17.

20. Wanders RJ, Vreken P, Ferdinandusse S, Jansen GA, Waterham HR, van Roermund CW, et al. Peroxisomal fatty acid alpha- and beta-oxidation in humans: enzymology, peroxisomal metabolite transporters and peroxisomal diseases. Biochemical Society transactions. 2001;29(Pt 2):250-67. Epub 2001/05/18.

21.   Lazarow PB. The role of peroxisomes in mammalian cellular metabolism. J Inherit Metab Dis. 1987;10 Suppl 1(Suppl 1):11-22. Epub 1987/01/01.

22.   Ferdinandusse S, Meissner T, Wanders RJ, Mayatepek E. Identification of the peroxisomal beta-oxidation enzymes involved in the degradation of leukotrienes. Biochem Biophys Res Commun. 2002;293(1):269-73. Epub 2002/06/11.

23.   Jansen GA, Wanders RJ. Alpha-oxidation. Biochim Biophys Acta. 2006;1763(12):1403-12. Epub 2006/08/29.

24.   Casteels M, Foulon V, Mannaerts GP, Van Veldhoven PP. Alpha-oxidation of 3-methyl-substituted fatty acids and its thiamine dependence. Eur J Biochem. 2003;270(8):1619-27. Epub 2003/04/16.

25.   Malheiro AR, da Silva TF, Brites P. Plasmalogens and fatty alcohols in rhizomelic chondrodysplasia punctata and Sjogren-Larsson syndrome. J Inherit Metab Dis. 2015;38(1):111-21. Epub 2014/11/30.

26.   Wanders RJ, Waterham HR. Peroxisomal disorders: the single peroxisomal enzyme deficiencies. Biochim Biophys Acta. 2006;1763(12):1707-20. Epub 2006/10/24.

27.   Nagan N, Zoeller RA. Plasmalogens: biosynthesis and functions. Progress in lipid research. 2001;40(3):199-229. Epub 2001/03/29.

28.   van den Bosch H, Schutgens RB, Wanders RJ, Tager JM. Biochemistry of peroxisomes. Annu Rev Biochem. 1992;61:157-97. Epub 1992/01/01.

29.   Hogenboom S, Tuyp JJ, Espeel M, Koster J, Wanders RJ, Waterham HR. Mevalonate kinase is a cytosolic enzyme in humans. J Cell Sci. 2004;117(Pt 4):631-9. Epub 2004/01/20.

30.   Bonekamp NA, Volkl A, Fahimi HD, Schrader M. Reactive oxygen species and peroxisomes: struggling for balance. Biofactors. 2009;35(4):346-55. Epub 2009/05/22.

31.   Angermuller S, Bruder G, Volkl A, Wesch H, Fahimi HD. Localization of xanthine oxidase in crystalline cores of peroxisomes. A cytochemical and biochemical study. Eur J Cell Biol. 1987;45(1):137-44. Epub 1987/12/01.

32.   Dhaunsi GS, Gulati S, Singh AK, Orak JK, Asayama K, Singh I. Demonstration of Cu-Zn superoxide dismutase in rat liver peroxisomes. Biochemical and immunochemical evidence. J Biol Chem. 1992;267(10):6870-3. Epub 1992/04/05.

33.   Immenschuh S, Baumgart-Vogt E. Peroxiredoxins, oxidative stress, and cell proliferation. Antioxid Redox Signal. 2005;7(5-6):768-77. Epub 2005/05/14.

34.   Singh AK, Dhaunsi GS, Gupta MP, Orak JK, Asayama K, Singh I. Demonstration of glutathione peroxidase in rat liver peroxisomes and its intraorganellar distribution. Arch Biochem Biophys. 1994;315(2):331-8. Epub 1994/12/01.

35.   Singh I. Mammalian peroxisomes: metabolism of oxygen and reactive oxygen species. Annals of the New York Academy of Sciences. 1996;804:612-27. Epub 1996/12/27.

36.   Danpure CJ. Primary hyperoxaluria type 1: AGT mistargeting highlights the fundamental differences between the peroxisomal and mitochondrial protein import pathways. Biochim Biophys Acta. 2006;1763(12):1776-84. Epub 2006/10/10.

37.   Antonenkov VD. Dehydrogenases of the pentose phosphate pathway in rat liver peroxisomes. Eur J Biochem. 1989;183(1):75-82. Epub 1989/07/15.

38.   Kunze M, Pracharoenwattana I, Smith SM, Hartig A. A central role for the peroxisomal membrane in glyoxylate cycle function. Biochim Biophys Acta. 2006;1763(12):1441-52. Epub 2006/10/24.

39.   Jedd G, Chua NH. A new self-assembled peroxisomal vesicle required for efficient resealing of the plasma membrane. NatCell Biol. 2000;2(4):226-31.

40.   Muller WH, Bovenberg RA, Groothuis MH, Kattevilder F, Smaal EB, Van der Voort LH, et al. Involvement of microbodies in penicillin biosynthesis. Biochim Biophys Acta. 1992;1116(2):210-3. Epub 1992/04/22.

41.   Reumann S, Weber AP. Plant peroxisomes respire in the light: some gaps of the photorespiratory C2 cycle have become filled--others remain. Biochim Biophys Acta. 2006;1763(12):1496-510. Epub 2006/10/19.

42.   Gould SJ, Keller GA, Subramani S. Identification of a Peroxisomal Targeting Signal at the Carboxy Terminus of Firefly Luciferase. Journal of Cell Biology. 1987;105(6):2923-31.

43.   Aubourg P, Wanders R. Peroxisomal disorders. Handbook of clinical neurology. 2013;113:1593-609. Epub 2013/04/30.

44.   Wanders RJ. Metabolic functions of peroxisomes in health and disease. Biochimie. 2014;98:36-44. Epub 2013/09/10.

45.   Moser AB, Rasmussen M, Naidu S, Watkins PA, McGuinness M, Hajra AK, et al. Phenotype of patients with peroxisomal disorders subdivided into sixteen complementation groups. The Journal of pediatrics. 1995;127(1):13-22. Epub 1995/07/01.

46.   Wanders RJ. Metabolic and molecular basis of peroxisomal disorders: a review. American journal of medical genetics Part A. 2004;126A(4):355-75. Epub 2004/04/21.

47.   Steinberg SJ, Dodt G, Raymond GV, Braverman NE, Moser AB, Moser HW. Peroxisome biogenesis disorders. Biochim Biophys Acta. 2006;1763(12):1733-48.

48.   Ebberink MS, Koster J, Visser G, Spronsen F, Stolte-Dijkstra I, Smit GP, et al. A novel defect of peroxisome division due to a homozygous non-sense mutation in the PEX11beta gene. J Med Genet. 2012;49(5):307-13. Epub 2012/05/15.

49.   Ebberink MS, Koster J, Stark Z, Ryan M, Chan E, Ta G, et al. PEX11β deficiency: a novel human peroxisome biogenesis disorder affecting peroxisome division. SSIEM 2014 Annual Symposium; Innsbruck, Austria: Springer Netherlands; 2014. p. 27-185.

50.   Waterham HR, Koster J, van Roermund CW, Mooyer PA, Wanders RJ, Leonard JV. A lethal defect of mitochondrial and peroxisomal fission. N Engl J Med. 2007;356(17):1736-41.

51.   Thoms S, Gartner J. First PEX11 patient extends spectrum of peroxisomal biogenesis disorder phenotypes. Journal of Medical Genetics. 2012;49(5):314-6.

52.   van Roermund CW, Visser WF, Ijlst L, van Cruchten A, Boek M, Kulik W, et al. The human peroxisomal ABC half transporter ALDP functions as a homodimer and accepts acyl-CoA esters. FASEB J. 2008;22(12):4201-8. Epub 2008/09/02.

53.   Berger J, Gartner J. X-linked adrenoleukodystrophy: clinical, biochemical and pathogenetic aspects. Biochim Biophys Acta. 2006;1763(12):1721-32. Epub 2006/09/05.

54.   Moser HW, Mahmood A, Raymond GV. X-linked adrenoleukodystrophy. Nature clinical practice Neurology. 2007;3(3):140-51. Epub 2007/03/08.

55.   Santos MJ, Quintanilla RA, Toro A, Grandy R, Dinamarca MC, Godoy JA, et al. Peroxisomal proliferation protects from beta-amyloid neurodegeneration. J Biol Chem. 2005;280(49):41057-68. Epub 2005/10/06.

56.   Cimini A, Benedetti E, D'Angelo B, Cristiano L, Falone S, Di Loreto S, et al. Neuronal response of peroxisomal and peroxisome-related proteins to chronic and acute Abeta injury. Curr Alzheimer Res. 2009;6(3):238-51. Epub 2009/06/13.

57.   Lizard G, Rouaud O, Demarquoy J, Cherkaoui-Malki M, Iuliano L. Potential roles of peroxisomes in Alzheimer's disease and in dementia of the Alzheimer's type. J Alzheimers Dis. 2012;29(2):241-54. Epub 2012/03/22.

58.   Gehrmann W, Elsner M, Lenzen S. Role of metabolically generated reactive oxygen species for lipotoxicity in pancreatic beta-cells. Diabetes, obesity & metabolism. 2010;12 Suppl 2:149-58. Epub 2010/11/05.

59.   Elsner M, Gehrmann W, Lenzen S. Peroxisome-generated hydrogen peroxide as important mediator of lipotoxicity in insulin-producing cells. Diabetes. 2011;60(1):200-8. Epub 2010/10/26.

60.   Snyder F, Wood R. Alkyl and alk-1-enyl ethers of glycerol in lipids from normal and neoplastic human tissues. Cancer Res. 1969;29(1):251-7. Epub 1969/01/01.

61.   Howard BV, Morris HP, Bailey JM. Ether-lipids, -glycerol phosphate dehydrogenase, and growth rate in tumors and cultured cells. Cancer Res. 1972;32(7):1533-8. Epub 1972/07/01.

62.   Albert DH, Anderson CE. Ether-linked glycerolipids in human brain tumors. Lipids. 1977;12(2):188-92. Epub 1977/02/01.

63.   Roos DS, Choppin PW. Tumorigenicity of cell lines with altered lipid composition. Proc Natl Acad Sci U S A. 1984;81(23):7622-6. Epub 1984/12/01.

64.   Benjamin DI, Cozzo A, Ji X, Roberts LS, Louie SM, Mulvihill MM, et al. Ether lipid generating enzyme AGPS alters the balance of structural and signaling lipids to fuel cancer pathogenicity. Proc Natl Acad Sci U S A. 2013;110(37):14912-7. Epub 2013/08/28.

65.   Valenca I, Pertega-Gomes N, Vizcaino JR, Henrique RM, Lopes C, Baltazar F, et al. Localization of MCT2 at peroxisomes is associated with malignant transformation in prostate cancer. Journal of cellular and molecular medicine. 2015. Epub 2015/02/03.

66.   Terlecky SR, Koepke JI, Walton PA. Peroxisomes and aging. Biochim Biophys Acta. 2006;1763(12):1749-54. Epub 2006/10/10.

67.   Leonov A, Titorenko VI. A network of interorganellar communications underlies cellular aging. IUBMB Life. 2013;65(8):665-74. Epub 2013/07/03.

68.   Fransen M, Nordgren M, Wang B, Apanasets O, Van Veldhoven PP. Aging, age-related diseases and peroxisomes. Sub-cellular biochemistry. 2013;69:45-65. Epub 2013/07/04.

69.   Odendall C, Kagan JC. Peroxisomes and the antiviral responses of mammalian cells. Sub-cellular biochemistry. 2013;69:67-75. Epub 2013/07/04.

70.   Distel B, Erdmann R, Gould SJ, Blobel G, Crane DI, Cregg JM, et al. A unified nomenclature for peroxisome biogenesis factors. J Cell Biol. 1996;135(1):1-3. Epub 1996/10/01.

71.   Kiel JA, Veenhuis M, van der Klei IJ. PEX genes in fungal genomes: common, rare or redundant. Traffic. 2006;7(10):1291-303. Epub 2006/09/19.

72.   Lazarow PB, Fujiki Y. Biogenesis of peroxisomes. Annual review of cell biology. 1985;1:489-530. Epub 1985/01/01.

73.   Schnell DJ, Hebert DN. Protein translocons: multifunctional mediators of protein translocation across membranes. Cell. 2003;112(4):491-505. Epub 2003/02/26.

74.   Leon S, Goodman JM, Subramani S. Uniqueness of the mechanism of protein import into the peroxisome matrix: transport of folded, co-factor-bound and oligomeric proteins by shuttling receptors. Biochim Biophys Acta. 2006;1763(12):1552-64. Epub 2006/10/03.

75.   Hettema EH, Erdmann R, van der Klei I, Veenhuis M. Evolving models for peroxisome biogenesis. Curr Opin Cell Biol. 2014;29:25-30. Epub 2014/04/01.

76.   Lametschwandtner G, Brocard C, Fransen M, Van Veldhoven P, Berger J, Hartig A. The difference in recognition of terminal tripeptides as peroxisomal targeting signal 1 between yeast and human is due to different affinities of their receptor Pex5p to the cognate signal and to residues adjacent to it. J Biol Chem. 1998;273(50):33635-43. Epub 1998/12/05.

77.   Brocard C, Hartig A. Peroxisome targeting signal 1: is it really a simple tripeptide? Biochim Biophys Acta. 2006;1763(12):1565-73. Epub 2006/09/30.

78.   Chowdhary G, Kataya AR, Lingner T, Reumann S. Non-canonical peroxisome targeting signals: identification of novel PTS1 tripeptides and characterization of enhancer elements by computational permutation analysis. BMC plant biology. 2012;12:142. Epub 2012/08/14.

79.   Lazarow PB. The import receptor Pex7p and the PTS2 targeting sequence. Biochim Biophys Acta. 2006;1763(12):1599-604. Epub 2006/09/26.

80.   Gatto GJ, Jr., Geisbrecht BV, Gould SJ, Berg JM. Peroxisomal targeting signal-1 recognition by the TPR domains of human PEX5. Nature structural biology. 2000;7(12):1091-5. Epub 2000/12/02.

81.   Rehling P, Marzioch M, Niesen F, Wittke E, Veenhuis M, Kunau WH. The import receptor for the peroxisomal targeting signal 2 (PTS2) in Saccharomyces cerevisiae is encoded by the PAS7 gene. EMBO J. 1996;15(12):2901-13. Epub 1996/06/17.

82.   Woodward AW, Bartel B. The Arabidopsis peroxisomal targeting signal type 2 receptor PEX7 is necessary for peroxisome function and dependent on PEX5. Mol Biol Cell. 2005;16(2):573-83. Epub 2004/11/19.

83.   Otera H, Harano T, Honsho M, Ghaedi K, Mukai S, Tanaka A, et al. The mammalian peroxin Pex5pL, the longer isoform of the mobile peroxisome targeting signal (PTS) type 1 transporter, translocates the Pex7p.PTS2 protein complex into peroxisomes via its initial docking site, Pex14p. J Biol Chem. 2000;275(28):21703-14. Epub 2000/04/18.

84.   Dodt G, Warren D, Becker E, Rehling P, Gould SJ. Domain mapping of human PEX5 reveals functional and structural similarities to Saccharomyces cerevisiae Pex18p and Pex21p. J Biol Chem. 2001;276(45):41769-81. Epub 2001/09/08.

85.   Titorenko VI, Nicaud JM, Wang H, Chan H, Rachubinski RA. Acyl-CoA oxidase is imported as a heteropentameric, cofactor-containing complex into peroxisomes of Yarrowia lipolytica. J Cell Biol. 2002;156(3):481-94. Epub 2002/01/30.

86.   Parkes JA, Langer S, Hartig A, Baker A. PTS1-independent targeting of isocitrate lyase to peroxisomes requires the PTS1 receptor Pex5p. Molecular membrane biology. 2003;20(1):61-9. Epub 2003/05/15.

87.   Islinger M, Li KW, Seitz J, Volkl A, Luers GH. Hitchhiking of Cu/Zn superoxide dismutase to peroxisomes--evidence for a natural piggyback import mechanism in mammals. Traffic. 2009;10(11):1711-21. Epub 2009/08/19.

88.   van der Klei IJ, Veenhuis M. PTS1-independent sorting of peroxisomal matrix proteins by Pex5p. Biochim Biophys Acta. 2006;1763(12):1794-800. Epub 2006/09/29.

89.   McNew JA, Goodman JM. An oligomeric protein is imported into peroxisomes in vivo. J Cell Biol. 1994;127(5):1245-57. Epub 1994/12/01.

90.   Freitag J, Ast J, Bolker M. Cryptic peroxisomal targeting via alternative splicing and stop codon read-through in fungi. Nature. 2012;485(7399):522-5. Epub 2012/05/25.

91.   Azevedo JE, Schliebs W. Pex14p, more than just a docking protein. Biochim Biophys Acta. 2006;1763(12):1574-84. Epub 2006/10/19.

92.   Williams C, Distel B. Pex13p: docking or cargo handling protein? Biochim Biophys Acta. 2006;1763(12):1585-91. Epub 2006/10/24.

93.   Niederhoff K, Meindl-Beinker NM, Kerssen D, Perband U, Schafer A, Schliebs W, et al. Yeast Pex14p possesses two functionally distinct Pex5p and one Pex7p binding sites. J Biol Chem. 2005;280(42):35571-8. Epub 2005/08/19.

94.   Pires JR, Hong X, Brockmann C, Volkmer-Engert R, Schneider-Mergener J, Oschkinat H, et al. The ScPex13p SH3 domain exposes two distinct binding sites for Pex5p and Pex14p. J Mol Biol. 2003;326(5):1427-35. Epub 2003/02/22.

95.   Natsuyama R, Okumoto K, Fujiki Y. Pex5p stabilizes Pex14p: a study using a newly isolated pex5 CHO cell mutant, ZPEG101. Biochem J. 2013;449(1):195-207. Epub 2012/09/27.

96.   Erdmann R, Schliebs W. Opinion: Peroxisomal matrix protein import: the transient pore model. Nature reviews Molecular cell biology. 2005;6(9):738-42.

97.   Freitas MO, Francisco T, Rodrigues TA, Alencastre IS, Pinto MP, Grou CP, et al. PEX5 protein binds monomeric catalase blocking its tetramerization and releases it upon binding the N-terminal domain of PEX14. J Biol Chem. 2011;286(47):40509-19. Epub 2011/10/07.

98.   Liu X, Ma C, Subramani S. Recent advances in peroxisomal matrix protein import. Curr Opin Cell Biol. 2012;24(4):484-9. Epub 2012/06/12.

99.   Wang D, Visser NV, Veenhuis M, van der Klei IJ. Physical interactions of the peroxisomal targeting signal 1 receptor pex5p, studied by fluorescence correlation spectroscopy. J Biol Chem. 2003;278(44):43340-5. Epub 2003/08/22.

100.   Kurochkin IV, Mizuno Y, Konagaya A, Sakaki Y, Schonbach C, Okazaki Y. Novel peroxisomal protease Tysnd1 processes PTS1- and PTS2-containing enzymes involved in beta-oxidation of fatty acids. EMBO J. 2007;26(3):835-45. Epub 2007/01/27.

101. Schuhmann H, Huesgen PF, Gietl C, Adamska I. The DEG15 serine protease cleaves peroxisomal targeting signal 2-containing proteins in Arabidopsis. Plant Physiol. 2008;148(4):1847-56. Epub 2008/10/28.

102. Okumoto K, Kametani Y, Fujiki Y. Two proteases, trypsin domain-containing 1 (Tysnd1) and peroxisomal lon protease (PsLon), cooperatively regulate fatty acid beta-oxidation in peroxisomal matrix. J Biol Chem. 2011;286(52):44367-79. Epub 2011/10/18.

103. Carvalho AF, Pinto MP, Grou CP, Alencastre IS, Fransen M, Sa-Miranda C, et al. Ubiquitination of mammalian Pex5p, the peroxisomal import receptor. J Biol Chem. 2007;282(43):31267-72. Epub 2007/08/30.

104. Okumoto K, Misono S, Miyata N, Matsumoto Y, Mukai S, Fujiki Y. Cysteine ubiquitination of PTS1 receptor Pex5p regulates Pex5p recycling. Traffic. 2011;12(8):1067-83. Epub 2011/05/11.

105. Grou CP, Carvalho AF, Pinto MP, Wiese S, Piechura H, Meyer HE, et al. Members of the E2D (UbcH5) family mediate the ubiquitination of the conserved cysteine of Pex5p, the peroxisomal import receptor. J Biol Chem. 2008;283(21):14190-7. Epub 2008/03/25.

106. Platta HW, El Magraoui F, Baumer BE, Schlee D, Girzalsky W, Erdmann R. Pex2 and pex12 function as protein-ubiquitin ligases in peroxisomal protein import. Molecular and cellular biology. 2009;29(20):5505-16. Epub 2009/08/19.

107. Williams C, van den Berg M, Geers E, Distel B. Pex10p functions as an E3 ligase for the Ubc4p-dependent ubiquitination of Pex5p. Biochem Biophys Res Commun. 2008;374(4):620-4. Epub 2008/07/23.

108. Miyata N, Fujiki Y. Shuttling mechanism of peroxisome targeting signal type 1 receptor Pex5: ATP-independent import and ATP-dependent export. Molecular and cellular biology. 2005;25(24):10822-32.

109. Platta HW, Grunau S, Rosenkranz K, Girzalsky W, Erdmann R. Functional role of the AAA peroxins in dislocation of the cycling PTS1 receptor back to the cytosol. Nat Cell Biol. 2005;7(8):817-22. Epub 2005/07/12.

110. Matsumoto N, Tamura S, Fujiki Y. The pathogenic peroxin Pex26p recruits the Pex1p-Pex6p AAA ATPase complexes to peroxisomes. Nat Cell Biol. 2003;5(5):454-60. Epub 2003/04/30.

111. Nashiro C, Kashiwagi A, Matsuzaki T, Tamura S, Fujiki Y. Recruiting mechanism of the AAA peroxins, Pex1p and Pex6p, to Pex26p on the peroxisomal membrane. Traffic. 2011;12(6):774-88. Epub 2011/03/03.

112. Hasan S, Platta HW, Erdmann R. Import of proteins into the peroxisomal matrix. Front Physiol. 2013;4:261. Epub 2013/09/27.

113. Fujiki Y, Nashiro C, Miyata N, Tamura S, Okumoto K. New insights into dynamic and functional assembly of the AAA peroxins, Pex1p and Pex6p, and their membrane receptor Pex26p in shuttling of PTS1-receptor Pex5p during peroxisome biogenesis. Biochim Biophys Acta. 2012;1823(1):145-9. Epub 2011/11/15.

114. Grimm I, Saffian D, Platta HW, Erdmann R. The AAA-type ATPases Pex1p and Pex6p and their role in peroxisomal matrix protein import in Saccharomyces cerevisiae. Biochim Biophys Acta. 2012;1823(1):150-8. Epub 2011/10/04.

115. Grou CP, Francisco T, Rodrigues TA, Freitas MO, Pinto MP, Carvalho AF, et al. Identification of ubiquitin-specific protease 9X (USP9X) as a deubiquitinase acting on ubiquitin-peroxin 5 (PEX5) thioester conjugate. J Biol Chem. 2012;287(16):12815-27. Epub 2012/03/01.

116. Baerends RJ, Rasmussen SW, Hilbrands RE, van der Heide M, Faber KN, Reuvekamp PT, et al. The Hansenula polymorpha PER9 gene encodes a peroxisomal membrane protein essential for peroxisome assembly and integrity. J Biol Chem. 1996;271(15):8887-94. Epub 1996/04/12.

117. Gotte K, Girzalsky W, Linkert M, Baumgart E, Kammerer S, Kunau WH, et al. Pex19p, a farnesylated protein essential for peroxisome biogenesis. Molecular and cellular biology. 1998;18(1):616-28. Epub 1998/01/07.

118.   Honsho M, Tamura S, Shimozawa N, Suzuki Y, Kondo N, Fujiki Y. Mutation in PEX16 is causal in the peroxisome-deficient Zellweger syndrome of complementation group D. American journal of human genetics. 1998;63(6):1622-30. Epub 1998/12/05.

119.   Matsuzono Y, Kinoshita N, Tamura S, Shimozawa N, Hamasaki M, Ghaedi K, et al. Human PEX19: cDNA cloning by functional complementation, mutation analysis in a patient with Zellweger syndrome, and potential role in peroxisomal membrane assembly. Proc Natl Acad Sci U S A. 1999;96(5):2116-21. Epub 1999/03/03.

120.   South ST, Gould SJ. Peroxisome synthesis in the absence of preexisting peroxisomes. J Cell Biol. 1999;144(2):255-66. Epub 1999/01/29.

121.   Ghaedi K, Honsho M, Shimozawa N, Suzuki Y, Kondo N, Fujiki Y. PEX3 is the causal gene responsible for peroxisome membrane assembly-defective Zellweger syndrome of complementation group G. American journal of human genetics. 2000;67(4):976-81. Epub 2000/09/01.

122.   Hettema EH, Girzalsky W, van Den Berg M, Erdmann R, Distel B. Saccharomyces cerevisiae pex3p and pex19p are required for proper localization and stability of peroxisomal membrane proteins. EMBO J. 2000;19(2):223-33. Epub 2000/01/19.

123.   Sacksteder KA, Jones JM, South ST, Li X, Liu Y, Gould SJ. PEX19 binds multiple peroxisomal membrane proteins, is predominantly cytoplasmic, and is required for peroxisome membrane synthesis. J Cell Biol. 2000;148(5):931-44. Epub 2000/03/08.

124.   South ST, Sacksteder KA, Li X, Liu Y, Gould SJ. Inhibitors of COPI and COPII do not block PEX3-mediated peroxisome synthesis. J Cell Biol. 2000;149(7):1345-60.

125.   Otzen M, Perband U, Wang D, Baerends RJ, Kunau WH, Veenhuis M, et al. Hansenula polymorpha Pex19p is essential for the formation of functional peroxisomal membranes. J Biol Chem. 2004;279(18):19181-90. Epub 2004/02/26.

126.   Brosius U, Gartner J. Cellular and molecular aspects of Zellweger syndrome and other peroxisome biogenesis disorders. Cell Mol Life Sci. 2002;59(6):1058-69. Epub 2002/08/10.

127.   Santos MJ, Imanaka T, Shio H, Small GM, Lazarow PB. Peroxisomal membrane ghosts in Zellweger syndrome--aberrant organelle assembly. Science. 1988;239(4847):1536-8. Epub 1988/03/25.

128.   Theodoulou FL, Bernhardt K, Linka N, Baker A. Peroxisome membrane proteins: multiple trafficking routes and multiple functions? Biochem J. 2013;451(3):345-52. Epub 2013/04/16.

129.   Schrader M, Bonekamp NA, Islinger M. Fission and proliferation of peroxisomes. Biochimica et Biophysica Acta (BBA) - Molecular Basis of Disease. 2012;1822(9):1343-57.

130.   Novikoff AB, Shin WY. The endoplasmic reticulum in the Golgi zone and its relations to microbodies, Golgi apparatus and autophagic vacuoles in rat liver cells. J Microsc. 1964;3:187-206.

131.   Kunau WH. Peroxisome biogenesis: end of the debate. Current biology : CB. 2005;15(18):R774-6. Epub 2005/09/20.

132.   Tabak HF, Hoepfner D, Zand A, Geuze HJ, Braakman I, Huynen MA. Formation of peroxisomes: present and past. Biochim Biophys Acta. 2006;1763(12):1647-54. Epub 2006/10/13.

133.   Ma C, Agrawal G, Subramani S. Peroxisome assembly: matrix and membrane protein biogenesis. J Cell Biol. 2011;193(1):7-16. Epub 2011/04/06.

134.   Otzen M, Rucktaschel R, Thoms S, Emmrich K, Krikken AM, Erdmann R, et al. Pex19p contributes to peroxisome inheritance in the association of peroxisomes to Myo2p. Traffic. 2012;13(7):947-59. Epub 2012/04/11.

135.   Sato Y, Shibata H, Nakatsu T, Nakano H, Kashiwayama Y, Imanaka T, et al. Structural basis for docking of peroxisomal membrane protein carrier Pex19p onto its receptor Pex3p. EMBO J. 2010;29(24):4083-93. Epub 2010/11/26.

136.   Schmidt F, Treiber N, Zocher G, Bjelic S, Steinmetz MO, Kalbacher H, et al. Insights into peroxisome function from the structure of PEX3 in complex with a soluble fragment of PEX19. J Biol Chem. 2010;285(33):25410-7. Epub 2010/06/18.

137.   Munck JM, Motley AM, Nuttall JM, Hettema EH. A dual function for Pex3p in peroxisome formation and inheritance. J Cell Biol. 2009;187(4):463-71. Epub 2009/12/02.

138.   Motley AM, Nuttall JM, Hettema EH. Pex3-anchored Atg36 tags peroxisomes for degradation in Saccharomyces cerevisiae. EMBO J. 2012;31(13):2852-68. Epub 2012/05/31.

139.   Nordgren M, Wang B, Apanasets O, Fransen M. Peroxisome degradation in mammals: mechanisms of action, recent advances, and perspectives. Front Physiol. 2013;4:145. Epub 2013/06/21.

140.   Aranovich A, Hua R, Rutenberg AD, Kim PK. PEX16 contributes to peroxisome maintenance by constantly trafficking PEX3 via the ER. J Cell Sci. 2014;127(Pt 17):3675-86. Epub 2014/07/09.

141.   Hua R, Gidda SK, Aranovich A, Mullen RT, Kim PK. Multiple Domains in PEX16 Mediate Its Trafficking and Recruitment of Peroxisomal Proteins to the ER. Traffic. 2015;16(8):832-52. Epub 2015/04/24.

142.   Karnik SK, Trelease RN. Arabidopsis peroxin 16 trafficks through the ER and an intermediate compartment to pre-existing peroxisomes via overlapping molecular targeting signals. Journal of experimental botany. 2007;58(7):1677-93. Epub 2007/04/14.

143.   Kim PK, Mullen RT, Schumann U, Lippincott-Schwartz J. The origin and maintenance of mammalian peroxisomes involves a de novo PEX16-dependent pathway from the ER. J Cell Biol. 2006;173(4):521-32. Epub 2006/05/24.

144.   Matsuzaki T, Fujiki Y. The peroxisomal membrane protein import receptor Pex3p is directly transported to peroxisomes by a novel Pex19p- and Pex16p-dependent pathway. J Cell Biol. 2008;183(7):1275-86. Epub 2008/12/31.

145.   Eitzen GA, Szilard RK, Rachubinski RA. Enlarged peroxisomes are present in oleic acid-grown Yarrowia lipolytica overexpressing the PEX16 gene encoding an intraperoxisomal peripheral membrane peroxin. J Cell Biol. 1997;137(6):1265-78. Epub 1997/06/16.

146.   Guo T, Gregg C, Boukh-Viner T, Kyryakov P, Goldberg A, Bourque S, et al. A signal from inside the peroxisome initiates its division by promoting the remodeling of the peroxisomal membrane. J Cell Biol. 2007;177(2):289-303. Epub 2007/04/18.

147.   Rucktaschel R, Girzalsky W, Erdmann R. Protein import machineries of peroxisomes. Biochim Biophys Acta. 2011;1808(3):892-900. Epub 2010/07/28.

148.   Fang Y, Morrell JC, Jones JM, Gould SJ. PEX3 functions as a PEX19 docking factor in the import of class I peroxisomal membrane proteins. Journal of Cell Biology. 2004;164(6):863-75.

149.   Jones JM, Morrell JC, Gould SJ. PEX19 is a predominantly cytosolic chaperone and import receptor for class 1 peroxisomal membrane proteins. Journal of Cell Biology. 2004;164(1):57-67.

150.   Jones JM, Morrell JC, Gould SJ. Multiple distinct targeting signals in integral peroxisomal membrane proteins. J Cell Biol. 2001;153(6):1141-50. Epub 2001/06/13.

151.   Rottensteiner H, Kramer A, Lorenzen S, Stein K, Landgraf C, Volkmer-Engert R, et al. Peroxisomal membrane proteins contain common Pex19p-binding sites that are an integral part of their targeting signals (mPTS). Mol Biol Cell. 2004;15:3406-17.

152.   Fransen M, Wylin T, Brees C, Mannaerts GP, Van Veldhoven PP. Human pex19p binds peroxisomal integral membrane proteins at regions distinct from their sorting sequences. Molecular and cellular biology. 2001;21(13):4413-24. Epub 2001/06/08.

153.   Saveria T, Halbach A, Erdmann R, Volkmer-Engert R, Landgraf C, Rottensteiner H, et al. Conservation of PEX19-binding motifs required for protein targeting to mammalian peroxisomal and trypanosome glycosomal membranes. Eukaryotic cell. 2007;6(8):1439-49. Epub 2007/06/26.

154.   Shibata H, Kashiwayama Y, Imanaka T, Kato H. Domain architecture and activity of human Pex19p, a chaperone-like protein for intracellular trafficking of peroxisomal membrane proteins. J Biol Chem. 2004;279(37):38486-94. Epub 2004/07/15.

155.   Kashiwayama Y, Asahina K, Shibata H, Morita M, Muntau AC, Roscher AA, et al. Role of Pex19p in the targeting of PMP70 to peroxisome. Biochim Biophys Acta. 2005;1746(2):116-28. Epub 2005/12/14.

156.   Matsuzono Y, Fujiki Y. In vitro transport of membrane proteins to peroxisomes by shuttling receptor Pex19p. J Biol Chem. 2006;281(1):36-42. Epub 2005/11/11.

157.   Girzalsky W, Saffian D, Erdmann R. Peroxisomal protein translocation. Biochim Biophys Acta. 2010;1803(6):724-31. Epub 2010/01/19.

158.   Schluter A, Real-Chicharro A, Gabaldon T, Sanchez-Jimenez F, Pujol A. PeroxisomeDB 2.0: an integrative view of the global peroxisomal metabolome. Nucleic Acids Res. 2010;38(Database issue):D800-5. Epub 2009/11/07.

159.   Fransen M, Vastiau I, Brees C, Brys V, Mannaerts GP, Van Veldhoven PP. Potential role for Pex19p in assembly of PTS-receptor docking complexes. J Biol Chem. 2004;279(13):12615-24. Epub 2004/01/13.

160.   Hoepfner D, Schildknegt D, Braakman I, Philippsen P, Tabak HF. Contribution of the endoplasmic reticulum to peroxisome formation. Cell. 2005;122(1):85-95. Epub 2005/07/13.

161.   Kragt A, Voorn-Brouwer T, van den Berg M, Distel B. Endoplasmic reticulum-directed Pex3p routes to peroxisomes and restores peroxisome formation in a Saccharomyces cerevisiae pex3Delta strain. J Biol Chem. 2005;280(40):34350-7. Epub 2005/08/16.

162.   Tam YY, Fagarasanu A, Fagarasanu M, Rachubinski RA. Pex3p initiates the formation of a preperoxisomal compartment from a subdomain of the endoplasmic reticulum in Saccharomyces cerevisiae. J Biol Chem. 2005;280(41):34933-9. Epub 2005/08/10.

163.   Lam SK, Yoda N, Schekman R. A vesicle carrier that mediates peroxisome protein traffic from the endoplasmic reticulum. Proc Natl Acad Sci U S A. 2010;107(50):21523-8. Epub 2010/11/26.

164.   Agrawal G, Joshi S, Subramani S. Cell-free sorting of peroxisomal membrane proteins from the endoplasmic reticulum. Proc Natl Acad Sci U S A. 2011;108(22):9113-8. Epub 2011/05/18.

165.   Yonekawa S, Furuno A, Baba T, Fujiki Y, Ogasawara Y, Yamamoto A, et al. Sec16B is involved in the endoplasmic reticulum export of the peroxisomal membrane biogenesis factor peroxin 16 (Pex16) in mammalian cells. Proc Natl Acad Sci U S A. 2011;108(31):12746-51. Epub 2011/07/20.

166.   Karnik SK, Trelease RN. Arabidopsis peroxin 16 coexists at steady state in peroxisomes and endoplasmic reticulum. Plant Physiol. 2005;138(4):1967-81. Epub 2005/07/26.

167.   Fujiki Y, Okumoto K, Mukai S, Honsho M, Tamura S. Peroxisome biogenesis in mammalian cells. Front Physiol. 2014;5:307. Epub 2014/09/02.

168.   Knoops K, Manivannan S, Cepinska MN, Krikken AM, Kram AM, Veenhuis M, et al. Preperoxisomal vesicles can form in the absence of Pex3. J Cell Biol. 2014;204(5):659-68. Epub 2014/03/05.

169.   Girzalsky W, Rehling P, Stein K, Kipper J, Blank L, Kunau WH, et al. Involvement of Pex13p in Pex14p localization and peroxisomal targeting signal 2-dependent protein import into peroxisomes. J Cell Biol. 1999;144(6):1151-62. Epub 1999/03/24.

170.   Motley AM, Hettema EH. Yeast peroxisomes multiply by growth and division. J Cell Biol. 2007;178(3):399-410. Epub 2007/07/25.

171.   van der Zand A, Braakman I, Tabak HF. Peroxisomal membrane proteins insert into the endoplasmic reticulum. Mol Biol Cell. 2010;21(12):2057-65. Epub 2010/04/30.

172.   Sparkes IA, Hawes C, Baker A. AtPEX2 and AtPEX10 are targeted to peroxisomes independently of known endoplasmic reticulum trafficking routes. Plant Physiol. 2005;139(2):690-700. Epub 2005/09/20.

173.   Titorenko VI, Rachubinski RA. Peroxisomal membrane fusion requires two AAA family ATPases, Pex1p and Pex6p. J Cell Biol. 2000;150(4):881-6. Epub 2000/08/23.

174.   van der Zand A, Gent J, Braakman I, Tabak HF. Biochemically distinct vesicles from the endoplasmic reticulum fuse to form peroxisomes. Cell. 2012;149(2):397-409. Epub 2012/04/17.

175.   Nuttall JM, Motley A, Hettema EH. Peroxisome biogenesis: recent advances. Curr Opin Cell Biol. 2011;23(4):421-6. Epub 2011/06/22.

176.   Schrader M, Burkhardt JK, Baumgart E, Luers G, Spring H, Volkl A, et al. Interaction of microtubules with peroxisomes. Tubular and spherical peroxisomes in HepG2 cells and their alterations induced by microtubule-active drugs. European Journal of Cell Biology. 1996;69(1):24-35.

177.   Schrader M, Reuber BE, Morrell JC, Jimenez-Sanchez G, Obie C, Stroh TA, et al. Expression of PEX11beta mediates peroxisome proliferation in the absence of extracellular stimuli. J Biol Chem. 1998;273(45):29607-14.

178.   Koch A, Thiemann M, Grabenbauer M, Yoon Y, McNiven MA, Schrader M. Dynamin-like protein 1 is involved in peroxisomal fission. Journal of Biological Chemistry. 2003;278(10):8597-605.

179.   Koch A, Schneider G, Luers GH, Schrader M. Peroxisome elongation and constriction but not fission can occur independently of dynamin-like protein 1. J Cell Sci. 2004;117(Pt 17):3995-4006. Epub 2004/08/03.

180.   Hicks L, Fahimi HD. Peroxisomes (microbodies) in the myocardium of rodents and primates. A comparative Ultrastructural cytochemical study. Cell Tissue Res. 1977;175(4):467-81. Epub 1977/01/04.

181.   Gorgas K. Morphogenesis of Peroxisomes in Lipid-Synthesizing Epithelia. In: Fahimi HD, Sies H, editors. Peroxisomes in Biology and Medicine: Springer Berlin Heidelberg; 1987. p. 3-17.

182.   Yamamoto K, Fahimi HD. Three-dimensional reconstruction of a peroxisomal reticulum in regenerating rat liver: evidence of interconnections between heterogeneous segments. J Cell Biol. 1987;105(2):713-22. Epub 1987/08/01.

183.   Roels F, Espeel M, Pauwels M, De Craemer D, Egberts HJ, van der Spek P. Different types of peroxisomes in human duodenal epithelium. Gut. 1991;32(8):858-65. Epub 1991/08/01.

184.   Fahimi HD, Baumgart E, Volkl A. Ultrastructural aspects of the biogenesis of peroxisomes in rat liver. Biochimie. 1993;75(3-4):201-8. Epub 1993/01/01.

185.   Schrader M, Baumgart E, Volkl A, Fahimi HD. Heterogeneity of peroxisomes in human hepatoblastoma cell line HepG2. Evidence of distinct subpopulations. Eur J Cell Biol. 1994;64(2):281-94. Epub 1994/08/01.

186.   Litwin JA, Bilinska B. Morphological heterogeneity of peroxisomes in cultured mouse Leydig cells. Folia histochemica et cytobiologica / Polish Academy of Sciences, Polish Histochemical and Cytochemical Society. 1995;33(4):255-8. Epub 1995/01/01.

187.   Schrader M, King SJ, Stroh TA, Schroer TA. Real time imaging reveals a peroxisomal reticulum in living cells. J Cell Sci. 2000;113 (Pt 20)(Pt 20):3663-71. Epub 2000/10/06.

188.   Marshall PA, Krimkevich YI, Lark RH, Dyer JM, Veenhuis M, Goodman JM. Pmp27 promotes peroxisomal proliferation. J Cell Biol. 1995;129(2):345-55. Epub 1995/04/01.

189.   Abe I, Fujiki Y. cDNA cloning and characterization of a constitutively expressed isoform of the human peroxin Pex11p. Biochem Biophys Res Commun. 1998;252(2):529-33. Epub 1998/11/25.

190.   Lingard MJ, Trelease RN. Five Arabidopsis peroxin 11 homologs individually promote peroxisome elongation, duplication or aggregation. Journal of Cell Science. 2006;119(9):1961-72.

191.   Opalinski L, Kiel JA, Williams C, Veenhuis M, van der Klei IJ. Membrane curvature during peroxisome fission requires Pex11. EMBO J. 2011;30(1):5-16. Epub 2010/11/30.

192.   Lingard MJ, Gidda SK, Bingham S, Rothstein SJ, Mullen RT, Trelease RN. Arabidopsis PEROXIN11c-e, FISSION1b, and DYNAMIN-RELATED PROTEIN3A cooperate in cell cycle-associated replication of peroxisomes. The Plant cell. 2008;20(6):1567-85. Epub 2008/06/10.

193.   Koch J, Pranjic K, Huber A, Ellinger A, Hartig A, Kragler F, et al. PEX11 family members are membrane elongation factors that coordinate peroxisome proliferation and maintenance. J Cell Sci. 2010;123(Pt 19):3389-400. Epub 2010/09/10.

194.   Koch J, Brocard C. Membrane elongation factors in organelle maintenance: the case of peroxisome proliferation. Biomol Concepts. 2011;2(5):353-64. Epub 2011/10/11.

195.   Chang J, Klute MJ, Tower RJ, Mast FD, Dacks JB, Rachubinski RA. An ancestral role in peroxisome assembly is retained by the divisional peroxin Pex11 in the yeast Yarrowia lipolytica. J Cell Sci. 2015;128(7):1327-40. Epub 2015/02/11.

196.   Erdmann R, Blobel G. Giant peroxisomes in oleic acid-induced Saccharomyces cerevisiae lacking the peroxisomal membrane protein Pmp27p. J Cell Biol. 1995;128(4):509-23. Epub 1995/02/01.

197.   Thoms S, Erdmann R. Dynamin-related proteins and Pex11 proteins in peroxisome division and proliferation. FEBS J. 2005;272(20):5169-81. Epub 2005/10/13.

198.   van Roermund CW, Tabak HF, van Den Berg M, Wanders RJ, Hettema EH. Pex11p plays a primary role in medium-chain fatty acid oxidation, a process that affects peroxisome number and size in Saccharomyces cerevisiae. J Cell Biol. 2000;150(3):489-98. Epub 2000/08/10.

199.   Krikken AM, Veenhuis M, van der Klei IJ. Hansenula polymorpha pex11 cells are affected in peroxisome retention. FEBS J. 2009;276(5):1429-39. Epub 2009/02/04.

200.   Voncken F, van Hellemond JJ, Pfisterer I, Maier A, Hillmer S, Clayton C. Depletion of GIM5 causes cellular fragility, a decreased glycosome number, and reduced levels of ether-linked phospholipids in trypanosomes. J Biol Chem. 2003;278(37):35299-310. Epub 2003/06/28.

201.   Kiel JA, van der Klei IJ, van den Berg MA, Bovenberg RA, Veenhuis M. Overproduction of a single protein, Pc-Pex11p, results in 2-fold enhanced penicillin production by Penicillium chrysogenum. Fungal genetics and biology : FG & B. 2005;42(2):154-64. Epub 2005/01/27.

202.   Lorenz P, Maier AG, Baumgart E, Erdmann R, Clayton C. Elongation and clustering of glycosomes in Trypanosoma brucei overexpressing the glycosomal Pex11p. EMBO J. 1998;17(13):3542-55. Epub 1998/07/03.

203.   Abe I, Okumoto K, Tamura S, Fujiki Y. Clofibrate-inducible, 28-kDa peroxisomal integral membrane protein is encoded by PEX11. FEBS Lett. 1998;431(3):468-72.

204.   Passreiter M, Anton M, Lay D, Frank R, Harter C, Wieland FT, et al. Peroxisome biogenesis: involvement of ARF and coatomer. J Cell Biol. 1998;141(2):373-83. Epub 1998/05/23.

205.   Li X, Baumgart E, Morrell JC, Jimenez-Sanchez G, Valle D, Gould SJ. PEX11 beta deficiency is lethal and impairs neuronal migration but does not abrogate peroxisome function. Molecular and cellular biology. 2002;22(12):4358-65. Epub 2002/05/25.

206.   Tanaka A, Okumoto K, Fujiki Y. cDNA cloning and characterization of the third isoform of human peroxin Pex11p. Biochem Biophys Res Commun. 2003;300(4):819-23. Epub 2003/02/01.

207.   Shimizu M, Takeshita A, Tsukamoto T, Gonzalez FJ, Osumi T. Tissue-selective, bidirectional regulation of PEX11 alpha- and perilipin genes through a common peroxisome proliferator response element. Molecular and cellular biology. 2004;24(3):1313-23.

208.   Li X, Baumgart E, Dong GX, Morrell JC, Jimenez-Sanchez G, Valle D, et al. PEX11alpha is required for peroxisome proliferation in response to 4-phenylbutyrate but is dispensable for peroxisome proliferator-activated receptor alpha-mediated peroxisome proliferation. Molecular and cellular biology. 2002;22(23):8226-40. Epub 2002/11/06.

209.   Weng H, Ji X, Endo K, Iwai N. Pex11a deficiency is associated with a reduced abundance of functional peroxisomes and aggravated renal interstitial lesions. Hypertension. 2014;64(5):1054-60. Epub 2014/08/13.

210.   Ahlemeyer B, Gottwald M, Baumgart-Vogt E. Deletion of a single allele of the Pex11beta gene is sufficient to cause oxidative stress, delayed differentiation and neuronal death in mouse brain. Dis Model Mech. 2012;5(1):125-40. Epub 2011/09/29.

211.   Bonekamp NA, Grille S, Cardoso MJ, Almeida M, Aroso M, Gomes S, et al. Self-interaction of human Pex11pbeta during peroxisomal growth and division. PLoS One. 2013;8(1):e53424. Epub 2013/01/12.

212.   Li XL, Gould SJ. The dynamin-like GTPase DLP1 is essential for peroxisome division and is recruited to peroxisomes in part by PEX11. Journal of Biological Chemistry. 2003;278(19):17012-20.

213.   Kobayashi S, Tanaka A, Fujiki Y. Fis1, DLP1, and Pex11p coordinately regulate peroxisome morphogenesis. Experimental cell research. 2007;313(8):1675-86. Epub 2007/04/06.

214.   Itoyama A, Michiyuki S, Honsho M, Yamamoto T, Moser A, Yoshida Y, et al. Mff functions with Pex11pbeta and DLP1 in peroxisomal fission. Biology open. 2013;2(10):998-1006. Epub 2013/10/30.

215.   Koch J, Brocard C. PEX11 proteins attract Mff and human Fis1 to coordinate peroxisomal fission. J Cell Sci. 2012;125(Pt 16):3813-26. Epub 2012/05/19.

216.   Delille HK, Agricola B, Guimaraes SC, Borta H, Luers GH, Fransen M, et al. Pex11pbeta-mediated growth and division of mammalian peroxisomes follows a maturation pathway. J Cell Sci. 2010;123(Pt 16):2750-62. Epub 2010/07/22.

217.   Cepinska MN, Veenhuis M, van der Klei IJ, Nagotu S. Peroxisome fission is associated with reorganization of specific membrane proteins. Traffic. 2011;12(7):925-37. Epub 2011/04/22.

218.   Drin G, Antonny B. Amphipathic helices and membrane curvature. FEBS Lett. 2010;584(9):1840-7. Epub 2009/10/20.

219.   Marshall PA, Dyer JM, Quick ME, Goodman JM. Redox-sensitive homodimerization of Pex11p: a proposed mechanism to regulate peroxisomal division. J Cell Biol. 1996;135(1):123-37. Epub 1996/10/01.

220.   Knoblach B, Rachubinski RA. Phosphorylation-dependent activation of peroxisome proliferator protein PEX11 controls peroxisome abundance. J Biol Chem. 2010;285(9):6670-80. Epub 2009/12/24.

221.   Yoshida Y, Niwa H, Honsho M, Itoyama A, Fujiki Y. Pex11mediates peroxisomal proliferation by promoting deformation of the lipid membrane. Biology open. 2015;4(6):710-21. Epub 2015/04/26.

222.   Williams C, Opalinski L, Landgraf C, Costello J, Schrader M, Krikken AM, et al. The membrane remodeling protein Pex11p activates the GTPase Dnm1p during peroxisomal fission. Proc Natl Acad Sci U S A. 2015. Epub 2015/05/06.

223.   Schrader M, Costello J, Godinho LF, Azadi AS, Islinger M. Proliferation and fission of peroxisomes - An update. Biochim Biophys Acta. 2015. Epub 2015/09/28.

224.   Schrader M. Shared components of mitochondrial and peroxisomal division. Biochim Biophys Acta. 2006;1763(5-6):531-41. Epub 2006/02/21.

225.   Delille HK, Alves R, Schrader M. Biogenesis of peroxisomes and mitochondria: linked by division. Histochem Cell Biol. 2009;131(4):441-6. Epub 2009/02/17.

226.   Bleazard W, McCaffery JM, King EJ, Bale S, Mozdy A, Tieu Q, et al. The dynamin-related GTPase Dnm1 regulates mitochondrial fission in yeast. Nat Cell Biol. 1999;1(5):298-304. Epub 1999/11/13.

227.   Smirnova E, Griparic L, Shurland DL, van der Bliek AM. Dynamin-related protein Drp1 is required for mitochondrial division in mammalian cells. Mol Biol Cell. 2001;12(8):2245-56. Epub 2001/08/22.

228.   Hinshaw JE. Dynamin and its role in membrane fission. Annual review of cell and developmental biology. 2000;16:483-519. Epub 2000/10/14.

229.   Praefcke GJ, McMahon HT. The dynamin superfamily: universal membrane tubulation and fission molecules? Nature reviews Molecular cell biology. 2004;5(2):133-47. Epub 2004/03/26.

230.   Roux A, Koster G, Lenz M, Sorre B, Manneville JB, Nassoy P, et al. Membrane curvature controls dynamin polymerization. Proc Natl Acad Sci U S A. 2010;107(9):4141-6. Epub 2010/02/18.

231. Roux A, Uyhazi K, Frost A, De Camilli P. GTP-dependent twisting of dynamin implicates constriction and tension in membrane fission. Nature. 2006;441(7092):528-31. Epub 2006/05/02.

232. Imoto Y, Kuroiwa H, Yoshida Y, Ohnuma M, Fujiwara T, Yoshida M, et al. Single-membrane-bounded peroxisome division revealed by isolation of dynamin-based machinery. Proc Natl Acad Sci U S A. 2013;110(23):9583-8. Epub 2013/05/23.

233. Ramachandran R, Surka M, Chappie JS, Fowler DM, Foss TR, Song BD, et al. The dynamin middle domain is critical for tetramerization and higher-order self-assembly. EMBO J. 2007;26(2):559-66. Epub 2006/12/16.

234. Chang CR, Manlandro CM, Arnoult D, Stadler J, Posey AE, Hill RB, et al. A lethal de novo mutation in the middle domain of the dynamin-related GTPase Drp1 impairs higher order assembly and mitochondrial division. J Biol Chem. 2010;285(42):32494-503. Epub 2010/08/11.

235. Tanaka A, Kobayashi S, Fujiki Y. Peroxisome division is impaired in a CHO cell mutant with an inactivating point-mutation in dynamin-like protein 1 gene. Experimental cell research. 2006;312(9):1671-84. Epub 2006/03/15.

236. Kuravi K, Nagotu S, Krikken AM, Sjollema K, Deckers M, Erdmann R, et al. Dynamin-related proteins Vps1p and Dnm1p control peroxisome abundance in Saccharomyces cerevisiae. J Cell Sci. 2006;119(Pt 19):3994-4001. Epub 2006/09/14.

237. Nagotu S, Saraya R, Otzen M, Veenhuis M, van der Klei IJ. Peroxisome proliferation in Hansenula polymorpha requires Dnm1p which mediates fission but not de novo formation. Biochim Biophys Acta. 2008;1783(5):760-9.

238. Fujimoto M, Arimura S, Mano S, Kondo M, Saito C, Ueda T, et al. Arabidopsis dynamin-related proteins DRP3A and DRP3B are functionally redundant in mitochondrial fission, but have distinct roles in peroxisomal fission. The Plant journal : for cell and molecular biology. 2009;58(3):388-400. Epub 2009/01/16.

239. Zhang X, Hu J. The Arabidopsis chloroplast division protein DYNAMIN-RELATED PROTEIN5B also mediates peroxisome division. The Plant cell. 2010;22(2):431-42. Epub 2010/02/25.

240. Chang CR, Blackstone C. Dynamic regulation of mitochondrial fission through modification of the dynamin-related protein Drp1. Annals of the New York Academy of Sciences. 2010;1201:34-9. Epub 2010/07/24.

241. Gomes LC, Di Benedetto G, Scorrano L. During autophagy mitochondria elongate, are spared from degradation and sustain cell viability. Nat Cell Biol. 2011;13(5):589-98. Epub 2011/04/12.

242. Schrader M, Costello J, Godinho LF, Islinger M. Peroxisome-mitochondria interplay and disease. J Inherit Metab Dis. 2015. Epub 2015/02/18.

243. Schollenberger L, Gronemeyer T, Huber CM, Lay D, Wiese S, Meyer HE, et al. RhoA regulates peroxisome association to microtubules and the actin cytoskeleton. PLoS One. 2010;5(11):e13886. Epub 2010/11/17.

244. Yoon Y, Krueger EW, Oswald BJ, McNiven MA. The mitochondrial protein hFis1 regulates mitochondrial fission in mammalian cells through an interaction with the dynamin-like protein DLP1. Molecular and cellular biology. 2003;23(15):5409-20.

245. Koch A, Yoon Y, Bonekamp NA, McNiven MA, Schrader M. A role for Fis1 in both mitochondrial and peroxisomal fission in mammalian cells. Mol Biol Cell. 2005;16(11):5077-86. Epub 2005/08/19.

246. Mozdy AD, McCaffery JM, Shaw JM. Dnm1p GTPase-mediated mitochondrial fission is a multi-step process requiring the novel integral membrane component Fis1p. Journal of Cell Biology. 2000;151(2):367-79.

247. Dohm JA, Lee SJ, Hardwick JM, Hill RB, Gittis AG. Cytosolic domain of the human mitochondrial fission protein fis1 adopts a TPR fold. Proteins. 2004;54(1):153-6. Epub 2004/01/06.

248.   Suzuki M, Neutzner A, Tjandra N, Youle RJ. Novel structure of the N terminus in yeast Fis1 correlates with a specialized function in mitochondrial fission. J Biol Chem. 2005;280(22):21444-52. Epub 2005/04/06.

249.   Delille HK, Schrader M. Targeting of hFis1 to peroxisomes is mediated by Pex19p. J Biol Chem. 2008;283(45):31107-15. Epub 2008/09/11.

250.   Gandre-Babbe S, van der Bliek AM. The Novel Tail-anchored Membrane Protein Mff Controls Mitochondrial and Peroxisomal Fission in Mammalian Cells. Mol Biol Cell. 2008;19(6):2402-12.

251.   Otera H, Wang C, Cleland MM, Setoguchi K, Yokota S, Youle RJ, et al. Mff is an essential factor for mitochondrial recruitment of Drp1 during mitochondrial fission in mammalian cells. J Cell Biol. 2010;191(6):1141-58. Epub 2010/12/15.

252.   Motley AM, Ward GP, Hettema EH. Dnm1p-dependent peroxisome fission requires Caf4p, Mdv1p and Fis1p. J Cell Sci. 2008;121(Pt 10):1633-40. Epub 2008/05/01.

253.   Palmer CS, Osellame LD, Stojanovski D, Ryan MT. The regulation of mitochondrial morphology: intricate mechanisms and dynamic machinery. Cell Signal. 2011;23(10):1534-45. Epub 2011/06/21.

254.   Zhao J, Liu T, Jin S, Wang X, Qu M, Uhlen P, et al. Human MIEF1 recruits Drp1 to mitochondrial outer membranes and promotes mitochondrial fusion rather than fission. EMBO J. 2011;30(14):2762-78. Epub 2011/06/28.

255.   Huber N, Guimaraes S, Schrader M, Suter U, Niemann A. Charcot-Marie-Tooth disease-associated mutants of GDAP1 dissociate its roles in peroxisomal and mitochondrial fission. EMBO Rep. 2013;14(6):545-52. Epub 2013/05/01.

256.   Niemann A, Berger P, Suter U. Pathomechanisms of mutant proteins in Charcot-Marie-Tooth disease. Neuromolecular medicine. 2006;8(1-2):217-42. Epub 2006/06/16.

257.   Cassereau J, Chevrollier A, Bonneau D, Verny C, Procaccio V, Reynier P, et al. A locus-specific database for mutations in GDAP1 allows analysis of genotype-phenotype correlations in Charcot-Marie-Tooth diseases type 4A and 2K. Orphanet journal of rare diseases. 2011;6:87. Epub 2011/12/28.

258.   Niemann A, Wagner KM, Ruegg M, Suter U. GDAP1 mutations differ in their effects on mitochondrial dynamics and apoptosis depending on the mode of inheritance. Neurobiol Dis. 2009;36(3):509-20. Epub 2009/09/29.

259.   Bonekamp NA, Sampaio P, de Abreu FV, Lüers GH, Schrader M. Transient complex interactions of mammalian peroxisomes without exchange of matrix or membrane marker proteins. Traffic. 2012:no-no.

260.   Huybrechts SJ, Van Veldhoven PP, Brees C, Mannaerts GP, Los GV, Fransen M. Peroxisome dynamics in cultured mammalian cells. Traffic. 2009;10(11):1722-33. Epub 2009/09/02.

261.   Hess R, Staubli W, Riess W. Nature of the hepatomegalic effect produced by ethyl-chlorophenoxy-isobutyrate in the rat. Nature. 1965;208(13):856-8.

262.   Fahimi HD, Reinicke A, Sujatta M, Yokota S, Ozel M, Hartig F, et al. The short- and long-term effects of bezafibrate in the rat. Annals of the New York Academy of Sciences. 1982;386:111-35. Epub 1982/01/01.

263.   Ishii H, Fukumori N, Horie S, Suga T. Effects of fat content in the diet on hepatic peroxisomes of the rat. Biochim Biophys Acta. 1980;617(1):1-11. Epub 1980/01/18.

264.   Goglia F, Liverini G, Lanni A, Iossa S, Barletta A. Morphological and functional modifications of rat liver peroxisomal subpopulations during cold exposure. Experimental biology. 1989;48(3):127-33. Epub 1989/01/01.

265.   Dzhekova-Stojkova S, Bogdanska J, Stojkova Z. Peroxisome proliferators: their biological and toxicological effects. Clinical chemistry and laboratory medicine : CCLM / FESCC. 2001;39(6):468-74. Epub 2001/08/17.

266.   Issemann I, Green S. Activation of a member of the steroid hormone receptor superfamily by peroxisome proliferators. Nature. 1990;347(6294):645-50.

267.   Dreyer C, Keller H, Mahfoudi A, Laudet V, Krey G, Wahli W. Positive regulation of the peroxisomal beta-oxidation pathway by fatty acids through activation of peroxisome proliferator-activated receptors (PPAR). Biology of the cell / under the auspices of the European Cell Biology Organization. 1993;77(1):67-76. Epub 1993/01/01.

268.   Pyper SR, Viswakarma N, Yu S, Reddy JK. PPARalpha: energy combustion, hypolipidemia, inflammation and cancer. Nuclear receptor signaling. 2010;8:e002. Epub 2010/04/24.

269.   Rakhshandehroo M, Knoch B, Muller M, Kersten S. Peroxisome proliferator-activated receptor alpha target genes. PPAR research. 2010;2010. Epub 2010/10/12.

270.   Gonzalez FJ. Recent update on the PPAR alpha-null mouse. Biochimie. 1997;79(2-3):139-44. Epub 1997/02/01.

271.   Schoonjans K, Staels B, Auwerx J. Role of the peroxisome proliferator-activated receptor (PPAR) in mediating the effects of fibrates and fatty acids on gene expression. J Lipid Res. 1996;37(5):907-25. Epub 1996/05/01.

272.   Klaunig JE, Babich MA, Baetcke KP, Cook JC, Corton JC, David RM, et al. PPARalpha agonist-induced rodent tumors: modes of action and human relevance. Critical reviews in toxicology. 2003;33(6):655-780. Epub 2004/01/20.

273.   Reddy JK, Lalwani ND. Carcinogenesis by hepatic peroxisome proliferators: Evaluation of the risk of hypolipidemic drugs and industrial plasticizers to humans. CRC Critical Rev Tox. 1983;12:1-58.

274.   Qi C, Zhu Y, Reddy JK. Peroxisome proliferator-activated receptors, coactivators, and downstream targets. Cell biochemistry and biophysics. 2000;32 Spring(Spring):187-204. Epub 2001/05/02.

275.   Bagattin A, Hugendubler L, Mueller E. Transcriptional coactivator PGC-1 promotes peroxisomal remodeling and biogenesis. Proceedings of the National Academy of Sciences. 2010;107(47):20376-81.

276.   Ribeiro D, Castro I, Fahimi HD, Schrader M. Peroxisome morphology in pathology. Histol Histopathol. 2012;27(6):661-76. Epub 2012/04/05.

277.   Manning G, Plowman GD, Hunter T, Sudarsanam S. Evolution of protein kinase signaling from yeast to man. Trends in biochemical sciences. 2002;27(10):514-20. Epub 2002/10/09.

278.   Bollen M, Peti W, Ragusa MJ, Beullens M. The extended PP1 toolkit: designed to create specificity. Trends in biochemical sciences. 2010;35(8):450-8. Epub 2010/04/20.

279.   Alberts B, Johnson A, Lewis J, Morgan D, Raff M, Roberts K, et al. Molecular Biology of the Cell. 6 ed. New York: Garland Science; 2015.

280.   van Wijk KJ, Friso G, Walther D, Schulze WX. Meta-Analysis of Arabidopsis thaliana Phospho-Proteomics Data Reveals Compartmentalization of Phosphorylation Motifs. The Plant cell. 2014;26(6):2367-89. Epub 2014/06/05.

281.   Tanaka AR, Tanabe K, Morita M, Kurisu M, Kasiwayama Y, Matsuo M, et al. ATP binding/hydrolysis by and phosphorylation of peroxisomal ATP-binding cassette proteins PMP70 (ABCD3) and adrenoleukodystrophy protein (ABCD1). J Biol Chem. 2002;277(42):40142-7. Epub 2002/08/15.

282.   Tanaka C, Tan LJ, Mochida K, Kirisako H, Koizumi M, Asai E, et al. Hrr25 triggers selective autophagy-related pathways by phosphorylating receptor proteins. J Cell Biol. 2014;207(1):91-105. Epub 2014/10/08.

283.   Tanaka K, Soeda M, Hashimoto Y, Takenaka S, Komori M. Identification of phosphorylation sites in Hansenula polymorpha Pex14p by mass spectrometry. FEBS open bio. 2013;3:6-10. Epub 2013/07/13.

284.   Elgersma Y, Kwast L, van den Berg M, Snyder WB, Distel B, Subramani S, et al. Overexpression of Pex15p, a phosphorylated peroxisomal integral membrane protein required for

peroxisome assembly in S.cerevisiae, causes proliferation of the endoplasmic reticulum membrane. EMBO J. 1997;16(24):7326-41. Epub 1998/02/21.

285.   Chang CR, Blackstone C. Cyclic AMP-dependent protein kinase phosphorylation of Drp1 regulates its GTPase activity and mitochondrial morphology. J Biol Chem. 2007;282(30):21583-7. Epub 2007/06/08.

286.   Cribbs JT, Strack S. Reversible phosphorylation of Drp1 by cyclic AMP-dependent protein kinase and calcineurin regulates mitochondrial fission and cell death. EMBO Rep. 2007;8(10):939-44. Epub 2007/08/28.

287.   Cho B, Cho HM, Kim HJ, Jeong J, Park SK, Hwang EM, et al. CDK5-dependent inhibitory phosphorylation of Drp1 during neuronal maturation. Experimental & molecular medicine. 2014;46:e105. Epub 2014/07/12.

288.   Kashatus JA, Nascimento A, Myers LJ, Sher A, Byrne FL, Hoehn KL, et al. Erk2 Phosphorylation of Drp1 Promotes Mitochondrial Fission and MAPK-Driven Tumor Growth. Mol Cell. 2015;57(3):537-51. Epub 2015/02/07.

289.   Lim S, Lee SY, Seo HH, Ham O, Lee C, Park JH, et al. Regulation of mitochondrial morphology by positive feedback interaction between PKCdelta and Drp1 in vascular smooth muscle cell. J Cell Biochem. 2015;116(4):648-60. Epub 2014/11/18.

290.   Joshi S, Agrawal G, Subramani S. Phosphorylation-dependent Pex11p and Fis1p interaction regulates peroxisome division. Mol Biol Cell. 2012;23(7):1307-15. Epub 2012/02/18.

291.   Reumann S. Specification of the peroxisome targeting signals type 1 and type 2 of plant peroxisomes by bioinformatics analyses. Plant Physiol. 2004;135(2):783-800. Epub 2004/06/23.

292.   Reumann S. Toward a definition of the complete proteome of plant peroxisomes: Where experimental proteomics must be complemented by bioinformatics. Proteomics. 2011;11(9):1764-79. Epub 2011/04/08.

293.   Lingner T, Kataya AR, Antonicelli GE, Benichou A, Nilssen K, Chen XY, et al. Identification of novel plant peroxisomal targeting signals by a combination of machine learning methods and in vivo subcellular targeting analyses. The Plant cell. 2011;23(4):1556-72. Epub 2011/04/14.

294.   Lester LB, Coghlan VM, Nauert B, Scott JD. Cloning and characterization of a novel A-kinase anchoring protein. AKAP 220, association with testicular peroxisomes. J Biol Chem. 1996;271(16):9460-5. Epub 1996/04/19.

295.   Schillace RV, Scott JD. Association of the type 1 protein phosphatase PP1 with the A-kinase anchoring protein AKAP220. Current biology : CB. 1999;9(6):321-4. Epub 1999/04/21.

296.   Tanji C, Yamamoto H, Yorioka N, Kohno N, Kikuchi K, Kikuchi A. A-kinase anchoring protein AKAP220 binds to glycogen synthase kinase-3beta (GSK-3beta) and mediates protein kinase A-dependent inhibition of GSK-3beta. J Biol Chem. 2002;277(40):36955-61. Epub 2002/07/31.

297.   Bloch DB, Li P, Bloch EG, Berenson DF, Galdos RL, Arora P, et al. LMKB/MARF1 localizes to mRNA processing bodies, interacts with Ge-1, and regulates IFI44L gene expression. PLoS One. 2014;9(4):e94784. Epub 2014/04/24.

298.   Dunster K, Lai FP, Sentry JW. Limkain b1, a novel human autoantigen localized to a subset of ABCD3 and PXF marked peroxisomes. Clin Exp Immunol. 2005;140(3):556-63. Epub 2005/06/04.

299.   Hendrickx A, Beullens M, Ceulemans H, Den Abt T, Van Eynde A, Nicolaescu E, et al. Docking motif-guided mapping of the interactome of protein phosphatase-1. Chemistry & biology. 2009;16(4):365-71. Epub 2009/04/25.

300.   Matre P, Meyer C, Lillo C. Diversity in subcellular targeting of the PP2A B'eta subfamily members. Planta. 2009;230(5):935-45. Epub 2009/08/13.

301.   Kataya AR, Heidari B, Hagen L, Kommedal R, Slupphaug G, Lillo C. Protein Phosphatase 2A Holoenzyme Is Targeted to Peroxisomes by Piggybacking and Positively Affects Peroxisomal beta-Oxidation. Plant Physiol. 2015;167(2):493-506. Epub 2014/12/10.

302. Kataya AR, Schei E, Lillo C. MAP kinase phosphatase 1 harbors a novel PTS1 and is targeted to peroxisomes following stress treatments. Journal of plant physiology. 2015;179:12-20. Epub 2015/03/31.

303. Xing Y, Jia W, Zhang J. AtMEK1 mediates stress-induced gene expression of CAT1 catalase by triggering H2O2 production in Arabidopsis. Journal of experimental botany. 2007;58(11):2969-81. Epub 2007/08/31.

304. Dammann C, Ichida A, Hong B, Romanowsky SM, Hrabak EM, Harmon AC, et al. Subcellular targeting of nine calcium-dependent protein kinase isoforms from Arabidopsis. Plant Physiol. 2003;132(4):1840-8. Epub 2003/08/13.

305. Coca M, San Segundo B. AtCPK1 calcium-dependent protein kinase mediates pathogen resistance in Arabidopsis. The Plant journal : for cell and molecular biology. 2010;63(3):526-40. Epub 2010/05/26.

306. Saleem RA, Rogers RS, Ratushny AV, Dilworth DJ, Shannon PT, Shteynberg D, et al. Integrated phosphoproteomics analysis of a signaling network governing nutrient response and peroxisome induction. Molecular & cellular proteomics : MCP. 2010;9(9):2076-88. Epub 2010/04/17.

307. Esteves SL, Korrodi-Gregorio L, Cotrim CZ, van Kleeff PJ, Domingues SC, da Cruz e Silva OA, et al. Protein phosphatase 1gamma isoforms linked interactions in the brain. Journal of molecular neuroscience : MN. 2013;50(1):179-97. Epub 2012/10/20.

308. Manning G, Whyte DB, Martinez R, Hunter T, Sudarsanam S. The protein kinase complement of the human genome. Science. 2002;298(5600):1912-34. Epub 2002/12/10.

309. Johnson SA, Hunter T. Kinomics: methods for deciphering the kinome. Nature methods. 2005;2(1):17-25. Epub 2005/03/25.

310. Bollen M. Combinatorial control of protein phosphatase-1. Trends in biochemical sciences. 2001;26(7):426-31. Epub 2001/07/07.

311. Alonso A, Sasin J, Bottini N, Friedberg I, Osterman A, Godzik A, et al. Protein tyrosine phosphatases in the human genome. Cell. 2004;117(6):699-711. Epub 2004/06/10.

312. Ceulemans H, Bollen M. Functional diversity of protein phosphatase-1, a cellular economizer and reset button. Physiological reviews. 2004;84(1):1-39. Epub 2004/01/13.

313. Virshup DM, Shenolikar S. From promiscuity to precision: protein phosphatases get a makeover. Mol Cell. 2009;33(5):537-45. Epub 2009/03/17.

314. Janssens V, Longin S, Goris J. PP2A holoenzyme assembly: in cauda venenum (the sting is in the tail). Trends in biochemical sciences. 2008;33(3):113-21. Epub 2008/02/23.

315. Fardilha M, Esteves SL, Korrodi-Gregorio L, Vintem AP, Domingues SC, Rebelo S, et al. Identification of the human testis protein phosphatase 1 interactome. Biochem Pharmacol. 2011;82(10):1403-15. Epub 2011/03/09.

316. Esteves SL, Domingues SC, da Cruz e Silva OA, Fardilha M, da Cruz e Silva EF. Protein phosphatase 1alpha interacting proteins in the human brain. Omics : a journal of integrative biology. 2012;16(1-2):3-17. Epub 2012/02/11.

317. Fardilha M, Esteves SL, Korrodi-Gregorio L, da Cruz e Silva OA, da Cruz e Silva FF. The physiological relevance of protein phosphatase 1 and its interacting proteins to health and disease. Current medicinal chemistry. 2010;17(33):3996-4017. Epub 2010/10/14.

318. Fardilha M, Esteves SL, Korrodi-Gregorio L, Pelech S, da Cruz ESOA, da Cruz ESE. Protein phosphatase 1 complexes modulate sperm motility and present novel targets for male infertility. Mol Hum Reprod. 2011;17(8):466-77. Epub 2011/01/25.

319. Cohen PT. Protein phosphatase 1--targeted in many directions. J Cell Sci. 2002;115(Pt 2):241-56. Epub 2002/02/13.

320. Shi Y. Serine/threonine phosphatases: mechanism through structure. Cell. 2009;139(3):468-84. Epub 2009/11/03.

321.   Barford D, Das AK, Egloff MP. The structure and mechanism of protein phosphatases: insights into catalysis and regulation. Annual review of biophysics and biomolecular structure. 1998;27:133-64. Epub 1998/07/01.

322.   Takizawa N, Mizuno Y, Ito Y, Kikuchi K. Tissue distribution of isoforms of type-1 protein phosphatase PP1 in mouse tissues and its diabetic alterations. Journal of biochemistry. 1994;116(2):411-5. Epub 1994/08/01.

323.   Egloff MP, Johnson DF, Moorhead G, Cohen PT, Cohen P, Barford D. Structural basis for the recognition of regulatory subunits by the catalytic subunit of protein phosphatase 1. EMBO J. 1997;16(8):1876-87. Epub 1997/04/15.

324.   Gibbons JA, Weiser DC, Shenolikar S. Importance of a surface hydrophobic pocket on protein phosphatase-1 catalytic subunit in recognizing cellular regulators. J Biol Chem. 2005;280(16):15903-11. Epub 2005/02/11.

325.   Wakula P, Beullens M, Ceulemans H, Stalmans W, Bollen M. Degeneracy and function of the ubiquitous RVXF motif that mediates binding to protein phosphatase-1. J Biol Chem. 2003;278(21):18817-23. Epub 2003/03/27.

326.   Meiselbach H, Sticht H, Enz R. Structural analysis of the protein phosphatase 1 docking motif: molecular description of binding specificities identifies interacting proteins. Chemistry & biology. 2006;13(1):49-59. Epub 2006/01/24.

327.   Connor JH, Frederick D, Huang H, Yang J, Helps NR, Cohen PT, et al. Cellular mechanisms regulating protein phosphatase-1. A key functional interaction between inhibitor-2 and the type 1 protein phosphatase catalytic subunit. J Biol Chem. 2000;275(25):18670-5. Epub 2000/04/05.

328.   Huang HB, Horiuchi A, Watanabe T, Shih SR, Tsay HJ, Li HC, et al. Characterization of the inhibition of protein phosphatase-1 by DARPP-32 and inhibitor-2. J Biol Chem. 1999;274(12):7870-8. Epub 1999/03/13.

329.   Hurley TD, Yang J, Zhang L, Goodwin KD, Zou Q, Cortese M, et al. Structural basis for regulation of protein phosphatase 1 by inhibitor-2. J Biol Chem. 2007;282(39):28874-83. Epub 2007/07/20.

330.   Terrak M, Kerff F, Langsetmo K, Tao T, Dominguez R. Structural basis of protein phosphatase 1 regulation. Nature. 2004;429(6993):780-4. Epub 2004/05/28.

331.   Ayllon V, Cayla X, Garcia A, Fleischer A, Rebollo A. The anti-apoptotic molecules Bcl-xL and Bcl-w target protein phosphatase 1alpha to Bad. Eur J Immunol. 2002;32(7):1847-55. Epub 2002/07/13.

332.   Godet AN, Guergnon J, Maire V, Croset A, Garcia A. The combinatorial PP1-binding consensus Motif (R/K)x((0,1))V/IxFxx(R/K)x(R/K) is a new apoptotic signature. PLoS One. 2010;5(4):e9981. Epub 2010/04/09.

333.   Brush MH, Weiser DC, Shenolikar S. Growth arrest and DNA damage-inducible protein GADD34 targets protein phosphatase 1 alpha to the endoplasmic reticulum and promotes dephosphorylation of the alpha subunit of eukaryotic translation initiation factor 2. Molecular and cellular biology. 2003;23(4):1292-303. Epub 2003/01/31.

334.   Yang J, Hurley TD, DePaoli-Roach AA. Interaction of inhibitor-2 with the catalytic subunit of type 1 protein phosphatase. Identification of a sequence analogous to the consensus type 1 protein phosphatase-binding motif. J Biol Chem. 2000;275(30):22635-44. Epub 2000/05/16.

335.   Heroes E, Lesage B, Gornemann J, Beullens M, Van Meervelt L, Bollen M. The PP1 binding code: a molecular-lego strategy that governs specificity. FEBS J. 2013;280(2):584-95. Epub 2012/03/01.

336.   Llanos S, Royer C, Lu M, Bergamaschi D, Lee WH, Lu X. Inhibitory member of the apoptosis-stimulating proteins of the p53 family (iASPP) interacts with protein phosphatase 1 via a noncanonical binding motif. J Biol Chem. 2011;286(50):43039-44. Epub 2011/10/15.

337.   Strack S, Kini S, Ebner FF, Wadzinski BE, Colbran RJ. Differential cellular and subcellular localization of protein phosphatase 1 isoforms in brain. The Journal of comparative neurology. 1999;413(3):373-84. Epub 1999/09/29.

338.   Baumgart E, Schad A, Volkl A, Fahimi HD. Detection of mRNAs encoding peroxisomal proteins by non-radioactive in situ hybridization with digoxigenin-labelled cRNAs. Histochem Cell Biol. 1997;108(4-5):371-9. Epub 1997/12/05.

339.   Luers GH, Schad A, Fahimi HD, Volkl A, Seitz J. Expression of peroxisomal proteins provides clear evidence for the presence of peroxisomes in the male germ cell line GC1spg. Cytogenet Genome Res. 2003;103(3-4):360-5.

340.   Luers GH, Thiele S, Schad A, Volkl A, Yokota S, Seitz J. Peroxisomes are present in murine spermatogonia and disappear during the course of spermatogenesis. Histochem Cell Biol. 2006;125(6):693-703.

341.   Huyghe S, Schmalbruch H, De Gendt K, Verhoeven G, Guillou F, Van Veldhoven PP, et al. Peroxisomal multifunctional protein 2 is essential for lipid homeostasis in Sertoli cells and male fertility in mice. Endocrinology. 2006;147(5):2228-36. Epub 2006/02/18.

342.   Nenicu A, Luers GH, Kovacs W, David M, Zimmer A, Bergmann M, et al. Peroxisomes in human and mouse testis: differential expression of peroxisomal proteins in germ cells and distinct somatic cell types of the testis. Biol Reprod. 2007;77(6):1060-72. Epub 2007/09/21.

343.   Powers JM, Schaumburg HH. The testis in adreno-leukodystrophy. Am J Pathol. 1981;102(1):90-8. Epub 1981/01/01.

344.   Wessel D, Flugge UI. A method for the quantitative recovery of protein in dilute solution in the presence of detergents and lipids. AnalBiochem. 1984;138(1):141-3.

345.   Kyhse-Andersen J. Electroblotting of multiple gels: a simple apparatus without buffer tank for rapid transfer of proteins from polyacrylamide to nitrocellulose. Journal of biochemical and biophysical methods. 1984;10(3-4):203-9. Epub 1984/12/01.

346.   Watanabe T, da Cruz e Silva EF, Huang HB, Starkova N, Kwon YG, Horiuchi A, et al. Preparation and characterization of recombinant protein phosphatase 1. Methods in enzymology. 2003;366:321-38. Epub 2003/12/17.

347.   Moorhead GB, Trinkle-Mulcahy L, Ulke-Lemee A. Emerging roles of nuclear protein phosphatases. Nature reviews Molecular cell biology. 2007;8(3):234-44. Epub 2007/02/24.

348.   Islinger M, Luers GH, Li KW, Loos M, Volkl A. Rat liver peroxisomes after fibrate treatment. A survey using quantitative mass spectrometry. J Biol Chem. 2007;282(32):23055-69.

349.   Shimozawa N, Nagase T, Takemoto Y, Suzuki Y, Fujiki Y, Wanders RJ, et al. A novel aberrant splicing mutation of the PEX16 gene in two patients with Zellweger syndrome. Biochem Biophys Res Commun. 2002;292(1):109-12. Epub 2002/03/14.

350.   Ebberink MS, Csanyi B, Chong WK, Denis S, Sharp P, Mooijer PAW, et al. Identification of an unusual variant peroxisome biogenesis disorder caused by mutations in the PEX16 gene. Journal of Medical Genetics. 2010;47(9):608-15.

351.   Shaheen R, Al-Dirbashi OY, Al-Hassnan ZN, Al-Owain M, Makhsheed N, Basheeri F, et al. Clinical, biochemical and molecular characterization of peroxisomal diseases in Arabs. Clin Genet. 2011;79(1):60-70. Epub 2010/08/05.

352.   Honsho M, Hiroshige T, Fujiki Y. The membrane biogenesis peroxin Pex16p. Topogenesis and functional roles in peroxisomal membrane assembly. J Biol Chem. 2002;277(46):44513-24. Epub 2002/09/12.

353.   Schliebs W, Kunau WH. Peroxisome membrane biogenesis: the stage is set. Current biology : CB. 2004;14(10):R397-9.

354.   Thieringer H, Moellers B, Dodt G, Kunau WH, Driscoll M. Modeling human peroxisome biogenesis disorders in the nematode Caenorhabditis elegans. J Cell Sci. 2003;116(Pt 9):1797-804. Epub 2003/04/01.

355.   Kim PK, Mullen RT. PEX16: a multifaceted regulator of peroxisome biogenesis. Front Physiol. 2013;4:241. Epub 2013/09/13.

356.   Titorenko VI, Rachubinski RA. Mutants of the yeast Yarrowia lipolytica defective in protein exit from the endoplasmic reticulum are also defective in peroxisome biogenesis. Molecular and cellular biology. 1998;18(5):2789-803. Epub 1998/05/05.

357.   Larkin MA, Blackshields G, Brown NP, Chenna R, McGettigan PA, McWilliam H, et al. Clustal W and Clustal X version 2.0. Bioinformatics. 2007;23(21):2947-8. Epub 2007/09/12.

358.   Nakayama M, Sato H, Okuda T, Fujisawa N, Kono N, Arai H, et al. Drosophila carrying pex3 or pex16 mutations are models of Zellweger syndrome that reflect its symptoms associated with the absence of peroxisomes. PLoS One. 2011;6(8):e22984. Epub 2011/08/10.

359.   GFP-Trap®_M.   ChromoTek   GmbH;   2015;   Available   from: http://www.chromotek.com/products/nano-traps/gfp-trap/gfp-trapr-m/.

360.   Brent R, Ptashne M. A eukaryotic transcriptional activator bearing the DNA specificity of a prokaryotic repressor. Cell. 1985;43(3 Pt 2):729-36. Epub 1985/12/01.

361.   Andreassen PR, Lacroix FB, Villa-Moruzzi E, Margolis RL. Differential subcellular localization of protein phosphatase-1 alpha, gamma1, and delta isoforms during both interphase and mitosis in mammalian cells. J Cell Biol. 1998;141(5):1207-15. Epub 1998/06/12.

362.   Lentze N, Auerbach D. Membrane-based yeast two-hybrid system to detect protein interactions. Current protocols in protein science / editorial board, John E Coligan [et al]. 2008;Chapter 19:Unit 19 7. Epub 2008/05/21.

363.   Petschnigg J, Groisman B, Kotlyar M, Taipale M, Zheng Y, Kurat CF, et al. The mammalian-membrane two-hybrid assay (MaMTH) for probing membrane-protein interactions in human cells. Nature methods. 2014;11(5):585-92. Epub 2014/03/25.

364.   Amino Acids Reference Chart. Sigma-Aldrich Co. LLC.;   [cited 2015]; Available from: http://www.sigmaaldrich.com/life-science/metabolomics/learning-center/amino-acid-reference-chart.html.

365.   Bonekamp NA. Towards an understanding of peroxisome dynamics in mammalian cells. Marburg: Phillip University of Marburg; 2012.

366.   Klomsiri C, Karplus PA, Poole LB. Cysteine-based redox switches in enzymes. Antioxid Redox Signal. 2011;14(6):1065-77. Epub 2010/08/31.

367.   Fomenko DE, Marino SM, Gladyshev VN. Functional diversity of cysteine residues in proteins and unique features of catalytic redox-active cysteines in thiol oxidoreductases. Molecules and cells. 2008;26(3):228-35. Epub 2008/07/24.

368.   Hu J. Molecular basis of peroxisome division and proliferation in plants. International review of cell and molecular biology. 2010;279:79-99. Epub 2010/08/28.

369.   Schrader M, Almeida M, Grille S. Postfixation detergent treatment liberates the membrane modelling protein Pex11beta from peroxisomal membranes. Histochem Cell Biol. 2012;138(3):541-7. Epub 2012/08/10.

370.   Thomas AS, Krikken AM, van der Klei IJ, Williams CP. Phosphorylation of Pex11p does not regulate peroxisomal fission in the yeast Hansenula polymorpha. Scientific reports. 2015;5:11493. Epub 2015/06/24.

371.   Guo T, Kit YY, Nicaud JM, Le Dall MT, Sears SK, Vali H, et al. Peroxisome division in the yeast Yarrowia lipolytica is regulated by a signal from inside the peroxisome. J Cell Biol. 2003;162(7):1255-66. Epub 2003 Sep 22.

372.   Schrader M, Grille S, Fahimi HD, Islinger M. Peroxisome Interactions and Cross-Talk with Other Subcellular Compartments in Animal Cells. In: del Río LA, editor. Peroxisomes and their Key Role in Cellular Signaling and Metabolism: Springer Science; 2013.

373.   Chu BB, Liao YC, Qi W, Xie C, Du X, Wang J, et al. Cholesterol transport through lysosome-peroxisome membrane contacts. Cell. 2015;161(2):291-306. Epub 2015/04/11.

374.   Nordgren M, Fransen M. Peroxisomal metabolism and oxidative stress. Biochimie. 2014;98:56-62. Epub 2013/08/13.

375.   Mast FD, Rachubinski RA, Aitchison JD. Signaling dynamics and peroxisomes. Curr Opin Cell Biol. 2015;35:131-6. Epub 2015/06/05.

376.   Oku M, Sakai Y. Peroxisomes as dynamic organelles: autophagic degradation. FEBS J. 2010;277(16):3289-94. Epub 2010/07/16.

377.   Schrader M, Wodopia R, Fahimi HD. Induction of tubular peroxisomes by UV irradiation and reactive oxygen species in HepG2 cells. The journal of histochemistry and cytochemistry : official journal of the Histochemistry Society. 1999;47(9):1141-8.

378.   Cimini A, Moreno S, D'Amelio M, Cristiano L, D'Angelo B, Falone S, et al. Early biochemical and morphological modifications in the brain of a transgenic mouse model of Alzheimer's disease: a role for peroxisomes. J Alzheimers Dis. 2009;18(4):935-52. Epub 2009/09/15.

379.   Schrader M, Fahimi HD. Peroxisomes and oxidative stress. Biochim Biophys Acta. 2006;1763(12):1755-66. Epub 2006/10/13.

Appendix
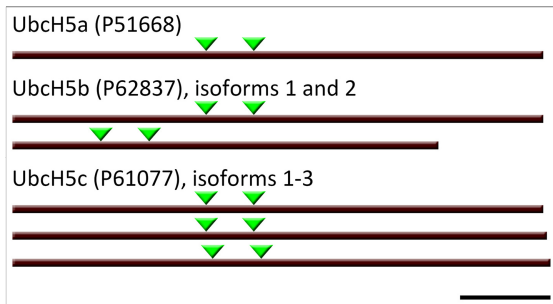
Supplementary Figure 1: Ubiquitin-conugated enzymes E2 UbcH5a/b/c have PP1-binding motifs
The sequences were collected from UniProtKB database and loaded in the ScanProsite program as well as the PP1-binding motifs canonical sequences listed on Table 5. Green triangles point matches with RVxF motifs. Bar, 25 amino acids. For more detailed information, such as sequences and position of the matches within the proteins see Supplementary Table 2.

Supplementary Table 1: Human peroxins and PP1-binding motifs

Peroxin	Accession number	FASTA sequence	PP1-binding motifs (aa x–y)
Pex1p	O43933	>sp|O43933|PEX1_HUMAN Peroxisome biogenesis factor 1 OS=Homo sapiens GN=PEX1 PE=1 SV=1 MWGSDRLAGAGGGGAAVTVAFTNARDCFLHLPRRLVAQLHLLQNQAIEVVWSHQPAFLSW VEGRHFSDQGENVAEINRQVGQKLGLSNGGQVFLKPCSHVVSCQQVEVEPLSADDWEILE LHAVSLEQHLLDQI**RIVF**PKAIFPVWVDQQTYIFIQIVALIPAASYGRLETDTKLLIQPK TRRAKENTFSKADAEYKKLHSYGRDQKGMMKELQTKQLQSNTVGITESNENESEIPVDSS SVASLWTMIGSIFSFQSEKKQETSWGLTEINAFKNMQSKVVPLDNIFRVCKSQPPSIYNA SATSVFHKHCAIHVFPWDQEYFDVEPSFTVTYGKLVKLLSPKQQQSKTKQNVLSPEKEKQ MSEPPLDQKKIRSDHNEEDEKACV**LQVVW**NGLEELNNAIKYTKNVEVLHLGKVWIPDDLRK RLNIEMHAVVRITPVEVTPKIPRSLKLQPRENLPKDISEEDIKTVFYSWLQQSTTTMLPL VISEEEFIKLETKDGLKEFSLSIVHSWEKEKDKNIFLLSPNLLQKTTIQVLLDPMVKEEN SEEIDFILPFLKLSSLGGVNSLGVSSLEHITHSLLGRPLSRQLMSLVAGLRNGALLLTGG KGSGKSTLAKAICKEAFDKLDAHVERVDCKALRGKRLENIQKTLEVAFSEAVWMQPSVVL LDDLDLIAGLPAVPEHEHSPDAVQSQRLAHALNDMIKEFISMGSLVALIATSQSQQSLHP LLVSAQGVHIFQCVQHIQPPNQEQRCEILCNVIKNKLDCDINKFTDLDLQHVAKETGGFV ARDFTVLVDRAIHSRLSRQSISTREKLVLTTLDFQKALRGFLPASLRSVNLHKPRDLGWD KIGGLHEVRQILMDTIQLPAKYPELFANLPIRQRTGILLYGPPGTGKTLLAGVIARESRM NFISVKGPELLSKYIGASEQAVRDIFIRAQAAKPCILFFDEFESIAPRRGHDNTGVTDRV VNQLLTQLDGVEGLQGVYVLAATSRPDLIDPALLRPGRLDKCVYCPPPDQVSRLEILNVL SDSLPLADDVDLQHVASVTDSFTGADLKALLYNAQLEALHGMLLSSGLQDGSSSSDSDLS LSSMVFLNHSSGSDDSAGDGECGLDQSLVSLEMSEILPDESKFNMYRLYFGSSYESELGN GTSSDLSSQCLSAPSSMTQDLPGVPGKDQLFSQPPVLRTASQEGCQELTQEQRDQLRADI SIIKGRYRSQSGEDESMNQPGPIKTRLAISQSHLMTALGHTRPSISEDDWKNFAELYESF QNPKRRKNQSGTMFRPGQKVTLA	135–138: R.IVF [1] 384–388: LQVVW [3]
Pex2p	P28328	>sp|P28328|PEX2_HUMAN Peroxisome biogenesis factor 2 OS=Homo sapiens GN=PEX2 PE=1 SV=2 MASRKENAKSANRVLRISQLDALELNKALEQLVWSQFTQCFHGFKPGLLARFEPEVKACL WVFLWRFTIYSKNATVGQSVLNIKYKNDFSPNLRYQPPSKNQKIWYAVCTIGGRWLEERC YDLFRNHHLASFGKVKQCVNFVIGLLKLGGLINFLI**FLQRGK**FATLTERLLGIHSVFCKP QNICEVGFEYMNRELLWHGFAEFLIFLLPLINVQKLKAKLSSWCIPLTGAPNSDNTLATS GKECALCGEWPTMPHTIGCEHIFCYFCAKSSFLFDVYFTCPKCGTEVHSLQPLKSGIEMS EVNAL	157–162: FLqRgK [5]
Pex3p	P56589	>sp|P56589|PEX3_HUMAN Peroxisomal biogenesis factor 3 OS=Homo sapiens GN=PEX3 PE=1 SV=1 MLRSVWN**FLKRHK**KKCIFLGTVLGGVYILGKYGQKKIREIQEREAAEYIAQARRQYHFES NQRTCNMTVLSMLPTLREALMQQLNSESLTALLKNRPSNKLEIWEDL**KIISF**TRSTVAVY STCMLVVLLRVQLNIIGGYIYLDNAAVGKNGTTILAPPDVQQQYLSSIQHLLGDGLTELI TVIKQAVQKVLGSVSLKHSLSLLDLEQKLKEIRNLVEQHKSSSWINKDGSKPLLCHYMMP DEETPLAVQACGLSPRDITTIKLLNETRDMLSPDFSTVLNTCLNRGFSRLLDNMAEFFR PTEQDLQHGNSMNSLSSVSLPLAKIIPIVNGQIHSVCSETPSHFVQDLLTMEQVKDFAAN VYEAFSTPQQLEK	8–13: FlkRhK [5] 108–112: KiISF [1]
Pex5p	P50542	>sp|P50542|PEX5_HUMAN Peroxisomal targeting signal 1 receptor OS=Homo sapiens GN=PEX5 PE=1 SV=3 MAMRELVEAECGGANPLMKLAGHFTQDKALRQEGLRPGPWPPGAPASEAASKPLGVASED ELVAEFLQDQNAPLVSRAPQTFKMDDLLAEMQQIEQSNFRQAPQRAPGVADLALSENWAQ EFLAAGDAVDVTQDYNETDWSQEFISEVTDPLSVSPARWAEEYLEQSEEKLWLGEPEGTA TDRWYDEYHPEEDLQHTASDFVAKVDDPKLANSEFLKFVRQIGEGQVSLESGAGSGRAQA EQWAAEFIQQQGTSDAWVDQFTRPVNTSALDMEFERAKSAIESDVDFWDKLQAELEEMAK RDAEAHPWLSDYDDLTSATYDKGYQFEEENPLRDHPQPFEEGLRRLQEGDLPNAVLLFEA AVQQDPKHMEAWQYLGTTQAENEQELLAISALRRCLELKPDNQTALMA**LAVSF**TNESLQR QACETLRDWLRYTPAYAHLVTPAEEGAGGAGLGPSKRILGSLLSDSLFLEVKELFLAAVR LDPTSIDPDVQCGLGVLFNLSGEYDKAVDCFTAALSVRPNDYLLWNKLGATLANGNQSEE AVAAYRRALELQPGYIRSRYNLGISCINLGAHREAVEHFLEALNMQRKSRGPRGEGGAMS ENIWSTLRLALSMLGQSDAYGAADARDLSTLLTMFGLPQ	409–413: LAVSF [3]
	P50542-2	>sp|P50542-2|PEX5_HUMAN Isoform 2 of Peroxisomal targeting signal 1 receptor OS=Homo sapiens GN=PEX5 MAMRELVEAECGGANPLMKLAGHFTQDKALRQEGLRPGPWPPGAPASEAASKPLGVASED ELVAEFLQDQNAPLVSRAPQTFKMDDLLAEMQQIEQSNFRQAPQRAPGVADLALSENWAQ EFLAAGDAVDVTQDYNETDWSQEFISEVTDPLSVSPARWAEEYLEQSEEKLWLGEPEGTA TDRWYDEYHPEEDLQHTASDFVAKVDDPKLANSEGTSDAWVDQFTRPVNTSALDMEFERA KSAIESDVDFWDKLQAELEEMAKRDAEAHPWLSDYDDLTSATYDKGYQFEEENPLRDHPQ PFEEGLRRLQEGDLPNAVLLFEAAVQQDPKHMEAWQYLGTTQAENEQELLAISALRRCLE LKPDNQTALMA**LAVSF**TNESLQRQACETLRDWLRYTPAYAHLVTPAEEGAGGAGLGPSKR ILGSLLSDSLFLEVKELFLAAVRLDPTSIDPDVQCGLGVLFNLSGEYDKAVDCFTAALSV RPNDYLLWNKLGATLANGNQSEEAVAAYRRALELQPGYIRSRYNLGISCINLGAHREAVE HFLEALNMQRKSRGPRGEGGAMSENIWSTLRLALSMLGQSDAYGAADARDLSTLLTMFGL PQ	372–376: LAVSF [3]
	P50542-3	>sp|P50542-3|PEX5_HUMAN Isoform 3 of Peroxisomal targeting signal 1 receptor OS=Homo sapiens GN=PEX5 MAMRELVEAECGGANPLMKLAGHFTQDKALRQEGLRPGPWPPGAPASEAASKPLGVASED ELVAEFLQDQNAPLVSRAPQTFKMDDLLAEMQQIEQSNFRQAPQRAPGVADLALSENWAQ EFLAAGDAVDVTQDYNETDWSQEFISEVTDPLSVSPARWAEEYLEQSEEKLWLGEPEGTA TDRWYDEYHPEEDLQHTASDFVAKVDDPKLANSEFLKFVRQIGEGQVSLESGAGSGRAQA EQWAAEFIQQQGTSDAWVDQFTRPVNTSALDMEFERAKSAIELQAELEEMAKRDAEAHPW LSDYDDLTSATYDKGYQFEEENPLRDHPQPFEEGLRRLQEGDLPNAVLLFEAAVQQDPKH MEAWQYLGTTQAENEQELLAISALRRCLELKPDNQTALMA**LAVSF**TNESLQRQACETLRD WLRYTPAYAHLVTPAEEGAGGAGLGPSKRILGSLLSDSLFLEVKELFLAAVRLDPTSIDP DVQCGLGVLFNLSGEYDKAVDCFTAALSVRPNDYLLWNKLGATLANGNQSEEAVAAYRRA LELQPGYIRSRYNLGISCINLGAHREAVEHFLEALNMQRKSRGPRGEGGAMSENIWSTLR LALSMLGQSDAYGAADARDLSTLLTMFGLPQ	401–405: LAVSF [3]
	P50542-4	>sp|P50542-4|PEX5_HUMAN Isoform 4 of Peroxisomal targeting signal 1 receptor OS=Homo sapiens GN=PEX5 MAMRELVEAECGGANPLMKLAGHFTQDKALRQEGLRPGPWPPGAPASEAVSVLEVESPGA ASEAASKPLGVASEDELVAEFLQDQNAPLVSRAPQTFKMDDLLAEMQQIEQSNFRQAPQR APGVADLALSENWAQEFLAAGDAVDVTQDYNETDWSQEFISEVTDPLSVSPARWAEEYLE QSEEKLWLGEPEGTATDRWYDEYHPEEDLQHTASDFVAKVDDPKLANSEFLKFVRQIGEG QVSLESGAGSGRAQAEQWAAEFIQQQGTSDAWVDQFTRPVNTSALDMEFERAKSAIESDV DFWDKLQAELEEMAKRDAEAHPWLSDYDDLTSATYDKGYQFEEENPLRDHPQPFEEGLRR LQEGDLPNAVLLFEAAVQQDPKHMEAWQYLGTTQAENEQELLAISALRRCLELKPDNQTA LMA**LAVSF**TNESLQRQACETLRDWLRYTPAYAHLVTPAEEGAGGAGLGPSKRILGSLLSD SLFLEVKELFLAAVRLDPTSIDPDVQCGLGVLFNLSGEYDKAVDCFTAALSVRPNDYLLW NKLGATLANGNQSEEAVAAYRRALELQPGYIRSRYNLGISCINLGAHREAVEHFLEALNM	424–428: LAVSF [3]

Peroxin	Accession number	FASTA sequence	PP1-binding motifs (aa x–y)
		QRKSRGPRGEGGAMSENIWSTLRLALSMLGQSDAYGAADARDLSTLLTMFGLPQ	
	Q8IYB4	sp|Q8IYB4|PEX5R_HUMAN PEX5-related protein OS=Homo sapiens GN=PEX5L PE=1 SV=2 MYQGHMQKSKEQGYGKLSSDEDLEIIVDQKQGKGSRAADKAVAMVMKEIPREESAEEKPL LTMTSQLVNEQQESRPLLSPSIDDFLCETKSEAIARPVTSNTAVLTTGLDLLDLSEPVSQ TQTKAKKSEPSSKTSSLKKKADGSDLISTDAEQRGQPLRVPETSSLDLDIQTQLEKWDDV KFHGDRNTKGHPMAERKSSSSRTGSKELLWSSEHRSQPELSGGKSALNSESASELELVAP TQARLTKEHRWGSALLSRNHSLEEEFERAKAAVESDTEFWDKMQAEWEEMARRNWISENQ EAQNQVTISASEKGYYFHTENPFKDWPGAFEEGLKRLKEGDLPVTILFMEAAILQDPGDA EAWQFLGITQAENENEQAAIVALQRCLELQPNNLKALMALAVSYTNTGHQQDACDALKNW IKQNPKYKYLVKSKKGSPGLTRRMSKSPVDSSVLEGVKELYLEAAHQNGDMIDPDLQTGL GVLFHLSGEFNRAIDAFNAALTVRPEDYSLWNRLGATLANGDRSEEAVEAYTRALEIQPG FIRSRYNLGISCINLGAYREAVSNFLTALSLQRKSRNQQQVPHPAISGNIWAALRIALSL MDQPELFQAANLGDLDVLLRAFNLDP	−
	Q8IYB4-2	>sp|Q8IYB4-2|PEX5R_HUMAN Isoform 2 of PEX5-related protein OS=Homo sapiens GN=PEX5L MYQGHMQVVGVTLKKKWHCLQKSDLTLALGKGSRAADKAVAMVMKEIPREESAEEKPLLT MTSQLVNEQQESRPLLSPSIDDFLCETKSEAIARPVTSNTAVLTTGLDLLDLSEPVSQTQ TKAKKSEPSSKTSSLKKKADGSDLISTDAEQRGQPLRVPETSSLDLDIQTQLEKWDDVKF HGDRNTKGHPMAERKSSSSRTGSKELLWSSEHRSQPELSGGKSALNSESASELELVAPTQ ARLTKEHRWGSALLSRNHSLEEEFERAKAAVESDTEFWDKMQAEWEEMARRNWISENQEA QNQVTISASEKGYYFHTENPFKDWPGAFEEGLKRLKEGDLPVTILFMEAAILQDPGDAEA WQFLGITQAENENEQAAIVALQRCLELQPNNLKALMALAVSYTNTGHQQDACDALKNWIK QNPKYKYLVKSKKGSPGLTRRMSKSPVDSSVLEGVKELYLEAAHQNGDMIDPDLQTGLGV LFHLSGEFNRAIDAFNAALTVRPEDYSLWNRLGATLANGDRSEEAVEAYTRALEIQPGFI RSRYNLGISCINLGAYREAVSNFLTALSLQRKSRNQQQVPHPAISGNIWAALRIALSLMD QPELFQAANLGDLDVLLRAFNLDP	−
	Q8IYB4-3	>sp|Q8IYB4-3|PEX5R_HUMAN Isoform 3 of PEX5-related protein OS=Homo sapiens GN=PEX5L MYQGHMQKSKEQGYGKLSSDEDLEIIVDQKQLVNEQQESRPLLSPSIDDFLCETKSEAIA RPVTSNTAVLTTGLDLLDLSEPVSQTQTKAKKSEPSSKTSSLKKKADGSDLISTDAEQRG QPLRVPETSSLDLDIQTQLEKWDDVKFHGDRNTKGHPMAERKSSSSRTGSKELLWSSEHR SQPELSGGKSALNSESASELELVAPTQARLTKEHRWGSALLSRNHSLEEEFERAKAAVES DTEFWDKMQAEWEEMARRNWISENQEAQNQVTISASEKGYYFHTENPFKDWPGAFEEGLK RLKEGDLPVTILFMEAAILQDPGDAEAWQFLGITQAENENEQAAIVALQRCLELQPNNLK ALMALAVSYTNTGHQQDACDALKNWIKQNPKYKYLVKSKKGSPGLTRRMSKSPVDSSVLE GVKELYLEAAHQNGDMIDPDLQTGLGVLFHLSGEFNRAIDAFNAALTVRPEDYSLWNRLG ATLANGDRSEEAVEAYTRALEIQPGFIRSRYNLGISCINLGAYREAVSNFLTALSLQRKS RNQQQVPHPAISGNIWAALRIALSLMDQPELFQAANLGDLDVLLRAFNLDP	−
Pex5pL	Q8IYB4-4	>sp|Q8IYB4-4|PEX5R_HUMAN Isoform 4 of PEX5-related protein OS=Homo sapiens GN=PEX5L MYQGHMQLVNEQQESRPLLSPSIDDFLCETKSEAIARPVTSNTAVLTTGLDLLDLSEPVS QTQTKAKKSEPSSKTSSLKKKADGSDLISTDAEQRGQPLRVPETSSLDLDIQTQLEKWDD VKFHGDRNTKGHPMAERKSSSSRTGSKELLWSSEHRSQPELSGGKSALNSESASELELVA PTQARLTKEHRWGSALLSRNHSLEEEFERAKAAVESDTEFWDKMQAEWEEMARRNWISEN QEAQNQVTISASEKGYYFHTENPFKDWPGAFEEGLKRLKEGDLPVTILFMEAAILQDPGD AEAWQFLGITQAENENEQAAIVALQRCLELQPNNLKALMALAVSYTNTGHQQDACDALKN WIKQNPKYKYLVKSKKGSPGLTRRMSKSPVDSSVLEGVKELYLEAAHQNGDMIDPDLQTG LGVLFHLSGEFNRAIDAFNAALTVRPEDYSLWNRLGATLANGDRSEEAVEAYTRALEIQP GFIRSRYNLGISCINLGAYREAVSNFLTALSLQRKSRNQQQVPHPAISGNIWAALRIALS LMDQPELFQAANLGDLDVLLRAFNLDP	−
	Q8IYB4-5	>sp|Q8IYB4-5|PEX5R_HUMAN Isoform 5 of PEX5-related protein OS=Homo sapiens GN=PEX5L MVMKEIPREESAEEKPLLTMTSQLVNEQQESRPLLSPSIDDFLCETKSEAIARPVTSNTA VLTTGLDLLDLSEPVSQTQTKAKKSEPSSKTSSLKKKADGSDLISTDAEQRGQPLRVPET SSLDLDIQTQLEKWDDVKFHGDRNTKGHPMAERKSSSSRTGSKELLWSSEHRSQPELSGG KSALNSESASELELVAPTQARLTKEHRWGSALLSRNHSLEEEFERAKAAVESDTEFWDKM QAEWEEMARRNWISENQEAQNQVTISASEKGYYFHTENPFKDWPGAFEEGLKRLKEGDLP VTILFMEAAILQDPGDAEAWQFLGITQAENENEQAAIVALQRCLELQPNNLKALMALAVS YTNTGHQQDACDALKNWIKQNPKYKYLVKSKKGSPGLTRRMSKSPVDSSVLEGVKELYLE AAHQNGDMIDPDLQTGLGVLFHLSGEFNRAIDAFNAALTVRPEDYSLWNRLGATLANGDR SEEAVEAYTRALEIQPGFIRSRYNLGISCINLGAYREAVSNFLTALSLQRKSRNQQQVPH PAISGNIWAALRIALSLMDQPELFQAANLGDLDVLLRAFNLDP	−
	Q8IYB4-6	>sp|Q8IYB4-6|PEX5R_HUMAN Isoform 6 of PEX5-related protein OS=Homo sapiens GN=PEX5L MYQGHMQGKGSRAADKAVAMVMKEIPREESAEEKPLLTMTSQLVNEQQESRPLLSPSIDD FLCETKSEAIARPVTSNTAVLTTGLDLLDLSEPVSQTQTKAKKSEPSSKTSSLKKKADGS DLISTDAEQRGQPLRVPETSSLDLDIQTQLEKWDDVKFHGDRNTKGHPMAERKSSSSRTG SKELLWSSEHRSQPELSGGKSALNSESASELELVAPTQARLTKEHRWGSALLSRNHSLEE EFERAKAAVESDTEFWDKMQAEWEEMARRNWISENQEAQNQVTISASEKGYYFHTENPFK DWPGAFEEGLKRLKEGDLPVTILFMEAAILQDPGDAEAWQFLGITQAENENEQAAIVALQ RCLELQPNNLKALMALAVSYTNTGHQQDACDALKNWIKQNPKYKYLVKSKKGSPGLTRRM SKSPVDSSVLEGVKELYLEAAHQNGDMIDPDLQTGLGVLFHLSGEFNRAIDAFNAALTVR PEDYSLWNRLGATLANGDRSEEAVEAYTRALEIQPGFIRSRYNLGISCINLGAYREAVSN FLTALSLQRKSRNQQQVPHPAISGNIWAALRIALSLMDQPELFQAANLGDLDVLLRAFNL DP	−
	Q8IYB4-7	>sp|Q8IYB4-7|PEX5R_HUMAN Isoform 7 of PEX5-related protein OS=Homo sapiens GN=PEX5L MVMKEIPREESAEEKPLLTMTSQLVNEQQESRPLLSPSIDDFLCETKSEAIARPVTSNTA DIQTQLEKWDDVKFHGDRNTKGHPMAERKSSSSRTGSKELLWSSEHRSQPELSGGKSALN SESASELELVAPTQARLTKEHRWGSALLSRNHSLEEEFERAKAAVESDTEFWDKMQAEWE EMARRNWISENQEAQNQVTISASEKGYYFHTENPFKDWPGAFEEGLKRLKEGDLPVTILF MEAAILQDPGDAEAWQFLGITQAENENEQAAIVALQRCLELQPNNLKALMALAVSYTNTG HQQDACDALKNWIKQNPKYKYLVKSKKGSPGLTRRMSKSPVDSSVLEGVKELYLEAAHQN GDMIDPDLQTGLGVLFHLSGEFNRAIDAFNAALTVRPEDYSLWNRLGATLANGDRSEEAV EAYTRALEIQPGFIRSRYNLGISCINLGAYREAVSNFLTALSLQRKSRNQQQVPHPAISG NIWAALRIALSLMDQPELFQAANLGDLDVLLRAFNLDP	−
	Q8IYB4-8	>sp|Q8IYB4-8|PEX5R_HUMAN Isoform 8 of PEX5-related protein OS=Homo sapiens GN=PEX5L MAERKSSSSRTGSKELLWSSEHRSQPELSGGKSALNSESASELELVAPTQARLTKEHRWG SALLSRNHSLEEEFERAKAAVESDTEFWDKMQAEWEEMARRNWISENQEAQNQVTISASE KGYYFHTENPFKDWPGAFEEGLKRLKEGDLPVTILFMEAAILQDPGDAEAWQFLGITQAE NENEQAAIVALQRCLELQPNNLKALMALAVSYTNTGHQQDACDALKNWIKQNPKYKYLVK SKKGSPGLTRRMSKSPVDSSVLEGVKELYLEAAHQNGDMIDPDLQTGLGVLFHLSGEFNR	−

Peroxin	Accession number	FASTA sequence	PP1-binding motifs (aa x–y)
		AIDAFNAALTVRPEDYSLWNRLGATLANGDRSEEAVEAYTRALEIQPGFIRSRYNLGISC INLGAYREAVSNFLTALSLQRKSRNQQQVPHPAISGNIWAALRIALSLMDQPELFQAANL GDLDVLLRAFNLDP	
Pex6p	Q13608	>sp|Q13608|PEX6_HUMAN Peroxisome assembly factor 2 OS=Homo sapiens GN=PEX6 PE=1 SV=2 MALAVLRVLEPFPTETPPLAVLLPPGGPWPAAELGLVLALRPAGESPAGPALLVAALEGP DAGTEEQGPGPPQLLVSRALLRLLALGSGAWV**RARA**VRRPPALGWALLGTSLGPGLGPRV GPLLVRRGETLPVPGPRVLETRPALQGLLGPGTRLAVTELRGRARLCPESGDSSRPPPPP VVSSFAVSGTVRRLQGVLGGTGDSLGVSRSCLRGLGLFQGEWVWVAQARESSNTSQPHLA RVQVLEPRWDLSDRLGPGSSGPLGEPLADGLALVPATLAFNLGCDPLEMGELRIQRYLEGS IAPEDKGSCSLLPGPPFARELHIEIVSSPHYSTNGNYDGVLYRHFQIPRVVQEGDVLCVP TIGQVEILEGSPEKLPRWREMFFKVKKTVGEAPDGPASAYLADTTHTSLYMVGSTLSPVP WLPSEESTLWSSLSPPGLEALVSELCAVLKPRLQPGGALLTGTSSVLLRGPPGCGKTTVV AAACSHLGLHLLKVPCSSLCAESSGAVETKLQAIFSRARRCRPAVLLTAVDLLGRDRDG LGEDARVMAVLRHLLLNEDPLNSCPPLMVVATTSRAQDLPADVQTAFPHELEVPALSEGQ RL**SILR**ALTAHLPLGQEVNLAQLARRCAGFVVGDLYALLTHSSRAACTRIKNSGLAGGLT EEDEGELCAAGFPLLAEDFGQALEQLQTAHSQAVGAPKIPSVSWHDVGGLQEVKKEILET IQLPLEHPELLSLGLRRSGLLLHGPPGTGKTLLAKAVATECSLTFLSVKGPELINMYVGQ SEENVREVFA**RARA**AAPCIIFFDELDSLAPSRGRSGDSGGVMDRVVSQLLAELDGLHSTQ DVFVIGATNRPDLLDPALLRPGRFDKLVFVGANEDRASQLRVLSAITRKFKLEPSVSLVN VLDCCPPQLTGADLYSLCSDAMTAALKRRVHDLEEGLEPGSSALMLTMEDLLQAAARLQP SVSEQELLRYKRIQRKFAAC	93–96: RARA [6] 603–606: SILR [4] 791–794: RARA [6]
Pex7p	O00628	>sp|O00628|PEX7_HUMAN Peroxisomal targeting signal 2 receptor OS=Homo sapiens GN=PEX7 PE=1 SV=1 MSAVCGGAARMLRTPGRHGYAAEFSPYLPGRLACATAQHYGIAGCGTLLILDPDEAGLRL FRSFDWNDGLFDVTWSENNEHVLITCSGDGSLQLWDTAKAAGPLQVYKEHAQEVYSVDWS QTRGEQLVVSGSWDQTVKLWDPTVGKSLCTFRGHESIIYSTIWSPHIPGCFASASGDQTL RIWDVKAAGVRIVIPAHQAEILSCDWCKYNENLLVTGAVDCSLRGWDLRNVRQPVFELLG HTYAI**RRVKF**SPFHASVLASCSYDFTVRFWNFSKPDSLLETVEHHTEFTCGLDFSLQSPT QVADCSWDETIKIYDPACLTIPA	246–250: RRVKF [1,2,3]
Pex10p	O60683	>sp|O60683|PEX10_HUMAN Peroxisome biogenesis factor 10 OS=Homo sapiens GN=PEX10 PE=1 SV=1 MAPAAASPPEVIRAAQKDEYYRGGLRSAAGGALHSLAGARKWLEWRKEVELLSDVAYFGL TTLAGYQTLGEEYVSIIQVDPSRIHVPSSLRRGVLVTLHAVLPYLLDKALLPLEQELQAD PDSGRPLQGSLGPGGRGCSGARRWMRHHTATLTEQQRRALLRAVFVLRQGLACLQR**LHVA W**FYIHGVFYHLAKRLTGITYLRVRSLPGEDLRARVSYRLLGVISLLHLVLSMGLQLYG**FR QRQR**ARKEWRLHRGLSHRRASLEERAVSRNPLCTLCLEERRHPTATPCGHLFCWECITAW CSSKAECPLCREKFPPQKLIYLRHYR	177–181: LHVAW [3] 239–244: FRqRqR [5]
Pex10p	O60683–2	>sp|O60683-2|PEX10_HUMAN Isoform 2 of Peroxisome biogenesis factor 10 OS=Homo sapiens GN=PEX10 MAPAAASPPEVIRAAQKDEYYRGGLRSAAGGALHSLAGARKWLEWRKEVELLSDVAYFGL TTLAGYQTLGEEYVSIIQVDPSRIHVPSSLRRGVLVTLHAVLPYLLDKALLPLEQELQAD PDSGRPLQGSLGPGGRGCSGARRWMRHHTATLTEQQRRALLRAVFVLRQGLACLQR**LHVA W**FYIHGVFYHLAKRLTGITYQALRPDPLRVLMSVAPSALQLRVRSLPGEDLRARVSYRLL GVISLLHLVLSMGLQLYG**FRQRQR**ARKEWRLHRGLSHRRASLEERAVSRNPLCTLCLEER RHPTATPCGHLFCWECITAWCSSKAECPLCREKFPPQKLIYLRHYR	177–181: LHVAW [3] 259–264: FRqRqR [5]
Pex11pα	O75192	>sp|O75192|PX11A_HUMAN Peroxisomal membrane protein 11A OS=Homo sapiens GN=PEX11A PE=1 SV=1 MDAFTRFTNQTQGRDRLFRATQYTCMLLRYLLEPKAGKEKVVMKLKKLESSVSTGRKWFR LGNVVHAIQATEQSIHATDLVPRLCLTLANLN**RVIYF**ICDTILWVRSVGLTSGINKEKWR TRAAHHYYYSLLLSLVRDLYEISLQMKRVTCDRAKKEKSASQDPLWFSVAEEETEWLQSF LLLLLFRSLKQHPPLLLDTVKNLCDILNPLDQLGIYKSNPGIIGLGGLVSSIAGMITVAYP QMKLKTR	93–97: RvIYF [1]
Pex11pα	O75192–2	>sp|O75192-2|PX11A_HUMAN Isoform 2 of Peroxisomal membrane protein 11A OS=Homo sapiens GN=PEX11A MDAFTRFTNQTQGRDRLFRATQYTCMLLRYLLEPKAGKEKVVMKLKKLESSVSTGRKSNL N**RVIYF**ICDTILWVRSVGLTSGINKEKWRTRAAHHYYYSLLLSLVRDLYEISLQMKRVTC DRAKKEKSASQDPLWFSVAEEETEWLQSFLLLLLFRSLKQHPPLLLDTVKNLCDILNPLDQ LGIYKSNPGIIGLGGLVSSIAGMITVAYPQMKLKTR	62–66: RvIYF [1]
Pex11pβ	O96011	>sp|O96011|PX11B_HUMAN Peroxisomal membrane protein 11B OS=Homo sapiens GN=PEX11B PE=1 SV=1 MDAWVRFSAQSQARERLCRAAQYACSLLGHALQRHGASPELQKQIRQLESHLSLGRKLLR LGNSADALESAKRAVHLSDVVLRFCITVSHLNRALYFACDNVLWAGKSGLAPRVDQEKWA QRSFRYYLFSLIMNLSRDAYEIRLLMEQESSACSRRLKGSGGGVPGGSETGGLGGPGTPG GGLPQLALKLRLQVLLLARVLRGHPPLLLDVVRNACDLFIPLDKLGLWRCGPGIVGLCGL VSSILSILTLIYPWLRLKP	–
Pex11pβ	O96011–2	>sp|O96011-2|PX11B_HUMAN Isoform 2 of Peroxisomal membrane protein 11B OS=Homo sapiens GN=PEX11B MGKLRAAQYACSLLGHALQRHGASPELQKQIRQLESHLSLGRKLLRLGNSADALESAKRA VHLSDVVLRFCITVSHLNRALYFACDNVLWAGKSGLAPRVDQEKWAQRSFRYYLFSLIMN LSRDAYEIRLLMEQESSACSRRLKGSGGGVPGGSETGGLGGPGTPGGGLPQLALKLRLQV LLLARVLRGHPPLLLDVVRNACDLFIPLDKLGLWRCGPGIVGLCGLVSSILSILTLIYPW LRLKP	–
Pex11pγ	Q96HA9	>sp|Q96HA9|PX11C_HUMAN Peroxisomal membrane protein 11C OS=Homo sapiens GN=PEX11G PE=1 SV=1 MASLSGLASALESYRGRDRLIRVLGYCCQLVGGVLVEQCPARSEVGTRLLVVSTQLSHCR TILRLFDDLAMFVYTKQYGLGAQEEDAFVRCVSVLGNLADQLYYPCEHVAWAADARVLHV DSSRWWTLSTTLWALSLLLGVARSLWMLLKLRQRLRSPTAPFTSPLPRGKRRAMEAQMQS EALSLLSNLADLANAVHWLP**RGVLW**AGRFPPWLVGLMGTISSILSMYQAARAGGQAEATT P	201–205: RgVLW [1]
Pex11pγ	Q96HA9–2	>sp|Q96HA9-2|PX11C_HUMAN Isoform 2 of Peroxisomal membrane protein 11C OS=Homo sapiens GN=PEX11G MFVYTKQYGLGAQEEDAFVRCVSVLGNLADQLYYPCEHVAWAADARVLHVDSSRWWTLST TLWALSLLLGVARSLWMLLKLRQRLRSPTAPFTSPLPRGKRRAMEAQMQSEALSLLSNLA DLANAVHWLP**RGVLW**AGRFPPWLVGLMGTISSILSMYQAARAGGQAEATTP	131–135: RgVLW [1]
Pex12p	O00623	>sp|O00623|PEX12_HUMAN Peroxisome assembly protein 12 OS=Homo sapiens GN=PEX12 PE=1 SV=1 MAEHGAHFTAASVADDQPSIFEVVAQDSLMTAVRPALQHVVKVLAESNPTHYGFLWRWFD EIFTLLDLLLQQHYLSRTSASFSENFYGLKRIVMGDTHKSQRLASAGLPKQQLW**KSIMF**L VLLPYLKVKLEKLVSSLREEDEYSIHPPSSRWKRFYRAFLAAYPFVNMAWEGWFLVQQLR YIILGKAQHHSPLLRLAGVQLGRLTVQDIQALEHKPAKASMMQQPARSVSEKINSALKKAV GGVALSLSTGLSVGVFFLQFLDWWYSSENQETIKSLTALPTPPPPVHLDYNSDSPLLPKM KTVCPLCRKTRVNDTVLATSGYVFCYRCVFHYVRSHQACPITGYPTEVQHLIKLYSPEN	115–119: KsIMF [1]

Peroxin	Accession number	FASTA sequence	PP1-binding motifs (aa x–y)
Pex13p	Q92968	>sp|Q92968|PEX13_HUMAN Peroxisomal membrane protein PEX13 OS=Homo sapiens GN=PEX13 PE=1 SV=2 MASQPPPPPKPWETRRIPGAGPGPGPGPTFQSADLGPTLMTRPGQPALTRVPPPILPRPS QQTGSSSVNTFRPAYSSFSSGYGAYGNSFYGGYSPYSYGYNGLGYNRLRVDDLPPSRFVQ QAEESSRGAFQSIESIVHAFASVSMMMDATFSAVYNSFRAVLDVANHFSRLKIHFTKVFS AFALVRTIRYLYRRLQRMLGLRRGSENEDLWAESEGTVACLGAEDRAATSAKSWPIFLFF AVILGGPYLIWKLLSTHSDEVTDSINWASGEDDHVVARAEYDFAAVSEEEISFRAGDMLN LALKEQQPKVRGWLLASLDGQTTGLIPANYVKILGKRKGRKTVESSKVSKQQQSFTNPTL TKGATVADSLDEQEAAFESVFVETNKVPVAPDSIGKDGEKQDL	171–175: LKIHF [1, 3]
Pex14p	O75381	>sp|O75381|PEX14_HUMAN Peroxisomal membrane protein PEX14 OS=Homo sapiens GN=PEX14 PE=1 SV=1 MASSEQAEQPSQPSSTPGSENVLPREPLIATAVKFLQNSRVRQSPLATRRAFLKKKGLTD EEIDMAFQQSGTAADEPSSLGPATQVVPVQPPHLISQPYSPAGSRWRDYGALAIIMAGIA FGFHQLYKKYLLPLILGGREDRKQLERMEAGLSELSGSVAQTVTQLQTTLASVQELLIQQ QQKIQELAHELAAAKATTSTNWILESQNINELKSEINSLKGLLLNRRQFPPSPSAPKIPS WQIPVKSPSPSSPAAVNHHSSSDISPVSNESTSSSPGKEGHSPEGSTVTYHLLGPQEEGE GVVDVKGQVRMEVQGEEEKREDKEDEEDEEDDDVSHVDEEDCLGVQREDRRGGDGQINEQ VEKLRRPEGASNESERD	–
	O75381-2	>sp|O75381-2|PEX14_HUMAN Isoform 2 of Peroxisomal membrane protein PEX14 OS=Homo sapiens GN=PEX14 MASSEQAEQPSQPSSTPGSENVLPREPLIATAVKFLQNSRVRQSPLATRRAFLKKKGPAG SRWRDYGALAIIMAGIAFGFHQLYKKYLLPLILGGREDRKQLERMEAGLSELSGSVAQTV TQLQTTLASVQELLIQQQQKIQELAHELAAAKATTSTNWILESQNINELKSEINSLKGLL LNRRQFPPSPSAPKIPSWQIPVKSPSPSSPAAVNHHSSSDISPVSNESTSSSPGKEGHSP EGSTVTYHLLGPQEEGEGVVDVKGQVRMEVQGEEEKREDKEDEEDEEDDDVSHVDEEDCL GVQREDRRGGDGQINEQVEKLRRPEGASNESERD	–
Pex16p	Q9Y5Y5	>sp|Q9Y5Y5|PEX16_HUMAN Peroxisomal membrane protein PEX16 OS=Homo sapiens GN=PEX16 PE=1 SV=2 MEKLRLLGLRYQEYVTRHPAATAQLETAVRGFSYLLAGRFADSHELSELVYSASNLLVLL NDGILRKELRKKLPVSLSQQKLLTWLSVLECVEVFMEMGAAKVWGEVGRWLVIALVQLAK AVLRMLLLLWFKAGLQTSPPIVPLDRETQAQPPDGDHSPGNHEQSYVGKRSNRVVRTLQN TPSLHSRHWGAPQQREGRQQQHHEELSATPTPLGLQETIAEFLYIARPLLHLLSLGLWGQ RSWKPWLLAGVVDVTSLSLLSDRKGLTRRERRELRRRTILLLYYLLRSPFYDRFSEARIL FLLQLLADHVPGVGLVTRPLMDYLPTWQKIYFYSWG	63–66: GILR [4] 298–301: R.ILF [1] 329–332: K.IYF [1]
	Q9Y5Y5-2	>sp|Q9Y5Y5-2|PEX16_HUMAN Isoform 2 of Peroxisomal membrane protein PEX16 OS=Homo sapiens GN=PEX16 MEKLRLLGLRYQEYVTRHPAATAQLETAVRGFSYLLAGRFADSHELSELVYSASNLLVLL NDGILRKELRKKLPVSLSQQKLLTWLSVLECVEVFMEMGAAKVWGEVGRWLVIALVQLAK AVLRMLLLLWFKAGLQTSPPIVPLDRETQAQPPDGDHSPGNHEQSYVGKRSNRVVRTLQN TPSLHSRHWGAPQQREGRQQQHHEELSATPTPLGLQETIAEFLYIARPLLHLLSLGLWGQ RSWKPWLLAGVVDVTSLSLLSDRKGLTRRERRELRRRTILLLYYLLRSPFYDRFSEARIL FLLQLLADHVPGVGLVTTSQRAASPCLPARPHTQPWSPPAFLPGHP	63–66: GILR [4] 298–301: R.ILF [1]
Pex19p	P40855	>sp|P40855|PEX19_HUMAN Peroxisomal biogenesis factor 19 OS=Homo sapiens GN=PEX19 PE=1 SV=1 MAAAEEGCSVGAEADRELEELLESALDDFDKAKPSPAPPSTTTAPDASGPQKRSPGDTAK DALFASQEKFFQELFDSELASQATAEFEKAMKELAEEEPHLVEQFQKLSEAAGRVGSDMT SQQEFTSCLKETLSGLAKNATDLQNSSMSEEELTKAMEGLGMDEGDGEGNILPIMQSIMQ NLLSKDVLYPSLKEITEKYPEWLQSHRESLPPEQFEKYQELFDSELASQATAEFEKAMKE LAEEEPHLVEQFQKLSEAAGRVGSDMTSQQEFTSCLKETLSGLAKNATDLQNSSMSEEEL TKAMEGLGMDEGDGEGNILPIMQSIMQNLLSKDVLYPSLKEITEKYPEWLQSHRESLPPE QFEKYQEQHSVMCKICEQFEAETPTDSETTQKARFEMVLDLMQQLQDLGHPPKELAGEMPPGLNFDLDALNLSGPPGASGEQCLIM	–
	P40855-5	>sp|P40855-5|PEX19_HUMAN Isoform 5 of Peroxisomal biogenesis factor 19 OS=Homo sapiens GN=PEX19 PPLRKAVVSGPKRTGNWRSFWKDALFASQEKFFQELFDSELASQATAEFEKAMKELAEEE PHLVEQFQKLSEAAGRVGSDMTSQQEFTSCLKETLSGLAKNATDLQNSSMSEEELTKAME GLGMDEGDGEGNILPIMQSIMQNLLSKDVLYPSLKEITEKYPEWLQSHRESLPPEQFEKY QEQHSVMCKICEQFEAETPTDSETTQKARFEMVLDLMQQLQDLGHPPKELAGEMPPGLNF DLDALNLSGPPGASGEQCLIM	–
Pex26p	Q7Z412	>sp|Q7Z412|PEX26_HUMAN Peroxisome assembly protein 26 OS=Homo sapiens GN=PEX26 PE=1 SV=2 MKSDSSTSAAPLRGLGGPLRSSEPVRAVPARAPAVDLLEEAADLLVVHLDFRAALETCER AWQSLANHAVAEEPAGTSLEVKCSLCVVGIQALAEMDRWQEVLSWVLQYYQVPEKLPPKV LELCILLYSKMQEPGAVLDVVGAWLQDPANQNLPEYGALAEFHVQRVLLPLGCLSEAEEL VVGSAAFGEERRLDVLQAIHTARQQQKQEHSGSEEAQKPNLEGSVSHKFLSLPMLVRQLW DSAVSHFFSLPFKKSLLAALILCLLVVRFDPASPSSLHFLYKLAQLFRWIRKAAFSRLYQ LRIRD	265–269: LVVRF [3]
	Q7Z412-2	>sp|Q7Z412-2|PEX26_HUMAN Isoform 2 of Peroxisome assembly protein 26 OS=Homo sapiens GN=PEX26 MKSDSSTSAAPLRGLGGPLRSSEPVRAVPARAPAVDLLEEAADLLVVHLDFRAALETCER AWQSLANHAVAEEPAGTSLEVKCSLCVVGIQALAEMDRWQEVLSWVLQYYQVPEKLPPKV LELCILLYSKMQEPGAVLDVVGAWLQDPANQNLPEYGALAEFHVQRVLLPLGCLSEAEEL VVGSAAFGEERRLDVLQAIHTARQQQKQEHSGSEEAQKPNLEASPSSLHFLYKLAQLFRW IRKAAFSRLYQLRIRD	–

The sequences were collected from UniProtKB database and loaded in ScanProsite program as well as the PP1-binding motifs canonical sequences listed on Table 5. The green- and blue-high lightened residues correspond to matches with the canonical sequences of RVxF and RVxF-cooperating motifs, respectively. [1]matches with the sequence [RK]-X(0,1)-[VI]-{P}-[FW]; [2]matches with the sequence [HKR]-[ACHKMNQRSTV]-V-[CHKNQRST]-[FW]; [3]matches with the sequence [KRL]-[KRSTAMVHNQ]-[VI]-{FIMYDP}-[FW]; [4]matches with the sequence [GS]-I-L-[RK]; [5]matches with the sequence F-X-X-[RK]-X-[RK]; [6]matches with the sequence R-A-R-A. Other canonical sequences were screened, with no hits (R-X-X-Q-[VIL]-[KR]-X-[YW], R-[KR]-X-H-Y, K-S-Q-K-W and R-N-Y-F). A graphic resume of this screening is depicted on Figure 9.

Supplementary Table 2: Human ubiquitin-conjugating enzymes and PP1-binding motifs

Ubiquitin-conjugating enzyme	Accession number	FASTA sequence	PP1-binding motifs (aa x–y)
UbcH5a	P51668	>sp|P51668|UB2D1_HUMAN Ubiquitin-conjugating enzyme E2 D1 OS=Homo sapiens GN=UBE2D1 PE=1 SV=1 MALKRIQKELSDLQRDPPAHCSAGPVGDDLFHWQATIMGPPDSAYQGGVFFLTVHFPTDY PFKPPKIAFTTKIYHPNINSNGSICLDILRSQWSPALTVSKVLLSICSLLCDPNPDDPLV PDIAQIYKSDKEKYNRHAREWTQKYAM	52–56: LTVHF [1] 66–69: K.IAF [2]
UbcH5b	P62837	>sp|P62837|UB2D2_HUMAN Ubiquitin-conjugating enzyme E2 D2 OS=Homo sapiens GN=UBE2D2 PE=1 SV=1 MALKRIHKELNDLARDPPAQCSAGPVGDDMFHWQATIMGPNDSPYQGGVFFLTIHFPTDY PFKPPKVAFTTRIYHPNINSNGSICLDILRSQWSPALTISKVLLSICSLLCDPNPDDPLV PEIARIYKTDREKYNRIAREWTQKYAM	52–56: LTIHF [1] 66–69: K.VAF [2]
	P62837-2	>sp|P62837-2|UB2D2_HUMAN Isoform 2 of Ubiquitin-conjugating enzyme E2 D2 OS=Homo sapiens GN=UBE2D2 MFHWQATIMGPNDSPYQGGVFFLTIHFPTDYPFKPPKVAFTTRIYHPNINSNGSICLDIL RSQWSPALTISKVLLSICSLLCDPNPDDPLVPEIARIYKTDREKYNRIAREWTQKYAM	23–27: LTIHF [1] 37–40: K.VAF [2]
UbcH5c	P61077	>sp|P61077|UB2D3_HUMAN Ubiquitin-conjugating enzyme E2 D3 OS=Homo sapiens GN=UBE2D3 PE=1 SV=1 MALKRINKELSDLARDPPAQCSAGPVGDDMFHWQATIMGPNDSPYQGGVFFLTIHFPTDY PFKPPKVAFTTRIYHPNINSNGSICLDILRSQWSPALTISKVLLSICSLLCDPNPDDPLV PEIARIYKTDRDKYNRISREWTQKYAM	52–56: LTIHF [1] 66–69: K.VAF [2]
	P61077-2	>sp|P61077-2|UB2D3_HUMAN Isoform 2 of Ubiquitin-conjugating enzyme E2 D3 OS=Homo sapiens GN=UBE2D3 MALKRINKELSDLARDPPAQCSAGPVGDDMFHWQATIMGPNDSPYQGGVFFLTIHFPTDY PFKPPKVAFTTRIYHPNINSNGSICLDILRSQWSPALTISKVLLSICSLLCDPNPDDPLV PEIARIYKTDRDKYNRLAREWTEKYAML	52–56: LTIHF [1] 66–69: K.VAF [2]
	P61077-3	>sp|P61077-3|UB2D3_HUMAN Isoform 3 of Ubiquitin-conjugating enzyme E2 D3 OS=Homo sapiens GN=UBE2D3 MLSNRKCLSKELSDLARDPPAQCSAGPVGDDMFHWQATIMGPNDSPYQGGVFFLTIHFPT DYPFKPPKVAFTTRIYHPNINSNGSICLDILRSQWSPALTISKVLLSICSLLCDPNPDDP LVPEIARIYKTDRDKYNRISREWTQKYAM	54–58: LTIHF [1] 68–71: K.VAF [2]

The sequences were collected from UniProtKB database and loaded in ScanProsite program as well as the PP1-binding motifs canonical sequences listed on Table 5. The green-lightened residues correspond to matches with the canonical sequences of RVxF motifs. [1]matches with the sequence [KRL]-[KRSTAMVHNQ]-[VI]-{FIMYDP}-[FW]; [2]matches with the sequence [RK]-X(0,1)-[VI]-{P}-[FW]. Other canonical sequences were screened, with no hits ([HKR]-[ACHKMNQRSTV]-V-[CHKNQRST]-[FW], [GS]-I-L-[RK], F-X-X-[RK]-X-[RK], R-A-R-A , R-X-X-Q-[VIL]-[KR]-X-[YW], R-[KR]-X-H-Y, K-S-Q-K-W and R-N-Y-F). A graphic resume of this screening is depicted on Supplementary Figure 1.

Supplementary Table 3: Proteins involved in peroxisome fission don't have PP1-binding motifs

Fission machinery protein	Accession number	FASTA sequence	PP1-binding motifs (aa x–y)
DLP1	O00429	>sp|O00429|DNM1L_HUMAN Dynamin-1-like protein OS=Homo sapiens GN=DNM1L PE=1 SV=2 MEALIPVINKLQDVFNTVGADIIQLPQIVVVGTQSSGKSSVLESLVGRDLLPRGTGIVTR RPLILQLVHVSQEDKRKTTGEENGVEAEEWGKFLHTKNKLYTDFDEIRQEIENETERISG NNKGVSPEPIHLKIFSPNVVNLTLVDLPGMTKVPVGDQPKDIELQIRELILRFISNPNSI ILAVTAANTDMATSEALKISREVDPDGRRTLAVITKLDLMDAGTDAMDVLMGRVIPVKLG IIGVVNRSQLDINNKKSVTDSIRDEYAFLQKKYPSLANRNGTKYLARTLNRLLMHHIRDC LPELKTRINVLAAQYQSLLNSYGEPVDDKSATLLQLITKFATEYCNTIEGTAKYIETSEL CGGARICYIFHETFGRTLESVDPLGGLNTIDILTAIRNATGPRPALFVPEVSFELLVKRQ IKRLEEPSLRCVELVHEEMQRIIQHCSNYSTQELLRFPKLHDAIVEVVTCLLRKRLPVTN EMVHNLVAIELAYINTKHPDFADACGLMNNNIEEQRRNRLARELPSAVSRDKSSKVPSAL APASQEPSPAASAEADGKLIQDSRRETKNVASGGGGVGDGVQEPTTGNWRGMLKTSKAEE LLAAEEKSKPIPIMPASPQKGHAVNLLDVPVPVARKLSAREQRDCEVIERLIKSYFLIVRK NIQDSVPKAVMHFLVNHVKDTLQSELVGQLYKSSLLDDLLTESEDMAQRRKEAADMLKAL QGASQIIAEIRETHLW	–
	O00429-2	>sp|O00429-2|DNM1L_HUMAN Isoform 4 of Dynamin-1-like protein OS=Homo sapiens GN=DNM1L MEALIPVINKLQDVFNTVGADIIQLPQIVVVGTQSSGKSSVLESLVGRDLLPRGTGIVTR RPLILQLVHVSQEDKRKTTGEENGVEAEEWGKFLHTKNKLYTDFDEIRQEIENETERISG NNKGVSPEPIHLKIFSPNVVNLTLVDLPGMTKVPVGDQPKDIELQIRELILRFISNPNSI ILAVTAANTDMATSEALKISREVDPDGRRTLAVITKLDLMDAGTDAMDVLMGRVIPVKLG IIGVVNRSQLDINNKKSVTDSIRDEYAFLQKKYPSLANRNGTKYLARTLNRLLMHHIRDC LPELKTRINVLAAQYQSLLNSYGEPVDDKSATLLQLITKFATEYCNTIEGTAKYIETSEL CGGARICYIFHETFGRTLESVDPLGGLNTIDILTAIRNATGPRPALFVPEVSFELLVKRQ IKRLEEPSLRCVELVHEEMQRIIQHCSNYSTQELLRFPKLHDAIVEVVTCLLRKRLPVTN EMVHNLVAIELAYINTKHPDFADACGLMNNNIEEQRRNRLARELPSAVSRDKSSKVPSAL APASQEPSPAASAEADGKVASGGGGVGDGVQEPTTGNWRGMLKTSKAEELLAEEKSKPIP IMPASPQKGHAVNLLDVPVPVARKLSAREQRDCEVIERLIKSYFLIVRKNIQDSVPKAVM HFLVNHVKDTLQSELVGQLYKSSLLDDLLTESEDMAQRRKEAADMLKALQGASQIIAEIR ETHLW	–
	O00429-3	>sp|O00429-3|DNM1L_HUMAN Isoform 2 of Dynamin-1-like protein OS=Homo sapiens GN=DNM1L MEALIPVINKLQDVFNTVGADIIQLPQIVVVGTQSSGKSSVLESLVGRDLLPRGTGIVTR RPLILQLVHVSQEDKRKTTGEENGVEAEEWGKFLHTKNKLYTDFDEIRQEIENETERISG NNKGVSPEPIHLKIFSPNVVNLTLVDLPGMTKVPVGDQPKDIELQIRELILRFISNPNSI ILAVTAANTDMATSEALKISREVDPDGRRTLAVITKLDLMDAGTDAMDVLMGRVIPVKLG IIGVVNRSQLDINNKKSVTDSIRDEYAFLQKKYPSLANRNGTKYLARTLNRLLMHHIRDC LPELKTRINVLAAQYQSLLNSYGEPVDDKSATLLQLITKFATEYCNTIEGTAKYIETSEL CGGARICYIFHETFGRTLESVDPLGGLNTIDILTAIRNATGPRPALFVPEVSFELLVKRQ IKRLEEPSLRCVELVHEEMQRIIQHCSNYSTQELLRFPKLHDAIVEVVTCLLRKRLPVTN EMVHNLVAIELAYINTKHPDFADACGLMNNNIEEQRRNRLARELPSAVSRDKLIQDSRRE TKNVASGGGGVGDGVQEPTTGNWRGMLKTSKAEELLAEEKSKPIPIMPASPQKGHAVNLL DVPVPVARKLSAREQRDCEVIERLIKSYFLIVRKNIQDSVPKAVMHFLVNHVKDTLQSEL VGQLYKSSLLDDLLTESEDMAQRRKEAADMLKALQGASQIIAEIRETHLW	–
	O00429-4	>sp|O00429-4|DNM1L_HUMAN Isoform 3 of Dynamin-1-like protein OS=Homo sapiens GN=DNM1L MEALIPVINKLQDVFNTVGADIIQLPQIVVVGTQSSGKSSVLESLVGRDLLPRGTGIVTR RPLILQLVHVSQEDKRKTTGEENGVEAEEWGKFLHTKNKLYTDFDEIRQEIENETERISG NNKGVSPEPIHLKIFSPNVVNLTLVDLPGMTKVPVGDQPKDIELQIRELILRFISNPNSI ILAVTAANTDMATSEALKISREVDPDGRRTLAVITKLDLMDAGTDAMDVLMGRVIPVKLG IIGVVNRSQLDINNKKSVTDSIRDEYAFLQKKYPSLANRNGTKYLARTLNRLLMHHIRDC LPELKTRINVLAAQYQSLLNSYGEPVDDKSATLLQLITKFATEYCNTIEGTAKYIETSEL CGGARICYIFHETFGRTLESVDPLGGLNTIDILTAIRNATGPRPALFVPEVSFELLVKRQ IKRLEEPSLRCVELVHEEMQRIIQHCSNYSTQELLRFPKLHDAIVEVVTCLLRKRLPVTN EMVHNLVAIELAYINTKHPDFADACGLMNNNIEEQRRNRLARELPSAVSRDKVASGGGGV GDGVQEPTTGNWRGMLKTSKAEELLAEEKSKPIPIMPASPQKGHAVNLLDVPVPVARKLS AREQRDCEVIERLIKSYFLIVRKNIQDSVPKAVMHFLVNHVKDTLQSELVGQLYKSSLLD DLLTESEDMAQRRKEAADMLKALQGASQIIAEIRETHLW	–
	O00429-5	>sp|O00429-5|DNM1L_HUMAN Isoform 5 of Dynamin-1-like protein OS=Homo sapiens GN=DNM1L MEALIPVINKLQDVFNTVGADIIQLPQIVVVGTQSSGKSSVLESLVGRDLLPRGTGIVTR RPLILQLVHVSQEDKRKTTGEENGVEAEEWGKFLHTKNKLYTDFDEIRQEIENETERISG NNKGVSPEPIHLKIFSPNVVNLTLVDLPGMTKVPVGDQPKDIELQIRELILRFISNPNSI ILAVTAANTDMATSEALKISREVDPDGRRTLAVITKLDLMDAGTDAMDVLMGRVIPVKLG IIGVVNRSQLDINNKKSVTDSIRDEYAFLQKKYPSLANRNGTKYLARTLNRLLMHHIRDC LPELKTRINVLAAQYQSLLNSYGEPVDDKSATLLQLITKFATEYCNTIEGTAKYIETSEL CGGARICYIFHETFGRTLESVDPLGGLNTIDILTAIRNATGPRPALFVPEVSFELLVKRQ IKRLEEPSLRCVELVHEEMQRIIQHCSNYSTQELLRFPKLHDAIVEVVTCLLRKRLPVTN EMVHNLVAIELAYINTKHPDFADACGLMNNNIEEQRRNRLARELPSAVSRDKSSKVPSAL APAVASGGGGVGDGVQEPTTGNWRGMLKTSKAEELLAEEKSKPIPIMPASPQKGHAVNLL DVPVPVARKLSAREQRDCEVIERLIKSYFLIVRKNIQDSVPKAVMHFLVNHVKDTLQSEL VGQLYKSSLLDDLLTESEDMAQRRKEAADMLKALQGASQIIAEIRETHLW	–
	O00429-6	>sp|O00429-6|DNM1L_HUMAN Isoform 6 of Dynamin-1-like protein OS=Homo sapiens GN=DNM1L MEALIPVINKLQDVFNTVGADIIQLPQIVVVGTQSSGKSSVLESLVGRDLLPRGTGIVTR RPLILQLVHVSQEDKRKTTGEENDPATWKNSRHLSKGVEAEEWGKFLHTKNKLYTDFDEI RQEIENETERISGNNKGVSPEPIHLKIFSPNVVNLTLVDLPGMTKVPVGDQPKDIELQIR ELILRFISNPNSIILAVTAANTDMATSEALKISREVDPDGRRTLAVITKLDLMDAGTDAM DVLMGRVIPVKLGIIGVVNRSQLDINNKKSVTDSIRDEYAFLQKKYPSLANRNGTKYLAR TLNRLLMHHIRDCLPELKTRINVLAAQYQSLLNSYGEPVDDKSATLLQLITKFATEYCNT IEGTAKYIETSELCGGARICYIFHETFGRTLESVDPLGGLNTIDILTAIRNATGPRPALF VPEVSFELLVKRQIKRLEEPSLRCVELVHEEMQRIIQHCSNYSTQELLRFPKLHDAIVEV VTCLLRKRLPVTNEMVHNLVAIELAYINTKHPDFADACGLMNNNIEEQRRNRLARELPSA VSRDKSSKVPSALAPASQEPSPAASAEADGKLIQDSRRETKNVASGGGGVGDGVQEPTTG NWRGMLKTSKAEELLAEEKSKPIPIMPASPQKGHAVNLLDVPVPVARKLSAREQRDCEVI ERLIKSYFLIVRKNIQDSVPKAVMHFLVNHVKDTLQSELVGQLYKSSLLDDLLTESEDMA QRRKEAADMLKALQGASQIIAEIRETHLW	–
	O00429-7	>sp|O00429-7|DNM1L_HUMAN Isoform 7 of Dynamin-1-like protein OS=Homo sapiens GN=DNM1L MFHKKINGKQQEKKMTLLHGKTQDTFLKGWKQKNGVNF`FTPKIR`SQLDINNKKSVTDSIR	39–44: FtpKiR [1]

Fission machinery protein	Accession number	FASTA sequence	PP1-binding motifs (aa x–y)
		DEYAFLQKKYPSLANRNGTKYLARTLNRLLMHHIRDCLPELKTRINVLAAQYQSLLNSYG EPVDDKSATLLQLITKFATEYCNTIEGTAKYIETSELCGGARICYIFHETFGRTLESVDP LGGGLNTIDILTAIRNATGPRPALFVPEVSFELLVKRQIKRLEEPSLRCVELVHEEMQRII QHCSNYSTQELLRFPKLHDAIVEVVTCLLRKKRLPVTNEMVHNLVAIELAYINTKHPDFAD ACGLMNNNIEEQRRNRLARELPSAVSRDKSSKVPSALAPASQEPSPAASAEADGKLIQDS RRETKNVASGGGGVGDGVQEPTTGNWRGMLKTSKAEELLAEEKSKPIPIMPASPQKGHAV NLLDVPVPVARKLSAREQRDCEVIERLIKSYFLIVRKNIQDSVPKAVMHFLVNHVKDTLQ SELVGQLYKSSLLDDLLTESEDMAQRRKEAADMLKALQGASQIIAEIRETHLW	
	O00429-8	>sp|O00429-8|DNM1L_HUMAN Isoform 8 of Dynamin-1-like protein OS=Homo sapiens GN=DNM1L MEALIPVINKLQDVFNTVGADIIQLPQIVVVGTQSSGKSSVLESLVGRDLLPRGTGIVTR RPLILQLVHVSQEDKRKTTGEENDPATWKNSRHLSKGVEAEEWGKFLHTKNKLYTDFDEI RQEIENETERISGNNKGVSPEPIHLKIFSPNVVNLTLVDLPGMTKVPVGDQPKDIELQIR ELILRFISNPNSIILAVTAANTDMATSEALKISREVDPDGRRTLAVITKLDLMDAGTDAM DVLMGRVIPVKLGIIGVVNRSQLDINNKKSVTDSIRDEYAFLQKKYPSLANRNGTKYLAR TLNRLLMHHIRDCLPELKTRINVLAAQYQSLLNSYGEPVDDKSATLLQLITKFATEYCNT IEGTAKYIETSELCGGARICYIFHETFGRTLESVDPLGGLNTIDILTAIRNATGPRPALF VPEVSFELLVKRQIKRLEEPSLRCVELVHEEMQRIIQHCSNYSTQELLRFPKLHDAIVEV VTCLLRKKRLPVTNEMVHNLVAIELAYINTKHPDFADACGLMNNNIEEQRRNRLARELPSA VSRDKSSKVPSALAPASQEPSPAASAEADGKVASGGGGVGDGVQEPTTGNWRGMLKTSKA EELLAEEKSKPIPIMPASPQKGHAVNLLDVPVPVARKLSAREQRDCEVIERLIKSYFLIV RKNIQDSVPKAVMHFLVNHVKDTLQSELVGQLYKSSLLDDLLTESEDMAQRRKEAADMLK ALQGASQIIAEIRETHLW	–
Fis1	Q9Y3D6	>sp|Q9Y3D6|FIS1_HUMAN Mitochondrial fission 1 protein OS=Homo sapiens GN=FIS1 PE=1 SV=2 MEAVLNELVSVEDLLKFEKKFQSEKAAGSVSKSTQFEYAWCLVRSKYNDDIRKGIVLLEE LLPKGSKEEQRDYVFYLAVGNYRLKEYEKALKYVRGLLQTEPQNNQAKELERLIDKAMKK DGLVGMAIVGGMALGVAGLAGLIGLAVSKSKS	–
GDAP1	Q8TB36	>sp|Q8TB36|GDAP1_HUMAN Ganglioside-induced differentiation-associated protein 1 OS=Homo sapiens GN=GDAP1 PE=1 SV=3 MAERQEEQRGSPPLRAEGKADAEVKLILYHWTHSFSSQKVRLVIAEKALKCEEHDVSLPL SEHNEPWFMRLNSTGEVPVLIHGENIICEATQIIDYLEQTFLDERTPRLMPDKESMYYPR VQHYRELLDSLPMDAYTHGCILHPELTVDSMIPAYATTRIRSQIGNTESELKKLAEENPD LQEAYIAKQKRLKSKLLDHDNVKYLKKILDELEKVLDQVETELQRRNEETPEEGQQPWLC GESFTLADVSLAVTLHRLKFLGFARRNWGNGKRPNLETYYERVLKRKTFNKVLGHVNNIL ISAVLPTAFRVAKKRAPKVLGTTLVVGLLAGVGYFAFMLFRKRLGSMILAFRPRPNYF	–
	Q8TB36-2	>sp|Q8TB36-2|GDAP1_HUMAN Isoform 2 of Ganglioside-induced differentiation-associated protein 1 OS=Homo sapiens GN=GDAP1 MRLNSTGEVPVLIHGENIICEATQIIDYLEQTFLDERTPRLMPDKESMYYPRVQHYRELL DSLPMDAYTHGCILHPELTVDSMIPAYATTRIRSQIGNTESELKKLAEENPDLQEAYIAK QKRLKSKLLDHDNVKYLKKILDELEKVLDQVETELQRRNEETPEEGQQPWLCGESFTLAD VSLAVTLHRLKFLGFARRNWGNGKRPNLETYYERVLKRKTFNKVLGHVNNILISAVLPTA FRVAKKRAPKVLGTTLVVGLLAGVGYFAFMLFRKRLGSMILAFRPRPNYF	–
Mff	Q9GZY8	>sp|Q9GZY8|MFF_HUMAN Mitochondrial fission factor OS=Homo sapiens GN=MFF PE=1 SV=1 MSKGTSSDTSLGRVSRAAFPSPTAAEMAEISRIQYEMEYTEGISQRMRVPEKLKVAPPNA DLEQGFQEGVPNASVIMQVPERIVVAGNNEDVSFSRPADLDLIQSTPFKPLALKTPPRVL TLSERPLDFLDLERPPTTPQNEEIRAVGRLKRERSMSENAVRQNGQLVRNDSLWHRSDSA PRNKISRFQAPISAPEYTVTPSPQQARVCPPHMLPEDGANLSSARGILSLIQSSTRRAYQ QILDVLDENRRPVLRGGSAAATSNPHHDNVRYGISNIDTTIEGTSDDLTVVDAASLRRQI IKLNRRLQLLEEENKERAKREMVMYSITVAFWLLNSWLWFRR	–
	Q9GZY8-2	>sp|Q9GZY8-2|MFF_HUMAN Isoform 2 of Mitochondrial fission factor OS=Homo sapiens GN=MFF MAEISRIQYEMEYTEGISQRMRVPEKLKVAPPNADLEQGFQEGVPNASVIMQVPERIVVA GNNEDVSFSRPADLDLIQSTPFKPLALKTPPRVLTLSERPLDFLDLERPPTTPQNEEIRA VGRLKRERSMSENAVRQNGQLVRNDSLVTPSPQQARVCPPHMLPEDGANLSSARGILSLI QSSTRRAYQQILDVLDENRRPVLRGGSAAATSNPHHDNVRYGISNIDTTIEGTSDDLTVV DAASLRRQIIKLNRRLQLLEEENKERAKREMVMYSITVAFWLLNSWLWFRR	–
	Q9GZY8-3	>sp|Q9GZY8-3|MFF_HUMAN Isoform 3 of Mitochondrial fission factor OS=Homo sapiens GN=MFF MAEISRIQYEMEYTEGISQRMRVPEKLKVAPPNADLEQGFQEGVPNASVIMQVPERIVVA GNNEDVSFSRPADLDLIQSTPFKPLALKTPPRVLTLSERPLDFLDLERPPTTPQNEEIRA VGRLKRERSMSENAVRQNGQLVRNDSLWHRSDSAPRNKISRFQAPISAPEYTYGISNIDT TIEGTSDDLTVVDAASLRRQIIKLNRRLQLLEEENKERAKREMVMYSITVAFWLLNSWLW FRR	–
	Q9GZY8-4	>sp|Q9GZY8-4|MFF_HUMAN Isoform 4 of Mitochondrial fission factor OS=Homo sapiens GN=MFF MAEISRIQYEMEYTEGISQRMRVPEKLKVAPPNADLEQGFQEGVPNASVIMQVPERIVVA GNNEDVSFSRPADLDLIQSTPFKPLALKTPPRVLTLSERPLDFLDLERPPTTPQNEEIRA VGRLKRERSMSENAVRQNGQLVRNDSLYGISNIDTTIEGTSDDLTVVDAASLRRQIIKLN RRLQLLEEENKERAKREMVMYSITVAFWLLNSWLWFRR	–
	Q9GZY8-5	>sp|Q9GZY8-5|MFF_HUMAN Isoform 5 of Mitochondrial fission factor OS=Homo sapiens GN=MFF MAEISRIQYEMEYTEGISQRMRVPEKLKVAPPNADLEQGFQEGVPNASVIMQVPERIVVA GNNEDVSFSRPADLDLIQSTPFKPLALKTPPRVLTLSERPLDFLDLERPPTTPQNEEIRA VGRLKRERSMSENAVRQNGQLVRNDSLPVLRGGSAAATSNPHHDNVRYGISNIDTTIEGT SDDLTVVDAASLRRQIIKLNRRLQLLEEENKERAKREMVMYSITVAFWLLNSWLWFRR	–

The sequences were collected from UniProtKB database and loaded in ScanProsite program as well as the PP1-binding motifs canonical sequences listed on Table 5. All the proteins returned no hits for all canonical sequences for PP1-binding motifs ([RK]-X(0,1)-[VI]-{P}-[FW], [HKR]-[ACHKMNQRSTV]-V-[CHKNQRST]-[FW], [KRL]-[KRSTAMVHNQ]-[VI]-{FIMYDP}-[FW], [GS]-I-L-[RK], F-X-X-[RK]-X-[RK], R-X-X-Q-[VIL]-[KR]-X-[YW], R-A-R-A, R-[KR]-X-H-Y, K-S-Q-K-W, R-N-Y-F). [1]isoform 7 of DLP1 returned one hit for an RVxF-cooperating motif which, alone, was considered irrelevant.

Supplementary Table 4: Similarity matrix between Pex16p homologs

	1	2	3	4	5	6	7	8	9	10	11	12	13	14	15	16	17	18	19	20	21	22	23	24	25	26	27	28	29	30
1:sp|O94516|PEX16_SCHPO	100.00	21.96	18.66	21.69	22.12	16.52	14.33	17.98	17.51	18.24	19.15	15.56	16.07	17.06	17.44	16.73	17.51	18.51	18.86	18.51	18.51	18.51	18.15	18.15	17.79	17.79	17.58	17.00	17.44	15.41
2:tr|Q5KG96|Q5KG96_CRYNJ	21.96	100.00	28.98	30.49	29.59	14.29	22.30	14.86	20.41	22.07	22.42	25.65	25.81	22.38	25.00	23.57	21.09	22.86	23.93	23.93	23.93	22.86	22.86	22.86	23.93	23.21	23.90	23.89	21.58	22.46
3:sp|P78980|PEX16_YARLI	18.66	28.98	100.00	34.25	34.84	15.19	22.36	17.01	24.69	20.86	24.18	25.26	24.41	23.89	25.67	24.25	23.16	24.33	25.00	24.67	24.33	23.59	23.26	22.92	25.00	24.33	25.17	25.37	20.40	22.92
4:sp|Q7SD18|Q7SD18_NEUCR	21.69	30.49	34.25	100.00	52.59	16.53	19.81	20.53	22.26	21.30	27.30	25.09	26.26	23.66	25.17	23.83	22.96	23.83	24.50	24.16	23.83	23.83	23.49	22.82	24.83	23.83	25.34	24.81	24.83	22.33
5:tr|Q4WJ13|Q4WJ13_ASPFU	22.12	29.59	34.84	52.59	100.00	15.06	21.54	21.72	22.67	20.99	28.43	29.07	27.42	27.43	27.67	25.91	24.26	27.33	27.67	27.33	27.00	26.58	26.25	25.91	27.33	27.00	28.23	27.99	24.58	25.74
6:tr|Q22X13|Q22X13_TETTS	16.52	14.29	15.19	16.53	15.06	100.00	20.46	21.03	22.14	12.62	19.41	21.30	20.59	20.26	20.08	19.67	20.33	21.34	20.92	20.92	20.92	20.16	19.76	19.76	22.18	21.76	22.94	24.15	21.10	21.40
7:sp|Q8S8S1|PEX16_ARATH	14.33	22.30	22.36	19.81	21.54	20.46	100.00	45.69	22.99	16.27	21.32	23.70	23.27	23.81	23.82	23.12	23.49	23.82	23.51	23.51	23.20	22.50	21.88	21.56	24.76	24.14	24.44	24.74	21.43	21.74
8:tr|Q0E4E2|Q0E4E2_ORYSJ	17.98	14.86	17.01	20.53	21.72	21.03	45.69	100.00	25.00	4.88	27.60	25.39	25.39	24.49	26.29	24.62	25.26	25.77	24.74	25.26	25.26	22.56	22.56	22.56	25.26	26.29	28.72	29.05	18.46	24.62
9:sp|Q550G0|PEX16_DICDI	17.51	20.41	24.69	22.26	22.67	22.14	22.99	25.00	100.00	17.98	25.00	24.37	26.54	28.14	27.47	25.85	27.36	27.47	28.70	27.78	27.47	27.08	26.15	25.85	28.70	28.70	28.71	28.18	21.21	20.30
10:tr|H2XTV0|H2XTV0_CIOIN	18.24	22.07	20.86	21.30	20.99	12.62	16.27	4.88	17.98	100.00	33.33	30.54	32.57	28.85	30.29	30.29	24.49	30.86	32.00	31.43	30.86	31.43	31.43	30.86	32.00	30.86	30.86	30.87	26.40	29.28
11:tr|B0JYZ2|PEX16_XENTR	19.15	22.42	24.18	27.30	28.43	19.41	21.32	27.60	25.00	33.33	100.00	51.70	57.36	58.08	60.78	55.99	48.69	56.59	57.49	57.19	56.89	53.29	52.99	52.69	57.78	57.49	57.98	57.33	34.58	36.67
12:tr|H3CGN5|H3CGN5_TETNG	15.56	25.65	25.26	25.09	29.07	21.30	23.70	25.39	24.37	30.54	51.70	100.00	65.85	58.96	62.77	57.85	54.55	62.15	62.77	63.08	62.77	58.46	58.46	58.15	62.46	63.08	64.47	63.70	36.10	35.22
13:sp|Q4QRH7|PEX16_DANRE	16.07	25.81	24.41	26.26	27.42	20.59	23.27	25.39	26.54	32.57	57.36	65.85	100.00	68.20	71.04	66.57	61.24	67.76	68.06	68.36	68.06	64.48	64.48	64.18	69.85	68.06	69.82	69.21	37.15	39.63
14:tr|E1BVC0|E1BVC0_CHICK	17.06	22.38	23.89	23.66	27.43	20.26	23.81	24.49	28.14	28.85	58.08	58.96	68.20	100.00	78.63	72.14	72.90	72.52	75.19	75.57	74.81	69.47	70.23	69.47	72.90	74.43	75.59	75.44	36.25	38.28
15:tr|F6W6D8|F6W6D8_MONDO	17.44	25.00	25.67	25.17	27.67	20.08	23.82	26.29	27.47	30.29	60.78	62.77	71.04	78.63	100.00	94.94	71.75	86.01	86.01	86.31	86.01	82.14	82.14	81.85	83.63	84.82	86.59	86.42	35.29	38.72
16:tr|F6WKY7|F6WKY7_MONDO	16.73	23.57	24.25	23.83	25.91	19.67	23.12	24.62	25.85	30.29	55.99	57.85	66.57	72.14	94.94	100.00	66.88	81.25	81.55	81.85	81.55	81.90	82.20	81.90	82.01	80.36	82.01	81.46	32.41	36.47
17:tr|Q5FVJ9|Q5FVJ9_RAT	17.51	21.09	23.16	22.96	24.26	20.33	23.49	25.26	27.36	24.49	48.69	54.55	61.24	72.90	71.75	66.88	100.00	78.90	79.87	79.55	79.22	75.32	74.68	74.35	86.04	80.84	81.00	79.56	32.20	35.00
18:tr|F6ZXH5|F6ZXH5_HORSE	18.51	22.86	24.33	23.83	27.33	21.34	23.82	25.77	27.47	30.86	56.59	62.15	67.76	72.52	86.01	81.25	78.90	100.00	91.96	92.56	92.26	88.10	88.39	88.10	89.88	91.96	93.29	92.38	37.46	37.20
19:tr|H9G207|H9G207_MACMU	18.86	23.93	25.00	24.50	27.67	20.92	23.51	24.74	28.70	32.00	57.49	62.77	68.06	75.19	86.01	81.55	79.87	91.96	100.00	98.21	97.92	94.94	93.45	93.15	91.07	92.56	92.99	93.05	37.15	38.41
20:tr|K7AV99|K7AV99_PANTR	18.51	23.93	24.67	24.16	27.33	20.92	23.51	25.26	27.78	31.43	57.19	63.08	68.36	75.57	86.31	81.85	79.55	92.56	98.21	100.00	99.40	93.75	95.24	94.64	91.07	92.86	92.99	92.72	37.46	38.11
21:sp|Q9Y5Y5|PEX16_HUMAN	18.51	23.93	24.33	23.83	27.00	20.92	23.20	25.26	27.47	30.86	56.89	62.77	68.06	74.81	86.01	81.55	79.22	92.26	97.92	99.40	100.00	93.45	94.64	95.24	90.77	92.56	92.68	92.38	37.15	37.80
22:tr|F7DTL5|F7DTL5_MACMU	18.51	22.86	23.59	23.83	26.58	20.16	22.50	22.56	26.15	31.43	52.99	58.46	64.48	69.47	82.14	81.90	75.32	88.10	94.94	93.75	93.45	100.00	97.40	96.82	86.90	92.56	92.68	92.38	34.26	37.80
23:tr|H2Q3H2|H2Q3H2_PANTR	18.15	22.86	23.26	23.49	26.25	19.76	21.88	22.56	26.15	31.43	52.99	58.46	64.48	70.23	82.14	82.20	74.68	88.39	93.45	95.24	94.64	97.40	100.00	99.13	86.61	88.10	88.41	87.75	34.57	36.17
24:tr|q9y5y5-2|PEX16_HUMAN	18.15	22.86	22.92	22.82	25.91	19.76	21.56	22.56	25.85	30.86	52.69	58.15	64.18	69.47	81.85	81.90	74.35	88.10	93.15	94.64	95.24	96.82	99.13	100.00	86.31	87.80	88.11	87.42	34.26	35.87
25:sp|Q91XC9|PEX16_MOUSE	17.79	23.93	25.00	24.83	27.33	22.18	24.76	25.26	28.70	32.00	57.78	62.46	69.85	72.90	83.63	82.01	86.04	89.88	91.07	91.07	90.77	86.90	86.61	86.31	100.00	92.26	91.77	91.39	36.22	39.63
26:tr|E2RES1|E2RES1_CANFA	17.79	23.21	24.33	23.83	27.00	21.76	24.14	26.29	28.70	30.86	57.49	63.08	68.06	74.43	84.82	80.36	80.84	91.96	92.56	92.86	92.56	88.10	88.10	87.80	92.26	100.00	94.82	94.04	37.15	38.41
27:sp|Q2KII1|PEX16_BOVIN	17.58	23.90	25.17	25.34	28.23	22.94	24.44	28.72	28.71	30.86	57.98	64.47	69.82	75.59	86.59	82.01	81.00	93.29	92.99	92.99	92.68	92.68	88.41	88.11	91.77	94.82	100.00	99.67	36.56	38.15
28:sp|Q2KII7-2|PEX16_BOVIN	17.00	23.89	25.37	24.81	27.99	24.15	24.74	29.05	28.18	30.87	57.33	63.70	69.21	75.44	86.42	81.46	79.56	92.38	93.05	92.72	92.38	92.38	87.75	87.42	91.39	94.04	99.67	100.00	35.71	38.80
29:sp|Q9VPB9|Q9VPB9_DROME	17.44	21.58	20.40	24.83	24.58	21.10	21.43	18.46	21.21	26.40	34.58	36.10	37.15	36.25	35.29	32.41	32.20	37.46	37.15	37.46	37.15	34.26	34.57	34.26	36.22	37.15	36.56	35.71	100.00	44.21
30:tr|Q7QKE2|Q7QKE2_ANOGA	15.41	22.46	22.92	22.33	25.74	21.40	21.74	24.62	20.30	29.28	36.67	35.22	39.63	38.28	38.72	36.47	35.00	37.20	38.41	38.11	37.80	37.80	36.17	35.87	39.63	38.41	38.15	38.80	44.21	100.00

The sequences were collected from UniProtKB database and aligned using the program Clustal Omega (version 1.2.1).

Supplementary Table 5: Pex16p homologs and PP1-binding motifs

Species (common name)	Accession number	FASTA sequence	PP1-binding motifs (aa x–y)
Anopheles gambiae (african malaria mosquito)	Q7QKE2	>tr|Q7QKE2|Q7QKE2_ANOGA AGAP002283-PA OS=Anopheles gambiae GN=AGAP002283 PE=4 SV=3 MSSPLAEVQNLYERYVKWVSGNPSALADVELTVKWLSYFVAGKINNSSAVSELVYSLSNL LVFFNDRIIEKASKKTPDDTQPLERHLNVLLTTLEYCEVFIELSAHKVWGTSGRWFFIVV IQTIKCIGRLILTLFCQNTKIIRNPPIPALNRKTIQTDNHHHDHPQSDNASFRDNLADGS SAIVLKRSGRVMRKVNCSPSLTSRSWKPPATGSSSHQPAVYGGKFLVSAEMLYIAKPLIH LASMRKFGTRSWTSYLIALALDSASLRMYYKNREVLSKDQRVELSRRCVSMLLYLMRSPF YDRYTHDKIACLLNGIGNNVPLTGSIARLILSYIPHWQETYFYMWST	14–18: RyVKW [1] 31–35: LTVKW [3]
Arabidopsis thaliana (mouse-ear cress)	Q8S8S1	>sp|Q8S8S1|PEX16_ARATH Peroxisome biogenesis protein 16 OS=Arabidopsis thaliana GN=PEX16 PE=1 SV=1 MEAYKQWVWRNREYVQSFGSFANGLTWLLPEKFSASEIGPEAVTAFLGIFSTINEHIIEN APTPRGHVGSSGNDPSLSYPLLIAILKDLETVVEVAAEHFYGDKKWNYIILTEAMKAVIR LALFRNSGYKMLLQGGETPNEEKDSNQSESQNRAGNSGRNLGPHGLGNQNHHNPWNLEGR AMSALSSFGQNARTTTSSTPGWSRRIQHQQAVIEPPMIKERRRTMSELLTEKGVNGALFA IGEVLYITRPLIYVLFIRKYGVRSWIPWAISLSVDTLGMGLLANSKWWGEKSKQVHFSGP EKDELRRRKLIWALYLMRDPFFTKYTRQKLESSQKKLELIPLIGFLTEKIVELLEGAQSR YTYISGS	293–297: KQVHF [1,2,3]
Bos taurus (bovine)	Q2KII7	>sp|Q2KII7|PEX16_BOVIN Peroxisomal membrane protein PEX16 OS=Bos taurus GN=PEX16 PE=2 SV=2 MEKLRLLGLRYQEYVTRHPAATAQLETAVRGLSYLLAGRFADSHELSELVYSASNLLVLL NDGILRKELRKKLPMSLSQQRLLTWLSVLECVEVFMEMGATKVWGEVGRWLVIALIQLAK AVLRMFLLIWFKAGLQTSPPIVPLDREIQAQSRDGDHSSGSQEQSYVGKRSNRVVRTLQN TPSLHSRHWGAPQQREELGVAPTPLGLQETIAESLHIARPLLHLLSLGLWGQRSWTPWLL SGVVDVTSLSLLSDRKGLTRRERLELRRRTILLLYYLLRSPFYDRFSEAKILFLLQLLAD HVPGIGLVTRPLMDYLPNWQKIYFYSWG	63–66: GILR [4] 290–293: K.ILF [1] 321–324: K.IYF [1]
	Q2KII7-2	>sp|Q2KII7-2|PEX16_BOVIN Isoform 2 of Peroxisomal membrane protein PEX16 OS=Bos taurus GN=PEX16 MEKLRLLGLRYQEYVTRHPAATAQLETAVRGLSYLLAGRFADSHELSELVYSASNLLVLL NDGILRKELRKKLPMSLSQQRLLTWLSVLECVEVFMEMGATKVWGEVGRWLVIALIQLAK EIQAQSRDGDHSSGSQEQSYVGKRSNRVVRTLQNTPSLHSRHWGAPQQREELGVAPTPLG LQETIAESLHIARPLLHLLSLGLWGQRSWTPWLLSGVVDVTSLSLLSDRKGLTRRERLEL RRRTILLLYYLLRSPFYDRFSEAKILFLLQLLADHVPGIGLVTRPLMDYLPNWQKIYFYS WG	63–66: GILR [4] 264–267: K.ILF [1] 295–298: K.IYF [1]
Canis familiaris (dog)	E2RES1	>tr|E2RES1|E2RES1_CANFA Uncharacterized protein OS=Canis familiaris GN=PEX16 PE=4 SV=1 MEKLRLLSLRYQEYVTRHPAATAQLETAVRGLSYLLAGRFADSHELSELVYSASNLLVLL NDGILRKELRKKLPVPLSQQKLLTWLSVLECVEVFMEMGAAKVWGEVGRWLVIALIQLAK AVLRMFLLIWFKAGLQTSPPIVPLDRETQAQSPDGDQSSGSQEQSYVGKRSNRVVRTLQN TPSLHTRHWGAPQQREGRQQQQREELNVPPTPLGLQETIAESLYIARPLLHLLSLGLWGQ RSWTPWLLSGVVDVTSLSLLSDRKGLTRRERLELRRRTILLLYYLLRSPFYDRFSEARIL FLLQLLTDHVPGIGVVARPLMDYLPTWQKIYFYSWG	63–66: GILR [4] 298–301: R.ILF [1] 329–332: K.IYF [1]
Ciona intestinalis (transparent sea squirt)	H2XTV0	>tr|H2XTV0|H2XTV0_CIOIN Uncharacterized protein OS=Ciona intestinalis GN=LOC100175223 PE=4 SV=1 MSDILKSARDRLNENLMEIKQAYVNFVSQNPEMVDQIEKTVKTSSYLFEALSKNYDNSIF ISELITSACNLFAYANTKILLKTRNLISQTDENKFVAKLKQALTVVEFSQAFLELSAGRL GGSGARWAVIVVITIIKTILRCLLLYMFDSGLQSPALVTMINKTNIATQATNSDENENIY IGRRTGHQMATLSSSYSK	95–100: FvaKlK [5]
Cryptococcus neoformans	Q5KG96	>tr|Q5KG96|Q5KG96_CRYNJ Peroxisomal membrane protein pex16, putative OS=Cryptococcus neoformans var. neoformans serotype D (strain JEC21 / ATCC MYA-565) GN=CNE04390 PE=4 SV=1 MSPLEAYHSFLLSNLSAVQTIESSISNITWLLPGRFEDAEVASEGLYALLSLVAGYHDKI LSSHLSSSLSLPPHPFAKPRTPTEPLSASQESVTTRIHPLLPPPSDHARYTRYWTESSSL YEKASRALSTISYLELLVEMVARKKLGDRRRWKVVLGLESLKTFLRLLMLKTRRPVLSQ PTPQREFDLASVPSEVLDPSSSQPQDGNNPVTPQLPAYSPLRSHLFPMAGNLPEKYLEHP LDLIPQLKGSEYIAEAVACCVGLARIYLLIRTSRQEVTRPYNPSSLPTLSRSMSPYLIPL ALLLLSRRLRSKSESPLLMSHYAQQDKKLALQAFMTGPMWIGWTRPKIVSVARALERLPI LGLVGDLVEGYLPLVDDYFFYTTS	–
Danio rerio (zebrafish)	Q4QRH7	>sp|Q4QRH7|PEX16_DANRE Peroxisomal membrane protein PEX16 OS=Danio rerio GN=pex16 PE=2 SV=1 MEKLTRVFERYQEYVRTSPAAASHLESTVRALSYLIAGRFSDSHEISELVYSASNLLVLL NDGILRKNLSRTLPMSISQQKLLTWLSVLEYVEVFVEMAAAKMWGDAGRWLVIVLIQIAK AVLRCLLLFWYKSGIQTSPPIIPLDRDSQLCSQDNNEEEDDEDSSFVGKRSNRVVRTLQN APSLQSRLWGLPRKKKVSRNQEEELHSSPTTPLGLQETIAESLYIARPLLHLASLGICGKR SWKPWILSGLLEITSFSLLSDMKALNRRERAEMRRRAFLLLYYLLRSPFYDRYSETKILF LLRFLADYVPGVGLVARPLMEYLPIWQKIYFYNWG	63–66: GILR [4] 297–300: K.ILF [1] 328–331: K.IYF [1]
Dictyostelium discoideum (slime mold)	Q550G0	>sp|Q550G0|PEX16_DICDI Peroxisome biogenesis factor 16 OS=Dictyostelium discoideum GN=pex16 PE=3 SV=1 MIPKQPKSNILIFLLENSDHLGLLKSLITFLPGRYGDSELFSEGLYSVANILQSYLDYRS SGILLSNNIDKISNGEKVPPPYYLTTLRWITTVQSLELFFEMLATKKGEQHDDSNSNNNN SNNNIKKMIIFIIELLKAILRLKLLIKTNGDMLVHHSFYVPSKDVKTILENNRNQQKFQ NKRPAVTMSINNNNNINNNDNNNINNNNNTNDDNFNNNNNNNNNRRTLSDQIFEQQRIVN QENNLLYQQQRELQQNESTLIKLLLFPPPPKDYNTKTIGEILFIFRPVIYWVSYCIFGKKS WKPWFLSLVTELLSKSFSEYGNFKQKIRLTLLEAKELNRRKLLFFYLIRSPFYEKFIGD GLLNKFLNFLKKIHIFKTLIDILINYLNVYRTRYFYTSAS	127–131: KmIIF [1] 323–328: FkqKiR [5]
Drosophila melanogaster (fruit fly)	Q9VPB9	>tr|Q9VPB9|Q9VPB9_DROME LD20358p OS=Drosophila melanogaster GN=Pex16 PE=2 SV=1 MDTLKGMLKAYEAWVGKNPDVVGDFETTAKWVSYFIAGRISSSNVVSELVYTLSNMLVFY NDRIIEKARNSEENSVIHLQSKLCYRLKVTLTTLEYSEVFIEISARRLFGQSGKWLVIAL IQAFKAAGRFFILKHSTSDIITSPPIAALNRRAKQRKNSGDGVASSTNDLLQSQHSITFQ LKRSGRVIRKVEGAPPLQYRDFKLHIDNNEAAKTQIPRKLLQAEYLYISKPLIHLVAMGL FGRRSWKQYMVALSIDLYSIHLYRQHRDLMSKQQKLELSRRCINIMYFLVRSPFYDSFTK SRLERILDFVATSVPIAKVVAKPLKDYIPTWQSTYFYLWST	–
Equus caballus (horse)	F6ZXH5	>tr|F6ZXH5|F6ZXH5_HORSE Uncharacterized protein OS=Equus caballus GN=PEX16 PE=4 SV=1 MEKLRLLGLRYQEYVTRHPAATAQLETAVRGLSYLLAGRFTDSHELSELVYSASNLLVLL NDGILRKELRKKLPVSLSQQKLLTWLSVLECVEVFMEMGAAKVWGEVGRWLVIALIQLAK AVLRMFLLIWFKAGLQTSPPIVPLDREAQAQPPGGGHSFSFYVPSKDVKTILENNRNQLS QPTPSLHSRHWGAPQQQEGRPRPHQEELSITPTPLGLQETIAESLYIARPLLHLLSLGLWGQ RSWTPWFLSGVVDVTSLSLLSDRRGLTRRERLELRHRTILLLYYLLRSPFYDRFSEARIL FLLQLLADHVPGIGVTRPLMDYLPTWQKIYFYNWG	63–66: GILR [4] 298–301: R.ILF [1] 329–332: K.IYF [1]
Gallus gallus	E1BVC0	>tr|E1BVC0|E1BVC0_CHICK Uncharacterized protein OS=Gallus gallus GN=PEX16 PE=4 SV=1	226–229: R.ILF [1]

Species (common name)	Accession number	FASTA sequence	PP1-binding motifs (aa x–y)
(chicken)		MSLPQQKLLTWLSVLECVEVFAEMGTARVWGEMGRWTIIVLIQLAKAILRLLLLLWYKAG IQTSPPIVPLNREQQQSLHSEDVEGSSSGKDQTFVGRRSSRVVRSLQNTPSLQSRHWGSP QQREETQSRRAEEMNQPPTPLGLQETIAESIYVTRPLLHLLSLGVWGQRSWKPWLLSAVL DISSLSLLSDLKDLNRRERAELRRRTILLLYYLLRSPFYDRYSEA<mark>RILF</mark>LLRLLADYVPG LGFVTRPLMDYLPAWQ<mark>KIYF</mark>YNWG	257–260: K.IYF [1]
Homo sapiens (human)	Q9Y5Y5	>sp|Q9Y5Y5|PEX16_HUMAN Peroxisomal membrane protein PEX16 OS=Homo sapiens GN=PEX16 PE=1 SV=2 MEKLRLLGLRYQEYVTRHPAATAQLETAVRGFSYLLAGRFADSHELSELVYSASNLLVLL ND<mark>GILR</mark>KELRKKLPVSLSQQKLLTWLSVLECVEVFMEMGAAKVWGEVGRWLVIALVQLAK AVLRMLLLLWFKAGLQTSPPIVPLDRETQAQPPDGDHSPGNHEQSYVGKRSNRVVRTLQN TPSLHSRHWGAPQQREGRQQQHHEELSATPTPLGLQETIAEFLYIARPLLHLLSLGLWGQ RSWKPWLLAGVVDVTSLSLLSDRKGLTRRERRELRRRTILLLYYLLRSPFYDRFSEA<mark>RIL</mark> <mark>F</mark>LLQLLADHVPGVGLVTRPLMDYLPTWQ<mark>KIYF</mark>YSWG	63–66: GILR [4] 298–301: R.ILF [1] 329–332: K.IYF [1]
	Q9Y5Y5-2	>sp|q9y5y5-2|PEX16_HUMAN Isoform 2 of Peroxisomal membrane protein PEX16 OS=Homo sapiens GN=PEX16 MEKLRLLGLRYQEYVTRHPAATAQLETAVRGFSYLLAGRFADSHELSELVYSASNLLVLL ND<mark>GILR</mark>KELRKKLPVSLSQQKLLTWLSVLECVEVFMEMGAAKVWGEVGRWLVIALVQLAK AVLRMLLLLWFKAGLQTSPPIVPLDRETQAQPPDGDHSPGNHEQSYVGKRSNRVVRTLQN TPSLHSRHWGAPQQREGRQQQHHEELSATPTPLGLQETIAEFLYIARPLLHLLSLGLWGQ RSWKPWLLAGVVDVTSLSLLSDRKGLTRRERRELRRRTILLLYYLLRSPFYDRFSEA<mark>RIL</mark> <mark>F</mark>LLQLLADHVPGVGLVTTSQRAASPCLPARPHTQPWSPPAFLPGHP	63–66: GILR [4] 298–301: R.ILF [1]
Macaca mulatta (rhesus monkey)	H9G207	>tr|H9G207|H9G207_MACMU Peroxisomal biogenesis factor 16 isoform 1 OS=Macaca mulatta GN=PEX16 PE=2 SV=1 MEKLRLLGLRYQEYVTRHPAATAQLETAVRGLSYLLAGRFADSHELSELVYSASNLLVLL ND<mark>GILR</mark>KELRKKLPVSLSQQKLLTWLSVLECVEVFMEMGAAKVWGEVGRWLVIALIQLAK AILRMLLLLWFKAGLQTSPPIVPLDRETQAQPPDGDHSHGSHEQSYVGKRSNRVVRTLQN TPSLHSRHWGAPQQREGWQQQHHEELSATPTPLGLQETIAEFLYIARPLLHLLSLGLWGQ RSWKPWLLAGVVDVTSLSLLSDRKGLTRRERRELRRRTILLLYYLLRSPFYDRFSEA<mark>RIL</mark> <mark>F</mark>LLQLLADHIPGVGLVTRPLMDYLPTWQ<mark>KIYF</mark>YSWG	63–66: GILR [4] 298–301: R.ILF [1] 329–332: K.IYF [1]
	F7DTL5	>tr|F7DTL5|F7DTL5_MACMU Uncharacterized protein OS=Macaca mulatta GN=PEX16 PE=4 SV=1 MEKLRLLGLRYQEYVTRHPAATAQLETAVRGLSYLLAGRFADSHELSELVYSASNLLVLL ND<mark>GILR</mark>KELRKKLPVSLSQQKLLTWLSVLECVEVFMEMGAAKVWGEVGRWLVIALIQLAK AVLRMLLLLWFKAGLQTSPPIVPLDRETQAQPPDGDHSHGSHEQSYVGKRSNRVVRTLQN TPSLHSRHWGAPQQREGWQQQHHEELSATPTPLGLQETIAEFLYIARPLLHLLSLGLWGQ RSWKPWLLAGVVDVTSLSLLSDRKGLTRRERRELRRRTILLLYYLLRSPFYDRFSEA<mark>RIL</mark> <mark>F</mark>LLQLLADHIPGVGLVTTSQRAAFPCLPARPCTQPWSPPAFFPGPS	63–66: GILR [4] 298–301: R.ILF [1]
Monodelphis domestica (gray short-tailed opossum)	F6W6D8	>tr|F6W6D8|F6W6D8_MONDO Uncharacterized protein OS=Monodelphis domestica GN=PEX16 PE=4 SV=1 MEKLRLLGLRYQEYVTRHPAATAQLETAVRGLSYLLAGRFADSHELSELVYSASNLLVLL ND<mark>GILR</mark>KELRQSLPVSLSQQKLLTWLSVLECVEVFMEMGAAKVWGEMGRWLIIVLIQLAK AVLRILLLLWYKAGLQTSPPIVPLDREMQLHSQGGEHNLGSQDRPYVGKRSNRVVRSLQS TPSLHSRHWGVPQQQEGRLSHRGEELEAGPTPLGLQETIAESVYIARPLLHLLSLGLWGQ RSWKPWLLSAILDVTSLSLLSDKKGLTRRERLELRRRTILLLYYLLRSPFYDRFSED<mark>RIL</mark> <mark>F</mark>LLRLLADYVPGVGLVTRPLMDYLPAWQ<mark>KIYF</mark>YNWG	63–66: GILR [4] 298–301: R.ILF [1] 329–332: K.IYF [1]
	F6WKY7	>tr|F6WKY7|F6WKY7_MONDO Uncharacterized protein OS=Monodelphis domestica GN=PEX16 PE=4 SV=1 MEKLRLLGLRYQEYVTRHPAATAQLETAVRGLSYLLAGRFADSHELSELVYSASNLLVLL ND<mark>GILR</mark>KELRQSLPVSLSQQKLLTWLSVLECVEVFMEMGAAKVWGEMGRWLIIVLIQLAK AVLRILLLLWYKAGLQTSPPIVPLDREMQLHSQGGEHNLGSQDRPYVGKRSNRVVRSLQS TPSLHSRHWGVPQQQEGRLSHRGEELEAGPTPLGLQETIAESVYIARPLLHLLSLGLWGQ RSWKPWLLSAILDVTSLSLLSDKKGLTRRERLELRRRTILLLYYLLRSPFYDRFSED<mark>RIL</mark> <mark>F</mark>LLRLLADYVPGVGLVTRKYQAAHPFSPSAPLPHSIPATMPKPASLPGEP	63–66: GILR [4] 298–301: R.ILF [1]
Mus musculus (mouse)	Q91XC9	>sp|Q91XC9|PEX16_MOUSE Peroxisomal membrane protein PEX16 OS=Mus musculus GN=Pex16 PE=2 SV=2 MEKLRLLSLRYQEYVTRHPAATAQLETAVRGLSYLLAGRFSDSHELSELVYSASNLLVLL ND<mark>GILR</mark>KELRKKLPVSLSQQKLLTWLSVLECVEVFMEMGAAKVWGEVGRWLVIALVQLAK AVLRMLLLIWFKAGIQTSPPIVPLDRETQAQPLDGDHNPGSQEPSYVGKRSHRVVRTLQN SPSLHSRYWGAPQQREIRQKQQQEELSTPPTPLGLQETIAESLYIARPLLHLLSLGLWGQ RSWTPWLLSGVVDMTSLSLLSDRKNLTRRERLELRRRTILLLYYLLRSPFYDRFSEA<mark>KIL</mark> <mark>F</mark>LLQLLTDHIPGVGLVARPLMDYLPSWQ<mark>KIYF</mark>YSWG	63–66: GILR [4] 298–301: R.ILF [1] 329–332: K.IYF [1]
Neosartorya fumigata	Q4WJ13	>tr|Q4WJ13|Q4WJ13_ASPFU Peroxisomal membrane protein pex16 (Peroxin-16) OS=Neosartorya fumigata (strain ATCC MYA-4609 / Af293 / CBS 101355 / FGSC A1100) GN=AFUA_1G07610 PE=4 SV=1 MNSDLKSHSPVSATLLQPSKWLTMYEDFVMKNASSVGQVESALRSLTYIIPGRYRDSEIS SESVHSGVQLLSLYHDSLVSRVIARLPSTVPRPAPTPHSRYTKYWISHSALYHQVALTLQ MVRYTELLWEMIARRRGE<mark>KVRW</mark>RVVVLIEIIKATCRLLLLRLTNSRPLVSPPLPEREVDP RSTEEEASDWNGMQTPVSERSADLSWTMPRTGLSLPSLPDANDISNFLISKVLTADDIKP PKSLLHRVSGQGQLAEVLHILRPVIYALALQRWRQDKRSWRPWLIGFAMEYGCRQLAKSD FRERVAGGLRGLTGLEREELRKRGWAMGWWLMRGAFYENITKSWLKGLTSKMKGKPLLDL VGSVIEDYEYLWENFYFSTATL	139–142: K.VRW [1]
Neurospora crassa	Q7SD18	>tr|Q7SD18|Q7SD18_NEUCR Peroxisomal membrane protein pex16 OS=Neurospora crassa (strain ATCC 24698 / 74-OR23-1A / CBS 708.71 / DSM 1257 / FGSC 987) GN=pex16 PE=4 SV=3 MSTAADVPRFKGPNPIIQSMSATKRSTTSTDVKSTMSTNWLGAYGNFITKNNHQVSQIES TLRSLTYIIPGRFRDAEIASESIHSGVQLLSLYHDTLLFRASSKLSQPSLANAPSPHK<mark>RY</mark> <mark>IRF</mark>WFLKSPLYRRVAYLLQIVNYVELLIEMAAKRRGERMRWRAVIIIEAIKAFCKLLLLR ITKSRPLITPVLPEREPLPEAPTDEESAFQGDDSGYASASGSPQQSSPDGEWTMPRTGMS LPTLPSPGDISSYLLSRVLTADDIKPAAKLVNQLQGSAQVAEILHILSPLAFAVAMARSK DKRKAWAPWVLGLAIELVARQLRDRSLRTTPLEREEWSRRGWALGWWMMRGAFYENITKS MVEGVRKRMPSLIGGILEDYEYLWENYHFSTSP	119–123: RyIRF [1]
Oryza sativa (rice)	Q0E4E2	>tr|Q0E4E2|Q0E4E2_ORYSJ Os02g0123200 protein OS=Oryza sativa subsp. japonica GN=Os02g0123200 PE=2 SV=1 MLLQGGEVANEEEINILDENFGAKSNGVPVIYPMNGHFQNGHGVASNGLDGKAGFVSKSL EGRAVAALNKFGQNAKMTSDPMWMKKALPPPDPPAMVVEKPTLASIWSAKGISGRLFLLG EVVHIFRPLLYVLLIKKFGIKSWTPWLVSLAVEITSLGIHSRATDLHQRGGKVHQLSSAE RDELKRRKMMWALYVMRDPFFTRYTKRHLQKAEKVLDPVPLIGFLTGKLVELVEGAQTRY TYTSGS	—
Pan troglodytes (chimpanzee)	K7AV99	>tr|K7AV99|K7AV99_PANTR Peroxisomal biogenesis factor 16 OS=Pan troglodytes GN=PEX16 PE=2 SV=1 MEKLRLLGLRYQEYVTRHPAATAQLETAVRGFSYLLAGRFADSHELSELVYSASNLLVLL ND<mark>GILR</mark>KELRKKLPVSLSQQKLLTWLSVLECVEVFMEMGAAKVWGEVGRWLVIALIQLAK AVLRMLLLLWFKAGLQTSPPIVPLDRETQAQPPDGDHSPGGHEQSYVGKRSNRVVRTLQN TPSLHSRHWGAPQQREGRQQQHHEELSATPTPLGLQETIAEFLYIARPLLHLLSLGLWGQ	63–66: GILR [4] 298–301: R.ILF [1] 329–332: K.IYF [1]

Species (common name)	Accession number	FASTA sequence	PP1-binding motifs (aa x–y)
		RSWKPWLLAGVVDVTSLSLLSDRKGLTRRERRELRRRTILLLYYLLRSPFYDRFSEA**RIL F**LLQLLADHVPGVGLVTRPLMDYLPTWQ**KIYF**YSWG	
	H2Q3H2	>tr|H2Q3H2|H2Q3H2_PANTR Uncharacterized protein OS=Pan troglodytes GN=PEX16 PE=4 SV=1 MEKLRLLGLRYQEYVTRHPAATAQLETAVRGFSYLLAGRFADSHELSELVYSASNLLVLL ND**GILR**KELRKKLPVSLSQQKLLTWLSVLECVEVFMEMGAAKVWGEVGRWLVIALIQLAK AVLRMLLLLWFKAGLQTSPPIVPLDRETQAQPPDGDHSPGGHEQSYVGKRSNRVVRTLQN TPSLHSRHWGAPQQREGRQQQHHEELSATPTPLGLQETIAEFLYIARPLLHLLSLGLWGQ RSWKPWLLAGVVDVTSLSLLSDRKGLTRRERRELRRRTILLLYYLLRSPFYDRFSEA**RIL F**LLQLLADHVPGVGLVTTSQRAASPCLPARPHTQPWSPPAFLPGPP	63–66: GILR [4] 298–301: R.ILF [1]
Rattus norvegicus (rat)	Q5FVJ9	>tr|Q5FVJ9|Q5FVJ9_RAT Peroxisomal biogenesis factor 16 OS=Rattus norvegicus GN=Pex16 PE=2 SV=1 MRKLGGNLDLPFKVASPIPTSCLSWCTLPLTCLCCSMTGSFGRSFEKKLPVSLSQQKLLT WLSVLECVEVFMEMGAAKVWGEVGRWLVIALIQLAKAVLRMFLLIWFKTGIQTSPPIVPL DRETQAQPLDGDHNLGSPEPSYVGKRSNRVVRTLQNSPSLHSRHWGAPQQREIRQKQQQE ELSTPPTPLGLQETIAESLYIARPLLHLLSLGLWGQRSWAPWLLSGVVDMTSLSLLSDRK NLTRRERLELRRRTILLLYYLLRSPFYDRFSEA**KILF**LLQLLADHIPGIGLVARPLMDYL PSWQ**KIYF**YSWG	274–277: K.ILF [1] 305–308: K.IYF [1]
Schizosaccharomyces pombe (fission yeast)	O94516	>sp|O94516|PEX16_SCHPO Peroxisomal membrane protein PEX16 OS=Schizosaccharomyces pombe (strain 972 / ATCC 24843) GN=pex16 PE=1 SV=2 MKPLAYYEDQLLKDEKSFLKVTEIERLLSYAAYLLPAEFRDDQLKSQTITSILLLLHQFH TGLLFRKIAELPKTEQAILKSERTQYLEYFRKKNPSFEKVSELLYFLNISTFPIELVISK YNPSRQYDSVLFLESVKFLLRVHIMWTTGGDLPLSNPVLQRDFNVKTFIHLHKKYSNSGS AVVLKNSKKVVPRLNTVNSSLDFLQNRTPRLSSILPDEIFTKRLPNLRIFSNFIKVCRPL IYMLFMWHWKRKQKSSSLKVRPWGPWIVAFVFEVISQLIDRRCESATSSRQGFGLERRTN QSQFQHFVVWAFTQGRFYDEFTKHWINRSLSWVNSIPVFGKYLLLSVEERQKSLENYISS VRNY	–
Tetrahymena thermophila	Q22X13	>tr|Q22X13|Q22X13_TETTS Peroxisomal membrane protein OS=Tetrahymena thermophila (strain SB210) GN=TTHERM_00633400 PE=4 SV=2 MDSQQENKSSQIYQSFQQYQHINKSLN**KLVSF**EFLLEQTLNYISNKST**FFNKDR**FLEILS LSQFV**KVYF**KLQKMNISQKQIYISEGNMQEELDEQNRQKSEAFEKFFTEDYIEKYRNLQP EEQIQKMAETLERIKNRQQNGMTFNEDFEEELQRSHKRVGLLSKLPIPKDLLETKQPNQK KSDYMIFVGEVLFIVRPLIYCILLRMFGVKSYTPYMISLIIDLFRLILQ**RKIKF**YQPAQR EE**FKTRNK**EMILNYLLRNPFYSHIFRNKVLIPMLDSLFGSRLQFLKSFILGIIEMRCSIC LLL	28–32: KlVSF [1] 49–54: FfnKdR [5] 66–69: K.VYF [1] 230–234: RKIKF [1, 3] 243–248: FktRnK [5]
Tetraodon nigroviridis (spotted green pufferfish)	H3CGN5	>tr|H3CGN5|H3CGN5_TETNG Uncharacterized protein OS=Tetraodon nigroviridis PE=4 SV=1 MEKASRYYERYSEFVRRNPAATAQLEGTVRTLSYLIAGRFTASHEMSELVYSASNLLVLL ND**SILR**RDLRWTGSMPVSQQRLLTWLEMGACKLWGKVGRWLVIALIQIFKAVLRLVLLLW YRSGIQTSPPIIPLDRSAELSPSDGERGQQEDSACFVGQRSGRVVRPLNRSAAPSPLTRR WGAPRPRTQPSSNMEKLLSRPTPLNLQETVGECVYIGRPLSAVLCLGLCGKQSWKPWLAC GCLSVGSVALLSEAKFQNGYERAEMRRRTFLLLYYLLRSPFYDKFSQG**KILF**LLRLLADH VPGIGLVARPLMDYLPTWQ**KIYF**YNWG	63–66: SILR [4] 289–292: K.ILF [1] 320–323: K.IYF [1]
Xenopus troplicalis (western clawed frog)	B0JYZ2	>sp|B0JYZ2|PEX16_XENTR Peroxisomal membrane protein PEX16 OS=Xenopus tropicalis GN=pex16 PE=2 SV=1 MAARYWDKLQDLSQKYKDYVIQNPTGATQLESAVRMLSYLIAGRFADSHELSELVYSASN LLALLND**GILR**KELLAPPPTEGSRRRLLTWLGVLESLEVFIEIGAARAWGDRTRWAAILI IQLLKACLRIVLLFWYRAGIQSSPPVTPLDREGILNQAEDNSNSGSSCFVGRRSSRAVRS LDDSASSHRRFWRSPQIHDGKQRNTGETESDKDGSELGTLGTLAEAIHILRPITHLLSLA TWGQKSWKPWMVAAALDITSISLLSDVRNLSHRERAELRRRMFLLLYYLLRSPFYNHYTE TRLLLLLRLLGDYVPGVGLVARPLMDYLPVWQ**KIYF**YNWG	68–71: GILR [4] 333–336: K.IYF [1]
Yarrowia lipolytica	P78980	>sp|P78980|PEX16_YARLI Peroxisomal membrane protein PEX16 OS=Yarrowia lipolytica (strain CLIB 122 / E 150) GN=PEX16 PE=3 SV=1 MTDKLVKVMQKKKSAPQTWLDSYDKFLVRNAASIGSIESTLRTVSYVLPGRFNDVEIATE TLYAVLNVLGLYHDTIIARAVAASPNAAAVYRPSPHNRYTDWFIKNRKGYKYAS**RAVTF**V KFGELVAEMVAKKNGGEMARWKCIIGIEGIKAGLRIYMLGSTLYQPLCTTPYPDREVTGE LLETICRDEGELDIEKGLMDPQWKMPRTGRTIPEIAPTNVEGYLLTKVLRSEDVDRPYNL LSRLDNWGVVAELL**SILR**PLIYACLLFRQHVNKTVPASTKSKFPFLNSPWAPWIIGLVIE ALSRKMMGSWLLRQRQSGKTPTALDQMEVKGRTNLLGWWLFRGEFYQAYTRPLLYSIVAR LEKIPGLGLFGALISDYLYLFDRYYFTASTL	aa 115–119: RAVTF [1] aa 255–258: SILR [4]

The sequences of the organisms listed on PeroxisomeDB 2.0 as having Pex16p homologs were collected from UniProtKB database and loaded in ScanProsite program as well as the PP1-binding motifs canonical sequences listed on Table 5. The sequences are alphabetically ordered by species Latin name. The green- and blue-high lightened residues correspond to matches with the canonical sequences of RVxF and RVxF-cooperating motifs, respectively. [1]matches with the sequence [RK]-X(0,1)-[VI]-{P}-[FW]; [2]matches with the sequence [HKR]-[ACHKMNQRSTV]-V-[CHKNQRST]-[FW]; [3]matches with the sequence [KRL]-[KRSTAMVHNQ]-[VI]-{FIMYDP}-[FW]; [4]matches with the sequence [GS]-I-L-[RK]; [5]matches with the sequence F-X-X-[RK]-X-[RK]. Other canonical sequences were screened, with no hits (R-X-X-Q-[VIL]-[KR]-X-[YW], R-A-R-A, R-[KR]-X-H-Y, K-S-Q-K-W and R-N-Y-F). A graphic resume of this screening is depicted on Figure 11.

```
sp|O75192|PX11A_HUMAN    ---MDAFTRFTNQTQGRDRLFRATQYTCMLLRYLLEPK-AGKEKVVMKLKKLESSVSTGR    56
sp|O96011|PX11B_HUMAN    ---MDAWVRFSAQSQARERLCRAAQYACSLLGHALQRH-GASPELQKQIRQLESHLSLGR    56
sp|Q96HA9|PX11C_HUMAN    MASLSGLASALESYRGRDRLIRVLGYCCQLVGGVLVEQCPARSEVGTRLLVVSTQLSHCR    60
                            :.. .     . :.*:** *.  * * *:    *  :  .  ::  ::  :.: :*   *

sp|O75192|PX11A_HUMAN    KWFRLGNVVHAIQATEQ---SIHATDLVPRLCLTLANLNRVIYFICDTILWVRSVGLTSG    113
sp|O96011|PX11B_HUMAN    KLLRLGNSADALESAKR---AVHLSDVVLRFCITVSHLNRALYFACDNVLWAGKSGLAPR    113
sp|Q96HA9|PX11C_HUMAN    TILRLFDDLAMFVYTKQYGLGAQEEDAFVRCVSVLGNLADQLYYPCEHVAWAADARV-LH    119
                         . :** :     :  ::: .  . : * . *    .:..*   :*: *: : *.. . :

sp|O75192|PX11A_HUMAN    INKEKWRTRAAHHYYYSLLLSLVRDLYEISLQMKRVT--CDRAKKEKSASQ---------    162
sp|O96011|PX11B_HUMAN    VDQEKWAQRSFRYYLFSLIMNLSRDAYEIRLLMEQESSACSRRLKGSGGGVPGGSETGGL    173
sp|Q96HA9|PX11C_HUMAN    VDSSRWWTLSTTLWALSLLLGVARSLWMLLKLRQRLRSPTAP----------------F    162
                         ::..:*    :    :  **:: : *. : :        ::

sp|O75192|PX11A_HUMAN    -DPLWFS-VAEEETEWLQSFLLLLFRSLKQHPPLLLDTVKNLCDIL-----NPLDQLGIY    215
sp|O96011|PX11B_HUMAN    GGPGTPGGGLPQLALKLRLQVLLLARVLRGHPPLLLDVVRNACDLF-----IPLDKLGLW    228
sp|Q96HA9|PX11C_HUMAN    TSPLPRG-KRRAMEAQMQSEA-------------LSLLSNLADLANAVHWLPRGVLWAG    207
                             *   .             ::                *. : * .*:      *   *

sp|O75192|PX11A_HUMAN    KSNPGIIGLGGLVSSIAGMITVAYPQMKLKTR--    247
sp|O96011|PX11B_HUMAN    RCGPGIVGLCGLVSSILSILTLIYPWLRLKP---    259
sp|Q96HA9|PX11C_HUMAN    RFPPWLVGLMGTISSILSMYQAARAGGQAEATTP    241
                         :   * ::** * :*** .:          : :
```

Supplementary Figure 2: Glycine-rich region of human Pex11pβ is absent in Pex11pα and Pex11pγ

The sequences were collected from UniProtKB database and aligned using the program Clustal Omega (version 1.2.1). Blue residues correspond to glycine-rich region.
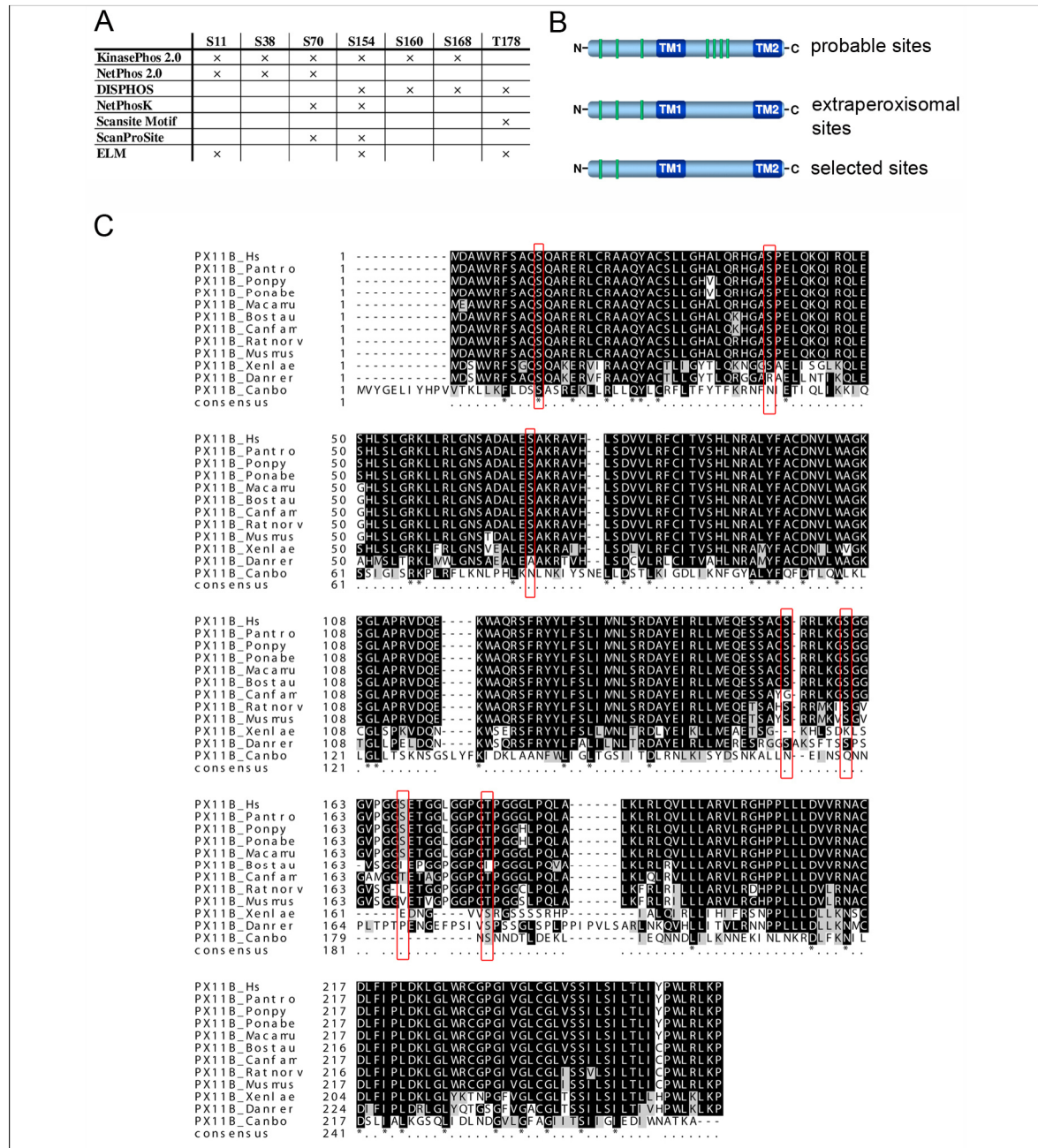
Supplementary Figure 3: Determination of potential phosphorylation sites within *Hs*Pex11pβ
(A) Overview of multiple hits for different amino acid positions. Several online screening tools were used to determine potential phosphorylation sites in the sequence of human Pex11pβ. The various tools were plotted against the positions given. (B) Scheme depicting phosphorylation-sites chosen for subsequent studies. Based on the screening, several putative phosphorylation sites were selected whose location is indicated in the upper scheme (potential sites). Based on our findings regarding the topology of Pex11pβ, intra-peroxisomal sites were excluded (extraperoxisomal sites). Furthermore, based in the studies regarding deletions of the N-terminus, the phosphorylation sites listed on the bottom were chosen. (C) Overview of conserved amino acids within Pex11pβ protein sequences across species. The putative phosphorylation-sites are depicted in red brackets. Note that position S11 is highly conserved. From (211).